

SULFORAPHANE & PROTEIN
EXPRESSION IN AN INFLAMMATORY
PROSTATE MODEL

Rosemary Louise McCall

Institute of Food Research

A thesis submitted for the degree of Doctor of Philosophy to the
University of East Anglia

June 2011

© This copy of the thesis has been supplied on condition that anyone who consults it is understood to recognise that its copyright rests with the author and that use of any information derived there from must be in accordance with current UK Copyright Law.

In addition, any quotation or extract must include full attribution.

Abstract

Benign prostatic hyperplasia (BPH) is a common condition that occurs in over 25% of men aged 50+, increasing to 50% amongst those over 80. Although the aetiology of the condition has not been ascertained, the majority of BPH specimens contain inflammatory infiltrates indicating inflammation plays an important role in the progression of the disease. Furthermore, a role for inflammation has also been suggested in prostate cancer (PCa). BPH is not a pre-cursor of PCa, but using BPH as a model of inflammation could result in findings that may apply and add to our understanding of PCa. Previous work has demonstrated that the consumption of broccoli can alter inflammatory pathways in the human prostate, and this may be due to the action of the isothiocyanate sulforaphane (SF), a phytochemical derived from broccoli. This dietary compound has a range of biological activities, including reducing inflammation, which has been demonstrated primarily by using *in vitro* models.

In this study, BPH tissue is cultured *ex vivo* as a model of prostate inflammation to more closely replicate *in vivo* conditions than established cell lines. Both targeted and untargeted approaches were employed to test the hypothesis that sulforaphane reduces inflammatory pathways, and beneficially alters protein expression in BPH tissue.

Analysis of the effect of SF on inflammatory markers revealed that SF significantly reduced levels of secreted IL-6 and IL-8, and to a lesser extent FGF-2. Global proteomic analysis demonstrated that there was, as expected, considerable variation between individuals, and that SF altered expression of several proteins in BPH tissue. From these, HSP90 β 1 was identified as a novel target for SF activity, a reduction of which was further verified in independent BPH patients. The biological relevance of the reduction of HSP90 β 1 by SF was investigated but not determined.

This work highlights the natural variation present within humans and the need to use a larger sample number in order to understand the complex effects of SF on prostate tissue. The results suggest that SF can reduce inflammatory markers and alter proteins within the human prostate, indicating a possible protective role for SF in pathogenesis of the prostate.

Acknowledgements

First and foremost, I would like to dedicate this thesis to my husband Darren, and thank him for all his love and support throughout my PhD, without which I doubt I would ever have reached this point.

I also wish to thank my family and friends, who have offered support, and shown an interest in my work.

I would like to thank my supervisor, Prof Richard Mithen, for giving me this opportunity and for all his guidance throughout, and my advisor, Dr Maria Traka, for her essential encouragement and advice.

Huge thanks goes to Dr. Robert Mills, and his team at the NNUH, for obtaining the BPH tissue samples that were so essential to my work, and Prof. Richard Ball for his help with the histological analysis of my samples. I also thank Julia Burton, and her team at the tissue bank, for embedding, sectioning and staining my tissue samples as required. Furthermore, I wish to acknowledge Dr Fran Mulholland for all his expert help and advice with the proteomics work, and Jack Dainty for his help with statistical analysis. Thanks also goes to the rest of my research group at large, including those who have left, for any help they have given me at any point in my PhD.

Finally, I wish to thank the BBSRC for funding my work.

Contents

Abstract	i
Acknowledgements	ii
Contents	iii
List of Figures	vii
List of Tables	ix
Abbreviations	x
Chapter 1. Introduction	1
1.1 The Prostate.....	1
1.1.1 Structure.....	1
1.1.2 Function.....	2
1.1.3 Regulation.....	2
1.1.4 Inflammatory System.....	4
1.2 Diseased Prostate.....	5
1.2.1 Benign Prostatic Hyperplasia.....	6
1.2.2 Prostate Cancer.....	11
1.2.3 Benign Prostatic Hyperplasia and Prostate Cancer.....	17
1.3 Diet and Disease.....	19
1.3.1 Diet and Benign Prostatic Hyperplasia.....	19
1.3.2 Diet and Prostate Cancer.....	20
1.3.3 Cruciferous Vegetables.....	22
1.3.4 Glucosinolates.....	22
1.3.5 Isothiocyanates.....	22
1.4 Sulforaphane.....	23
1.4.1 Modes of Action.....	27
1.5 Models to Explore Diet Interactions.....	37
1.5.1 In Vitro.....	37
1.5.2 Ex Vivo.....	38
1.5.3 In Vivo.....	39
1.6 Thesis Aims.....	40
Chapter 2. Tissue Culture Method Development	41
2.1 Introduction.....	42
2.2 Materials & Methods.....	44
2.2.1 Tissue Collection.....	44

2.2.2	<i>Tissue Preparation</i>	44
2.2.3	<i>Tissue Culture</i>	44
2.2.4	<i>Sample collection and storage</i>	45
2.2.5	<i>LDH Assay</i>	45
2.2.6	<i>PSA Assay</i>	46
2.2.7	<i>Histological evaluation</i>	46
2.2.8	<i>Statistics</i>	46
2.3	Results.....	48
2.3.1	<i>Comparison of the effect of culture media on BPH tissue viability</i>	48
2.3.2	<i>Determining the effect of DHT on BPH tissue viability</i>	50
2.3.3	<i>Histological structure of BPH tissue</i>	52
2.4	Discussion.....	60
2.4.1	<i>Tissue Viability</i>	60
2.4.2	<i>Tissue Function</i>	62
2.4.3	<i>DHT Supplementation</i>	63
2.4.4	<i>Conclusions</i>	64
Chapter 3.	Benign Prostatic Hyperplasia & Inflammation	66
3.1	Introduction.....	67
3.2	Methods.....	69
3.2.1	<i>Tissue Collection and Preparation</i>	69
3.2.2	<i>Tissue Culture</i>	69
3.2.3	<i>Sample collection and storage</i>	69
3.2.4	<i>ELISA</i>	69
3.2.5	<i>Statistics</i>	71
3.3	Results.....	72
3.3.1	<i>Inflammatory cytokines in BPH tissue</i>	72
3.3.2	<i>Modulation of inflammatory cytokines by sulforaphane</i>	73
3.3.3	<i>Dose-dependent effect of SF on IL-6 secretion</i>	76
3.4	Discussion.....	78
3.4.1	<i>Inflammatory markers in BPH tissue</i>	78
3.4.2	<i>Reduction of inflammatory markers by SF</i>	82
3.4.3	<i>Conclusions</i>	84
Chapter 4.	Proteomics & Protein Identification	85
4.1	Introduction.....	86

4.2	Methods.....	88
4.2.1	<i>Tissue collection</i>	88
4.2.2	<i>Protein extraction</i>	88
4.2.3	<i>Protein quantification</i>	88
4.2.4	<i>2D gels</i>	89
4.2.5	<i>Mass spectrometry</i>	91
4.2.6	<i>Identification of proteins using Mascot</i>	92
4.2.7	<i>Statistics</i>	96
4.3	Results.....	97
4.3.1	<i>Analysis of sources of variation within 2D gels</i>	97
4.3.2	<i>Selection of protein spots for identification</i>	101
4.3.3	<i>Identification of proteins</i>	105
4.4	Discussion.....	111
4.4.1	<i>Sources of Variation</i>	111
4.4.2	<i>The effect of SF on global protein expression</i>	115
4.4.3	<i>Spots chosen for identification</i>	115
4.4.4	<i>Identification of proteins</i>	116
4.4.5	<i>Conclusions</i>	117
Chapter 5.	Analysis of proteins altered in BPH tissue	118
5.1	Introduction	119
5.2	Methods.....	120
5.2.1	<i>Classification of proteins by molecular function and biological process</i>	120
5.3	Results.....	121
5.3.1	<i>Analysis of proteins significantly altered between 2D gels</i>	121
5.3.2	<i>Biological process and molecular function analysis</i>	128
5.3.3	<i>The link between protein binding proteins and apoptosis</i>	131
5.4	Discussion.....	138
5.4.1	<i>Natural variation of protein expression in BPH tissue</i>	138
5.4.2	<i>The biological processes and molecular functions altered by SF</i>	142
5.4.3	<i>Apoptosis and chaperone proteins</i>	151
5.4.4	<i>Conclusions</i>	159
Chapter 6.	Biological Relevance of HSP90β1	160
6.1	Introduction	161
6.2	Materials & Methods	166

6.2.1	<i>Tissue culture and sample collection</i>	166
6.2.2	<i>Cell Line Culture</i>	168
6.2.3	<i>Western Blotting</i>	172
6.2.4	<i>Taqman</i>	173
6.2.5	<i>Statistics</i>	174
6.3	<i>Results</i>	175
6.3.1	<i>The effect of SF on HSP90B1 in BPH tissue</i>	175
6.3.2	<i>Modulation of HSP90B1 by SF in cell lines</i>	179
6.3.3	<i>siRNA Method Optimization</i>	181
6.3.4	<i>Optimising HSP90B1 knockdown</i>	183
6.3.5	<i>The effect of HSP90B1 knockdown on the cell</i>	186
6.4	<i>Discussion</i>	188
6.4.1	<i>Modulation of HSP90B1 by SF</i>	188
6.4.2	<i>Artificial knockdown of HSP90B1</i>	192
6.4.3	<i>The effect of HSP90B1 reduction on cell function</i>	194
6.4.4	<i>Conclusions</i>	197
Chapter 7.	Final Discussion	198
7.1	<i>Contributions to thesis aims</i>	198
7.1.1	<i>Ex vivo model of prostate inflammation</i>	199
7.1.2	<i>Reduction of inflammation by sulforaphane</i>	200
7.1.3	<i>Sulforaphane and protein expression in BPH tissue ex vivo</i>	204
7.1.4	<i>Novel target for sulforaphane activity</i>	205
7.2	<i>Further Contributions</i>	209
7.2.1	<i>Ex Vivo models versus In Vitro Models</i>	209
7.2.2	<i>Targeted versus Untargeted Approaches</i>	212
7.3	<i>Summary</i>	215
7.4	<i>Future Work</i>	217
7.4.1	<i>Further Ex Vivo Tissue Culture Optimization</i>	217
7.4.2	<i>HSP90B1</i>	217
7.4.3	<i>In Vivo Models</i>	220
Annex	222	222
BPH Tissue Patients	222
References	223	223

List of Figures

Figure 1.1. Prostate structure: zones and lobes.	2
Figure 1.2. Haematopoiesis and inflammatory cell development.	5
Figure 1.3. Immune response and cytokine expression in BPH progression.	8
Figure 1.4. Inflammatory pathways in BPH.	10
Figure 1.5. Gleason grades.	12
Figure 1.6. Inflammatory pathways in PCa.	16
Figure 1.7. Prostatic disease progression.	18
Figure 1.8. Glucosinolate and isothiocyanate structure.	23
Figure 1.9. Conversion of glucoraphanin to sulforaphane.	24
Figure 1.10. Modes of action of sulforaphane (excluding apoptosis).	28
Figure 1.11. Activation of apoptosis by SF.	34
Figure 2.1. Tissue sample preparation.	45
Figure 2.2. PSA Assay Protocol.	47
Figure 2.3. Comparison of the effect of media on BPH tissue <i>ex vivo</i>	49
Figure 2.4. Determining the effect of DHT on BPH tissue <i>ex vivo</i>	51
Figure 2.5. Normal prostate structure.	52
Figure 2.6. Diathermy edge effect.	55
Figure 2.7. BPH tissue in culture for 5 days.	56
Figure 2.8. Abnormal histological features in prostate tissue.	57
Figure 2.9. BPH tissue in culture for 24 hours.	59
Figure 3.1. Quantikine ELISA Protocol.	70
Figure 3.2. Basal Levels of Inflammatory cytokines in BPH tissue.	72
Figure 3.3. The effect of 25 μ M SF on inflammatory cytokines in BPH tissue.	75
Figure 3.4. Dose-dependent effect of SF on IL-6 secretion from BPH tissue.	77
Figure 4.1. Proteomic analysis overview.	87
Figure 4.2. Mascot search result.	94
Figure 4.3. Position of spot 397 on a 2D gel.	94
Figure 4.4. Peptide Sequence of endoplasmic (P14625).	95
Figure 4.5. Peptide Sequence of collagen alpha-1(VI) chain (P12109).	95

Figure 4.6. 2D Gels of protein extracted from BPH tissue cultured with or without 10 μ M SF. .	99
Figure 4.7. Spots picked for identification.	103
Figure 4.8. Overlap between spots picked for identification due to the effect of SF on each patient.....	104
Figure 4.9. Spots identified from 2D Gels.....	106
Figure 4.10. Technical Sources of Error in 2D Gel Analysis.....	114
Figure 5.1. Spots significantly altered between BPH samples ran by 2D gel electrophoresis..	121
Figure 5.2. The effect of SF on HSP90 β 1.....	133
Figure 5.3. The effect of SF on calreticulin.....	134
Figure 5.4. The effect of SF on 14-3-3 ϵ	135
Figure 5.5. The effect of SF on GRP78.....	136
Figure 5.6. The effect of SF on HSP70.....	137
Figure 6.1. Immunohistochemistry Protocol.	167
Figure 6.2. siRNA Transfection Protocol.	169
Figure 6.3. The effect of SF on HSP90 β 1.....	176
Figure 6.4. HSP90 β 1 expression in BPH tissue.....	178
Figure 6.5. The effect of SF on HSP90 β 1 in cell lines.	180
Figure 6.6. Optimisation of siRNA delivery.	182
Figure 6.7. HSP90B1 siRNA dose effect.....	183
Figure 6.8. Time course for HSP90 β 1 knockdown.	185
Figure 6.9. Effect of HSP90 β 1 siRNA on cell viability.	186
Figure 6.10. Effect of HSP90 β 1 siRNA on cell proliferation.	187
Figure 7.1. Inhibition of IL-6 production by sulforaphane.	203
Figure 7.2. HSP90 β 1 and apoptosis.	206

List of Tables

Table 4.1. Possible identifications for spot 397.	93
Table 4.2. Statistical analysis of the sources of variation within the 2D gels.	100
Table 4.3. Number of spots found to be statistically significantly altered (p -value <0.05) and chosen for identification.	102
Table 4.4. Identification of protein spots by mass spectrometry.	107
Table 5.1. Fold-change of proteins identified as statistically significantly ($p \leq 0.05$) different between individuals at baseline.	122
Table 5.2. Fold-change of proteins identified as statistically significantly ($p > 0.05$) altered in the population as a whole as a result of sulforaphane treatment.	123
Table 5.3. Fold-change of proteins identified as statistically significantly ($p \leq 0.05$) altered in patient 13 as a result of $10\mu\text{M}$ SF treatment.	124
Table 5.4. Fold-change of proteins identified as statistically significantly ($p \leq 0.05$) altered in patient 14 as a result of $10\mu\text{M}$ SF treatment.	125
Table 5.5. Fold-change of proteins identified as statistically significantly ($p \leq 0.05$) altered in patient 16 as a result of $10\mu\text{M}$ SF treatment.	127
Table 5.6. Proteins identified from 2D gels classified by biological process.	129
Table 5.7. Proteins identified from 2D gels organised into molecular functional groups.	130
Table 5.8. Apoptotic proteins altered by SF: Their role in apoptosis and relationship with SF.	145
Table 5.9. The role of molecular chaperones in apoptosis.	153
Table 6.1. 18S Primers and probe sequences.	173
Table 7.1. Advantages and limitations of <i>ex vivo</i> and <i>in vitro</i> models.	211

Abbreviations

-ve	Negative
+ve	Positive
2D	Two dimensional
Ab	Antibody
ACT	Actin
ACTN	Actinin
Akt	RAC-alpha serine/threonine-protein kinase
ALB	Serum albumin
ANOVA	Analysis of variance
ANX	Annexin
AP-1	Activator protein 1
APC	Antigen presenting cell
AR	Androgen receptor
ARE	Antioxidant response element
ATP5A1	ATP synthase subunit alpha
BPH	Benign prostatic hyperplasia
BrdU	Bromodeoxyuridine
BSA	Bovine serum albumin
CALR	Calreticulin
CCR	c-c motif receptor
CDK	Cyclin-dependent kinase
CKB	Creatine kinase B
CLL	Chronic lymphoid leukemia
COL6A3	Collagen alpha-3 (VI)
COX-2	Cyclooxygenase-2
CTC	Circulating tumour cell
CYP450	Cytochrome P450
CXCR	C-X-C chemokine receptor type
DES	Desmin
DHT	Dihydrotestosterone
DMSO	Dimethyl sulfoxide
DNA	Deoxyribonucleic acid
DR	Death receptor

EC	Epithelial cell
EEF1A1	Elongation factor 1-alpha 1
EGF	Epidermal growth factor
ELISA	Enzyme-linked immunosorbent assay
ER	Endoplasmic reticulum
ERG	ets related gene
ERK	Extracellular-signal-regulated kinase
ESC	Embryonic stem cell
FBLN	Fibulin
FCS	Fetal calf serum
FGF	Fibroblast growth factor
FLNA	Filamin-A
FOXO	Forkhead members of the class O (FOXO) transcription factors
GA	Geldanamycin
GAPDH	Glyceraldehyde 3-phosphate dehydrogenase
GF	Growth factor
GITR	Glucocorticoid-induced tumour necrosis factor receptor
GO	Gene ontology
GLS	Glucoconinolate
GM-CSF	Granulocyte-macrophage colony-stimulating factor
GRP	Glucose regulated protein
GST	Glutathione-s-transferase
H&E	Haemotoxylin and eosin
HADHB	Trifunctional enzyme subunit beta
HDAC	Histone deacetylase
HGF	Hepatocyte growth factor
HIF-1	Hypoxia-inducible factor-1
HLA-DR	Human Leukocyte Antigen DR
HMA	Herbimycin A
HO-1	Heme oxygenase-1
HSF	Heat shock transcription factor
HSP	Heat shock protein
HSP90B1	Endoplasmin
HUVEC	Human umbilical vein endothelial cell

ICAM	Intercellular adhesion molecule
IFN	Interferon
IGF	Insulin-like growth factor
IHC	Immunohistochemistry
IL	Interleukin
IL-18BP α	Interleukin-18 binding protein α
iNOS	Inducible nitric oxide synthase
IRAK	Interleukin-receptor associated kinase
ITC	Isothiocyanate
JNK	c-Jun N-terminal kinases
Keap-1	kelch-like ECH-associated protein 1
KGM	Keratinocyte growth medium
KRT	Keratin
LDH	Lactate dehydrogenase
LPS	Lipopolysaccharide
LUM	Lumican
LUTS	Lower urinary tract symptoms
MAPK	Mitogen-activated protein kinase
MEK	MAPK/ERK kinases
MFAP4	Microfibril-associated glycoprotein 4
MHC	Major histocompatibility complex
MIC-1	Macrophage inhibitory cytokine 1
MMP	Matrix metalloproteinase
mRNA	Messenger ribonucleic acid
MYH11	Myosin-11
MYL6B	Myosin light chain 6B
NADE	p75 ^{NTR} -associated cell death executor
NDMA	N-nitrosodimethylamine
NDRG1	N-myc downstream regulated gene 1
NF κ B	Nuclear factor kappa-light-chain-enhancer of activated B cells
NHS	National health service
NQO1	NAD(P)H: quinine oxidoreductase 1
Nrf-2	NF-E2-related factor 2
NT	Non-targeting

OR	Oestrogen receptor
p75NTR	p75 neurotrophin receptor
PCa	Prostate cancer
PDIA4	Protein disulfide-isomerase A4
pI	Isoelectric focussing point
PI3K	Phosphatidylinositol 3-kinases
PIA	Proliferative inflammatory atrophy
PIN	Prostatic intraepithelial neoplasia
PMA	Phorbol myristate acetate
PSA	Prostate specific antigen
PTEN	Phosphatase and tensin homolog
PUFA	Polyunsaturated fatty acid
Rb	Retinoblastoma
RNA	Ribonucleic acid
ROS	Reactive oxygen species
RT-PCR	Reverse transcription polymerase chain reaction
s.e.	Standard error
SF	Sulforaphane
siRNA	Silencing ribonucleic acid
SMC	Smooth muscle cell
SOD	Superoxide dismutase
STAT3	Signal transducer and activator of transcription 3
TAGLN	Transgelin
T β R1	Human type 1 TGF β receptor
T _c	CD8 ⁺ cytotoxic T cells
TF	Serotransferrin
TGF	Transforming growth factor
T _H	CD4 ⁺ helper T cells
TLR	Toll-like receptor
TNF α	Tumour necrosis factor alpha
TPI1	Triosephosphate isomerise
TR	Thioredoxin reductase
TRA	Tumour rejection antigen
TRAIL	Tumour necrosis factor-related apoptosis-inducing ligand

TRPS1	Trichorhinophalangeal syndrome I
TUBB2C	Tubulin beta-2C chain
UK	United Kingdom
VCAM	Vascular cell adhesion molecule 1
VEGF	Vascular endothelial growth factor

Chapter One

General Introduction

Chapter 1. Introduction

1.1 The Prostate

The prostate is an exocrine gland of the male reproductive system that is located at the neck of the bladder surrounding the urethra. In the embryo, the prostate starts developing at week 11 and by week 22 is well developed, continuing to grow progressively until at birth it weighs a few grams. After birth the prostate enters a regression period followed by a period of quiescence until 12 - 14 years old and a maturation period between 14 – 18 years old. During this time it increases in weight to approximately 20g by the age of 20 at which point the weight stabilises until later life [1].

1.1.1 Structure

The prostate is surrounded by a capsule of thin fibroblastic tissue and can be divided into either zones (most common in pathology) or lobes (more often used in anatomy) (Figure 1.1). There are four histologically distinct zones: central, which accounts for approximately 25% of the gland, peripheral, which accounts for up to 70%, transition, and anterior fibro-muscular (or stroma), which together account for approximately 5% [2]. Anatomically the prostate can be divided into five lobes; anterior, posterior and median, which roughly correspond to the transitional, peripheral and central zones respectively, and two lateral lobes, which span all zones, although the lobes are not easily identifiable in the healthy prostate. The prostate is composed of 30-50 glands, 16-32 excretory ducts, stroma, blood vessels, lymphatics, and nerves, and contains a number of different cell types including basal, stem, neuroendocrine and five types of acinar cells which line the ducts; microvillar, secretory, holey, crater and bare cells [3].

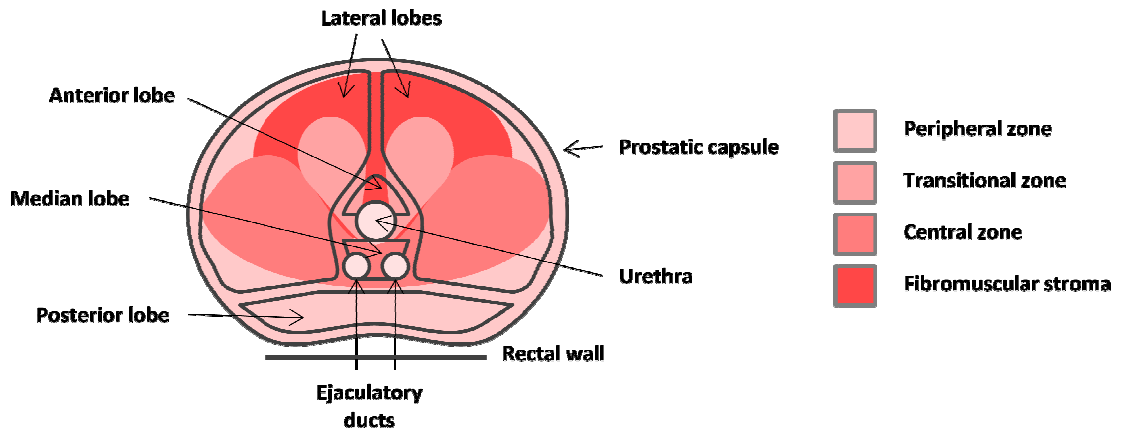


Figure 1.1. Prostate structure: zones and lobes.

Adapted from the National Cancer Institute SEER Training website, <http://training.seer.cancer.gov/>.

1.1.2 Function

The primary function of the prostate is to produce a slightly acidic (pH 6.6) milky fluid that constitutes approximately 15% of the volume of semen. This secretion contains a mixture of enzymes, lipids, metal ions and amines which facilitate fertility and are involved in coagulation [4]. The pH of the secretion is essential to reduce the acidity of the urethra increasing sperm viability, whilst albumin helps stimulate sperm motility, and zinc acts as an antibacterial agent [5]. Acting as an endocrine gland, the prostate helps convert testosterone, the main androgen synthesized by the testes, to its more potent form, dihydrotestosterone (DHT). Dihydrotestosterone is key in the development of male reproductive tissues and in secondary sexual characteristics such as the growth of body and facial hair, deepening of the voice and muscle development [6]. Further to this, due to its physical mass and musculature the prostate is also involved in the control of urination and ejaculation [3].

1.1.3 Regulation

1.1.3.1 Hormones

Key in the regulation of the prostate are steroid hormones including androgens, oestrogen and progesterone. The two main androgens found in the prostate are testosterone and DHT which control male characteristics by signalling via the androgen receptor and are essential for both the structure and function of the prostate. Androgens can alter DNA, RNA and protein synthesis and play a key role in the maintenance of cellular structures, such as the

endoplasmic reticulum and nuclei, as well as being involved in the control of stromal growth and secretory activity.

Loss of androgen stimulation, such as the result of castration, leads to a reduction in protein content of the prostate both by increasing protein degradation and by decreasing protein synthesis. Such a loss also causes metabolic changes resulting in a reduction in size of the prostate [3]. Despite their essential nature in homeostasis of the normal prostate, androgens have also been implicated as crucial in the development of both benign prostatic hyperplasia (BPH) and prostate cancer (PCa) [7]. It is interesting though that androgen levels naturally decrease with age, whilst the levels of oestrogens remain stable or increase with age, and it may well be the ratio of androgens to oestrogens that is related to disease onset.

The function of oestrogens in prostate regulation is still being investigated but research suggests a complex role. Firstly, oestrogens are able to suppress pituitary gonadotrophin secretion subsequently reducing testosterone production by the testes. They are also capable of promoting proliferation of the prostatic basal epithelial cells and altering the inflammatory state of the prostate. Oestrogens signal through both oestrogen receptors (OR)- α and $-\beta$ and it appears that whether they mediate adverse or beneficial effects depends on which receptor is activated [8].

Other hormones involved in the control of the prostate include prolactin, which works synergistically with androgens, progesterone, which is able to stimulate or maintain the weight and activity of the gland, and insulin, which is required for normal growth of the prostate [3].

1.1.3.2 Growth Factors

The prostate is also under the regulation of growth factors (GFs) including fibroblast growth factors (FGFs), insulin-like growth factor 1 (IGF-1), epidermal growth factor (EGF), and transforming growth factor-beta (TGF β) [3].

There are nine different FGF genes but it is FGF7 followed by FGF2 (or bFGF) and FGF1 (aFGF) that are the main FGFs expressed in the prostate. Fibroblast growth factors are produced by the stromal cells in response to androgen stimulation and their receptors are expressed by both epithelial cells, which express FGFR-3 IIIc isoform and FGFR-2 IIIc which bind FGF2 and

FGF7, and stromal cells, which express FGFR-1 IIIc and FGFR-2 IIIc which bind FGF1 and FGF2. They are involved in the growth of both epithelial and stromal cells and can stimulate angiogenesis.

Insulin-like growth factor 1 promotes the transition of cells from G1 to S phase of the cell cycle having a mitogenic effect and both IGF-1 and the homologous IGF-2 are required for normal epithelial cells. Insulin-like growth factor 2 is produced by fibroblast cells in the prostate but it is unknown which cells produce IGF-1. Prostatic epithelium produces EGF, which is mitogenic to epithelial cells, in response to androgens and is also found in prostatic secretion suggesting it may also have a post-ejaculatory role. Transforming growth factor-beta suppresses epithelial cell growth but increases stromal growth and also controls angiogenesis. Both TGF β protein and receptor expression are negatively regulated by androgens [9].

1.1.4 Inflammatory System

The prostate is one of the few organs that has contact with the outside world and therefore is regularly exposed to a range of antigens. In the healthy prostate there are very low levels of T cells, B cells & macrophages (Figure 1.2) which are found throughout the interstitium and in between the epithelial cells (ECs) [10].

The T cells can be divided into two classes with CD8⁺ cytotoxic T cells (T_c) being more prevalent than CD4⁺ helper T cells (T_H). In the healthy prostate the T_c cells are believed to prevent an autoimmune response to sperm and other prostatic antigens. Both ECs and stromal cells express toll-like receptors (TLRs) which can activate immune responses via the TLR-dependent signalling pathway as a result of exposure to microbes resulting in the induction of interleukin-1 and -15 (IL-1 and IL-15) expression. [10].

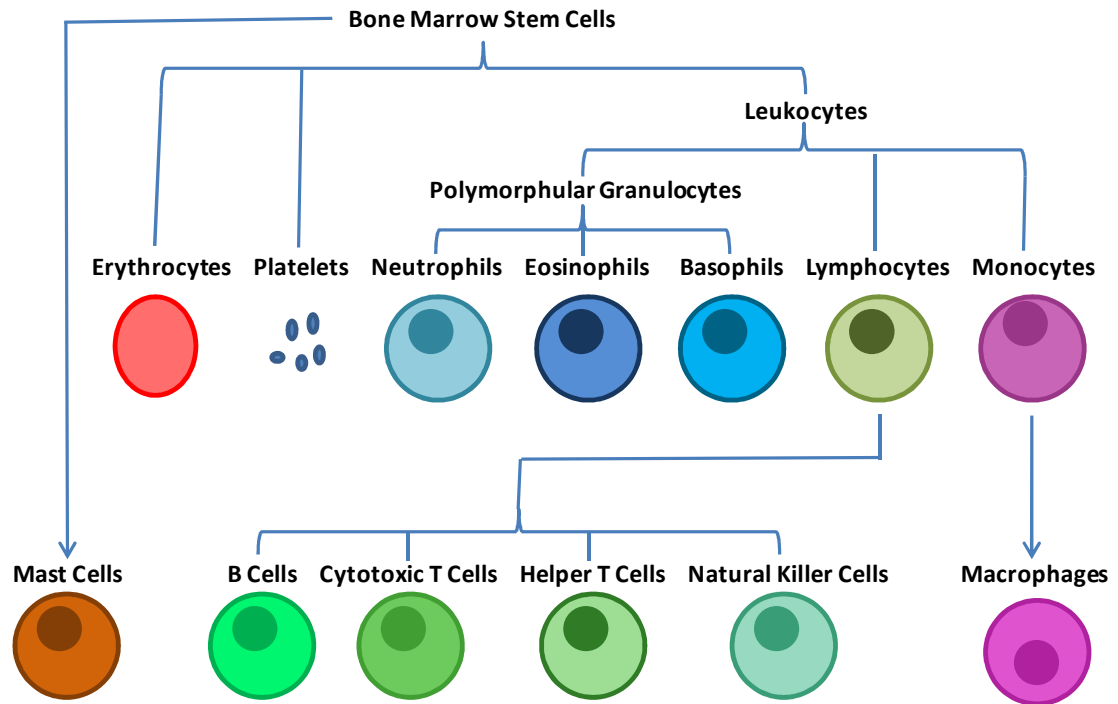


Figure 1.2. Haematopoiesis and inflammatory cell development.

Simplified diagram demonstrating the development of and relationship between blood cells and cells involved in the inflammatory process. Adapted from Vander, Sherman & Luciano's Human Physiology 9th edition [11].

1.2 Diseased Prostate

There are three main conditions that may affect the prostate; prostatitis, benign prostatic hyperplasia (BPH) and cancer (PCa). Unlike prostatitis which can occur at any age the incidence of both BPH and PCa increases with age. With an aging population the incidence of these diseases is increasing, putting a greater burden on the National Health Service (NHS). Therefore, now more than ever, it is important we understand the aetiology and development of these diseases to try and reduce their occurrence thereby easing the strain on healthcare budgets. In both BPH and PCa it has been hypothesised that inflammation may play an important role so along with a summary of how the diseases develop and progress the possible role of inflammation in both conditions is discussed.

1.2.1 Benign Prostatic Hyperplasia

Benign prostatic hyperplasia (BPH) is a highly common disease that occurs in a quarter of men over 50, a third of men over 60 and half of all men over 80 [12] although the initial development may start before the age of 30 [13]. It is a condition in which the prostate becomes enlarged due to over proliferation of cells in the tissue surrounding the urethra ultimately leading to lower urinary tract symptoms (LUTS) such as urinary frequency and urgency, nocturia, incomplete bladder emptying and weak urine stream [12]. Although BPH is not a life-threatening condition it can still have a large impact on the quality of life as patients report problems with mobility, self-care, pain and anxiety [14].

1.2.1.1 Development

In BPH, the areas of enlargement in the prostate are termed nodules and most commonly arise in the internal transition and peripheral zones (Figure 1.1) adjacent to the proximal urethra in an area that normally accounts for 2% of the healthy prostate [15]. The majority of the mass of BPH tissue is composed of nodules from the transition zone which are believed to develop first and mainly consist of epithelium.

Nodules from the peripheral zone develop later and are smaller, fewer in number and mainly consist of fibroblastic tissue. As a result, in the initial stages of BPH, prior to clinical manifestation, the transition zone becomes enlarged due to microscopic nodule formation as a result of glandular budding and branching [15]. As the condition develops the nodules further increase in size and more ducts become involved in the process so the prostate becomes much enlarged, although at this stage it is not necessarily clinically apparent.

The final stage of BPH is the development of clinical symptoms, although prostatic enlargement alone is not enough to cause this, other factors such as prostatic infarction, the response of the prostatic capsule or incidental adenocarcinomas may determine the point at which BPH becomes clinically evident [12, 15]. It is estimated that approximately 50% of pathological BPH develops into clinical BPH [16].

The cause of BPH is not clearly defined although advancing age appears to be a major factor in its development [16]. Not all patients who develop clinical BPH go on to need treatment as the condition may not be severe enough or the individual may be tolerant of the symptoms. If left to develop naturally and left untreated BPH may result in urinary tract infection, urinary retention, renal failure and bladder stones, so it is important to treat it before it progresses to this stage [16]. Current treatments include drugs, such as α_1 -AR antagonists and 5- α -reductase inhibitors, as well as surgery [12].

1.2.1.2 Inflammation

Although increasing age is associated with the development of BPH other factors such as androgen levels, in particular DHT, oestrogen levels, growth factors, and lifestyle have been implicated in the aetiology of the disease [17]. Historically the idea that inflammation may be the cause of BPH was first proposed in the first half of the 20th century although this was superseded by the embryonal reawakening theory for the majority of the century. It was only in the latter half of the century that interest shifted back to relevance of inflammation in BPH progression [10]. Since then research has identified inflammatory markers commonly found in BPH tissue leading to the hypothesis that BPH may be an immune-mediated inflammatory disease as the majority of BPH samples exhibit inflammatory infiltrates, despite a lack of infection or correlation with foreign antigens in the patient.

The type of immune response seen in BPH tissue is determined by the cytokines produced by the T_H cells. These cells can be either of the T_{H1} lineage, which control the cell-mediated immune response and are characterised by the secretion of IFN- γ and IL-2, the T_{H2} lineage, which control the humoral immune response and secrete IL-4 and IL-13, or the T_{H0} lineage which produce both responses. It is thought in the initial phase of BPH the response is T_{H1} as illustrated by the increased mRNA expression of IL-2 and IFN- γ 10- and 3-fold respectively. As BPH progresses a shift towards a T_{H0} response is seen with IFN- γ and IL-4 mRNA both increasing by 10-fold and IL-13 increasing 3-fold. A progression towards T_{H2} response is observed in fully developed BPH with IL-4 and IL-13 increasing 3- and 2-fold respectively with lower levels of IFN- γ and much reduced levels of IL-2 mRNA (Figure 1.3) [18].

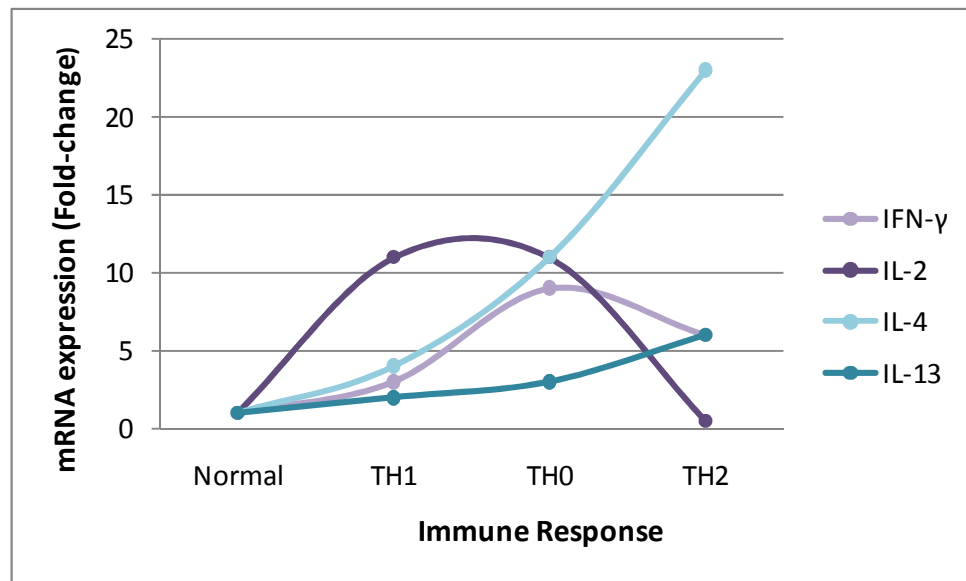


Figure 1.3. Immune response and cytokine expression in BPH progression.

As BPH progresses the immune response changes as shown by the changing cytokine expression profile of $CD4^+$ T helper cells. The cytokine expression alters from baseline expression in normal tissue to a T_H1 response at BPH initiation developing to a T_H2 response in established BPH. IFN- γ and IL-2 (purple plots) are associated with the T_H1 response whilst IL-4 and IL-13 (blue plots) are associated with T_H2 . Data taken from Steiner *et al* 2003 [18].

The inflammatory infiltrates found within BPH tissue contain approximately 70% T cells, 15% B cells and 15% macrophages as well as mast cells (Figure 1.2). T cell infiltrates naturally increase with age but in BPH the level of T cells increases 28-fold. In comparison to the healthy prostate the ratio of T_C cells to T_H cells is reversed with 55% of T cells being T_H cells, a 60-fold increase, and 28% T_C cells.

The remaining T cells found in BPH are approximately 8% $CD4^+/CD8^+$ and 10% $CD4^-/CD8^-$ T cells [18]. Increased levels of macrophages may be a result of reduced levels of macrophage inhibitory cytokine 1 (MIC-1). The inflammatory process may be initiated by *de novo* expression of MHC class II antigen human leukocyte antigen (HLA)-DR and heat shock proteins 72 and 73, up-regulation of which can be measured in 1 - 5% of glands analysed in prostates of men aged 25 and over [10].

As well as an increase in inflammatory cells there are a number of changes to the cytokines expressed in the prostate in BPH. These can be divided into two main functions; those involved in recruiting leukocytes and those involved in prostate cell growth [10].

Proliferation of normal prostate-derived stromal cells is inhibited by IL-4 and not effected by IFN- γ , IL-2 or IL-7, but BPH-derived stromal cells barely respond to IL-4 and instead proliferate in response to IFN- γ , IL-2 and IL-7. IFN- γ was also shown to increase proliferation of BPH-derived epithelial cells [19]. Interestingly there is a 3-fold increase in IFN- γ and *de novo* expression of IL-4 and IL-2 in BPH tissue [20]. Furthermore, IFN- γ causes a 2-fold increase in the expression of IL-15 by stromal cells which along with an increase in the expression of IL-15 by smooth muscle cells can cause a 100-fold increase in the growth of memory T cells and increase in recruitment of more T lymphocytes [21].

Another cytokine that is increased in BPH is IL-17 which is produced by activated T cells and some epithelial and smooth muscle cells. IL-17 stimulates the expression of pro-inflammatory molecules by epithelial, endothelial and fibroblast cells including increasing IL-6 expression by stromal cells by 9-fold and IL-8 by 26-fold [22]. Both IL-6 and IL-8 stimulate stromal growth (Figure 1.4).

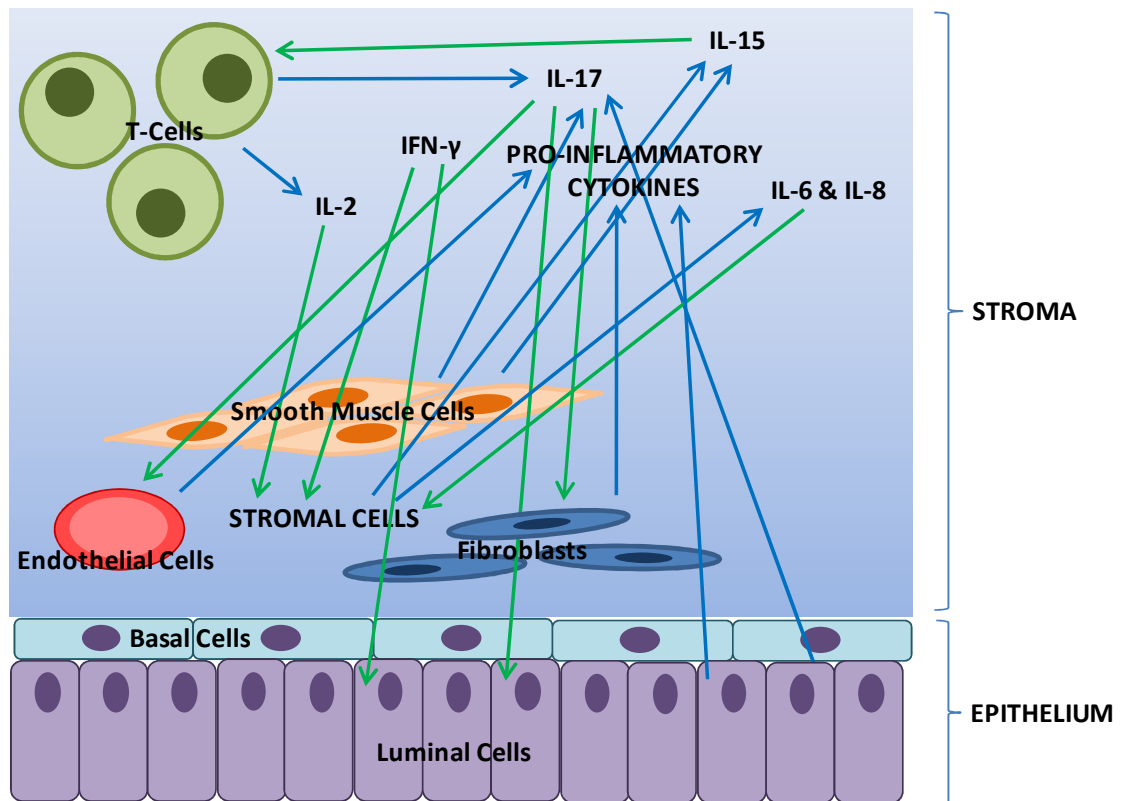


Figure 1.4. Inflammatory pathways in BPH.

Simplified drawing illustrating some of the inflammatory cytokines expressed in BPH and their relationships with cells. Cytokines can stimulate cells to modulate cytokine expression and/or promote proliferation (green arrows). Different cell types express varying inflammatory cytokines (blue arrows). Stromal cells encompasses endothelial, smooth muscle and fibroblast cells.

1.2.2 Prostate Cancer

Prostate cancer (PCa) is the fourth most common cancer in the UK after breast, lung and colorectal cancer. In 2007 there were 36,101 new cases and 10,168 deaths, accounting for 12% of all new cases of cancer and 6% of all cancer deaths. From the mid 1980s to the early 1990s there was a sharp increase in the incidence of prostate cancer in the UK which can partly be attributed to new methods of diagnosis leading to increased detection. These rates started to fall in the mid 1990s but have recently started to increase again, which has been partially attributed to a rise in the aging population.

Thankfully despite this increase in incidence the death rate is decreasing, in the 1970s only 20% survived for more than ten years past diagnosis but this has now increased to nearly 70% [23]. Although cure rates for cancers localised to the prostate are relatively high most cases are not diagnosed until a later stage when metastasis has already occurred. With current treatment, around 80% of these individuals go into remission, but within two years many of them relapse, developing a disease resistant to current treatments which is therefore incurable [24-25].

1.2.2.1 Development

Cancer is a disease in which a mutation or mutations within a cell alters its response to normal control mechanisms causing it to grow unregulated eventually leading to invasion and metastasis away from the site of origin. There are six main steps in the development of cancer: development of growth signal autonomy; unresponsiveness to growth inhibition; insensitivity to apoptotic signals; evasion of senescence; promotion of angiogenesis and the ability to invade and metastasise [26].

What makes cancer so difficult to understand and treat is that each cancer behaves differently according to the individual mutations it has accumulated. Prostate tumours often arise as a result of a pre-cursor condition, such as prostatic intraepithelial neoplasia (PIN) and are often diagnosed as a result of a patient exhibiting symptoms similar to those seen in BPH, such as problems with urination. Often a blood test will be performed to measure prostate specific antigen (PSA) as increased levels are associated with PCa but ultimately the cancer will be diagnosed by biopsy and assigned a Gleason score (Figure 1.5).

The Gleason system was developed in the 1960s – 1970s by Dr Donald F Gleason and assigns a grade to the tumour dependent on the arrangement of carcinoma cells in haematoxylin and eosin (H&E)-stained tissue samples. This grade is correlated to the progression of the disease and the likely prognosis for the patient. The lowest Gleason grade (1) is assigned when the tumour has well-defined smooth edges but as the cancer progresses and the tumour becomes less defined and stromal invasion becomes more extensive the grade increases (<5) (Figure 1.5) [27].

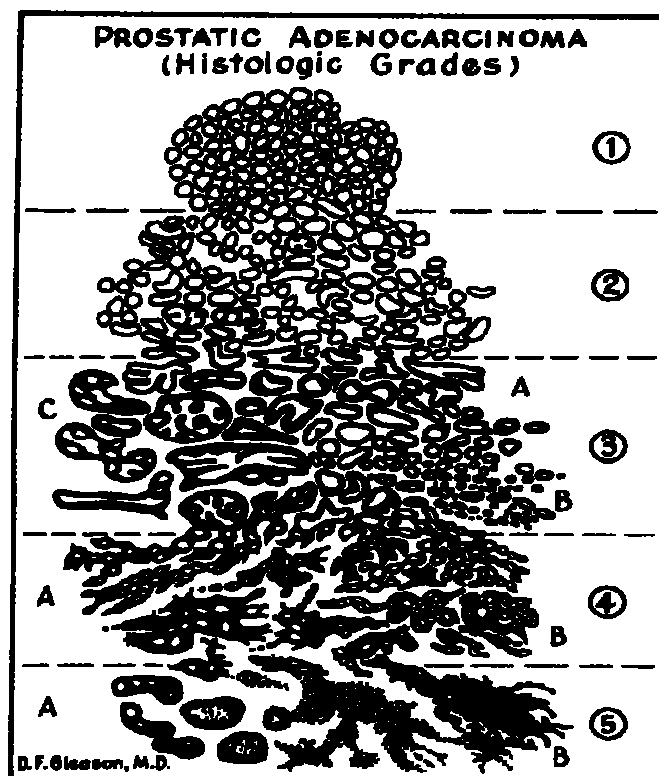


Figure 1.5. Gleason grades.

Extensively used standard drawing originally by Dr D. F. Gleason. Gleason grade assigns a value according to certain features to the two largest areas of cancer within the tissue sample. Metastasis is rarely seen in cancer with a grade of 3 but more commonly so in grades 4 and 5. The two grades are added together to produce a Gleason score. The higher the score the more advanced the cancer is: a score of 2-4 is low grade, 5-7 is intermediate and 8-10 is high grade.

One of the main treatments for PCa is androgen ablation as during the early stages the tumour is dependent on androgens for growth. This therapy is initially effective for the majority of patients however the majority of patients relapse with an aggressive form of the disease that is independent of androgenic control known as hormone-refractory PCa [28].

1.2.2.2 Inflammation

Although many factors have been suggested as possible determinants for PCa the only established risk factors are family history, increasing age, and ethnicity.

More recently it has been hypothesised that inflammation may play a role in PCa [29]. An established risk factor for many cancers, chronic inflammation has been accepted as playing a key role in the aetiology of 20% of all cancers including cancers of the stomach, liver and intestine. In normal tissue, after an inflammatory response anti-inflammatory cytokines and proteins are produced to end the inflammation but in chronic inflammation this homeostasis does not occur and the inflammation persists.

As the prostate ages inflammation naturally increases, due to infections and other factors, and it has been suggested this may be linked to the initiation of PCa by causing cellular and genomic damage, increasing cell turnover, and producing an environment conducive to tumour cell growth and angiogenesis, promoting carcinogenesis [30]. In one study in which biopsies were taken at baseline and five years from men with suspected malignancies they reported that those with inflammation at baseline had a 20% chance of developing PCa within the five years compared with a 6% chance for those who did not [31].

Injury to the prostatic epithelium can often result in proliferative inflammatory atrophy (PIA) lesions in which cells do not fully differentiate and are associated with chronic inflammation. The majority of PIA lesions arise in the peripheral zone which is where the majority of cancers originate [32] and it has been suggested that PIA can transform into prostatic intraepithelial neoplasia (PIN), a precursor of cancer (Figure 1.7) [33-34].

In PIA, PIN and PCa an over-expression of cyclooxygenase-2 (COX-2) has been reported which leads to an increase in prostaglandin expression, an event associated with prostate carcinogenesis. Prostaglandins can inhibit apoptosis and promote angiogenesis and metastasis. COX-2 expression can be controlled by a number of factors including IL-6 and NF κ B [30].

The chronic inflammation observed in the prostate is similar to that seen in BPH with regards to the inflammatory cells including lymphocytes, monocytes and macrophages. Macrophages have been linked to both tumour progression and suppression as they are involved in killing tumour cells by secreting TNF α . However TNF α , and also IL-2, can promote the expression of prostate derived factor/macrophage inhibitory cytokine (MIC-1) by monocytes, which in turn inhibits TNF α secretion reducing the effectiveness of macrophages in protecting against the tumour.

MIC-1 is a member of the TGF β superfamily and has been implicated as a link between inflammation and PCa due to the correlation between MIC-1 levels and tumour grade. Although MIC-1 is not normally detectable in the prostate, it has been found in samples from patients with no PCa suggesting that MIC-1 may be involved in the initiation rather than development of PCa. It is therefore suggested that MIC-1 is an early response to inflammation leading to the production of an environment favourable to tumour growth due to its proliferative effects [35].

Another member of the TGF β superfamily, TGF β 1, has also been implicated in PCa although it has a very complex relationship with prostate regulation. TGF β 1 is able to inhibit the growth and proliferation of non-malignant cells but conversely promotes survival and proliferation of tumour cells and is linked with the metastatic potential of the disease.

Many other alterations in cytokine levels have also been associated with prostate cancer including increased IL-1 which has been shown to promote tumour growth and is necessary for metastasis of prostate cancer cells. Increased IL-6 levels have also been correlated to metastatic PCa and it is known that this cytokine can promote proliferation and inhibit apoptosis of many malignant cell types. Furthermore, the activity of IL-6 may be linked to the androgen response status of the cell.

IL-17, a very potent pro-inflammatory cytokine, is involved in angiogenesis and can promote tumour cell growth as well as stimulating the secretion of TNF α and IL-1. It has also been found to be increased in many PCa samples and can further stimulate IL-6 and IL-8 expression. IL-17 may therefore be able to act indirectly by altering the secretion of other proinflammatory cytokines implicated in carcinogenesis, and also directly by promoting angiogenesis and increasing tumour cell growth.

IL-8 is able to promote tumour cell growth and may also assist in angiogenesis and metastasis by increasing the secretion of matrix metalloproteinases (MMPs), including MMP-9, that break down the ECM; elevated levels of IL-8 and MMP-9 have been found to correlate to PCa metastasis.

Increased TNF- α is also correlated with disease progression and decreased survival in PCa patients and has been found to stimulate MMP-9 expression [36]. Different expression patterns of cytokines have been linked to cancer progression. Hepatocyte growth factor (HGF) and IL-18 binding protein a (IL-18BP α) are increased in patients with extensive PCa. IL-17, glucocorticoid-induced tumour necrosis factor receptor (GITR), intercellular adhesion molecule 1 (ICAM-1) and IL-18BP α are elevated in PCa specimens with neutrophilic inflammation into glands; whilst IL-18BP α , IL-17, GITR and ICAM-1 are higher in samples with lymphocytic inflammation in the stroma [37]. All these studies are suggestive of a link between PCa and inflammation but do not definitively show that inflammation is essential for PCa initiation (Figure 1.6).

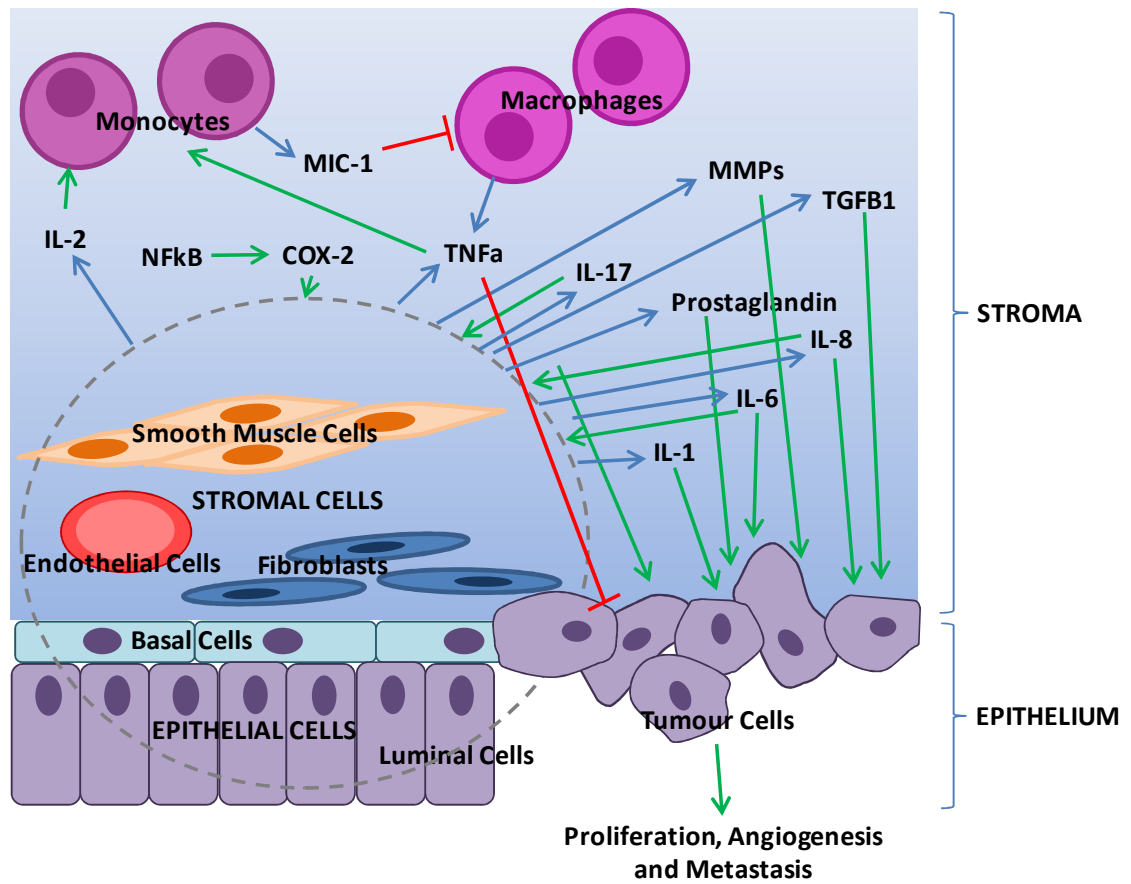


Figure 1.6. Inflammatory pathways in PCa.

Simplified drawing illustrating some of the inflammatory cytokines expressed in PCa and their relationships with cells. Cytokines and other molecules can stimulate cells to modulate cytokine expression and/or promote proliferation, angiogenesis and metastasis (green arrows) whilst others can inhibit these processes (red arrows). Different cell types express varying inflammatory molecules (blue arrows). The area within the grey dashed line represents all the cell types present within the tissue, all of which can secrete cytokines and other molecules.

1.2.3 Benign Prostatic Hyperplasia and Prostate Cancer

The relationship between BPH and PCa (Figure 1.7) has been investigated on a number of separate occasions. The first investigations were conducted over 30 years ago in two separate studies which resulted in opposing conclusions- one suggesting a link between the two [38], the other indicating no increase in risk of PCa as a result of BPH [39]. More recently a further study also concluded that the presence of BPH does not increase the risk of PCa [40], and no epidemiological evidence has successfully demonstrated a role for BPH in the aetiology of PCa.

Although both diseases are associated with increasing age, epidemiological evidence suggests that BPH develops earlier than PCa. Anatomical evidence highlights that BPH nodules almost exclusively arise in the transitional zone in comparison with PCa where two thirds originate in the peripheral zone, a quarter in the transition zone and the rest in the central zone [41].

Research into the aetiology of both diseases has demonstrated that androgens and oestrogens are crucial to the development of both diseases although this may just highlight the importance of steroid hormones in the prostate rather than suggest a link between BPH and PCa.

With the knowledge that the majority of BPH specimens contain inflammatory infiltrates and the growing body of evidence to suggest a role of inflammation in PCa it could be that this may be a link. Comparison of inflammatory molecules that have been noted as altered in either BPH or PCa reveals there are a number that overlap, including the powerful pro-inflammatory IL-17 and subsequently IL-6 and IL-8 whose expression it promotes. On the other side of the coin the expression of toll-like receptors (TLRs) has been found to be different in the two diseases with TLRs 4, 5, 7 and 9 more highly expressed in BPH in contrast to TLRs 1, 2 and 3 in PCa.

Other inflammatory markers such as CCR-3, COX-2 and CXCR-4 have also been noted to be increased in BPH as opposed to PCa where Rantes, IL-8, MMP-2 and -9, and CCR-5 are found at higher levels [42]. Interestingly in samples taken from the normal peripheral and transition zones of PCa patients MIC-1 was found to be higher in the peripheral zone, the site of origin of most tumours, compared to the transition zone, where the majority of BPH arises [35].

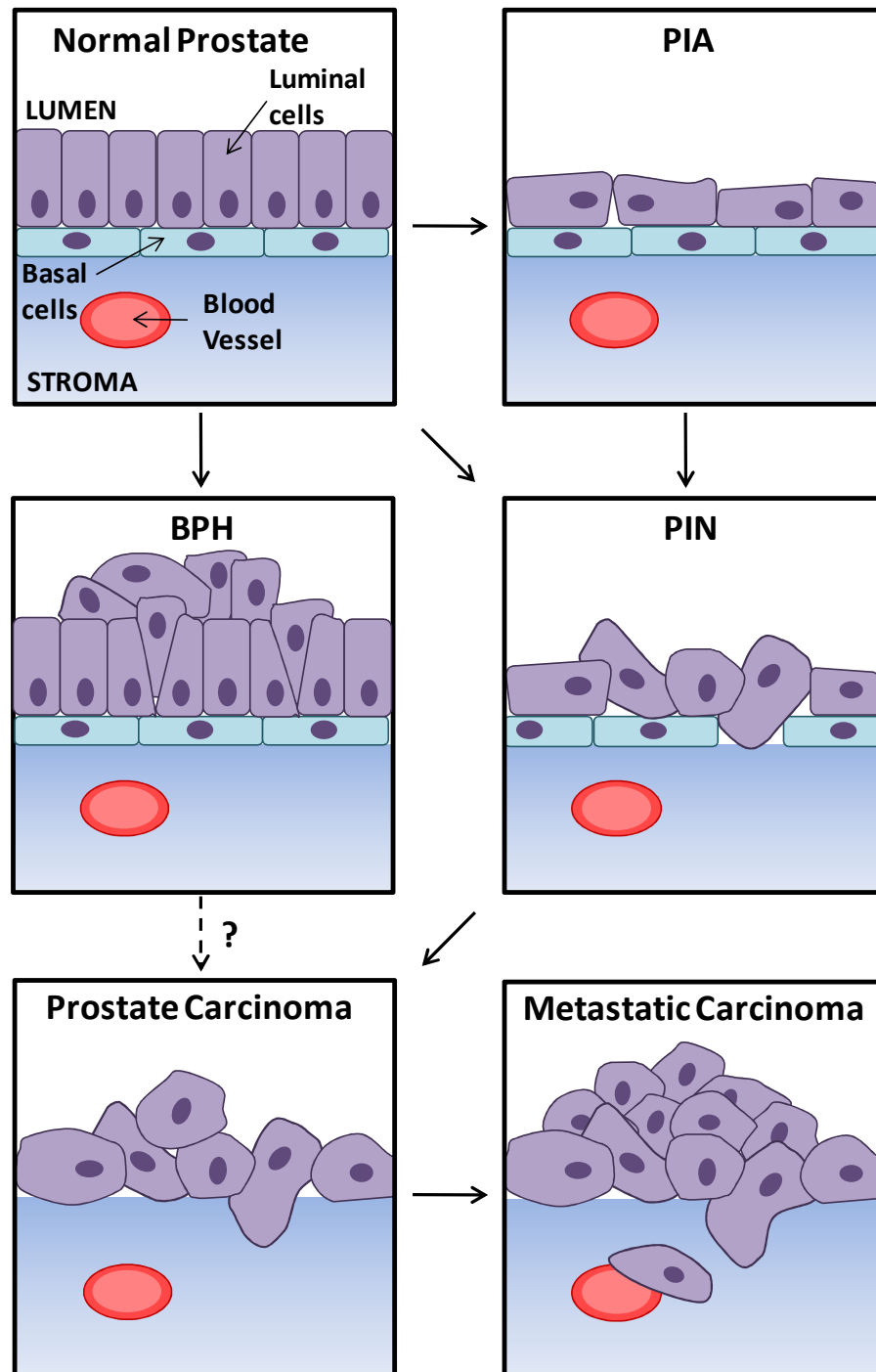


Figure 1.7. Prostatic disease progression.

PIA = proliferative inflammatory atrophy, BPH = benign prostatic hyperplasia, PIN = prostatic intraepithelial neoplasia. Inflammation in the prostate is associated with both BPH and PIA. BPH is not considered a pre-cursor of PCa but it has been suggested there could be a link. PIA has been shown to develop into PIN, a known pre-cursor of PCa, but this is not an essential step in PIN development. Once PCa has developed, as the disease progresses metastasis can occur. Adapted from Vasto, 2008 [30].

1.3 Diet and Disease

It has long been known that what we eat can have a great influence on our health. The exact nature of the relationship between foods and human health is extremely complex and is subject to a vast amount of research [43]. In particular, the link between major diseases and diet are well researched with estimates suggesting 30% of tumours in the Western world are caused by diet alone [44]. Dietary agents are both able to increase and decrease our risk of disease and how specific foods and nutrients can alter our disease risk depend upon each individual disease. Epidemiological studies further support the idea that diet influences disease, as the prevalence of many diseases alters due to the diet consumed within a region. The evidence for the role diet can play in both BPH and PCa is reviewed.

1.3.1 Diet and Benign Prostatic Hyperplasia

A number of studies have suggested a role for diet in the aetiology of BPH although any associations are still under debate. Traditionally BPH occurrence is much higher in the western world than Asia where the typical diet is low in fat and high in fibre [45]. However in recent years the number of cases of BPH in Asia is starting to rise, an increase associated with the Westernisation of the diet including increased consumption of fats and animal proteins coupled to reduced vegetable and wholegrain intake [46].

Epidemiological studies, including case-control and prospective cohort studies, have investigated the role of diet in BPH risk. Of the studies that examined the effect of total calorie intake or BMI on BPH risk neither found an association [47-48].

Examination of the main nutrient groups shows no relationship with BPH risk for total carbohydrate [49] or sugar consumption [47] but there is conflicting evidence on the effect of protein consumption, with one study finding no effect [47], one finding an increased risk [49] and another reporting a decreased risk if a high percentage of total energy came from protein [48].

With regards to total fats, Bravi and colleagues [47] and Suzuki and colleagues [49] found no change in BPH risk but Bravi and colleagues found a reduced risk due to polyunsaturated fatty acids (PUFAs), linoleic and linolenic consumption. In contrast, Suzuki and colleagues found PUFAs increased risk which corresponded with two other studies [48, 50], both of which found

total fat consumption increased BPH risk. Bravi and colleagues also reported that starch increased risk [47] although in further analysis neither pasta, rice or potatoes had any effect but both cereals and bread increased risk [51].

Past knowledge suggests that fruit and vegetables should be beneficial which is confirmed by these studies although only one found an effect from total fruit and vegetable consumption [48]. This study further suggested that the fruits and vegetables that were most beneficial contained vitamin D and lycopene.

In a separate study Rohrmann and colleagues found no effect of total fruit and vegetable consumption [52] but instead saw an effect from vegetable consumption only, in particular naming the rutaceae, legumes and cruciferous vegetable families as most beneficial. They further suggested that β -carotene, lutein and vitamin C reduced risk, the last of which correlates with the indication that orange juice [52] and citrus fruits [51] reduce risk. Bravi and colleagues [51] also suggested that cooked vegetables offered more protection than raw and from the same data Galeone and colleagues suggested allium vegetables may also be of particular benefit [53].

Further food groups implicated in increasing risk include eggs and meat whilst pulses are believed to reduce risk [48, 51]. This data suggests that diet may well influence BPH risk but the best diet to protect against BPH is still unclear.

1.3.2 Diet and Prostate Cancer

As with BPH, diet is believed to play a role in prostate cancer risk due in part to the observation that Japanese migrants living in the US and who had adopted a Western diet increased their risk of developing Western cancers, including prostate cancer, to a level comparable to that of native US citizens [54-55], an observation that cannot be attributed entirely to genetics.

Examination of total energy intake showed no correlation with PCa risk in a study in the Netherlands [56] but was found to be correlated to increased risk in other studies [57-58]. The correlation of fats appears complex with some reporting no effect [56, 59-60] and other reporting an increase in risk [57-58, 61], although Slattery and colleagues noted this increase in

risk only applied if a high fat diet was consumed as an adult compared to as an adolescent [61]. Further analysis of fat consumption suggested that animal fats [62-63] and oleic acid [56] were responsible for increased risk whereas linoleic and leniolenic acids [56] and marine fats reduce risk [64].

The other major nutrient groups, proteins and carbohydrates are less extensively studied with only one study reporting any findings which was that there was no correlation with PCa risk [59, 65]. Hsing and Chokkalingam reported no correlation between meat consumption and PCa risk [66] but Schuurman and colleagues suggested this was true for fresh meat but that cured meat increased risk [65]. It has further been reported that red meat is associated with higher risk [58]. Augustsson and colleagues reported that fish reduced risk significantly [64] but others have found no effect [65].

Dairy products have been reported both as having no correlation [66-67] and as increasing risk [68] although Schuurman and colleagues reported milk had a detrimental effect on prostate health whereas eggs and cheese had no effect [65]. Dairy products are the main source of calcium in the diet and this has been correlated with increased risk by many studies [57, 67-69] although just as many found no relationship [59, 62, 65].

The major body of research with regards to PCa and diet surrounds fruit and vegetables and their associated phytochemicals. Total fruit [70] and vegetable consumption was found to have no effect in one study [66] but they are often implicated in reducing risk [69, 71], especially vegetables [70] and most notably those of the cruciferous family [70, 72-78]. In a number of these studies they suggested that cruciferous vegetables may offer protection at different stages of the disease, including during initiation [74] and progression [76] of PCa, or development of an extra-prostatic tumour [77]. Tomatoes and lycopene have been linked to a reduction in PCa risk [79-81] but not all studies support this suggestion [60, 62, 70]. Likewise β -carotene and other carotenoids have also been suggested as offering protective effects [59-60, 80]. α - and γ -tocopherol, the major forms of vitamin E found in supplements, and selenium have also been observed to reduce risk [58, 82].

Further suggested to reduce risk are vitamin A [59, 83], vitamin C [58, 84], soy foods and isoflavones [85], vitamin B6, garlic, beans and peas [60].

1.3.3 Cruciferous Vegetables

As previously discussed a link between vegetable consumption and health has long been established. Furthermore, recent evidence has shown that cruciferous vegetables in particular are more strongly associated with the reduction of cancer risk than vegetable consumption in general [72, 75] and have been suggested as protective against both BPH and PCa. In particular, consumption of cruciferous vegetables has been reported to reduce the risk of PCa by 39, 40 and 32% [70, 73, 78], reduce the risk of extra-prostatic PCa by up to 40% [77], and reduce the risk of progression by 59% in men diagnosed with non-metastatic disease [76].

Crucifers or alternatively brassicas are members of the *Cruciferae* or *Brassicaceae* family that consist of some of the most commonly consumed vegetables in Asian and European diets. Members of this family include cabbage, turnips, cauliflower, watercress, rocket, mustard, Chinese cabbage and broccoli among others [86]. The *Cruciferae* family are so-called as they produce flowers which have four petals in the shape of a cross otherwise known as a 'crucifer' and the term 'brassica' is the Latin word for cabbage. They are known to contain a number of nutrients and bioactive compounds such as fibre, flavonoids, minerals, vitamins and glucosinolates (GLS), many of which are known to have chemopreventive properties.

1.3.4 Glucosinolates

It is the latter group of phytochemicals, GLS, which are highly characteristic of this group of vegetables and are responsible for their distinctive aromas and taste [87]. Glucosinolates are a group of approximately 120 sulphur-rich phytochemicals that share a common structure consisting of a β -D-thioglucose group, a sulfonated oxime group and a variable side chain, derived from one of eight amino acids (Figure 1.8a) [88]. They are not biologically active compounds but under the correct conditions and in the presence of certain enzymes they can undergo reactions to produce a number of chemically related bioactive compounds such as cyanoepithioalkanes, nitriles, indole-3-carbinol and isothiocyanates (ITC).

1.3.5 Isothiocyanates

Isothiocyanates are a group of bioactive compounds derived from GLS which are found in cruciferous vegetables. The hydrolysis of GLS to ITC occurs upon release of endogenous myrosinase, a native β -thioglucosidase, from the plant cell due to disruption of the structure caused by harvesting, processing or chewing [89]. The reaction yields glucose and a

thiohydroxamate-*O*-sulfonate as myrosinase catalyzes the hydrolysis of the glucosidic bond in the GLS. The thiohydroxamate-*O*-sulfonate is highly unstable and depending on the reaction conditions, for example the presence of co-reactors and the temperature, the side chain structure spontaneously rearranges to form a number of possible structures. If the reaction occurs at a relatively neutral pH (6-7) the most common products are stable ITC although other outcomes can occur (Figure 1.8b) [90].

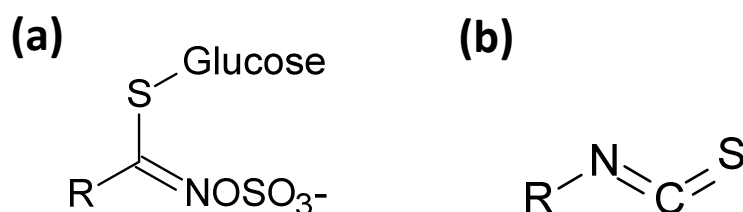


Figure 1.8. Glucosinolate and isothiocyanate structure.

R represents a variable amino acid side chain specific to the (a) glucosinolate or (b) isothiocyanate. There are approximately 120 known side chain structures.

1.4 Sulforaphane

Of the ITCs one of the most studied compound with respect to cancer prevention is sulforaphane (SF) which is derived primarily from broccoli and produced from glucoraphanin, its chemically related GLS (Figure 1. 9). Glucoraphanin is either converted to SF by the endogenous myrosinase, as previously described, or once consumed, if the myrosinase has been denatured by cooking [91], by microbial thioglucosidases in the gut [89, 92]. Sulforaphane is then absorbed and conjugated with glutathione before being metabolized via the mercapturic acid pathway prior to excretion from the body in the urine.

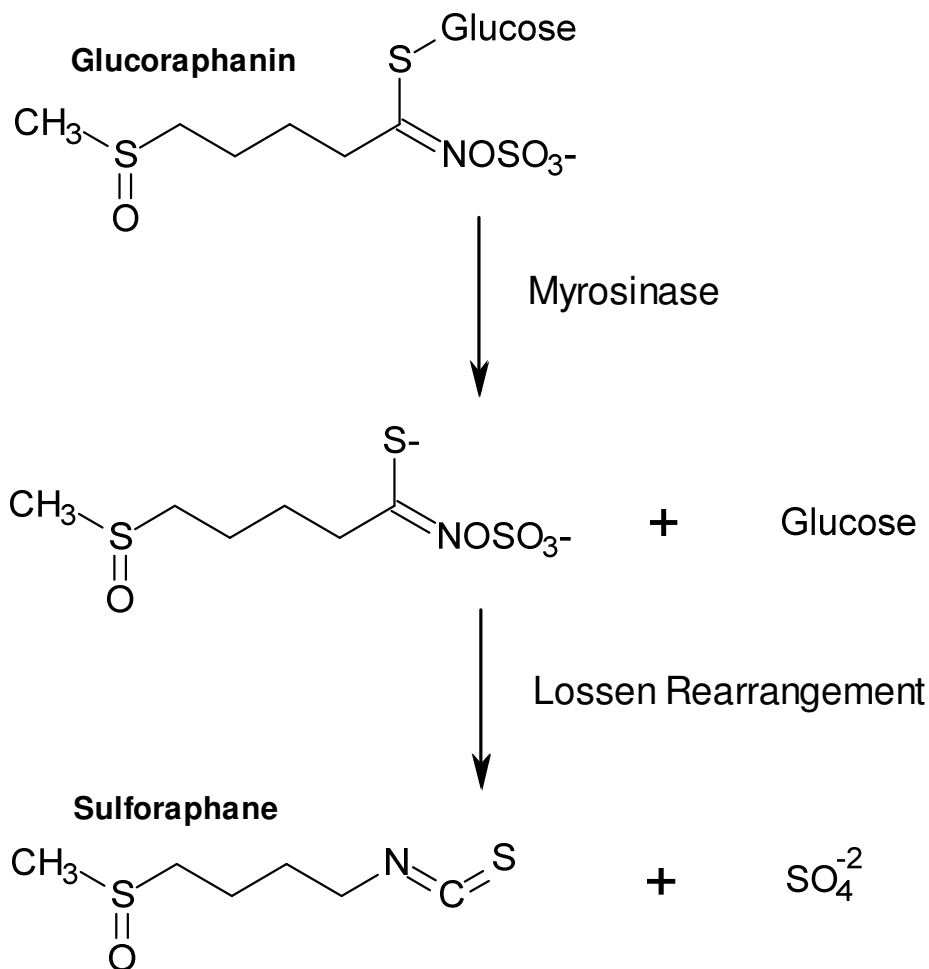


Figure 1.9. Conversion of glucoraphanin to sulforaphane.

Myrosinase cleaves the thio-glucose bond of glucoraphanin to give rise to an aglycone which is unstable and undergoes a Lossen rearrangement to produce sulforaphane.

The conjugation of SF and glutathione is catalyzed by glutathione S-transferases (GSTs) although it can occur non-enzymatically. Glutathione S-transferases are categorized into three different families: cytosolic, mitochondrial and microsomal. The cytosolic GSTs are dimers formed from approximately 17 subunits divided between 7 different classes [93]. The two members of this family that have been shown to have the greatest catalytic activity on SF and glutathione conjugation are GSTM1 and GSTP1, although even in the presence of these GSTs SF conjugation occurs much slower than that of other ITCs. Glutathione S-transferases also assist the disassociation of ITCs from glutathione, although this occurs at a significantly lower rate than the association [94].

Polymorphisms in many of the GST genes have been recorded including a null mutation in GSTM1 which results in the absence of a functional gene product. This polymorphism is thought to be so common that it can be found in 50% of the population [95].

A number of epidemiological studies conducted on Western subjects have gathered evidence that suggests GSTM1 +ve individuals gain greater cancer protection from the consumption of crucifers, in particular broccoli, than their GSTM1 -ve counterparts [75, 96-97]. One of these studies even goes as far as to suggest that consuming just one portion of broccoli a week can decrease prostate cancer risk by 50% [75]. However in contrast, studies from Asia suggest that GSTM1-ve individuals gain the most benefit although this may be due to the identity of the major crucifer being consumed, which in these studies was Chinese cabbage, not broccoli [98-99].

Despite accumulating evidence for the protective effects of broccoli it is unknown by what mechanism it occurs as after absorption SF is found in relatively low concentrations in the plasma before being quickly excreted. A study by Gasper and colleagues observed faster excretion of SF metabolites in the 6 hours immediately proceeding consumption of broccoli as well as a higher percentage of total SF excretion during the first 24 hours in GSTM1 -ve subjects compared to GSTM1 +ve individuals. The difference between the two is statistically significant as GSTM1 +ve individuals only excrete approximately 60% of SF within 24hrs of consumption compared to 100% for those who are GSTM1 -ve. Despite this, genotype appears to have no significant effect on the levels of SF conjugates found in plasma [100].

The same paper posits three possible hypotheses to explain these results which include GSTM1 +ve individuals absorbing less SF from the gut, metabolizing and excreting it via an alternative pathway, or retaining the SF in certain tissues. Although there is no experimental evidence to support any of these hypotheses there are some epidemiological observations to back up all three ideas, none of which is conclusive [100].

Although GSTM1 is the GST with the greatest catalytic activity with regards to SF conjugation there are other enzymes, such as GSTP1, that can also catalyze the reaction. Similarly these enzymes have common polymorphisms and are often deleted so it may be that whether an individual gains the greatest possible protective benefit from cruciferous vegetables may be

due to the combination of genetic polymorphisms. Or in other words just being GSTM1 +ve or -ve may not be enough to determine the benefit a person receives from cruciferous vegetables, but whether a person is +ve or -ve for a number of different enzymes may be the determinant, as other enzymes may be able to fulfill the role of a single missing enzyme but not of multiple deletions. This idea was investigated by Steinbrecher *et al* who evaluated the risk of PCa and GLS with regards to polymorphisms in a number of enzymes including GSTM1. They reported that polymorphisms in these genes modulated the risk of PCa in response to GLS intake, in particular noting that deletion of GSTM1 and GSTT1 combined had a greater protective effect than either deletion alone [101]. Therefore supporting the hypothesis it is the combination of polymorphisms that determines the benefit derived from cruciferous vegetables, so measuring the effect in terms of a single polymorphism may give misleading results. As such the conflicting results in terms of whether being GSTM1 +ve or -ve provides greater protection against PCa from GLS may be due to other polymorphisms present in the populations studied.

1.4.1 Modes of Action

The means by which SF may confer beneficial effects are well investigated and it has been demonstrated that SF has many possible mechanisms of action. The effect of SF on carcinogenesis has in particular been intensely studied, the evidence from which suggests SF is able to both help prevent initiation [102] and slow progression of the disease. The many modes by which SF acts and pathways it alters can often overlap making defining its precise role difficult to determine. Here the main mechanisms by which SF can help protect health, namely suppression of oxidative stress, regulation of phase I and II enzymes, reduction of inflammation, initiation of the heat shock response, inhibition of histone deacetylases, suppression of the cell cycle, induction of apoptosis, inhibition of angiogenesis, and reduction of migration and metastasis, are discussed (Figure 1.10 and Figure 1 .11).

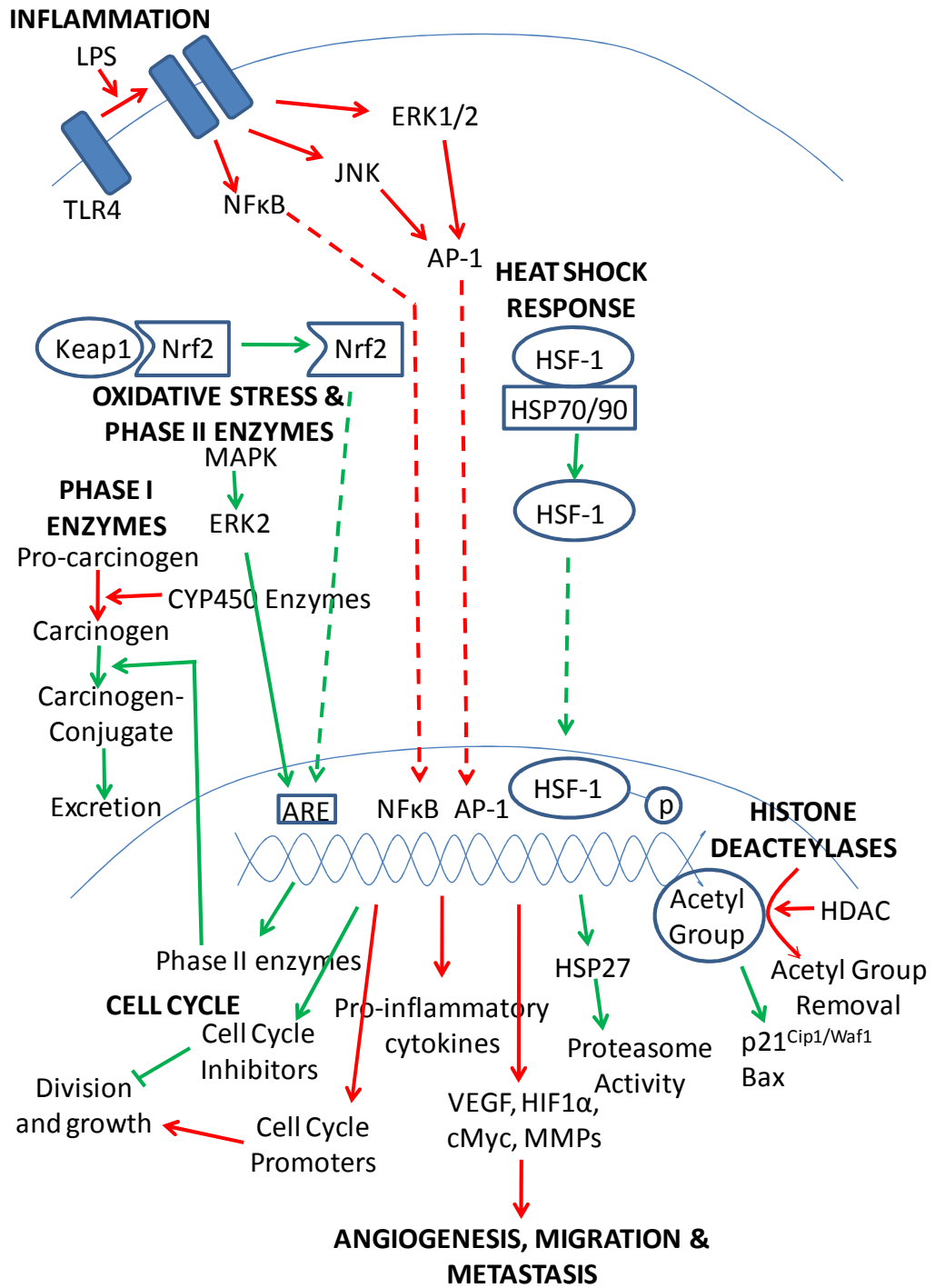


Figure 1.10. Modes of action of sulforaphane (excluding apoptosis).

Simplified drawing of the direct and indirect cytoprotective mechanisms of SF. Green and red lines represent pathways up and down-regulated respectively by SF. The dotted lines indicate translocation to the nucleus.

1.4.1.1 Oxidative Stress

Oxidative stress occurs when there is an imbalance between the production and elimination of reactive oxygen species (ROS) which can result in cellular damage. Antioxidants that act to protect the cell from ROS induced damage can either act as direct antioxidants, scavenging ROS directly, or as indirectly by initiating defensive mechanisms.

Sulforaphane acts as an indirect antioxidant regulating cellular defence mechanisms notably activating the nuclear factor (erythroid-derived)-like 2 (Nrf2) pathway. Nrf2 is a transcription factor that plays a key role in regulating the enzymes and other molecules that help protect the cell from oxidative stress. Under normal circumstances Nrf2 is sequestered in the cytoplasm by kelch-like ECH-associated protein 1 (Keap1) which targets it for degradation.

During oxidative stress Keap1 is modified causing a conformational change that leads to the release and activation of Nrf2. Nrf2 translocates to the nucleus where it binds to promoters containing the antioxidant response element (ARE) upregulating the transcription of cytoprotective enzymes. SF is able to activate this pathway by activating Nrf2 leading to an increase in downstream markers such as heme oxygenase-1 (HO-1) and NAD(P)H: quinone oxidoreductase 1 (Nqo1) protecting against oxidative damage [103-104].

1.4.1.2 Phase 1 and 2 Enzymes

Along with ROS, other molecules, including foreign chemicals from the environment and food, are capable of causing cellular damage. Foreign chemicals are metabolised by phase I cytochrome P450 (CYP450) enzymes that catalyze their conversion to a more hydrophilic form, allowing their conjugation to endogenous ligands, a process catalyzed by phase II detoxification enzymes, in order for them to be excreted from the body. In metabolising these foreign chemicals phase I enzymes convert pre-cursors of chemical carcinogens to their active state. Without sufficient phase II enzyme activity to clear them from the body cellular damage will occur which can ultimately lead to disease.

Sulforaphane inhibits the activity of phase I enzymes [105] including CYP2E1, a phase I iso-enzyme which is expressed in the liver where it metabolically activates a number of carcinogens including N-nitrosodimethylamine (NDMA), a carcinogen found in tobacco smoke,

cured meats and fish. Sulforaphane thereby reduces NDMA mutagenicity and unscheduled DNA synthesis protecting against malignancy [106].

In conjunction with this, SF stimulates transcription of phase II enzymes which help protect against carcinogenic intermediates including HO-1, NQO1, superoxide dismutase (SOD) and thioredoxin reductase (TR) [107-108]. As mentioned above, SF activates the Nrf2 pathway whose targets include a number of phase II enzymes [108-109]. In addition to this SF stimulates mitogen-activated protein kinase (MAPK) which in turn activates extracellular signal-regulated protein kinase 2 (ERK2) thereby inducing the activation of AREs promoting the expression of quinone reductase, a phase II detoxifying enzyme and ARE-linked reporter gene [110]. SF also increases the expression of the phase II enzymes GSTM1 and NQO1 [111]. By both inhibiting phase I enzymes and activating phase II enzymes SF is able to improve cellular defence against carcinogens and help prevent potential mutagenic events.

1.4.1.3 Inflammation

More recently SF has been implicated in protection against inflammation. It has been shown that in rat microglia cells SF significantly reduces lipopolysaccharide (LPS)-induced expression of proinflammatory cytokines IL-1B, IL-6 and TNF α , inhibits nitric oxide production, reduces phosphorylation of ERK1/2 and JNK, and attenuates NF κ B p65 translocation to the nucleus. Additionally in the murine microglia cell line, BV2, SF inhibits LPS-induced activator protein 1 (AP1) and NF κ B mediated reporter activity [103].

Also involved in inflammation are TLRs which recognise microorganisms and non-microbial endogenous molecules initiating an inflammatory response. SF is able to inhibit oligomerization of TLR4 thereby reducing interleukin-receptor associated kinase-1 (IRAK-1) degradation, an early marker of TLR4 activation, in turn suppressing the activation of downstream transcription factors NF κ B and IRF3, and reducing LPS-induced proinflammatory cytokine expression [112]. In endothelial cells, the activation of the Nrf2 pathway by SF, as mentioned previously, is able to reduce inflammation by inhibiting p38-VCAM-1 signalling [113]. SF can also inhibit LPS-induced expression of TNF- α , IL-1 β , COX-2 and iNOS via the Nrf-2 pathway [114].

Further evidence of pro-inflammatory cytokine inhibition by SF includes reduction of IL-8, granulocyte-macrophage colony-stimulating factor (GM-CSF) and IL-1 β in airway epithelial cells [111]. Overall all these factors combine to demonstrate how SF is capable of suppressing inflammation.

1.4.1.4 Heat Shock Response

One of the most recent hypotheses regarding cytoprotection by SF is the suggestion that SF is capable of initiating a heat shock response. The heat shock response is the induction of the expression of heat shock proteins in response to misfolded proteins which occurs as a result of stressed conditions. Of prime importance in this response is the proteasome which acts to control the normal turnover of proteins and also to remove abnormal proteins.

Sulforaphane increases proteasome activity by causing the dissociation of heat shock transcription factor 1 (HSF-1) from heat shock protein (HSP) 90 and 70, which sequester it in the cytoplasm. This results in the translocation of HSF-1 to the nucleus and subsequent hyperphosphorylation, both markers of HSF-1 activation, leading to a HSF-1-dependent increase in HSP27, a known regulator of proteasome activity [115].

Hu and colleagues also suggested a role for SF in proteasome activity as they observed that SF altered the expression of Nrf2-dependent proteasome subunit genes. In their study they further noted the Nrf2-dependent increase of a number of heat shock proteins in response to SF treatment including glucose regulated protein (GRP) 78 and HSP-1, -8 and -105 [116].

Sulforaphane indirectly alters the activation state of HSP90, a molecular chaperone whose clients include many involved in apoptosis, suggesting another method by which SF may help induce apoptosis and therefore help protect the cell [117].

1.4.1.5 Histone Deacetylases

Histone deacetylases (HDACs) are proteins that can remove acetyl groups from other proteins controlling gene expression and protein function. HDACs are often up-regulated in cancer and other diseases. It has been reported that SF can inhibit their activity thereby preventing any HDAC-induced changes [118]. Sulforaphane can inhibit HDAC activity increasing histone

acetylation leading to an increase in p21 and Bax expression which can alter cell cycle progression, induce caspase-dependent apoptosis [119] and can suppress tumour development [120].

1.4.1.6 Cell Cycle

The cell cycle is the process by which the cell proliferates and this process is divided into five phases: quiescence/senescence (G_0); gap phase where the cell increases in size (G_1); S phase when DNA replication occurs (S); gap 2 during which the cell prepares to divide (G_2); and mitosis when the cell divides (M). There are three major checkpoints that control progression to the next phase: G_1/S , G_2/M and metaphase. The progression of the cell cycle is controlled by the expression of cyclins, cyclin-dependent kinase (CDK) inhibitors and other proteins.

Sulforaphane has been shown to inhibit cell cycle progression by modulating a number of these proteins increasing the expression of cyclin A and B1, cell cycle inhibitors p21 and p27^{KIP1}, causing retinoblastoma (Rb) hyperphosphorylation and inhibiting cyclin d1 [89, 121-124]. A single study by Hu and colleagues suggested that SF increased cell cycle proteins by a Nrf-2 dependent manner including CDK4, CDK7, CDK9, CDK11A, cyclin D1, cyclin E2, and cyclin T2 [116].

1.4.1.7 Apoptosis

A major well-researched activity of sulforaphane is the induction of apoptosis, which has been recorded in a number of different cell lines. In HT29 human colon carcinoma cells, SF-induced condensation of nuclear chromatin and cell surface expression of the phospholipid phosphatidylserine, both hallmarks of apoptosis [122]. Whilst in pancreatic cancer cells, SF was observed to induce apoptosis by increasing caspase-3 activation. Furthermore, SF also reduced the phosphorylation of AKT and ERK inhibiting the PI3K/AKT and MEK/ERK pathways respectively, activating forkhead members of the class O (FOXO) transcription factors which control apoptosis [123].

Tumour necrosis factor-related apoptosis-inducing ligand (TRAIL) induces apoptosis in a number of cancer cells but not in normal cells by binding to death receptors (DR)-4 and -5. Some cells are TRAIL-resistance but can be sensitised by inhibiting AKT and NF- κ B, both

pathways that SF can inhibit. Sulforaphane increased TRAIL-induced apoptosis in PC3 prostate cancer cells and sensitised TRAIL-resistant LNCaP prostate cancer cells. Sulforaphane-induced apoptosis correlated with increased ROS production, collapse of mitochondrial membrane potential, activation of caspase-3 and -9, and increase in DR4 and DR5. Further to this, SF induced the expression of pro-apoptotic proteins Bax, Bak, Bim and Noxa, and inhibited the expression of anti-apoptotic proteins Bcl-2, Bcl-X_L and Mcl-1 [125]. SF also increased phosphorylation of JNK1/2, Elk-1 and c-Jun inducing AP-1 leading to an increase in apoptosis via decreased Bcl-2 [126]. Furthermore, SF increased intracellular free Ca²⁺, upregulating calpain, activating caspase-12 and subsequently caspase-9. Sulforaphane also induced Bax, and inhibited Bcl-2, triggering the release of cytochrome c from the mitochondria leading to the activation of caspase-9 and then caspase-3. There was also a decrease in NFκB and increase in NFκBα all of which combine to induce apoptosis in glioblastoma cells [127] (Figure 1.11).

1.4.1.8 Angiogenesis

Angiogenesis is essential to cancer progression as without the formation of new blood vessels tumour growth is limited as all cells must be within 200µm of blood vessels, the diffusion limit of oxygen [26].

Using human umbilical vein endothelial cells (HUVECs), a model of angiogenesis, SF was shown to reduce proliferation by increasing apoptosis and thereby inhibiting angiogenesis [128]. Sulforaphane also inhibits the expression of vascular endothelial growth factor (VEGF) and its receptor, and the angiogenesis-associated transcription factors hypoxia-inducible factor-1α and c-Myc as well as MMP-2, reducing cell migration thereby preventing angiogenesis [129].

1.4.1.9 Migration and Metastasis

Metastasis is an important step in the carcinogenic process as once the cancer cells travel away from the site of origin, establishing new tumours, it becomes much more difficult to treat. Inhibiting this process would keep the tumour contained making treatment easier and improving the prognosis of a large number of patients. Sulforaphane has been shown to increase the lifespan of animals with metastatic tumours by inhibiting migration and metastasis via reducing the secretion of matrix metalloproteinases (MMPs) [89, 130-131].

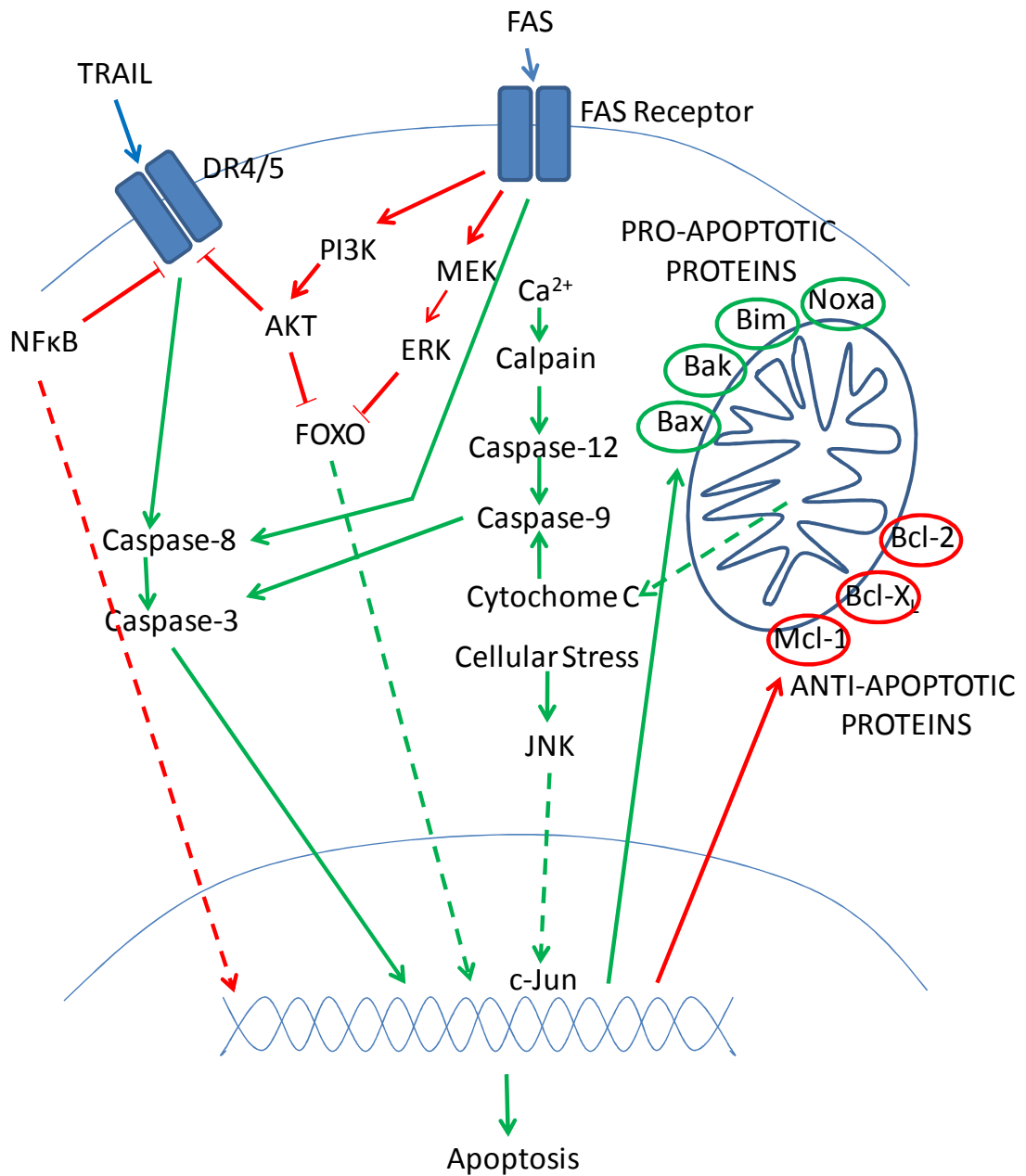


Figure 1.11. Activation of apoptosis by SF.

Simplified drawing showing the major pathways SF alters to induce apoptosis. Green and red lines represent pathways and processes promoted and inhibited respectively by SF, the blue line represents the normal mode of action of pathways shown. The dotted lines indicate translocation.

1.4.1.10 Sulforaphane in the Prostate

From the evidence above it is clear that SF is able to act via a number of mechanisms to beneficially alter cellular processes in a wide range of tissues. Due to the natural variations in tissue and cell types in the body it may be that some of the mechanisms by which SF can act and subsequent effects may be tissue or cell type specific. The effect of SF on the prostate in particular has been much researched and has suggested some prostate specific effects.

Global analysis of the effects of SF on gene expression in LNCaP prostate cancer cells revealed 25µM SF altered 2579 transcripts, 10µM SF altered 3601 transcripts and broccoli sprouts (lyophilised and reconstituted to 10µM SF) altered 1496 transcript compared to untreated cells. The 10µM SF and broccoli sprout results had the highest degree of overlap which is not surprising considering the broccoli sprouts were reconstituted to a concentration of 10µM SF. The expression patterns of 575 transcripts were found to be highly similar between the three treated datasets and of these genes the greatest association was seen with cell cycle regulation. Of the transcripts observed to be altered, the greatest increase was in genes associated with phase 2 enzymes, including NQO1 and GSTM1. Other functions identified as important included cellular assembly and organization, and cancer associated pathways. Analysis of cell cycle phase showed that SF increased the expression of many transcripts associated with G2/M suggesting that SF may act at this point of the cell cycle to induce growth arrest [132].

Androgens and the androgen receptor (AR) have been implicated as essential to prostate health and inhibition of this pathway is of interest in both prevention and treatment of disease. Evidence is accumulating to suggest that SF can inhibit AR indicating a novel method by which SF can be of particular benefit to prostate health. The AR is a known client of HSP90, itself a target of HDAC6. Histone deacetylase 6 is known to deacetylate and activate HSP90, leading to enhanced binding to client proteins inhibiting degradation of these proteins. It has been shown that in LNCaP PCa cells, SF inhibits HDAC6 enzymatic function increasing HSP90 acetylation leading to dissociation from AR and degradation of AR by the proteasome. As a result of this there is less AR bound to androgen response elements (AREs) and subsequently a reduction in AR target gene expression such as PSA [117].

A further study confirmed that SF treatment decreases AR levels and thereby reduced AR nuclear translocation but suggest that this is due to suppressed AR transcription as opposed to

increased AR degradation. In addition, they further went on to demonstrate that SF inhibited androgen-induced LNCaP cell growth suggesting that SF may be able to inhibit tumour cell growth *in vivo* [133].

Myzak and colleagues have also demonstrated the ability of SF to inhibit HDAC activity in prostate cells including BPH-1, LNCaP and PC3 cells resulting in increased histone acetylation levels. This resulted in increased p21 expression and altered expression of pro- and anti-apoptotic proteins including decreasing Bcl-2 and increasing Bax. They also demonstrated increased caspase activity and showed that SF caused cell cycle arrest at G2/M phase leading to an increase in apoptosis [119]. They then went on to show that SF specifically inhibited the growth of PC3 xenografts in mice and in these tumours observed reduced HDAC activity. The same effect was seen in mouse prostates as well as mouse monoclonal blood cells and human peripheral blood mononuclear cells [134].

Hypoxia-inducible factor-1 (HIF-1) is a transcription factor that is over-expressed in many cancers including PCa. Hypoxia-inducible factor-1 expression can be induced by hypoxia, growth factors and oncogenes and its activity is associated with tumorigenicity, angiogenesis and metastasis. Under normoxia, HIF-1 is constitutively expressed but rapidly degraded by the proteasome, however under hypoxia HIF-1 accumulates. Hypoxia-inducible factor-1 controls the transcription of VEGF, a key player in tumour angiogenesis, growth and metastasis, so it is clear to see how increased HIF-1 can positively influence tumour progression. In DU145 PCa cells, SF is able to inhibit HIF-1 expression by activating the ERK and JNK signalling pathways, which are known to regulate HIF-1, thereby reducing its synthesis. The observed reduction in HIF-1 also correlated with reduced VEGF demonstrating another mechanism by which SF can act [135].

1.5 Models to Explore Diet Interactions

In order to test hypotheses and investigate the relationships between what we consume and the effect on our bodies researchers need models in which to explore these interactions. There are three main methods available; *in vitro* models such as cell culture, the simplest model that allows the investigation of interactions with a single cell type; *ex vivo* models, for example tissue culture, which allows the exploration of relationships between different types of cells within a single tissue type; and *in vivo* models of whole organisms (human and animal studies), where the complex interactions that occur within our bodies come into play. All three systems have a role to play in understanding how our bodies work hopefully ultimately allowing us to develop new treatments and prevent diseases from occurring.

1.5.1 In Vitro

In vitro cell culture techniques have been in common laboratory use since the mid-20th century to directly investigate how cells behave. There are two main types of cell culture: primary, cells that are cultured directly from a subject and typically have a limited lifespan; and established cell lines, immortalized cells which can proliferate indefinitely due to either random mutations or deliberate modification. With particular reference to cell lines these are often cells which are representative of a cell type and are well characterised allowing researchers to use the cell type most relevant to their investigations. Working with cell lines allows experiments to be repeated many times confirming the reproducibility of results.

In comparison to other methods cell culture is by far the cheapest and the simplicity of this system makes it easier to elucidate how compounds act and cells respond. Cell culture experiments have most value in allowing researchers to investigate the exact relationship between molecules, without the confounding effects caused by natural variation, if the experiments were to be performed in a more complex subject.

Established cell lines have long been derived from prostate tissue at various stages of dysregulation, from healthy through to BPH and onto highly metastatic PCa. These cell lines can be highly useful in initially establishing and studying the effect of certain conditions but their relevance is limited as other factors such as the stroma play an important role in the function of the prostate, something cell culture models do not replicate. Established human

prostate cell lines include PNT1a, a normal epithelial prostatic cell line, and DU145, a tumorigenic cell line.

The use of cell lines has greatly improved our understanding of signalling pathways in the prostate including the discovery that SF can cause transcriptional repression of the androgen receptor and prevent its translocation to the nucleus in PCa cell lines, an important piece of information considering the crucial role AR plays in prostate development and disease [133].

1.5.2 Ex Vivo

Compared to cell culture, *ex vivo* tissue culture is less routinely performed. This may be due to the availability of tissue as there are stringent rules regarding the use of human samples and strict ethical procedures must be adhered to before commencing any work. Sourcing suitable tissue can be difficult depending on the exact nature of the experiment, and reproducibility of results is impossible as each sample is unique.

Understanding results can also be much more complex as natural variation within humans, and therefore human samples, will ultimately lead to greater variation in results. However, despite these issues, tissue culture has great experimental value providing a much more complex and more relevant experimental model than cell culture alone is able to offer. A number of previous studies have been undertaken to develop and characterise models for human prostate organ culture, in order to study the effects of various conditions and treatments on the tissue.

By establishing a method for the viable culture of prostate tissue it will allow studies to be conducted that will more precisely replicate the *in vivo* condition although there will still be limitations on the value of results obtained. Larger sample numbers will help reduce the effect of human variation and make it easier to identify patterns within results.

The relevance of this technique was demonstrated by Bronte and colleagues who, using prostate samples in culture, showed that the tumour microenvironment is immunosuppressive for T_c cells and were able to inhibit this suppression, which coupled with immunotherapy may provide a novel therapy for patients with metastatic hormone-refractory PCa [136].

1.5.3 In Vivo

A further step up from both laboratory culture methods is the use of whole organisms in either *in vivo* animal or human studies. There are of course a number of issues that need to be dealt with including the many rules and regulations, expense, recruitment of volunteers, or selection of the most appropriate animal model. Researchers must also contend with the variation in results that comes with using such a complex system, but these studies allow researchers to test hypotheses developed in less complex systems in a whole organism.

Among the most commonly used animal models are rats and mice due to practical aspects in ease of their care, their rapid maturation and quick breeding turnaround. Many strains have been developed to provide suitable systems to test hypothesis, including those with mutations leading to spontaneous tumour development. With specific regards to PCa, murine models include transgenic adenocarcinoma of the mouse prostate (TRAMP) and PTEN^{L/L};PB-Cre4 mice.

Using the TRAMP murine model Singh and colleagues observed that SF was able to inhibit prostate carcinogenesis and reduce metastasis providing further evidence for the anti-carcinogenic properties of SF [137].

Although the use of animal model can add to our understanding, the ideal model for examining the effect of dietary agents on health is human studies. Such studies allow researchers to gather data on the effect of diet on the body but due to the complexity of our bodies and the vast natural variation that exists between individuals large sample numbers are often required in order to obtain statistically significant data. Smaller targeted studies can be just as useful, as demonstrated by Traka and colleagues. Using a sample number of 21 men with high-grade PIN, they showed that broccoli consumption altered gene expression in the prostate dependent on GSTM1 genotype, resulting in changes to signalling pathways involved in inflammation and carcinogenesis [95].

In conclusion, the use of *in vitro*, *ex vivo*, and *in vivo* models, both separately or in combination with each other, is essential to facilitate and enhance our understanding of mechanisms within the human body with the long-term aim of helping to prevent and cure disease.

1.6 Thesis Aims

Previously the majority of studies to investigate the effect of SF on prostate health have been undertaken using *in vitro* models. In this study, an *ex vivo* model of BPH tissue was used to more closely replicate *in vivo* conditions in the prostate.

As inflammation has been proposed to have a crucial role in both BPH and PCa, the BPH tissue was initially used as a model of inflammation to test the hypothesis that SF can reduce inflammation. Following on from this, the effect of SF on global protein expression in BPH tissue was investigated. The four major objectives of my thesis were:

1. Develop a method for the culture of BPH tissue to replicate *in vivo* conditions using an *ex vivo* model.
2. Establish whether SF is able to modulate inflammation in the *ex vivo* model as has been previously observed in *in vitro* models.
3. Determine what effect SF has on global protein expression in BPH tissue *ex vivo*.
4. Confirm the effect of SF on a selected protein, as identified from aim 3, using a greater sample number and investigate further to determine whether this effect may have any biological significance for prostate health.

Chapter Two

Tissue Culture Method Development

Chapter 2. Tissue Culture Method Development

2.0.1. Summary

In this chapter, the development of a method for the culture of benign prostatic tissue (BPH) tissue as an *ex vivo* model which more closely replicates conditions *in vivo* than *in vitro* cell lines is described. More specifically, the effect of different culture media formulations and the addition of dihydrotestosterone (DHT) to the culture medium on the tissue were investigated by measuring prostate specific antigen (PSA) and lactate dehydrogenase (LDH) secretion. The histology of the tissue was also assessed to determine the effect of culture.

No significant difference was observed between the RPMI and KGM media with regards to PSA or LDH secretion. Prostate specific antigen levels were seen to rapidly drop when tissue was cultured for longer than 24 hours, correlating with the histological observation that large portions of epithelium died within the same time period. Thereby suggesting this method was not suitable for culturing tissue for long periods of time. The addition of DHT was not seen to have any effect on either PSA or LDH levels.

Histological evaluation showed increased cell death as culture time progressed, although some cells persisted. There was also evidence of basal cells differentiating into squamous cells in a manner similar to that seen after injury. An edge effect caused by the diathermy was also evident.

Evaluation of these results resulted in the decision to culture the tissue in KGM media without DHT supplementation for a maximum of 24 hours.

This method is used in the proceeding chapters to investigate the effect of SF on inflammatory markers using a targeted method, and global protein expression using an untargeted approach.

2.1 Introduction

The establishment of a suitable tissue culture method is essential in order to investigate the effect of sulforaphane (SF) on prostate tissue *ex vivo*, so that the model replicates conditions *in vivo* as closely as possible.

Previous work investigating the effect of SF on the prostate, have primarily used either *in vitro* cell line models, or *in vivo* models. Using an *ex vivo* model provides closer replication of *in vivo* conditions than *in vitro* models, but allows easier manipulation of the system and measurement of the response, than *in vivo* models.

Although studies have reported similar experimental protocols to establish and maintain prostate tissue culture, to date a standard method has not been established. In previous reports, human prostate tissue has been obtained from patients undergoing radical prostatectomy. The tissue is then examined to determine its health status, or to perform histological and pathological evaluation (BPH, PIN and PCa detection). Tissue was transported to the laboratory as soon as possible after surgery in either ice cold medium 199, supplemented with antibiotics and glutamine [138], or DMEM, with the addition of antibiotics [139]. The samples were then processed within 2-4 hours [138-139]. Sections were routinely taken for histological analysis, and the remaining tissue prepared for culture by the removal of necrotic tissue.

The most commonly used preparation method of prostate tissue is cutting it into 1-3mm³ pieces [136, 140]. More recently, a method using precision cut slices has been developed. The tissue is then commonly cultured in 6- or 24- well tissue culture plates, with often multiple pieces in a single well. In the study performed by Nevalainen and colleagues [138], samples were laid on lens paper on stainless steel grids within Petri dishes, whilst others placed the tissue pieces on collagen sponges in 6-well plates [136, 139].

Concerning tissue culture media, different formulations have been evaluated to date. Both Varani and colleagues [141], and Parrish and colleagues [142], reported the use of Keratinocyte Growth Medium (KGM) supplemented with epidermal growth factor, insulin, pituitary extract (PE), hydrocortisone and antibiotics. Further to this, they experimented with the addition of dihydrotestosterone (DHT), CaCl₂ and phorbol myristate acetate (PMA) [141]. Other media have been used, such as RPMI 1640 [136], medium 199 supplemented with 5%

fetal calf serum (FCS) [138], and DMEM with 10% fetal calf serum (FBS) and DHT [139]. Media were commonly changed every other day, and tissue cultured for around a week, although some studies cultured the tissue for longer in order to test the long term viability of their system [138, 141].

To measure the viability of the tissue, and to evaluate the culture method used, the majority of studies examined the histology of the tissue at various time points during the culture period. Further tests performed to determine viability include measuring prostate specific antigen (PSA), and lactate dehydrogenase (LDH) activity.

Prostate specific antigen, or kallikrein III, is a serine protease secreted by epithelial cells in the prostate, which is widely used as a cancer biomarker. A high level of PSA in the plasma is correlated with prostate carcinoma (PCa), and is used as a screening tool [143]. Prostate specific antigen secretion naturally increases with age, so the upper limit for the normal range is age-adjusted. Although widely used to detect PCa, it is common for hyperplastic conditions to be associated with increased PSA, whilst some cases of PCa do not manifest with a higher PSA level. As such this has led some to question its validity as a method for the detection of prostate disease. Regardless of this issue, secretion of PSA is a function of healthy prostate, so it is suitable for use as a method for measuring whether normal prostate homeostasis is maintained in culture. An ideal culture method would result in the constant secretion of PSA as would occur naturally in the body.

Lactate dehydrogenase (LDH) is a cytoplasmic enzyme found within cells that reduces nicotinamide adenine dinucleotide (NAD⁺) to NADH. This reaction can be utilized in the conversion of a dye, resulting in a coloured compound that can be measured spectrophotometrically. Lactate dehydrogenase is only released from the cell when there is a loss of membrane integrity. Measuring LDH in the media of cells or tissue can be used as an indicator of cell viability in culture. The viability test is necessary in order to assess the effectiveness of the culture method, and for how long it may be appropriate to culture tissue for in such conditions [144-145].

The use of the two tests in combination gives a clearer representation of the viability of the culture sample as PSA secretion is specific to luminal cells, whilst LDH is released by all cell types.

2.2 Materials & Methods

2.2.1 Tissue Collection

Tissue was obtained from Partners in Cancer Research Human Tissue Bank (Norwich, UK). Ethical consent for the project was received from the Essex 2 Research Ethics Committee (project reference 09/H0302/75). Tissue was collected by transurethral resection of the prostate (TURP) as part of routine clinical treatment for benign prostatic hyperplasia (BPH) at the Norwich and Norfolk University Hospital. Informed consent was obtained by standard hospital procedures to allow tissue to be used for research. Tissue was transported in saline solution and prepared for culture within four hours.

2.2.2 Tissue Preparation

Samples were prepared by removing any tissue that appeared necrotic, or had a visible diathermy¹ effect, using a disposable scalpel. Tissue was cut into ~2mm³ pieces and six pieces placed in each well (Figure 2.1) with each well acting as a biological replicate. Where specified technical replicates are where multiple measurements are made from a single biological replicate (one well).

2.2.3 Tissue Culture

Tissue was cultured at 37°C in Corning® 24-well plates with 1ml media per well in a humidified atmosphere with 5% CO₂. Culture media used were either RPMI 1640 supplemented with 50 mg/ml penicillin/streptomycin antibiotics (Invitrogen) and 10% (v/v) fetal calf serum (FCS), or KGM (Lonza, Switzerland) media supplemented with the KGM BulletKit containing bovine pituitary extract, human epidermal growth factor, insulin, hydrocortisone and GA-1000 (Gentamicin, Amphotericin). When required, DHT (5α-Androstan-17β-ol-3-one; Sigma-Aldrich) was dissolved in water and added to media at a final concentration of 0.8µg/ml.

¹ Surgical technique where electrically induced heat is used to cut tissue or seal blood vessels

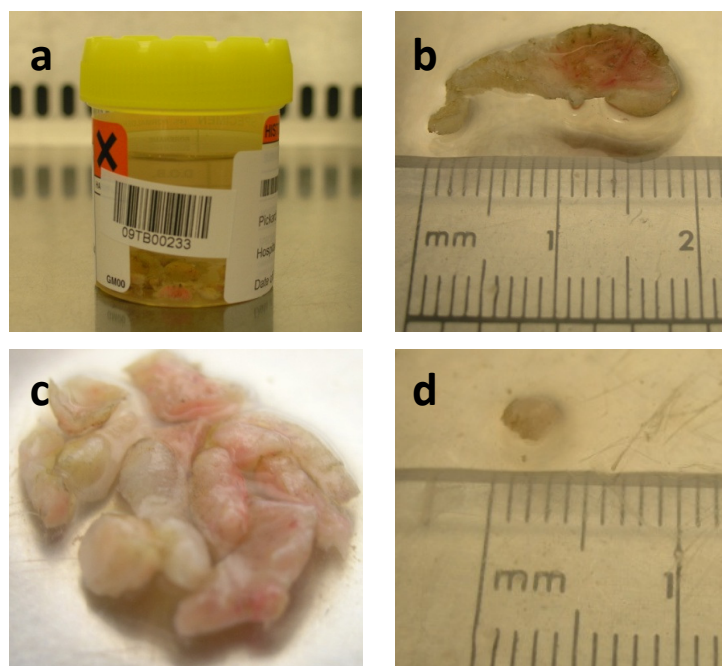


Figure 2.1. Tissue sample preparation.

(a) Tissue in saline solution as obtained from the tissue bank, (b) An unprocessed TURP chip, (c) With necrotic tissue removed, (d) $\sim 2\text{mm}^3$ piece of tissue prepared for culture.

2.2.4 Sample collection and storage

Media were collected in aliquots, immediately frozen in dry ice and stored at -80°C prior to analysis. Tissue for histological evaluation was placed in Accustain[®] Formalin Solution 10% Neutral Buffered (Sigma-Aldrich) for 24 hours and then transferred to 70% ethanol, both at 4°C . Samples were then transferred to the Cotman Centre (Norfolk & Norwich University Hospital, UK) for paraffin wax-embedding and sectioning using standard methods. Sections from each block were stained with haematoxylin and eosin (H&E).

2.2.5 LDH Assay

The LDH concentration of the tissue culture media was quantified using the *In Vitro* Toxicology Assay Kit Lactate Dehydrogenase Based (Sigma-Aldrich). The method was adapted from the provided protocol to ensure its suitability for tissue culture. Briefly, a $100\mu\text{l}$ sample of the media was incubated with $200\mu\text{l}$ LDH Assay Mixture in a 96-well plate for 30 minutes at room temperature in the dark. The reaction was terminated by adding $30\mu\text{l}$ HCl 1N to each well. Absorbance was measured at 490nm , and background absorbance measured at 690nm , using

the Benchmark Plus Microplate Spectrophotometer (Bio-Rad). Duplicate readings were performed for each sample.

2.2.6 PSA Assay

PSA concentration was measured using an enzyme-linked immunosorbent assay (ELISA) (R&D Systems). ELISA was performed as per protocol (see Figure 2.2), duplicate wells performed for all standards and samples. Antibodies (Ab) provided in kit: capture Ab, mouse anti-human PSA; detection Ab, biotinylated goat anti-human PSA. Absorbance at 450nm with wavelength correction set at 540nm was measured using the Benchmark Plus Microplate Spectrophotometer (Bio-Rad). Microplate Manager 5.2.1. (Bio-Rad) was used to reduce the data from the standards to generate a four parameter logistic (4-PL) graph, and sample concentrations calculated from the curve.

2.2.7 Histological evaluation

Histological evaluation of tissue sections with H&E staining was performed under the guidance of Professor Richard Ball, Consultant Histopathologist at the Cotman Centre (Norfolk and Norwich University Hospital, UK). Slides were assessed for any changes in architecture, cytological characteristics and viability over the time period studied. Slides were viewed using an Olympus BX60 microscope with Brightfield illumination, and representative images were taken using the attached Olympus U-TV1X camera controlled by ProgRes Capture 2.1.0. software (JENOPTIK Laser, Optik, Systeme GmbH, Germany).

2.2.8 Statistics

Statistical analysis performed in Minitab 15 (LEAD Technologies, Ltd). Student's paired t-test performed to compare treatments at each time point (see Figures 2.3 and 2.4).

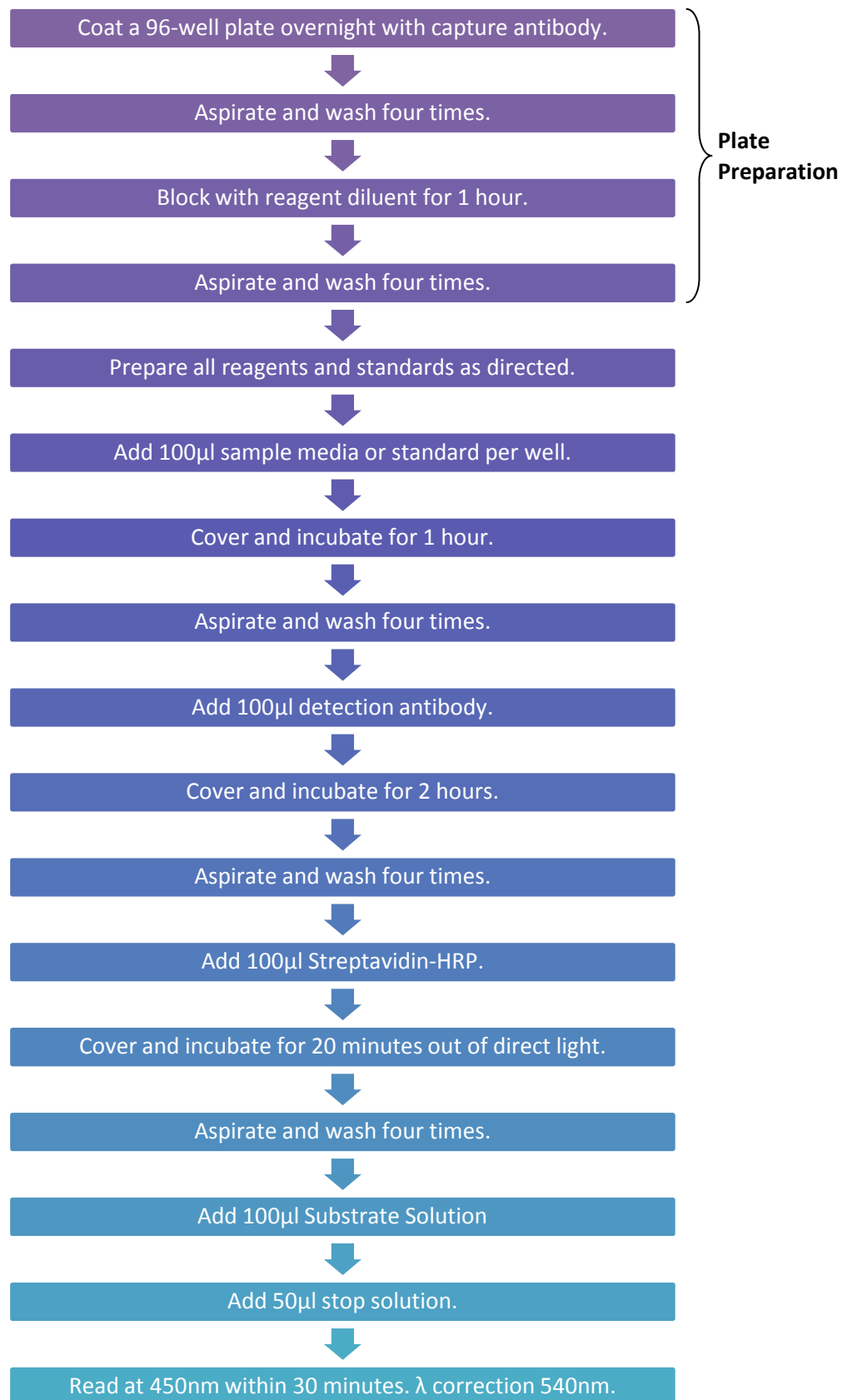


Figure 2.2. PSA Assay Protocol.

Diagram to show the ELISA method for detection of PSA in media using the Human Kallikrein 3/PSA DuoSet (R&D Systems). Adapted from the provided datasheet.

2.3 Results

2.3.1 Comparison of the effect of culture media on BPH tissue viability

Initially, a suitable culture medium to develop a method for the BPH tissue culture was evaluated. Previous studies have used a range of media [136, 138-139, 141-142] and two of the most commonly used were selected, RPMI and KGM. To determine the effect of both media on the tissue, two markers were measured: LDH, which is secreted from cells when a loss of membrane integrity occurs and represents a measure of cell viability, and PSA, which is specifically secreted by normal epithelial cells and can therefore be used to determine their health.

In both culture media, LDH secretion was at its highest on day one, with both peaking at an absorbance of 3.75, after which it started to decline. LDH secretion in the KGM media decreased steadily, until on day five the secretion was 25% of the starting value. LDH secretion in RPMI media also reduced by 75% over the five day period, but initially declined dramatically reaching this level by day three, at which point it reached a plateau. Statistical analysis showed there to be no significant difference between the LDH levels in the two media for all days, except day three (p -value = 0.024). On this day, the level of LDH in the RPMI was lower than that in KGM (Figure 2.3a).

At day one, PSA was present in both media, but rapidly reduced until on day four and five there was no detectable PSA. PSA secretion in KGM reduced at a marginally lower rate than in RPMI, and at day three was still measurable, whilst the PSA concentration in RPMI was, in all but one replicate, undetectable. The only significant difference between the two media was on day three when PSA secretion in KGM media was on average 10.8ng/ml compared to 1.7ng/ml in RPMI (p -value = 0.009) (Figure 2.3b).

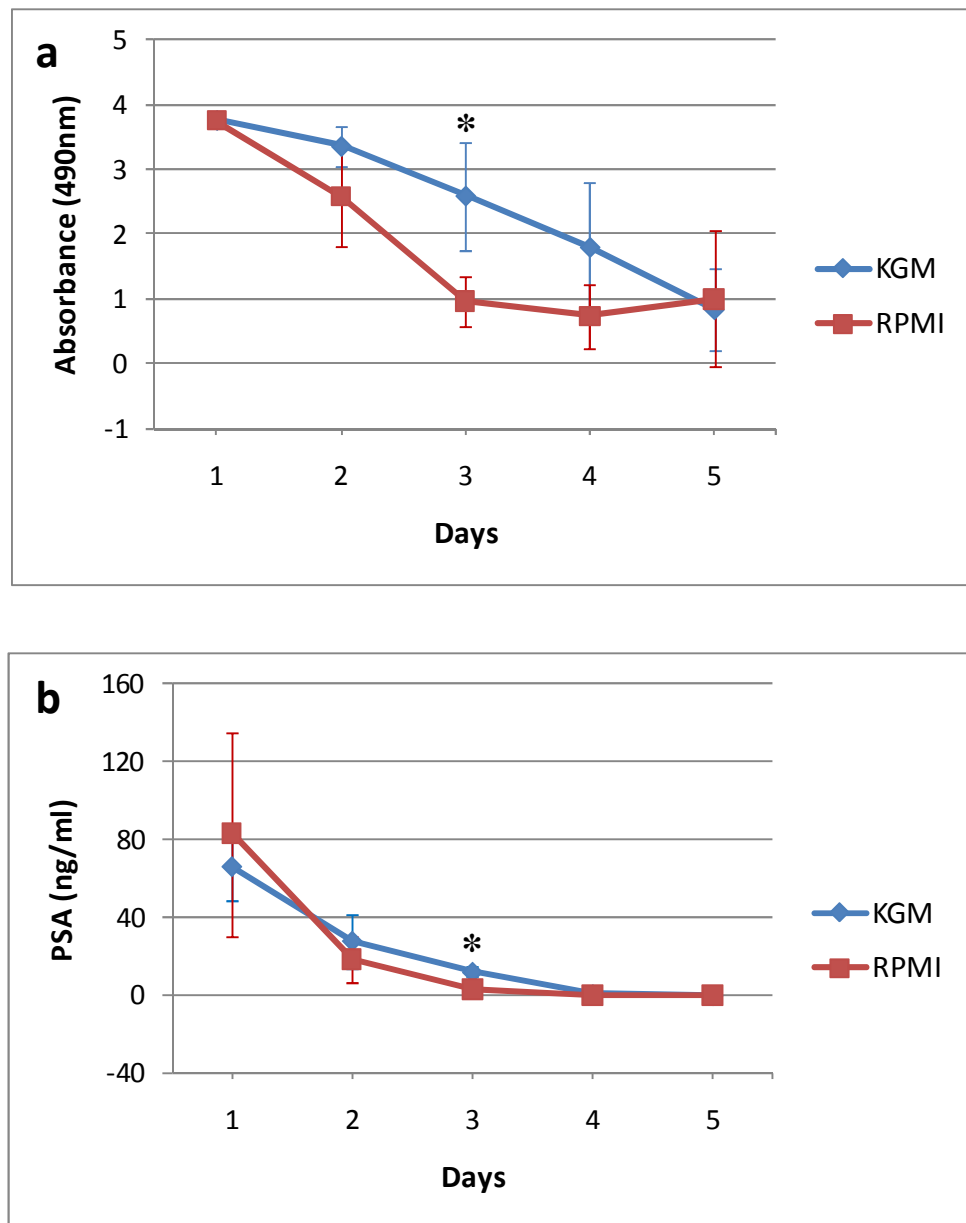


Figure 2.3. Comparison of the effect of media on BPH tissue *ex vivo*.

BPH tissue from a single patient was cultured in either KGM or RPMI media for five days at 37°C with four biological replicates of each condition. Media were collected and replaced daily. (a) LDH and (b) PSA secretion were measured. Means \pm standard deviation are plotted. There was no significant difference (p -values >0.05) between either LDH or PSA secretion in the two media except at day three ($*p$ -values ≤ 0.03 , Student's paired t -test).

2.3.2 Determining the effect of DHT on BPH tissue viability

In previous studies, addition of DHT to the culture medium had a positive effect on BPH tissue in culture [139, 141]. In this study, the effect of DHT on tissue viability was also determined.

On day one, LDH secretion both with and without DHT supplementation was at similar levels. Over the five days, both treatments were associated with a reduction in LDH secretion. However, during this time the LDH levels stayed higher only in the tissue samples cultured with DHT supplementation, although not reaching statistical significance. In the samples with no DHT supplementation, LDH secretion reduced by 70% from day one to day two, and then another 26% from day two to day five. LDH secretion in the samples with DHT supplementation reduced at a steadier rate, with daily reductions of 35, 21, 24 and 8% over the five days (Figure 2.4a).

The concentrations of PSA both with and without DHT supplementation were at comparable levels, although the DHT supplemented samples had a higher starting concentration, but not significantly so. The DHT supplemented samples had almost undetectable levels of PSA by day five, but those without DHT still secreted an average of 20ng/ml on day five (Figure 2.4b).

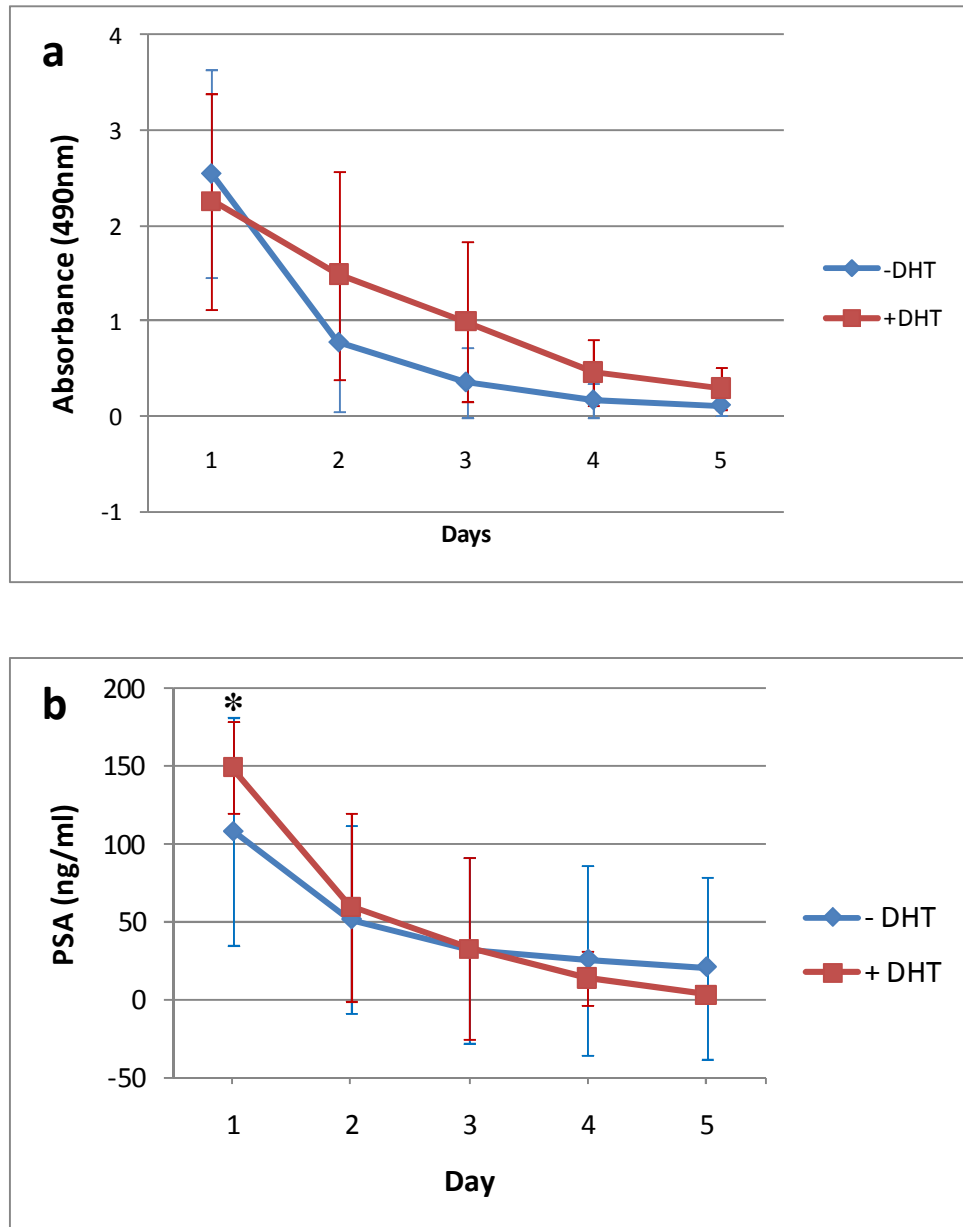


Figure 2.4. Determining the effect of DHT on BPH tissue *ex vivo*.

BPH tissue from three patients with three biological replicates for each condition was cultured with or without DHT for five days at 37°C. Media were collected and replaced daily. (a) LDH and (b) PSA secretion were measured. Means \pm standard deviation are plotted. The only significant difference (*p-value ≤ 0.05) was seen on day one when PSA secretion was significantly higher in the presence of DHT.

2.3.3 Histological structure of BPH tissue

To further study the effect of culture on the BPH tissue, pieces were fixed, wax-embedded, sectioned, and stained with H&E for histological assessment. The normal structure of prostate tissue is made up of fibro-muscular stroma punctuated with glands and ducts. The glandular epithelium consists of a base layer of basal cells upon which sit luminal (or epithelial) secretory cells (Figure 2.5).

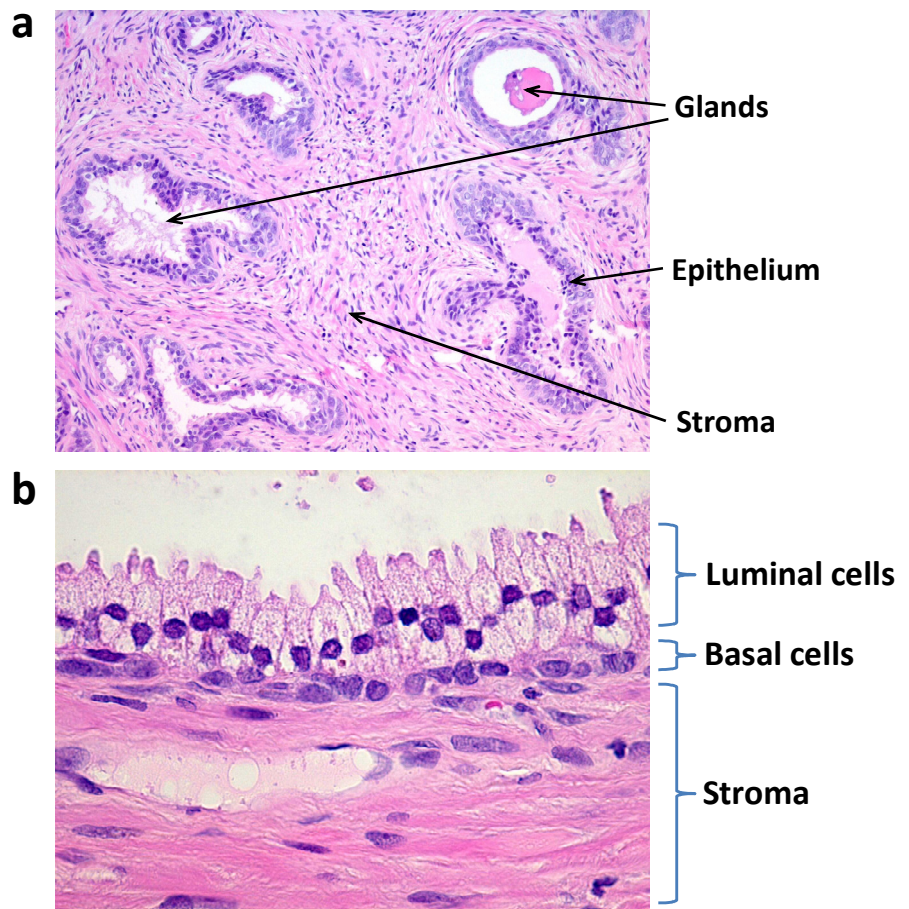


Figure 2.5. Normal prostate structure.

Images from H&E stained prostate tissue showing the normal structure of the prostate. (a) The normal structure of glands and stroma (x10 magnification), (b) the structure of the glandular epithelium (x40 magnification).

2.3.3.1 Histological assessment of tissue in culture for up to five days

BPH tissue samples cultured for up to five days were fixed and wax-embedded prior to H&E staining for histological evaluation. Unprocessed tissue was examined and good gland architecture was observed (Figure 2.6). However, the effect of diathermy due to cauterisation during the TURP procedure was clearly noted (Figure 2.6). The diathermy edge effect resulted in a band of either dead and/or distorted cells resulting in a smudgy nuclear appearance at the periphery of the section (Figure 2.6a + c).

Tissue that had been prepared for culture was fixed at time zero to act as a control for the effect of culture. Examination of this tissue showed that removal of visibly necrotic or cauterised tissue had removed tissue affected by diathermy (Figure 2.7). At time zero, the tissue looked viable.

On day one, reduced staining of nuclei was seen, indicating reduced cell number, thereby suggesting extensive cell death, although some epithelial cells were surviving.

On day two, there was further cell death, but some surviving areas with enlarged nuclei, suggesting proliferation (Figure 2.8a). Also observed, was the presence of dead cells (pink cytoplasm with very dark condensed nuclei) in the middle of a gland similar to that observed in comedocarcinoma² (Figure 2.8a), so this observation may be inherent to the tissue sample as opposed to an effect of culture.

Further cell death with some surviving areas and enlarged nuclei, as seen on day two, were also observed on day three.

On day four, in some sections of surviving epithelium, the basal cells had elongated with enlarged nuclei, suggesting they had started to differentiate into squamous cells, a process known as squamous metaplasia, with visible intercellular bridges (Figure 2.8b), making them more resilient. When cells become squamous, they form tight junctions, and upon fixing, the cells shrink, causing the appearance of 'hairs', or intercellular bridges, between the cells where the membranes are being pulled.

² A malignant intraductal neoplasm of the breast in which the central cells degenerate

By day five, squamous differentiation was more apparent, but viability had further decreased. Examination of the tissue showed random sample piece specific death, with some sections surviving better than others. It was also clear that as time progressed, tissue viability decreased, although a small percentage of cells persisted, and started to adapt to the culture conditions. There was also evidence of the presence of inflammatory cells in the stroma (Figure 2.8c).

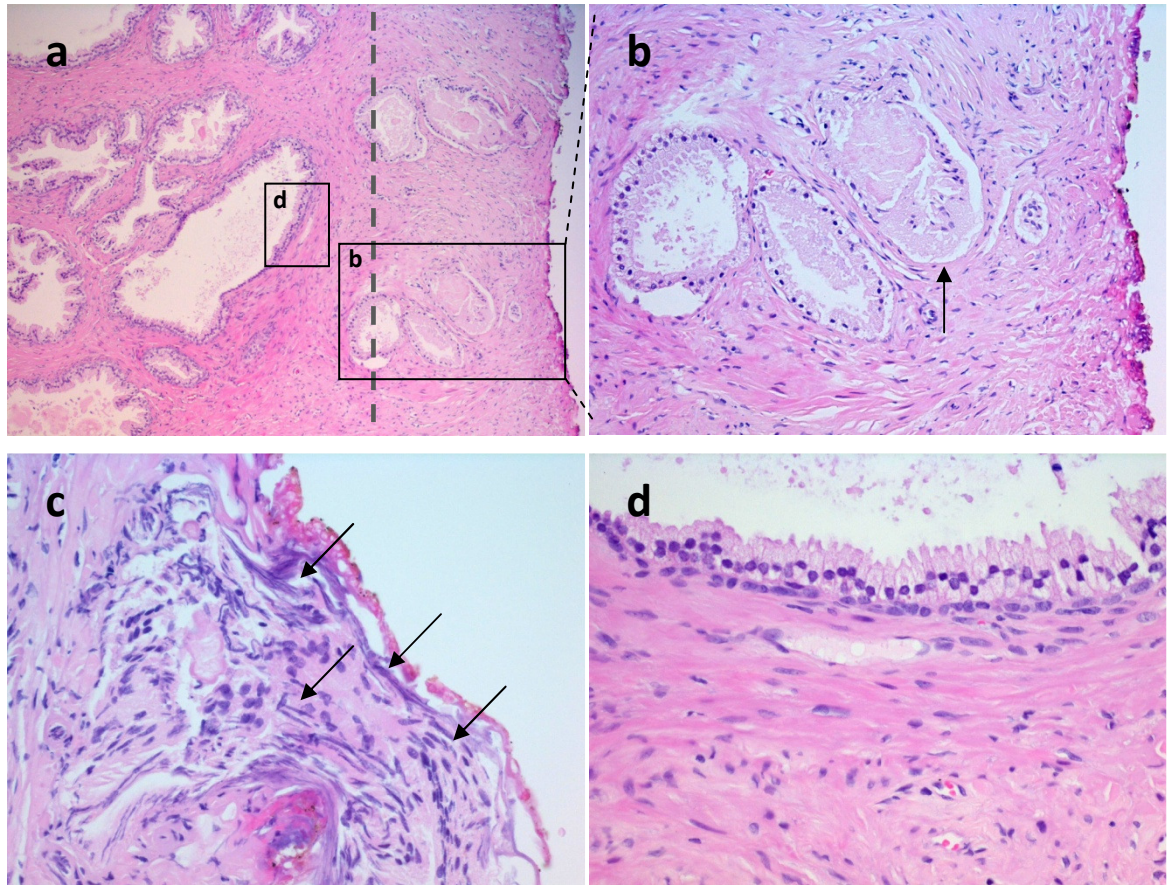


Figure 2.6. Diathermy edge effect.

BPH tissue removed by TURP is performed using cauterisation which causes a diathermy edge effect. Abnormal features were identified and examples shown here. (a) On the right side of the tissue the cauterised edge is visible, and the band of cells close to this edge are dead or dying, whilst those cells further away from the edge display normal morphology (dotted line indicates the approximate boundary of the diathermy edge effect), (b) the diathermy edge effect with loss of normal glandular epithelium (indicated by arrow; magnified section of image (a) lower right edge), (c) smudgy nuclei (examples indicated by arrows) as a result of diathermy, (d) further away from the cauterised edge normal tissue morphology is maintained (magnified centre section of image (a)). Magnification: (a) x4, (b) x10, (c) and (d) x20.

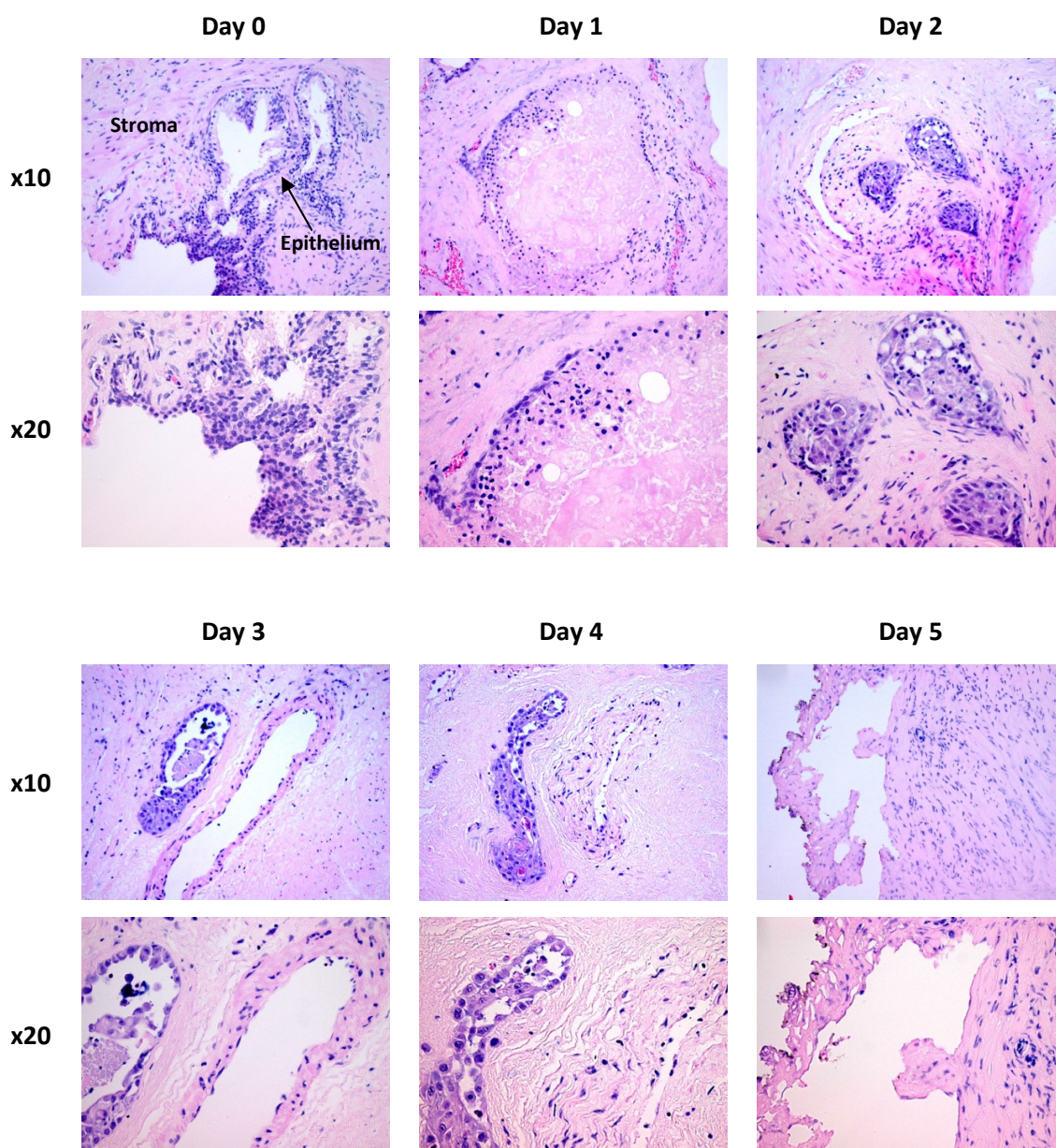


Figure 2.7. BPH tissue in culture for 5 days.

BPH tissue was cultured for up to 5 days, samples fixed and wax-embedded, sectioned, and stained with H&E. Samples assessed for histological changes. Experiment was performed with tissue from two samples and representative images from one sample shown here. x10/20 magnification as specified.

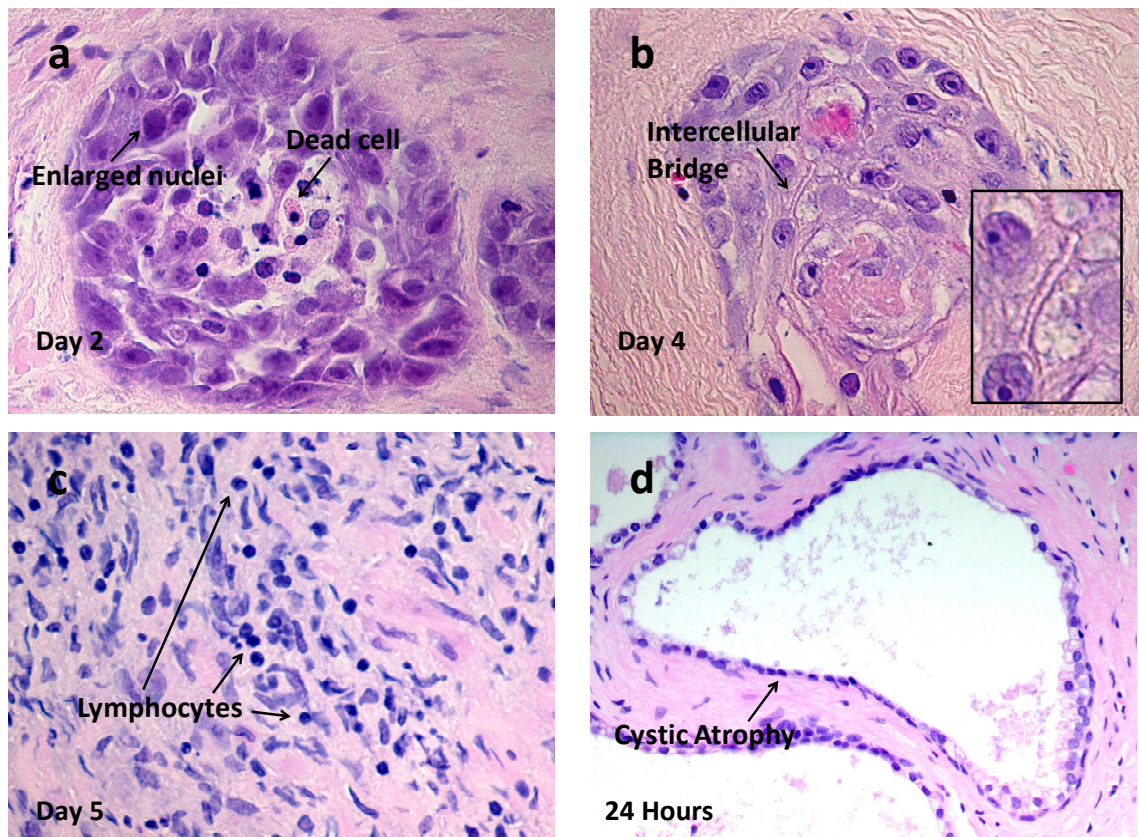


Figure 2.8. Abnormal histological features in prostate tissue.

(a) Cells with enlarged nuclei and central dead cells reminiscent of comedocarcinoma, (b) an intercellular bridge between cells in an area of squamous metaplasia (inset: close-up of the intercellular bridge), (c) lymphocytes infiltrating the stroma, (d) enlarged gland exhibiting cystic atrophy of luminal cells. All images x40 magnification.

2.3.3.2 24 Hours

Fixed and embedded tissue cultured for various times up to 24 hours was stained with H&E (Figure 2.9). Tissue at time zero was fixed to act as a control for the effect of culture.

The experiment was performed with two individual tissue samples, but upon histological examination one was diagnosed as high-grade cancer (image not shown) so the effect of culture was assessed using a single BPH sample.

At time 0, prior to culture, it was clear to see enlarged glands, a hallmark of BPH, exhibiting cystic atrophy, where the luminal cells had increased in number but decreased in size (Figure 2.8d). At 2 and 6 hours, good preservation was seen but at 9 hours the tissue was looking less viable, with the viability decreasing further at 18 hours. By 24 hours, although some sections remained viable, there was a great loss in viability.

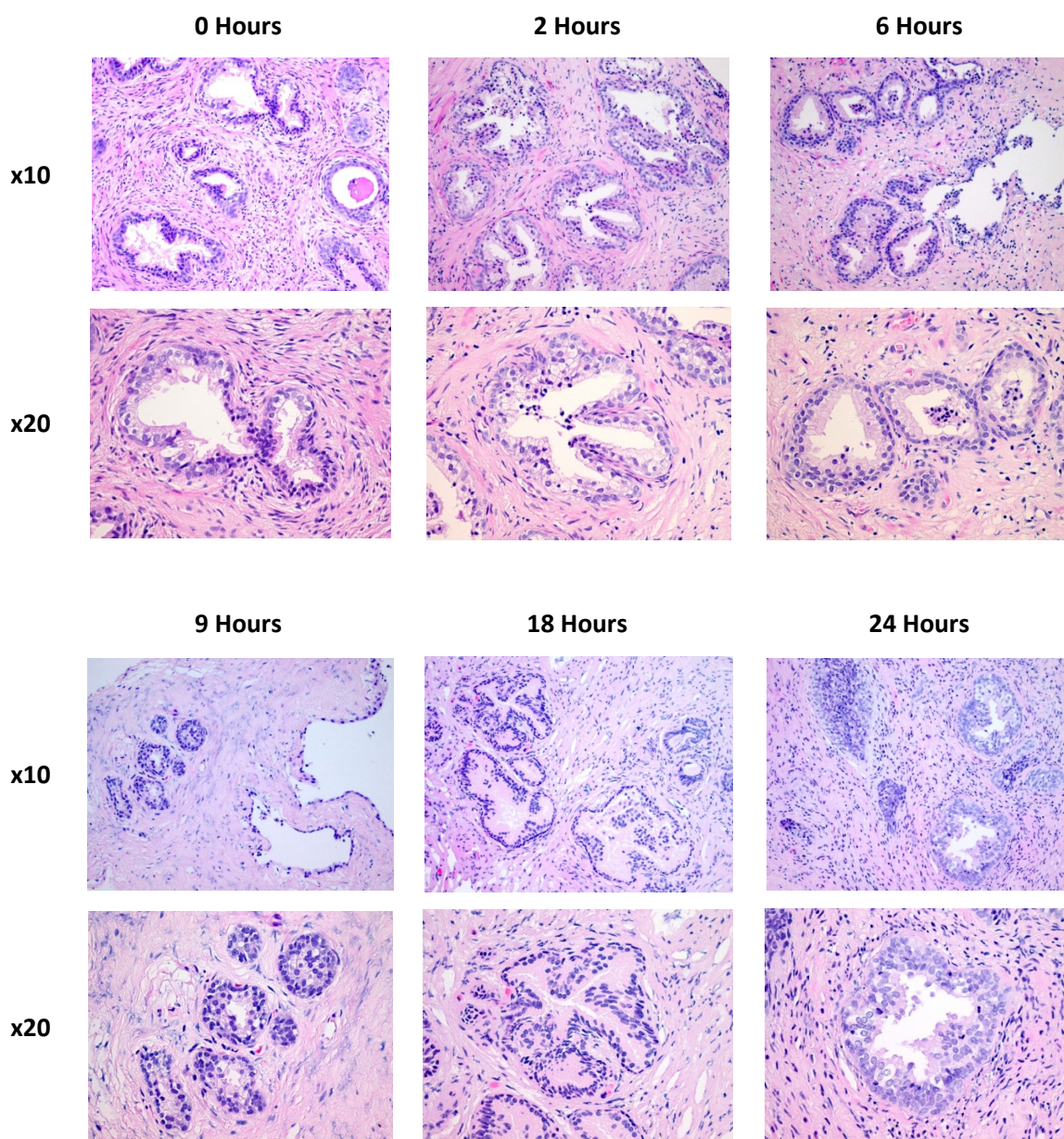


Figure 2.9. BPH tissue in culture for 24 hours.

BPH tissue was cultured for up to 24 hours, samples fixed and wax-embedded, sectioned, and stained with H&E. Samples were then assessed for histological changes. Experiment was performed with tissue from two samples and example images from one sample are shown as the other was identified as high-grade cancer upon histological examination. Images shown of x10/20 magnification.

2.4 Discussion

To investigate the effect of SF on BPH tissue, an *ex vivo* method of tissue culture has been optimised to replicate conditions *in vivo*. A review of previous methods used resulted in the decision to test two different media, and to assess the effect of DHT supplementation. To investigate the effects of the different culture conditions, both tissue viability and functionality were measured by LDH and PSA secretion, respectively. Additionally, data obtained have been confirmed by histological evaluation.

2.4.1 Tissue Viability

To determine the effect of different culture conditions on the tissue, the accumulation of LDH in the media was measured (Figure 2.3a). LDH is released from cells only when there is a loss of membrane integrity, or the cell membrane is in some way injured allowing its release. As such, LDH levels in the media can be used as a measure of cell viability.

In all samples tested, LDH secretion was highest within the first 24 hours. During this period, the high release of LDH may largely be attributed to the collection and the processing of the tissue. Removal of the tissue from the body, cauterisation of the sample and storage in saline solution, can all induce stress in the tissue triggering cell death. Furthermore, during preparation of the tissue, cutting the sample with a scalpel may physically break open a number of cells allowing the release of LDH. As a result, when the tissue is first placed in the culture dish, due to these external factors, a high number of cells may release LDH into the media immediately, leading to the high reading on day one. Another contributing factor to the high LDH concentration on day one may be cell death due to the culture process itself, as cells need time to adjust to the new environment.

During the rest of the culture period, LDH secretion steadily declined (media was collected and replenished daily so there is no cumulative effect), suggesting three possible explanations: 1) cells are adjusting to the culture medium and therefore fewer are dying; 2) cells surviving after the first day are less sensitive to the *ex vivo* conditions; and 3) previous cell death reduces the number of cells in culture, and low LDH secretion is not related to better growth conditions preventing cell death, but to the decreasing number of cells (eg. if 10% of all the cells die each day the actual number of cells within that 10% would get smaller: Day 1: 10% of 1000 = 100 die

so 900 left, Day 2: 10% of 900 = 90 die etc resulting in the appearance that 10% less cells died on day two than day one, so a reduction in LDH secretion is seen).

From histological evaluation of the tissue (Figure 2.7) it was apparent to see that there was a significant loss of viability within the first 24 hours. Over the remaining culture period, further cell death was apparent but the differences in viability between the time points reduced, correlating with LDH secretion which was detected at all time points, but at reducing concentrations as time progressed.

From examination of the tissue, it appears there are three zones or sets of cells: those that died due to diathermy (Figure 2.6), those that died within the first 24 hours, and those that are still persisting and surviving. Due to the first massive loss as a result of diathermy, it is essential to ensure all affected tissue is removed prior to culture.

In the tissue there was also evidence of karyolysis³, evidenced by nuclei fading away, which occurs mainly as a result of necrosis, not apoptosis. However, in some areas there was evidence of apoptosis, suggesting that some cells were able to carry on normal cellular processes during culture.

It must also be taken into account that there is variability within tissue samples obtained from a single patient. For example, within a single TURP sample there is both glandular and muscular stromal tissue. Although the assignment of tissue pieces to each culture well is as random as possible, it may be that the different wells have different proportions of tissue type, making it difficult to compare fairly between all days.

With regards to the effect of diathermy, this is an effect of the TURP collection procedure, and does not occur as a result of radical prostatectomy, so using tissue collected using an alternative method may eliminate this issue. However, collection of prostate tissue by radical prostatectomy is a longer procedure compared to TURP, which is very rapid. This may result in alternative issues, such as reduced viability, which may arise as a result of the different collection procedure, as each collection procedure may have its own unique inherent associated issues. Furthermore, radical prostatectomy is often carried out as treatment for

³ Complete dissolution of the chromatin matter of a dying cell

PCa, so by its very nature the tissue will behave differently due to its disease state, and therefore could not be used to answer questions regarding BPH.

2.4.2 Tissue Function

PSA is secreted from luminal cells in the prostatic epithelium, and in previous research these cells have been observed to be lost during tissue culture [138-139, 141]. Therefore, PSA was measured to assess the presence of these cells in the culture and the maintenance of normal prostate architecture.

At day one, PSA is present in all samples but then rapidly reduces to negligible levels (Figure 2.3b). The loss of PSA secretion suggests that these cells have either been lost or have stopped producing PSA. Histological evaluation showed luminal cell death, suggesting that the reduction in PSA was due to loss of these cells, and not to their compromised functional activity (Figure 2.7).

The initial death of the luminal cells correlates with observations of other studies [138-139, 141], including Nevalainen and colleagues, who also observed a considerable loss of secretory epithelium during the first few days, followed by adjustment to the culture conditions. In their study, Nevalainen and colleagues maintained the tissue culture for up to fourteen days, although seven days culture was sufficient for their experimental protocol [138]. However, in the study performed here, the tissue was cultured for a short period and significant tissue adaptation was not observed during this time. Results obtained suggest that this experimental protocol may not be suitable for use as a long-term *ex vivo* model of prostate tissue as a major cell type was rapidly lost during the culture period.

At the same time as the death of luminal cells was witnessed, there were still small sections of tissue surviving, primarily composed of basal cells [141], that had started to adapt to the environment and undergo squamous metaplasia (Figure 2.9b), also observed by others [138-139]. Squamous metaplasia refers to reversible benign changes to epithelium in which cells start to take on a more squamous appearance becoming larger and flatter. It often occurs as a result of stress to the tissue such as that cause of injury or infection [146], so it may be that this metaplasia was triggered either by injury during TURP or as a result of stress during culture. In this tissue, the luminal cells die, but there is a selective advantage for the underlying

basal cells which are tougher, and adapt to the environment by undergoing squamous metaplasia.

It has long been thought that the PCa originates from the luminal cells in the prostatic epithelium, as the disease is characterised by luminal cell expansion and loss of basal cells [147]. More recently, research has reported that different factors may be involved in this process. It has been shown that over expression of Akt and ets related gene (ERG), two oncogenes commonly upregulated in PCa, in basal and luminal cells results in the development of abnormal structures resembling PIN in the basal cells only. Furthermore, additional overexpression of AR resulted in progression to cancer [148]. It is therefore interesting that the cells from which PCa can arise, are the ones that can adapt to the culture conditions. However, it must be noted that evidence contrarily suggests PCa can arise from other cell types.

Although the role of luminal cells in the prostate is clear, producing and secreting growth factors and enzymes, the function of basal cells is less well understood. However, it has been suggested that they are essential for maintaining ductal integrity and ensuring correct differentiation of luminal cells [149]. Research has also shown that the majority of proliferation that occurs in the normal adult prostate is in the basal layer, which may contribute to these cells surviving longer than luminal cells [150-151]. This may suggest that basal cells are more tolerant and more responsive to change than any other cell type in the prostatic epithelium, explaining the reason for their ability to survive and adapt in response to the new conditions in *ex vivo* models.

2.4.3 DHT Supplementation

Dihydrotestosterone (DHT) is the more potent form of testosterone, and is essential in normal function of the prostate. Previous studies suggested it was necessary in culture to maintain normal tissue function and architecture. Following results obtained in previous studies [139, 141], the effect of the addition of DHT to the culture medium was investigated. In this study, DHT supplementation was seen to have no significant effect on either tissue viability or PSA secretion, suggesting that in the culture method used it was not able to influence the behaviour of the tissue (Figure 2.4).

Nevalainen and colleagues reported that DHT prevented metaplastic changes, such as squamous metaplasia, and maintained the luminal cells [138]. Our results suggest that DHT did not have a positive effect on the luminal cells viability or function, or viability of the tissue in general, as both PSA and LDH secretion were not significantly altered by DHT supplementation (Figure 2.4). It must be noted though, that Nevalainen and colleagues were using tissue collected by radical prostatectomy, which may behave differently in culture.

Nevalainen and colleagues also noted an increase in immunohistochemical staining for PSA in the tissue cultured with DHT, but we found no difference in PSA secretion between tissue cultured with or without DHT. Varani and colleagues suggested that without the addition of DHT squamous differentiation was more apparent [141], and in another study DHT was found to maintain the luminal cell layer [139].

Histological examination of DHT treated tissue was not performed in our study, but from our data it is clear that the DHT supplementation had no effect on PSA or LDH secretion in the culture media. Histological examination of these samples may have been beneficial, as it would allow us to confirm whether DHT offered any protective effect on the architecture of the tissue. However, the significant reduction of PSA over time observed in the samples supplemented with DHT, was in line with that observed in tissue minus DHT. Thus suggesting that in this study DHT had no protective effect on luminal cell functionality as has been reported by others [138-140]. Furthermore, as no effect was seen on LDH concentration with DHT, this suggests that, in this study, DHT did not have a positive effect on the viability of the tissue in culture.

2.4.4 Conclusions

Considering data obtained from culturing the prostate tissue with either KGM or RPMI medium, supplemented or not with DHT, it was decided to use KGM medium. KGM medium was selected as our method presented some similarities with the study carried out by Varani and colleagues in which they successfully cultured tissue in this medium [140]. As DHT supplementation showed no significant effect it appears unnecessary to include it, and all further experiments were performed without DHT. Furthermore, it is obvious that the tissue rapidly loses viability, and the majority of epithelial cells are lost after 24 hours. For this

reason, any results obtained after 24 hours culture will not be considered to be a realistic comparison for the behaviour of BPH *in vivo*.

The method developed here will be implemented in the next two chapters to investigate the effect of SF on protein expression. Two approaches will be used: a targeted method to measure inflammatory cytokines, and a non-targeted approach to assess global protein expression.

Chapter Three

Benign Prostatic Hyperplasia & Inflammation

Chapter 3. Benign Prostatic Hyperplasia & Inflammation

3.0.1 Summary

Following successful determination of *ex vivo* culture conditions for prostate tissue, the effect of SF on inflammatory markers was investigated. The majority of benign prostatic hyperplasia (BPH) specimens contain inflammatory infiltrates, and the levels of a number of pro- and anti-inflammatory cytokines have been noted as altered in BPH compared to normal prostate tissue. Previous work has suggested a protective role for sulforaphane (SF) in the prostate, whilst recent evidence has suggested that SF can reduce inflammation. The use of the *ex vivo* model will replicate more closely the *in vivo* environment than the use of a cell line, but still allows targeted treatment with SF, and direct measurement of the response.

This chapter reports the concentration of selected inflammatory cytokines secreted from BPH tissue *ex vivo*, and the effect of SF on these levels. Cytokines IL-4, IL-6, IL-8, IL-17, IFN- γ and FGF-2 were all measured by ELISA, but IL-4, IL-17 and IFN- γ were not detected. IL-6 and IL-8 were shown to be secreted at similar levels, but FGF-2 was four-fold lower. 25 μ M SF significantly reduced both basal levels of IL-6 and IL-8 secretion, but had no effect on FGF-2. A dose-dependent effect of SF on IL-6 secretion was observed, with a concentration as low as 10 μ M having a significant effect.

These results support the hypothesis that SF has anti-inflammatory properties, and suggest that SF may be beneficial to those suffering from BPH by reducing inflammation in the prostate.

3.1 Introduction

The majority of BPH specimens contain inflammatory infiltrates and display altered expression of a wide range of cytokines [18, 20-22]. Cytokines are a large group of signalling molecules that are involved in cell communication, and are often modulated during inflammation [152]. They can be categorised as either pro- or anti-inflammatory, but due to their pleiotropic nature, many can function as both, depending on circumstance, making classification difficult. Included amongst the cytokines that have been observed to be altered in BPH are interleukins (IL) -4, -6, -8, & -17, as well as interferon- γ (IFN- γ), and fibroblast growth factor 2 (FGF-2) [10]. In particular IL-6 has been demonstrated to be important in prostate pathogenesis, and has been implicated in PCa progression through activation of androgen receptor (AR) [153-156]. More recently, it has been shown that in benign prostate epithelial cells, IL-6 can induce tumorigenic conversion and further progression to an invasive phenotype [157].

Previously, consumption of broccoli was reported to reduce symptoms associated with BPH and alter inflammatory pathways within the prostate [95]. This may be due to sulforaphane (SF), the main bioactive compound derived from broccoli. Sulforaphane is suggested to have anti-inflammatory activity, and research has shown that SF can reduce the levels of pro-inflammatory cytokines, including IL-6 [103, 158-159] and IL-8 [111].

To investigate the effect of SF in an *ex vivo* model, SF is added to the culture media, and therefore is directly applied to the tissue. However, *in vivo* the route for SF to the prostate is much more indirect, as broccoli has to first be consumed, glucoraphanin converted to SF, SF absorbed and conjugated with glutathione, before circulation in the plasma. Therefore, consumption of broccoli does not necessarily guarantee that SF will reach the prostate *in vivo*, whilst *ex vivo* and *in vitro* experiments directly add a known concentration of SF.

Biological relevance is of huge importance when investigating the role of dietary agents in human health. To know whether the concentrations of SF being used are of any relevance, it is crucial to know whether, and at what concentration, SF reaches the prostate after broccoli consumption. Indirect evidence that SF reaches the prostate after broccoli consumption is provided in a human study by Traka and colleagues [95]. They reported that consumption of broccoli altered signalling pathways in the prostate, indicating that SF did reach the prostate, eliciting an effect. Evidence that the alteration in signalling arises from SF is provided by a further study by Traka and colleagues [160]. In this study, mice were fed a diet supplemented

with SF, which resulted in changes in prostate gene expression similar to that seen in humans on a broccoli-rich diet. This suggests that the consumption of broccoli can alter gene expression in the prostate due to its SF content.

Analysis of plasma SF levels after consumption of high-glucosinolate broccoli has shown SF in the circulation at concentrations of up to $7.4\mu\text{M} \pm 3.08$ at 2 hours after consumption. After this, the level of SF rapidly drops and only trace concentrations are detectable at 24 hours [100], providing direct evidence that broccoli consumption results in an increase in SF in the circulation. A pilot study with eight participants reported the presence of SF metabolites in breast tissue 50 minutes after consumption of a single dose of broccoli sprouts, with a maximum concentration of $2 \text{ pmol/mg tissue} \pm 1.95$ [161]. This observation indicates that SF reaches tissue rapidly after consumption, leading to the hypothesis that if it is detectable in breast tissue it is likely to be detectable in other tissues, including the prostate.

All this data combined provides evidence that the consumption of broccoli results in an increase in circulating SF, and that it is likely to reach the prostate at a concentration at which it can modulate gene expression influencing prostate health.

Taking into consideration the prevalence of inflammatory cytokines in BPH tissue, the proposed role for inflammation in prostate pathogenesis, and the evidence suggesting a protective role for sulforaphane in prostate health, the hypothesis that SF can reduce the secretion of inflammatory cytokines from BPH tissue in culture is tested.

3.2 Methods

3.2.1 Tissue Collection and Preparation

Tissue was collected and prepared for culture as described in Chapter 2.1.1-2.

3.2.2 Tissue Culture

Tissue was cultured in KGM media as previously described in Chapter 2.2.3. Sulforaphane (SF; LKT Laboratories) diluted in dimethyl sulfoxide (DMSO; Sigma) to 100mM and subsequently diluted to 1mM in 10% PBS (Invitrogen). Sulforaphane added to media at final concentration of 2, 5, 10 or 25 μ M. Final DMSO concentration <0.025%, final PBS concentration <0.25%. Control samples supplemented with DMSO and PBS to a final concentration of 0.025 and 0.25% respectively.

3.2.3 Sample collection and storage

Media were collected in aliquots, and tissue collected in pairs and washed in 10% PBS, immediately frozen in dry ice and stored at -80°C prior to analysis.

3.2.4 ELISA

Media collected from tissue culture were analysed for inflammatory markers using commercially available Quantikine ELISA (R&D Systems) for IL-4, IL-6, IL-8, IL-17, FGF-2, and IFN- γ . Limit of detection was 10, 0.70, 1.5-7.5 (mean 3.5), 15, 3 and 8 pg/ml respectively. ELISA performed according to kit instructions (see Figure 3.1). Media was diluted 1:100 prior to measuring IL-6. Absorbance was measured at 450nm with wavelength correction set at 540nm using the Benchmark Plus Microplate Spectrophotometer (Bio-Rad). Microplate Manager 5.2.1. (Biorad) was used to reduce the data from the standards to generate a four parameter logistic (4-PL) graph and sample concentrations calculated from the curve.

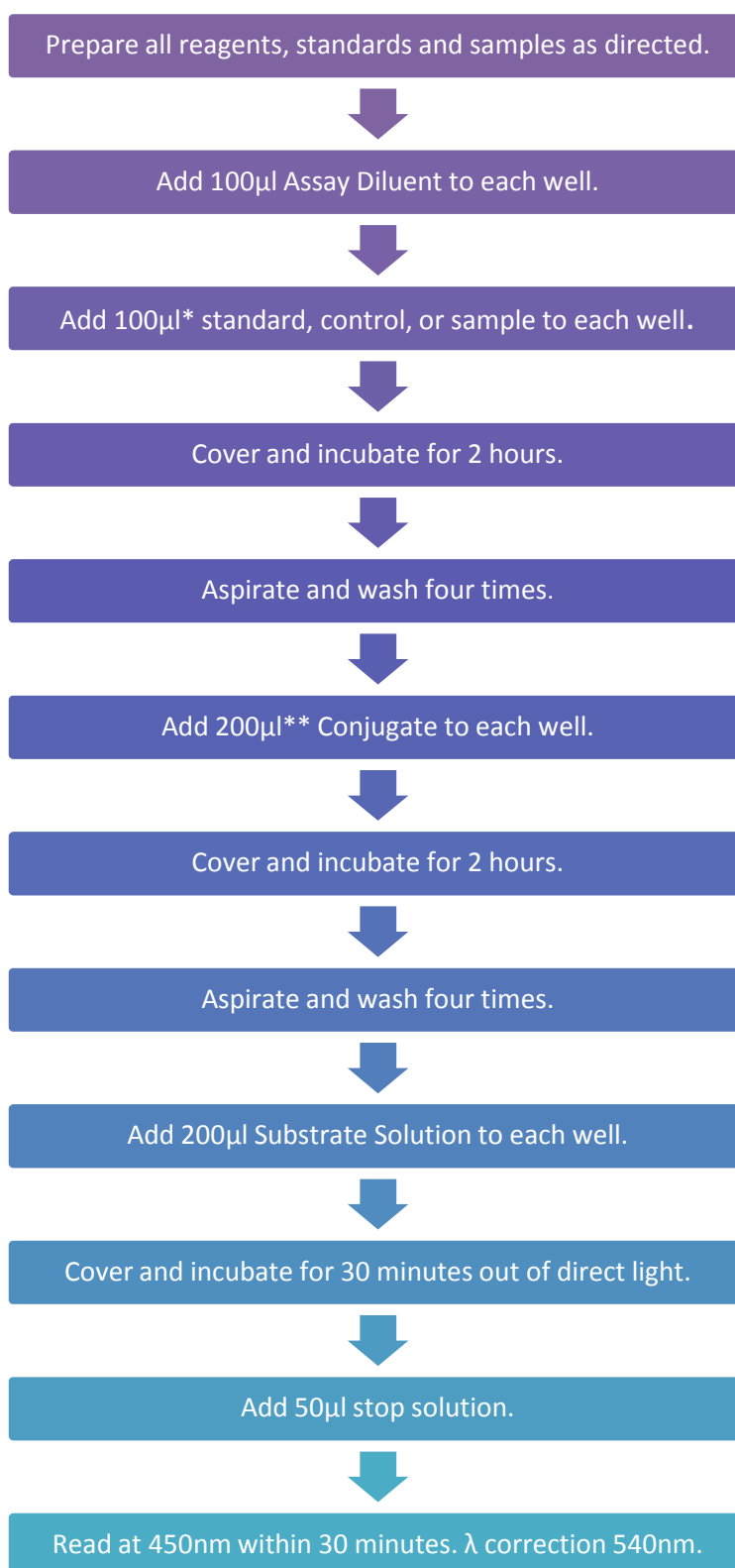


Figure 3.1. Quantikine ELISA Protocol.

Taken from kit protocol provided by R&D Systems, same protocol used for all ELISAs but with the following changes: *50µl for IL-4 and IL-8 ELISA, **100µl for the IL-8 ELISA.

3.2.5 Statistics

Statistical analysis performed in Minitab 15 (LEAD Technologies, Ltd) and R as necessary. Analysis in R was performed by Dr Jack Dainty. Minitab was used to perform Student's paired t-tests to compare treatment at each time point (see Figure 3.3). Data for the dose-dependent effect of SF on IL-6 (Figure 3.4) was normalised to minimise between patient variation, and then transformed to ensure normal distribution of residuals. Data was analysed in R using repeated measures ANOVA, with subsequent Dunnett's *post hoc* tests for pair-wise comparison.

3.3 Results

3.3.1 Inflammatory cytokines in BPH tissue

The majority of BPH specimens contain inflammatory infiltrates, suggesting that inflammation plays a key role in the aetiology of the disease. A number of inflammatory cytokines have been observed as elevated in BPH tissue, so selected cytokines were analysed as a measure of inflammation in the tissue. The cytokines measured were IL-4, IL-6, IL-8, IL-17, FGF-2 and IFN- γ . Media from tissue samples incubated for 24 hours were analysed by ELISA to detect cytokine level. IL-4, IL-17 and IFN- γ were not detectable in the sample media, so if they were present in the media it was at levels below the detection limit of the ELISA. Both IL-6 and IL-8 were found to have an average concentration of 4ng/ml, which was approximately four times higher than FGF-2, which had an average concentration of 1ng/ml (Figure 3.2).

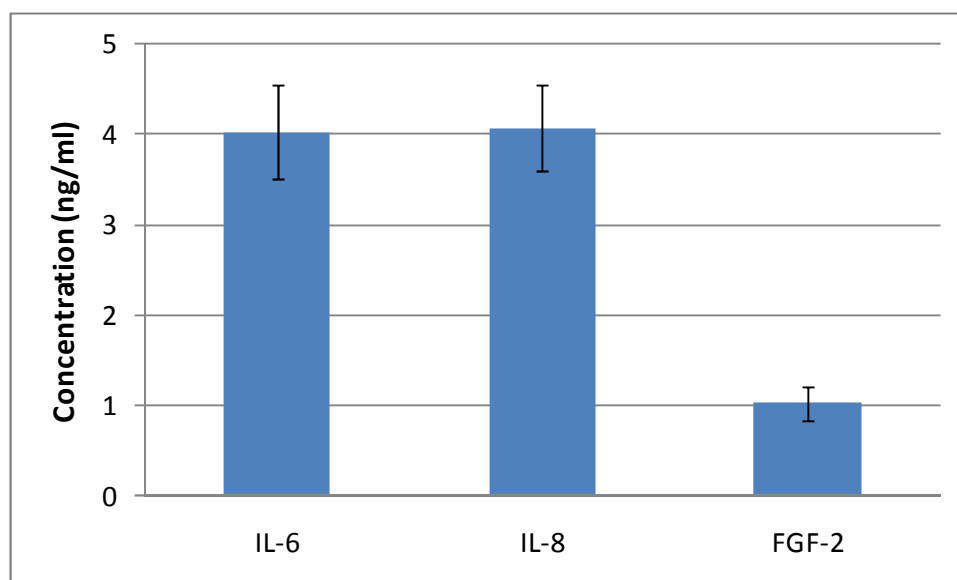


Figure 3.2. Basal Levels of Inflammatory cytokines in BPH tissue.

BPH tissue samples from three patients with three biological replicates were cultured for 24 hours at 37°C. Media was collected and inflammatory marker levels measured by ELISA. Means plotted \pm standard deviation. IL-4, IL-17 and IFN- γ were all assayed but not detected in any samples (data not shown). IL-6 and IL-8 levels were highly similar, but FGF-2 levels were 4-fold lower.

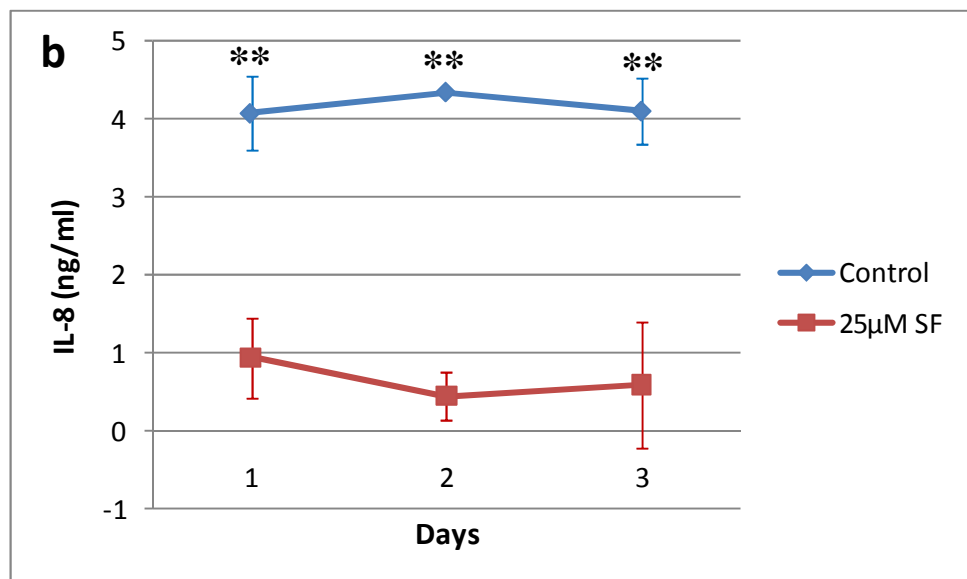
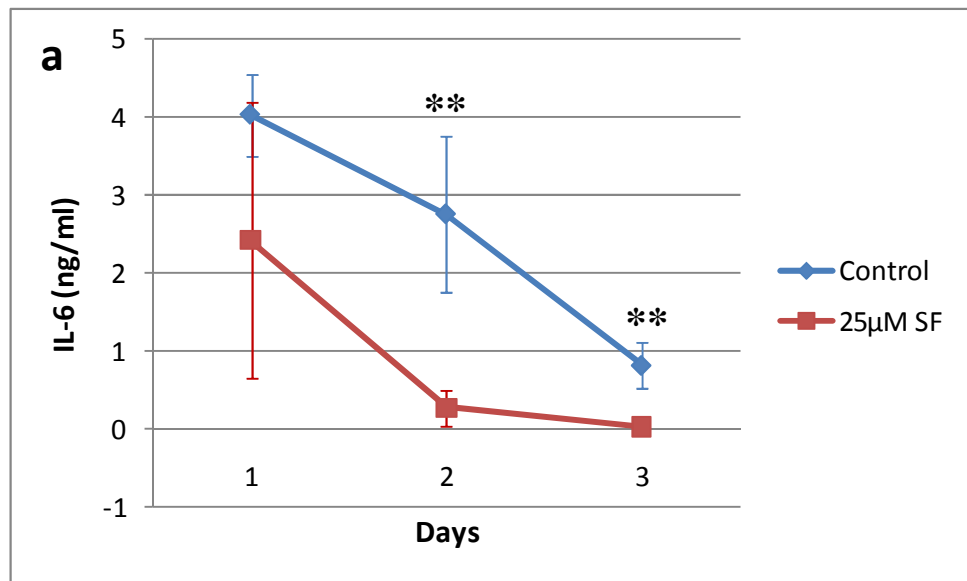
3.3.2 Modulation of inflammatory cytokines by sulforaphane

Sulforaphane has been demonstrated to have anti-inflammatory properties, so whether SF could reduce the secretion of inflammatory markers from BPH tissue *ex vivo* was investigated. Tissue was cultured with 25 μ M SF for three days, with media collected and replenished daily. Media samples from each day were analysed by ELISA. An initial concentration of 25 μ M SF was investigated as this corresponds to concentrations often used in the literature [117, 132-133, 135, 162], and this high concentration of SF would most likely make any effect more visible as this *ex vivo* model is more complex than the *in vitro* models most commonly used.

Over the three day period IL-6 secretion declined, starting at 4.03ng/ml, reducing by 32% in the next 24 hours to 2.76ng/ml, and by day three had reduced to 0.82ng/ml, a reduction of 80% compared to day one. In a similar pattern to the control samples, IL-6 secretion in the treated samples also declined over the three days, reducing 89% from day one to day two, and by day three secretion had decreased 98% compared to day one. On day one, IL-6 in the samples treated with 25 μ M SF was 40% lower than the control (p-value = 0.089). However by day two, SF had almost abolished IL-6 secretion from BPH tissue, and compared to the control samples, IL-6 secretion was significantly reduced on both day two and three (p-values \leq 0.001) (Figure 3.3a).

In contrast, IL-8 secretion remained fairly stable throughout the three day culture period in both the control and treated samples. In the control samples, IL-8 secretion was measured at 4.07ng/ml on day one, increasing slightly on day two to 4.35ng/ml, and ending on 4.10ng/ml on day three. In the samples cultured with 25 μ M SF, IL-8 secretion was significantly reduced on all three days, with levels decreased by 75, 90 and 85% on days one, two and three respectively (p-values \leq 0.001) (Figure 3.3b).

In a similar pattern to IL-6, FGF-2 secretion reduced over the time period measured. In contrast to both IL-6 and IL-8, the initial concentration of FGF-2 was four times lower at 1.03ng/ml in the control samples. This reduced by 48% to 0.50ng/ml on day two, dropping to 0.23ng/ml on day three, a total reduction of 78% compared to day one. Sulforaphane reduced FGF-2 secretion by 20, 55 and 43% on the three days respectively compared to the levels in the control samples, but this was not statistically significant (Figure 3.3c).



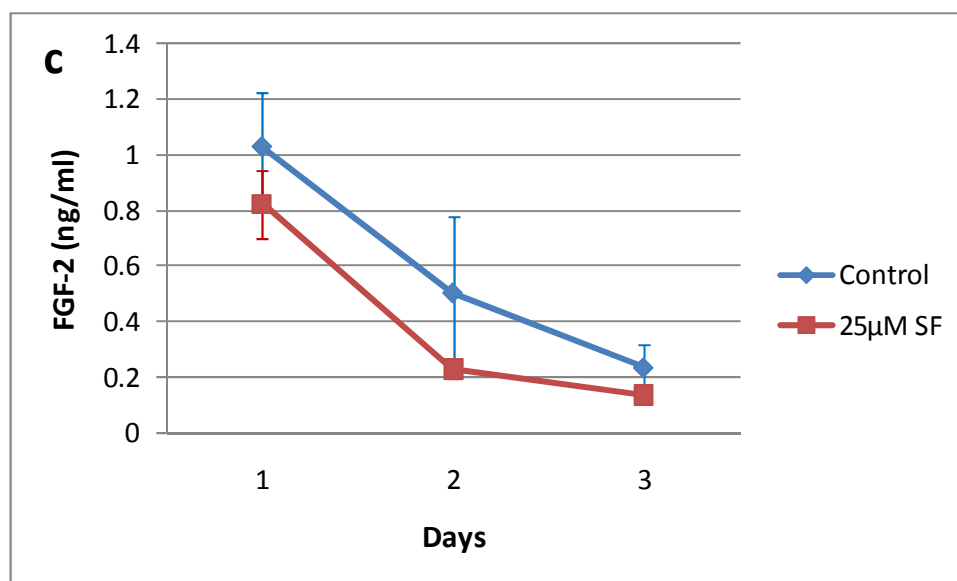


Figure 3.3. The effect of 25µM SF on inflammatory cytokines in BPH tissue.

BPH tissue samples from three patients were cultured for three days with three biological replicates with or without 25µM SF. Media was removed and replenished daily. Media samples from each day were assayed using ELISA for (a) IL-6, (b) IL-8 and (c) FGF-2. Means \pm standard deviation are plotted. IL-6 was significantly reduced by 25µM SF on days two and three, IL-8 was significantly reduced on all three days (**p-values ≤ 0.001) but FGF-2 was not significantly altered at any point.

3.3.3 Dose-dependent effect of SF on IL-6 secretion

As it was seen that 25 μ M SF was able to reduce the secretion of inflammatory cytokines, the dose-dependent effect of SF on IL-6 secretion was investigated.

Notably, the average IL-6 secretion concentration without SF varied from sample to sample, with a range of values from 5907pg/ml to 45776pg/ml. Therefore, data were normalised to 0 μ M SF for each sample to allow clearer comparison between all patients with regard to reduction for each treatment. Data was then transformed to ensure normal distribution of the residuals. Repeated measures ANOVA revealed treatment to be highly significant (p-value <0.001). *Post hoc* Dunnett's tests showed that both the 10 μ M (p-value = 0.0086) and the 25 μ M (p-value <0.001) treatments had a significant effect on the level of IL-6 secreted compared to the control tissue. 10 and 25 μ M SF reduced the levels of IL-6 by 40% and 75% respectively. The 2 μ M and the 5 μ M treatments resulted in non-significant p-values of 0.366 and 0.756, with reductions of 25 and 13% respectively (Figure 3.4).

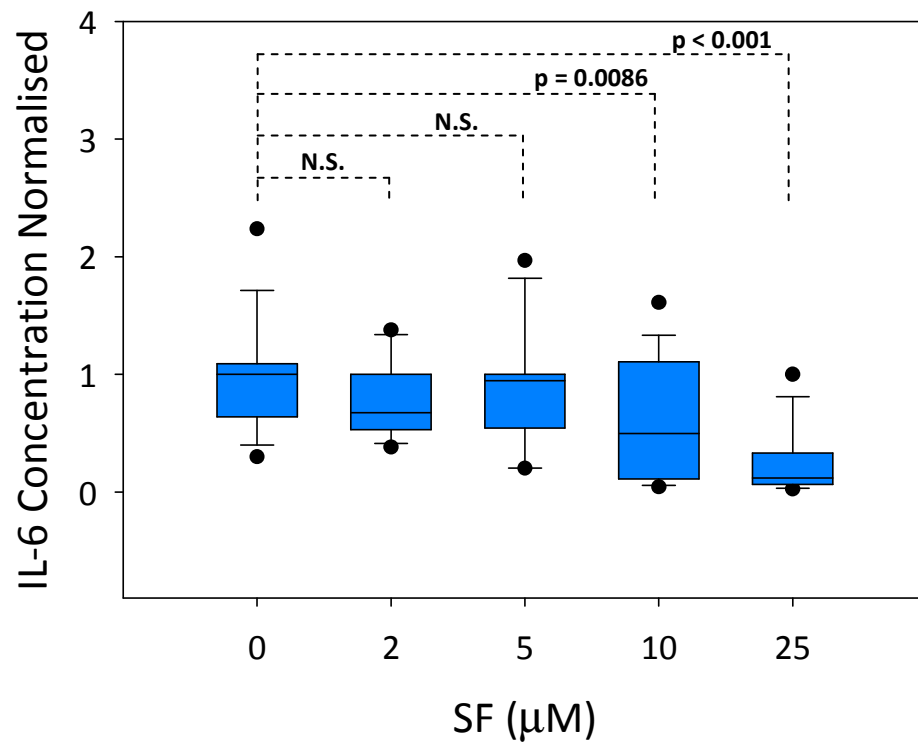


Figure 3.4. Dose-dependent effect of SF on IL-6 secretion from BPH tissue.

BPH tissue samples from five patients with biological triplicates each were cultured with 0, 2, 5, 10 or 25µM SF for 24 hours. Media was collected and assayed for IL-6 using ELISA. Results normalised to 0µM SF for each sample to allow for variations in baseline IL-6 secretion. Medians (line in box) plotted along with 25th and 75th percentiles (box), 10th and 90th percentiles (whiskers), and outliers (black circles). Compared to control, no significant effect was observed in the 2 or 5µM SF treatments but 10 and 25µM both significantly reduced IL-6 secretion. N.S. = non-significant.

3.4 Discussion

3.4.1 Inflammatory markers in BPH tissue

As it has previously been shown that BPH samples express altered levels of cytokines, a range of cytokines that had previously been reported to be expressed and altered in BPH were selected for analysis (Figure 3.2) [163-165]. Of the six cytokines selected and assayed in the media, three could not be measured: IL-4, IL-17 and IFN- γ , despite being previously measured in BPH. This may either be because they were not present in the media sample, or they were below the limit of detection of the ELISA.

It is interesting to note that the limit of detection of the ELISAs for these three cytokines were higher than those for the cytokines that were successfully measured. The lower limit of detection for the IL-4, IL-17 and IFN- γ ELISAs were 10, 15 and 8 pg/ml respectively, compared to 0.7, 3.5 and 3pg/ml for IL-6, IL-8 and FGF-2. However, if these cytokines were not measurable as they were below the limit of detection of the ELISA, then their levels would still be far smaller than those detected for IL-6, IL-8 and FGF-2, which were recorded as 4000 pg/ml for both IL-6 and IL-8, and 1000 pg/ml for FGF-2, suggesting that if they were secreted, then they were at negligible concentrations.

It is interesting that these cytokines were not detected in these samples as their expression in BPH has previously been recorded. It was expected that IL-4 would be detected as previous work has shown *de novo* IL-4 mRNA expression in BPH tissue compared to healthy prostates [20]. That IL-4 has been shown to be expressed in BPH tissue, but not healthy prostates, is interesting, as it has been shown to inhibit the proliferation of normal prostate-derived stromal cells (SCs), but this control is lost in BPH-derived SCs. IL-4 has been shown to activate androgen receptor (AR) and can promote the growth of androgen-responsive cancer cells. Thus suggesting that the *de novo* IL-4 expression observed in BPH may work through the AR to contribute to the progression of BPH, and possibly further disease development [166]. The fact that IL-4 was not detected here may be because *de novo* expression had not occurred, it had degraded in the media, or it may not have been secreted from the cells.

Also assayed, but not detected, was IFN- γ , which stimulates BPH-derived, but not normal prostate-derived, SC proliferation [20]. Whether IFN- γ expression is increased or decreased in BPH is unclear, as levels in seminal plasma have been reported to decrease from 25pg/ml in healthy tissue to 15pg/ml in BPH tissue [167], whilst another study found that IFN- γ mRNA

increased in BPH compared to healthy prostate tissue [20]. The study in which IFN- γ was measured in the seminal plasma also measured IL-6 and IL-8 concentration, and reported both of these to be much higher than the levels of IFN- γ [167]. If IFN- γ was secreted by the tissue in the present culture experiments at a similar ratio to IL-6 and IL-8 as seen in that study, it would have been below the detection limit of the ELISA, suggesting a possible explanation as to why it was not detected here.

Finally, it is surprising that IL-17 is not detected as it has been reported as over-expressed in 79% of BPH tissue samples, although further investigation suggests it is only released by activated T cells [22]. It is possible that the samples cultured here were in the 21% of BPH samples that were reported to not over-express IL-17, or that there were either no T cells, or the T cells that were present were not activated, leading to lack of IL-17 secretion. Lymphocytes were observed in the tissue (Figure 2.8c) during histological examination, although whether these were T cells is unknown. However, the use of specific stains such as CD45, selective for T cells, would allow us to confirm their identity.

Leading on from the detectable absence of IL-17, it is interesting that both IL-6 and IL-8 were easily detectable, when it has been shown that IL-17 stimulates their production [22]. It could be that the levels of IL-6 and IL-8 measured would be comparable to levels detected in healthy tissue treated in the same way, or that their secretion was stimulated by an alternative pathway. Furthermore, IL-17 may have been present in the tissue but not detectable in the media, as it may not have been secreted or may have been degraded.

Of the cytokines that were successfully measured, it is interesting that the two with the greatest concentration were IL-6 and IL-8, the favoured executors of stromal growth in BPH [165, 168]. IL-6 is an autocrine growth factor [168] whilst IL-8 is a paracrine inducer of FGF-2 [169], the third cytokine that was detected in the media. The results of the ELISAs revealed that secretion of IL-6 and IL-8 was highly comparable, at $\sim 4000\text{pg/ml}$, but were 4-fold higher than the concentration of FGF-2, which was $\sim 1000\text{pg/ml}$. There are no previous data concerning secretion concentrations of these cytokines in BPH tissue in culture with which to directly compare these results, but their relative levels, and effect on prostate health have been reported.

IL-6 has been reported to be increased 3-fold in expressed prostatic secretions of large prostates (>60g) compared to small prostates (<40g), suggesting it is involved in prostate enlargement [170]. Similarly IL-6 protein expression in prostate tissue has been observed to increase in BPH and PCa compared to normal prostates [163]. Drachenburg and colleagues further investigated the correlation between circulating IL-6 levels in serum, and prostatic disease. Their results revealed a mean concentration of 0.7pg/ml in healthy patients compared to 1.9pg/ml in BPH patients, 1.1pg/ml in PIN and 1.7pg/ml in those with localized PCa. IL-6 levels further increased to 3.9pg/ml \pm 1.6 in advance hormone-dependent disease, and 5.7pg/ml \pm 1.9 in advanced hormone-refractory disease [171]. Thereby suggesting that IL-6 is positively correlated with prostate dysregulation. It is interesting to note that IL-6 was recorded as higher in BPH patients compared to those with PIN and localized PCa, although this may be because inflammation plays a greater role in BPH than PCa. All of these results confirm that IL-6 is positively correlated with BPH, suggesting a role for IL-6 in either BPH initiation or progression.

The correlation of IL-8 with prostate health has also previously been investigated. Hochreiter and colleagues reported no difference in the IL-8 concentration of expressed prostatic secretions from control and BPH samples (approx. 3000pg/ml) [164]. Measurement of IL-8 in serum also showed no significant difference between healthy and BPH patients, with concentrations of 6.8pg/ml and 6.5pg/ml respectively. However, IL-8 was seen to be elevated in PCa, increasing to a mean of 15.6pg/ml in localized disease, and 27.8pg/ml in metastatic disease [172]. Levels of IL-8 were found to be positively correlated with prostate size and cellular senescence, and IL-8 found to promote proliferation of both primary and immortalized prostatic epithelial cells in culture [165]. Such data suggests that there is little relation between IL-8 and BPH, but that it is correlated with PCa, indicating it can play a role in prostate pathogenesis, but that it may not be of direct importance in the study of BPH tissue.

Basal levels of IL-6 and IL-8 secretion have been measured from PCa cell lines in culture, with IL-6 secreted at 8.5pg/ml and 155pg/ml in LNCaP and PC3 cell lines respectively, whilst IL-8 was measured at 442pg/ml and 378pg/ml [42]. These results once again demonstrate that IL-6 increases when PCa progresses to a hormone refractory state [171]. In contrast, these results suggest that IL-8 decreases, although it is not known whether this reduction is significant as statistical comparison was not performed.

In a study by Penna and colleagues of cytokines in seminal plasma from healthy and BPH prostates, the median IL-6 concentration was seen to increase from 16pg/ml to 74pg/ml in healthy and BPH samples respectively. Likewise, IL-8 increased from 1984pg/ml to 5044pg/ml [167]. Compared to the results I obtained, it is interesting to see that IL-8 in seminal plasma from BPH tissue was so much higher than IL-6, when I found them to be at highly similar concentrations. In terms of comparison to my results, this is probably the closest comparison, as both measured the secreted concentration as opposed to mRNA expression or tissue protein levels.

However, in my experimental setup the tissue was cultured prior to cytokine measurement. Therefore, the culture environment may have had an effect on cytokine secretion either stimulating IL-6 or inhibiting IL-8 secretion, so that the levels secreted were highly similar. Unfortunately, due to the nature of the method used in this study, it is not possible to obtain a time zero secretion value, so the question remains whether this result is representative of the tissue sample, or caused by culture.

A further explanation for the discrepancy between the two results, may be due to the sample being assayed, as they were measuring levels in seminal plasma, whilst I was measuring culture media, so their constituents may naturally differ. It is interesting that in the study by Penna and colleagues, they found IL-8 increased in BPH. This does not correspond with other data discussed above [164, 172], where no correlation was reported, suggesting the possibility that there may be some relationship between IL-8 and BPH, although the role is not clear.

The expression of FGF-2 has previously been observed to be unchanged in BPH samples compared to normal tissue [20]. This was corroborated in a further study that reported FGF2 mRNA remained stable in 54% of BPH samples analysed, whilst it was overexpressed in 44% of PCa samples. However, statistical analysis indicated a similar expression pattern in both BPH and PCa, suggesting a common role for FGF-2 in both disease states [173]. Others have observed an increase in FGF-2 in BPH, and reported a role in stromal proliferation [169, 174-175]. These data indicate that FGF-2 may be involved in BPH and PCa, although less data exists concerning the relationship between FGF-2 and prostate dysregulation, making it difficult to draw firm conclusions.

Overall the above data confirms the importance of cytokines in BPH highlighting the inflammatory nature of the disease.

3.4.2 Reduction of inflammatory markers by SF

Previously, SF has been shown to reduce the levels of some cytokines. This led to the hypothesis that SF would reduce the secretion of pro-inflammatory cytokines from the BPH tissue *ex vivo*. The results of my experiment suggest this hypothesis to be true, as 25 μ M SF was seen to reduce both IL-6 and IL-8 secretion (Figure 3.3). This correlates with results in the literature, including reports that SF inhibits diesel extract-induced IL-8 production in airway epithelial cells [111]. Although some cytokines assayed were undetected in this study, SF has also been shown to inhibit IL-17 production by rheumatoid T cells [176], and reduce expression of IL-4, IL-6 and IFN- γ in aggressive breast carcinoma cells [158].

Initially, the effect of SF on cytokine secretion was measured using 25 μ M SF, as this corresponds to concentrations often used in the literature [117, 132-133, 135, 162]. It was hoped this high concentration of SF would make any effect more apparent, as due to the complexity of the tissue model compared to cell models most commonly used, it was thought a higher dose may be needed to elicit an effect.

Using concentrations of biological relevance is of great importance when investigating dietary components. Levels of SF recorded in plasma after broccoli consumption, have been recorded at a maximum of 7.4 μ M \pm 3.08 [100], much lower than the 25 μ M SF used here. However, 25 μ M SF could be achieved by supplementation, meaning it is not outside the bounds of human relevance. In this study, 25 μ M SF was shown to have a more significant effect on IL-8 secretion than IL-6. Despite this, due to evidence suggesting an important role for IL-6 in prostate inflammation and pathogenesis in general, and a clearer correlation between IL-6 levels and BPH than IL-8, it was decided to further investigate the dose-dependent effect of SF on IL-6, not IL-8.

Results from the dose-dependent experiment showed that the lowest concentration at which significance was achieved, was 10 μ M SF and that 2 and 5 μ M had no significant effect (Figure 3.4). 10 μ M SF was therefore chosen as the concentration for all subsequent experiments, as not only were the results statistically significant, but it is a more biologically relevant

concentration than 25 μ M SF. As mentioned above, SF levels in plasma after consumption of high-glucosinolate broccoli have been recorded at 7.4 μ M \pm 3.08 (n = 7), suggesting that 10 μ M SF is at the upper limit of levels achievable in plasma through diet [100].

Reduction of IL-6 by SF corresponds with the literature, although this effect has not previously been shown in prostatic tissue. Previously, it has been shown that 1 μ M SF can significantly reduce LPS-induced IL-6 expression in rat microglia [103], and that 2.5 and 5 μ M SF reduced the secretion of IL-6 20% and 35% respectively in aggressive breast carcinoma cells after 48 hours [158]. 10 and 20 μ M SF were also shown to reduce norepinephrine-induced IL-6 secretion by pancreatic duct epithelial cells by 50 and 80% respectively [159]. Compared to the first two of these studies, the concentration of SF needed to see a significant effect here was much greater. This may be due to the more complex model being investigated, as previous reports were using *in vitro* cell models which are much simpler systems.

Sulforaphane has also been shown to inhibit IL-6-induced activation of signal transducer and activator of transcription 3 (STAT3), which has anti-apoptotic and proliferative effects, contributing to the induction of apoptosis by SF. This suggests a mechanism by which the reduction of IL-6 by SF may contribute to the pro-apoptotic protective effects of SF [177]. However, the mechanism by which SF is reducing cytokine secretion in the tissue model is unknown.

In the tissue SF may modulate cytokine secretion by two difference mechanisms. Firstly, SF may reduce the expression or secretion of the cytokines, subsequently decreasing the concentrations in the media. Secondly, it may be inducing cell death, thereby reducing the number of cells secreting cytokines into the media.

Previous work has shown that SF can modulate pathways controlling cytokine expression and secretion whilst not altering cell death [111], suggesting that this may be a possible explanation for the reduction seen here. However, as SF is known to have pro-apoptotic properties, it can not be ruled out that SF may be inducing cell death in this model. Further evidence for this possibility is provided in Chapter 5, where SF is reported to alter the expression of a number of proteins involved in the apoptotic process, suggesting SF can promote apoptosis in this model.

As neither hypothesis can be proven or discredited, it must also be considered that the reduction observed here could be due to a combination of the two, with SF both increasing cell death, but also reducing the expression and secretion of cytokines from the surviving cells.

3.4.3 Conclusions

It is apparent from the experiments performed that BPH tissue *ex vivo* secretes a range of cytokines, supporting the idea that inflammation is a key component of BPH. It has also been shown that SF can reduce pro-inflammatory cytokines in a dose-dependent manner, thereby demonstrating a possible method by which SF can have a beneficial effect on prostate health. As such this may help to explain why the consumption of broccoli is associated with improved prostate health, and correlates with the observation that broccoli can reduce BPH-related symptoms and alter inflammatory pathways in the prostate [95]. To further investigate the activity of SF in the *ex vivo* model, the next chapter will employ an untargeted method which will hopefully allow for the discovery of novel targets of SF activity in the prostate.

Chapter Four

Proteomics & Protein Identification

Chapter 4. Proteomics & Protein Identification

4.0.1 Summary

Chapter 3 described the effect of sulforaphane (SF) on inflammatory cytokines in benign prostatic hyperplasia (BPH) tissue *ex vivo* using a targeted approach. The next two chapters will describe the effect of SF in the *ex vivo* model using an untargeted approach to assess changes in global protein expression, with the aim of identifying novel targets of SF activity. This chapter focuses on the technical aspects of proteomics, whilst discussion of the proteins identified will be undertaken in the following chapter.

Protein extracted from BPH tissue from three patients cultured with or without 10 μ M SF in triplicate, was separated by 2D gel electrophoresis, and the resulting gels compared. Analysis of the gels identified four sources of variation: replicate, patient, treatment and technical. Assessment of baseline global protein expression showed a significant difference between patients 13 and 14, and patient 16. In each patient, a number of individual spots were found to be altered due to SF treatment, but total global protein expression was only significantly altered in patients 13 and 14. Comparison of the spots altered by SF in each patient revealed there was very little overlap, indicating that the samples from the individual patients responded in unique and varying ways. Protein spots that were altered due to patient or treatment variation were selected, corrected for technical variation, and identified by mass spectrometry.

These results show that SF can alter proteins within BPH tissue, but that there is a high degree of human variation evident.

4.1 Introduction

In the previous chapter, the hypothesis that SF could reduce the secretion of pro-inflammatory cytokines from BPH tissue in culture was tested using a targeted method to measure the effect of SF on specific selected cytokines. In this chapter, this work is expanded with the use of a non-targeted approach to investigate the effect of SF on global protein expression in BPH tissue *ex vivo* (Figure 4.1).

Compared to a targeted approach, a non-targeted approach will remove any bias in the selection of proteins measured, and will hopefully allow for the identification of novel targets of modulation by SF. Furthermore, the use of the two techniques will hopefully mitigate any limitations intrinsic to each. For example, 2D gel electrophoresis is often not sensitive enough to detect inflammatory cytokines, so the use of the targeted ELISA, which has higher sensitivity, will facilitate the detection and measurement of these markers. However, 2D gel electrophoresis has advantages over ELISA due to its untargeted nature. One such advantage, is that it allows the identification of different protein isoforms or modifications, which may, due to the specificity of the antibodies used in ELISA, lead to a false negative [178].

The aim of this work is to investigate the effect of SF on global protein expression, and to identify the proteins altered, providing a greater understanding of the mechanisms by which SF can have a beneficial effect on the prostate. In addition, it is also hoped that a novel target of SF activity may be identified for further investigation. 2D gels have previously been used to identify targets of SF activity, including: down-regulation of serotonin receptors in a colorectal cancer cell line [179]; induction of apoptosis by down regulation of phosphoglucomutase 3 in a prostate cancer cell line [180]; and inhibition of cell growth and induction of apoptosis by binding to tubulin and inhibiting its polymerization in a lung cancer cell line [181]. The use of this technique in the analysis of BPH tissue cultured *ex vivo*, which is novel in itself, is hoped to elicit a novel target for SF activity, as has been achieved in studies using established cell lines.

In this chapter, I will use 2D gel electrophoresis to separate proteins extracted from BPH tissue cultured with or without 10 μ M SF, the lowest concentration at which SF significantly reduced IL-6 secretion (see Chapter 3). I will analyse the overall effect on global protein expression, and then select specific spots for identification. The aim of this work is to provide a greater understanding of which proteins SF is capable of modulating, and to try and understand how SF may have a beneficial effect on prostate health.

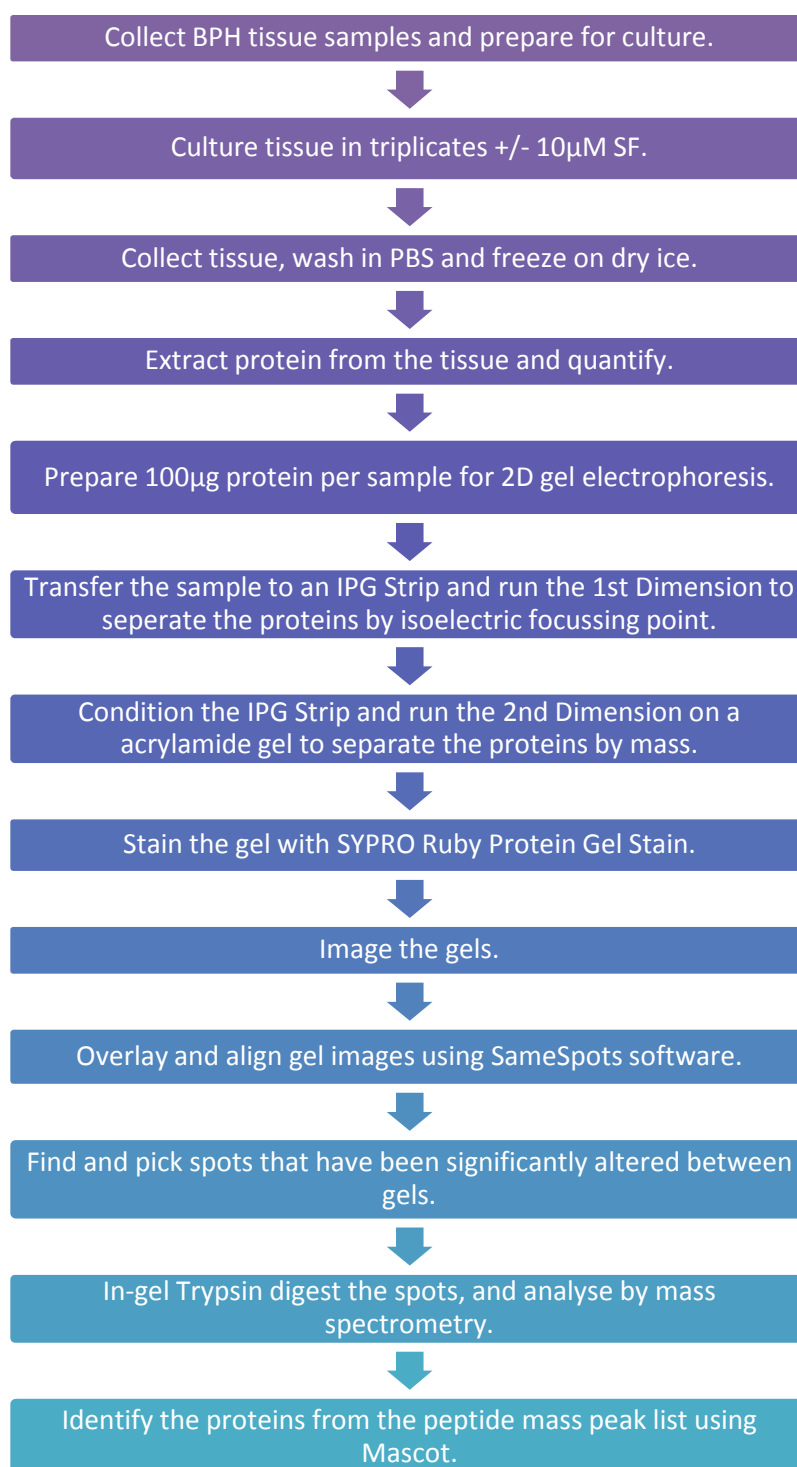


Figure 4.1. Proteomic analysis overview.

Simplified process diagram showing the major steps in sample collection, preparation and proteomic analysis using 2D gel electrophoresis.

4.2 Methods

4.2.1 Tissue collection

BPH prostate tissue collected in Chapter 3 was used in this chapter. Previously, media samples from tissue culture were assessed for the dose-dependent effect of SF on IL-6 secretion (see Chapter 3.3.3). The lowest concentration of SF at which an effect was seen was 10 μ M. Tissue samples from five patients were cultured for 24 hours and media samples assayed. The three tissue samples which showed the greatest response to 10 μ M SF were selected for the 2D gel electrophoresis work. The samples were washed in warm PBS, collected in pairs, immediately frozen in dry ice, and stored at -80°C for later analysis.

4.2.2 Protein extraction

Two pieces of snap-frozen tissue were transferred into a grind tube (Sample Grinding Kit, GE Healthcare) with 100 μ l Reagent 1 (40mM Tris-BASE (5ml), supplemented with 15 μ l 1M MgCl₂, 12.5 μ l Protease Inhibitor Cocktail (Sigma P-8340), 25 μ l DNase (1 unit/ μ l Promega M6101) and 2.5 μ l RNase A (10mg/ml Sigma R6513)), and ground using a pestle until homogenized. The sample was centrifuged at 10,000rpm and 4°C for 1 minute and the supernatant collected. A further 100 μ l Reagent 1 was added, and the sample ground and centrifuged again as before, and the supernatant collected. 100 μ l of ReadyPrep Sequential Extraction Kit Reagent 3 supplemented 1:100 with Tributylphosphine (TBP) Reducing Reagent (both BioRad) was added to the sample, ground and centrifuged (at 15°C) as before; and the supernatant collected in a new tube, this step was then repeated. Both supernatants were spun for 5 mins at 15,000 rpm and 5°C or 15°C for Reagent 1 and 3 supernatants respectively. Supernatants were removed and labelled 'Supernatant 1' (Reagent 1) and 'Supernatant 2' (Reagent 3) and stored at -80°C. Supernatant 2 (Reagent 3) was used for all protein analysis.

4.2.3 Protein quantification

Protein extracted from tissue was quantified using the 2D Quant Kit (GE Healthcare) as per instructions. Briefly: a standard curve was prepared using the BSA standard provided, samples were prepared using 15 μ l supernatant 2, 500 μ l precipitant was added to all standards and samples prior to a brief vortex, and incubated for 2-3 minutes. 500 μ l co-precipitant was added and mixed by inversion, samples centrifuged at 10,000 x g for 5 minutes, supernatants immediately decanted, tubes briefly re-centrifuged, and all remaining supernatant carefully

removed using a pipette. 100µl copper solution and 400µl distilled water was added to each tube and vortexed. 1ml working colour reagent added, mixed by inversion, and incubated for 15-20 minutes. Samples were transferred to cuvettes (Sarstedt), and the absorbance read at 480nm, with water as a blank, in a spectrophotometer (DU 640 Spectrophotometer (Beckman)). Standards were plotted to produce a curve, which was then used to calculate sample concentrations.

4.2.4 2D gels

Protein was run on 2D gels to separate the proteins by both mass and isoelectric focussing point. For each patient three biological triplicates with or without 10µM SF were run.

4.2.4.1 Sample Preparation

A sample volume equivalent to 100µg protein was added to a Biomax 5K NMWL Membrane Ultrafree 0.5ml centrifugal filter (Millipore) along with 400µl non-bromophenol blue rehydration buffer (7M Urea, 2M Thiourea and 2% CHAPS) and concentrated to approximately 50µl at 12,000g and 20°C. The concentrate was mixed with an IPG Strip Rehydration Buffer, containing 7M Urea, 2M Thiourea, 2% CHAPS, bromophenol blue, 0.018M DTT and 0.5% pH 3-11NL IPG Buffer (GE Healthcare), to a final volume of 450µl.

4.2.4.2 1st Dimension

The whole volume was transferred into one well of the Immobiline Dry Strip re-swelling tray, and IPG strips (24cm, pH 3-11; GE Healthcare) were rehydrated overnight at 20°C. Each strip was then transferred to a ceramic strip-holder, and the iso-electric focusing run with a 'step-n-hold' at 500 V for 1 hour, a gradient step up to 1000V over 1 hour, a gradient step up to 8,000V over 3 hours and a 'step-n-hold' at 8000 V for 3.75 hours (Ettan IPGphor Manifold IEF System, GE Heathcare). After completion strips were stored at -80°C.

4.2.4.3 2nd Dimension

The second-dimension was carried out on 1mm thick 10% polyacrylamide (Duracryl) gels prepared in 28 x 23cm gel-plate cassettes. Focused IPG strips were rinsed free of excess

mineral oil and conditioned in filtered (0.45µm) equilibration buffer (Tris Acetate Equilibration Buffer (5% SDS, 0.01% bromophenol blue, 0.122M Tris/Acetate,)), supplement with a further 5mg/ml final volume SDS, 360mg/ml final volume urea and 30% final volume glycerol). To re-enforce disulphide bond separation and prevent proteins from re-folding, strips were first treated with 8mg/ml DTT in the equilibration buffer (9ml for 30 minutes with gentle shaking) and then transferred into 25mg/ml iodoacetamide in equilibration buffer (9ml for 30 minutes with gentle shaking). Acrylamide gels (28 x 23cm, 1mm thick) were prepared for use in the 2nd Dimension Running System (Millipore), and IPG strips placed in the well of the gel cassette ensuring good contact with the gel. The top reservoir contained the cathode buffer (14mM SDS, 200mM Tris Base, 200mM Tricine), and the bottom reservoir contained the anode buffer (26mM Tris Base, 0.08% Acetic Acid). Electrophoresis conditions were set to give a maximum voltage of 500 V, power of 20,000mW/gel and a total run time ~4 hours.

4.2.4.4 Sypro Ruby Staining

After electrophoresis, the gels were fixed overnight in 400ml Fixing Solution (40% methanol, 10% acetic acid), and then stained overnight using 330ml SYPRO Ruby Protein Gel Stain (Invitrogen) in the dark. They were then destained for 4 hours in a 400ml 10% methanol, 6% acetic acid solution in the dark.

4.2.4.5 Imaging

Gels were imaged at 100µm resolution using the Pharos FX Plus Molecular Imager with the GS800 Calibration Densitometer and Quantity One imaging software (all Bio-Rad) employing the Excitation 532nm laser and 605nm BP Emission filter. The photo multiplier tube (PMT) laser strength was determined empirically for each gel, the range used was 48-60%, using the strongest spot on each gel to achieve the maximum signal (65,500) without causing bleaching or peak slicing.

4.2.4.6 SameSpots Software

Images were analysed using Progenesis SameSpots software (Nonlinear Dynamics). Each gel was aligned to a reference gel prior to automatic spot detection. Each gel then had the same spot shown on that position on the image. Spurious spots were filtered out and the gels were

then grouped into their experimental conditions. Finally, manual editing was performed to ensure spots were correctly defined. Comparisons of spots on gels were made between multiple groups to look at the inter-individual variation, intra-individual variation and the effect of treatment on the group as a whole.

4.2.4.7 Spot picking

Selected spots were excised from a gel using the ProPick excision robot (Genomic Solutions). Gel plugs underwent manual in-gel Trypsin digestion. Gel plugs were first conditioned with two 20 minute incubations in 200mmol/L ammonium bicarbonate (ABC) in 50% acetonitrile, followed by washing, and a 10 minute incubation with acetonitrile, before air-drying for 10 minutes. 50ng Trypsin Gold (Promega) dissolved in 10mM ABC was added to each gel plug (5µl per well) and incubated at 37°C for 3 hours. Digestion was stopped and peptides extracted using 5µl 5% formic acid incubated for 10 minutes. Samples were flash frozen in liquid nitrogen and stored at -70°C.

4.2.5 Mass spectrometry

Samples were analysed by mass spectrometry by Dr Fran Mulholland as a service as part of the IFR Proteomics Partnership using the following procedure.

4.2.5.1 Sample preparation

The supernatant from the in-gel digest was recovered from digest reaction tube and put into a 1.5ml Eppendorf tube. To extract further peptides 20µl 50% Acetonitrile was added to the gel piece and left at room temperature for 3-5mins before the liquid removed and added to the Eppendorf tube. The sample was then dried down at the Low Drying setting (no heat) on a Speed Vac SC110 (Savant) fitted with a Refrigerated Condensation Trap and a Vac V-500 (Buchi). The sample was frozen at -70°C or immediately reconstituted for LC-MS/MS analysis.

To prepare the sample for the LC-MS/MS analysis, the sample was redissolved in 30-100µl 0.5% formic acid and vortexed for 20 seconds before sitting in a sonicating water bath (Kerry) for 5 minutes at room temperature to facilitate dissolution. The sample was then briefly pulse centrifuged before the appropriate volume (25-50µl) was dispensed into a 0.2ml skirted 96-

well PCR plate (ThermoAB-800). Once all samples were added to the plate it was sealed with an adhesive PCR foil seal.

4.2.5.2 LC-MS/MS analysis

LC-MS/MS analysis was performed using a LTQ-Orbitrap mass spectrometer (Thermo Electron) and a nanoflow-HPLC system (nanoACQUITY; Waters, US). Peptides were trapped on line to a Symmetry C18 Trap (5 μm , 180 μm x 20 mm) which was then switched in-line to a UPLC BEH C18 Column, (1.7 μm , 75 μm x 250 mm) held at 45°C. Peptides were eluted by a gradient of 0–80% acetonitrile in 0.1% formic acid over 50 min at a flow rate of 250 nL min⁻¹. The mass spectrometer was operated in positive ion mode with a nano-spray source at a capillary temperature of 200°C.

The Orbitrap was run with a resolution of 60,000 over the mass range m/z 300–2000 and an MS target of 10^6 and 1 s maximum scan time. The MS/MS was triggered by a minimal signal of 2000 with an Automatic Gain Control target of 30000 ions and maximum scan time of 150 ms. For MS/MS events selection of 2+ and 3+ charge states selection were used. Dynamic exclusion was set to 1 count and 30 s exclusion time with an exclusion mass window of ± 20 ppm.

4.2.6 Identification of proteins using Mascot

Proteins were identified from the mfg file (prepared from the Orbitrap-derived RAW data file using DTASupercharger) using an in-house version of the Mascot LC-MS-MS search tool from Matrix Science. The search parameters were as follows: the taxonomy group searched was *Homo sapiens* of the SPTrEMBL database, tryptic digest was assumed to have a maximum of up to two missed cleavages, the carbamidomethylation of cysteine residues was a fixed modification, and oxidation of methionine residues was a variable modification, peptide masses were monoisotopic and either 2+ or 3+ charged, and the peptide and fragment mass tolerances were set at 5 ppm and 0.5 Da respectively. Individual ions scores >23 indicated identity or extensive homology (p-value <0.05). From the resulting analysis identified proteins with overall scores >100 were investigated further. The predicted pI and mass were noted for all hits with an overall protein score >100, and compared to the position of the spot on the gel. The peptide coverage pattern of the sequence was examined to determine whether the protein may have fragmented, in which case the predicted pI and molecular weight of the

fragment were calculated using the ExPASy Proteomics Server Compute pI/Mw tool (http://www.expasy.ch/tools/pi_tool.html). Proteins with a mass or pI which did not correspond with the position of the spot on the gel were eliminated. The process used to identify proteins using the Mascot results is described in greater detail below using spot 397 as an example.

Spot number 397 returned 22 protein hits with 11 of these scoring >100. One of these hits was a control and the other possible identifications included endoplasmic reticulum chaperonin, desmin, collagen- α 1 (IV) and several keratins (Table 4.1).

Table 4.1. Possible identifications for spot 397.

ID No.	Accession	Name	Score	Mass	pI
1	P14625	Endoplasmic reticulum chaperonin	2212	92696	4.76
2	P04264	Keratin, type II cytoskeletal 1	990	66170	8.15
3	P35527	Keratin, type I cytoskeletal 9	531	62255	5.14
4	P13645	Keratin, type I cytoskeletal 10	327	59020	5.13
5	P35908	Keratin, type II cytoskeletal 2	292	65678	8.07
		- Fragment		33628	5.04
6	P02533	Keratin, type I cytoskeletal 14	277	51872	5.09
7	P12109	Collagen alpha-1(VI) chain	213	109602	5.26
8	P13647	Keratin, type II cytoskeletal 5	168	62568	7.59
9	P17661	Desmin	116	53560	5.21
10	P04259	Keratin, type II cytoskeletal 6B	108	60315	8.09

Possible protein identifications for spot 397 as elicited from searching Orbitrap data using Mascot. 22 possible matches were found but all IDs with a score <100 were eliminated (data not shown) as these were below the arbitrary threshold.

From noting down the mass and pI of each possible ID (Figure 4.2), and comparing to the position of the spot on the gel (Figure 4.3), IDs 2, 5 (un-fragmented), 8 & 10 can be eliminated as their pIs are too high. It is unlikely to be IDs 3, 4, 5 (fragment), 6 & 9 as their mass would indicate they would have run further down the gel. Keratins are also recognised contaminants of this type of experimental data and can usually be ignored. This leaves only two possible IDs; (1) endoplasmic reticulum chaperone protein or (7) collagen alpha-1(VI) chain.

{MATRIX} SCIENCE Mascot Search Results

Protein View

Match to: P14625 Score: 2212
 RecName: Full=Endoplasmic reticulum chaperone protein; AltName: Full=Heat shock protein 90 kDa beta member 1; AltName: Full=94
 Found in search of \\Nbi-cfs2\proteomicpartnership\OrbitrapData\100201\mgffiles\fm100201_06.mgf

Nominal mass (M_r): 92696; Calculated pI value: 4.76
 NCBI BLAST search of [P14625](#) against nr
 Unformatted [sequence string](#) for pasting into other applications

Taxonomy: [Homo sapiens](#)

Figure 4.2. Mascot search result.

Information shown includes accession number, score, name, mass and pI of a possible ID for spot 397. This information is generated for each possible ID.

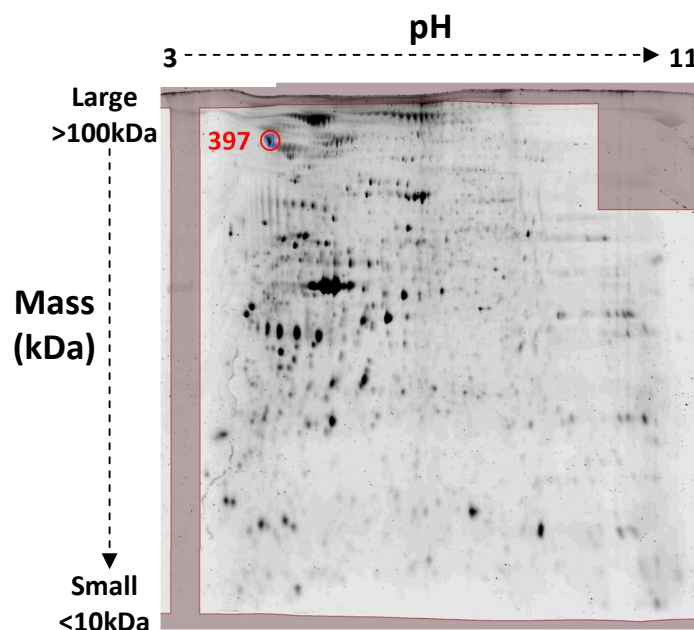


Figure 4.3. Position of spot 397 on a 2D gel.

An example image of a 2D gel showing the position of spot 397. The spot is positioned towards the top left of the gel indicating that it has a low pI and the mass is relatively large.

Assessment of the sequence coverage reveals 38% coverage for endoplasmin (Figure 4.4), and 5% coverage for collagen alpha-1(VI) chain (Figure 4.5), suggesting the most likely ID for spot 397 is (1) endoplasmin. Previous papers have also been published that had identified endoplasmin (also known as gp96, GRP94 and HSP90 β 1) in the same position on the gel further validating the identification [182-183].

```

1 MRALWVLGLC CVLLTFGSVR ADDEVVDVGT VEEDLGKSRE GSRTDDEVVQ
51 REEEAIQLDG LNASQIRELR EKSEKFAFQA EVNRMMKLII NSLYKNKEIF
101 LRELISNASD ALDKIRLISL TDENALSGNE ELTVKIKCDK EKNLLHVTDT
151 GVGMTREELV KNLGTIAKSG TSEFLNKMTE AQEDGQSTSE LIGQFGVGFY
201 SAFLVADKVI VTSKHNNDTQ HIWESDSNEF SVIADPRGNT LGRGTTITLV
251 LKEEASDYLE LDTIKNLVKK YSQFINFPIY VWSSKTETVE BPMEEBEAAK
301 EEKEESDDEA AVEEEEEEEK PKTKKVEKTV WDWELMNDIK PIWQRPSKEV
351 EEDEYKAFYK SFSKESDDPM AYIHFTAEGE VTFKSILFVP TSAPRGLFDE
401 YGSKKSDYIK LYVRRVFITD DFHDMMPKYL NFVKGVVDS DLPLNVSRET
451 LQQHKLLKVI RKKLVRKTL D MIKKIADDKY NDTFWKEFGT NIKLGVIEDH
501 SNRTRLAKLL RFQSSHPTD ITSLDQYVER MKEKQDKIYF MAGSSRKEAE
551 SSPFVERLLK KGYEVIYLTE PVDEYCIQAL PEFDGKRFQN VAKEGPKFDE
601 SEKTESREA VEKEFEPLLN WMKDKALKDK IEKAVVSQRL TESPCALVAS
651 QYGWSGNMER IMKAQAYQTG KDISTNYIAS QKKTFEINPR HPLIRDMLRR
701 IKEDEDDKIV LDLAVVLFET ATLRSGYLLP DTKAYGDRIE RMLRSLNID
751 PDAKVEEPEE EEPEETAEDT TEDEQDEDE EMDVGTDEE ETAKESTAEK
801 DEL

```

Figure 4.4. Peptide Sequence of endoplasmin (P14625).

Matched peptides shown in bold red with 38% sequence coverage.

```

1 MRAARALLPL LLQACWTAAQ DEPETPRAVA FQDCPVDLFF VLDTSESVAL
51 RLKPYGALVD KVSFTKRFI DNLRDRYYRC DRNLVWNAGA LHYSDEVEII
101 QGLTRMPGGR DALKSSVDV KYFGKGTYTD CAIKKGLEQL LVGGSHLKEN
151 KYLIVVTDGH PLEGYKEPCG GLEDAVNEAK HLGVKVFSVA ITPDHLEPRL
201 SIATDHTYR RNFTAADWGQ SRDAEEAISQ TIDTIVDMIK NNVEQVCCSF
251 ECQPARGPPG LRGDPGFEGE RGKPLPGEK GEAGDPGRPG DLGPFVYQGM
301 KGEKGSRGEK GSRGPKGYKG EKGRGIDGV DGVKGEMGYP GLPGCKGSPG
351 FDGIQPPPGP KGDPGAFLK GEKGEFGADG EAGRPGSSGP SGDEGQPGEP
401 GPPGEKGEAG DEGNPGPDGA FGERGGPGER GPRGTPGTRG PRGDPGEAGP
451 QGDQGREGFV GVPDPGEAG FIGPKGYRGD EGPPGSEGAR GAPGPAGPPG
501 DPGLMGERGE DGPAGNGTEG FPGFPGYPGN RGAPGINGTK GYPGLKGDG
551 EAGDPGDDNN DIAPRGVKA KGYRGEPPGQ GPPGHQSPG PDECEILDII
601 MKMCSCECK CGPIDLLFVL DSSESIGLQN FEIAKDFVVK VIDRLSRDEL
651 VKFEPGQSYA GVVQYSHSQM QEHVSLRSPS IRNVQELKEA IKSLQWMAGG
701 TFTGEALQYT RDQLLPPSPN NRIALVITDG RSDTQRDTP LNVLCSPGIQ
751 VVSVGIKDV DFIPGSDQLN VISCQGLAPS QGRPGLSLVK ENYAELEDA
801 FLKNVTAQIC IDKKCPDYTC PITFSSPADI TILLDGSASV GSHNFDTKR
851 FAKRLAERFL TAGRTDPAHD VRVAVVQYSG TGQQRPERAS LQFLQNYTAL
901 ASAVDAMDFI NDATDVNDAL GYVTRFYREA SSGAAKKRLL LFSDBGNSQGA
951 TPAATIEKAVQ EAQRAGIEIF VVVVGRQVNE PHIRVLVTGK TAEYDVAYGE
1001 SHLFRVPSYQ ALLRGVFHQ T VSRKVALG

```

Figure 4.5. Peptide Sequence of collagen alpha-1(VI) chain (P12109).

Matched peptides shown in bold red with 5% sequence coverage.

In some cases, if there was good coverage in a specific section of the sequence but no matches throughout the rest of the sequence, fragmentation of the protein was considered and the mass and pI of the proposed fragment calculated using the online Protein Mass Calculator (Bioinformatics at the Cancer Research UK Clinical Centre, University of Leeds, <http://www.proteomics.leeds.ac.uk/cgi-bin/masscalc>) and Compute pI/Mw tool (ExPASy Proteomics Server, Swiss Institute of Bioinformatics, http://www.expasy.ch/tools/pi_tool.html) respectively. The calculated mass and pI were compared to the position of the spot on the gel to decide whether this proposed fragment could be a possible ID for the spot of interest.

4.2.7 Statistics

Data was statistically analysed to identify sources of variation using ANOVA, repeated measures and 1-way, and subsequent Tukey HSD *post hoc* tests as appropriate (Table 4.2). Individual protein spots were analysed by 1-way ANOVA (Table 4.3). Analysis was performed in R by Dr Jack Dainty. Results were not corrected for multiple testing, as this was deemed to stringent for this type of data, due to the natural variation present within human samples. Production of a Venn diagram, showing the overlap between protein spots altered by 10 μ M SF, and selected for identification in the three patients, was performed in R under the guidance of Dr Maria Traka (Figure 4.6).

4.3 Results

4.3.1 Analysis of sources of variation within 2D gels

To investigate the effect of SF on global protein expression in BPH tissue in culture, tissue stored from a previous experiment (Chapter 3.3.3), where samples were cultured with or without 10 μ M SF for 24 hours in triplicate, was used. Protein was extracted from the tissue, and then run by 2D gel electrophoresis to separate the proteins, firstly by isoelectric point, and secondly by mass. Gels were stained with SYPRO Ruby, a fluorescent stain which binds to proteins, with a lower detection limit of 1-10ng, to visualise the spots. Images of each gel were taken, and analysed using SameSpots software (Figure 4.6). Initial analysis was performed to identify any sources of variation between the gels. Three sources of variation were examined: replicate, patient and treatment.

4.3.1.1 Replicate

Analysis for replicate effect throughout the gels using repeated measures ANOVA indicated there was significant difference between the replicates (p-value <0.001) (Table 4.2). 1-way ANOVA of the control and 10 μ M treatment groups showed that the difference was arising from the control group (p-value = 0.068 compared to 0.672 for the 10 μ M SF group). Further 1-way ANOVA of the control group revealed that the variation resulted from patient 16 (p-value = 0.0072) and not patients 13 or 14 (p-value = 0.649 and 0.614 respectively). Tukey HSD *post hoc* tests indicated that replicate 2 was significantly different to replicates 1 and 3 (p-values for replicate 1 vs. 3 = 0.734, 2 vs. 3 = 0.0073, and 2 vs. 1 = 0.061). Removal of the second replicate from all groups reduced the overall significance of replicate effect greatly (from p-value <0.001 to 0.0462), although the p-value remained just within the values for significance, which is likely due to the decreased sample size from which the calculation was made.

This data demonstrated that overall there was little replicate variation, suggesting that the replicate variation observed from replicate 2 of patient 16 control group was an anomaly. This may have been caused by either technical issues that occurred during running and staining, or inherent biological variability in the sample, such as the presence of different cell types. All further analysis using data from patient 16 control group was performed with replicate 2 removed from all groups involved to ensure balanced statistical analysis.

4.3.1.2 Patient

Comparison of tissue from the three patients without treatment using 1-way ANOVA revealed significant difference between the patients (p -value = 0.001) (Table 4.2). Further analysis using Tukey HSD *post hoc* tests, for pair-wise comparison with in-built multiple test correction, showed that patients 13 and 14 were statistically similar (p -value = 0.3429), but that patient 16 was significantly different to both patients 13 and 14 (p -value = 0.037 and <0.001 respectively). This highlights that the global protein expression in BPH tissue naturally varies from patient to patient.

4.3.1.3 Treatment

Lastly, the effect of treatment was examined to determine whether 10 μ M SF had altered the global protein expression of the tissue compared to the control group, also referred to as the baseline. Repeated measures ANOVA showed there was a statistically significant effect of treatment (p value <0.001) (Table 4.2). Further 1-way ANOVA showed that the greatest effect of treatment occurred in patient 14 (p -value <0.001), and that patient 13 was also significantly effected by the SF (p -value = 0.0037). No significant effect of treatment was observed on patient 16 (p -value = 0.9265).

It is interesting that it was patient 16 which showed the least response to treatment. Patient 16 showed the greatest variance to the other patients without treatment, and displayed an effect of replicate in the control group.

These results suggest that 10 μ M SF is capable of altering global protein expression in BPH after 24 hours of culture, but that different patients respond in diverse ways, once again highlighting the natural variation between individuals.

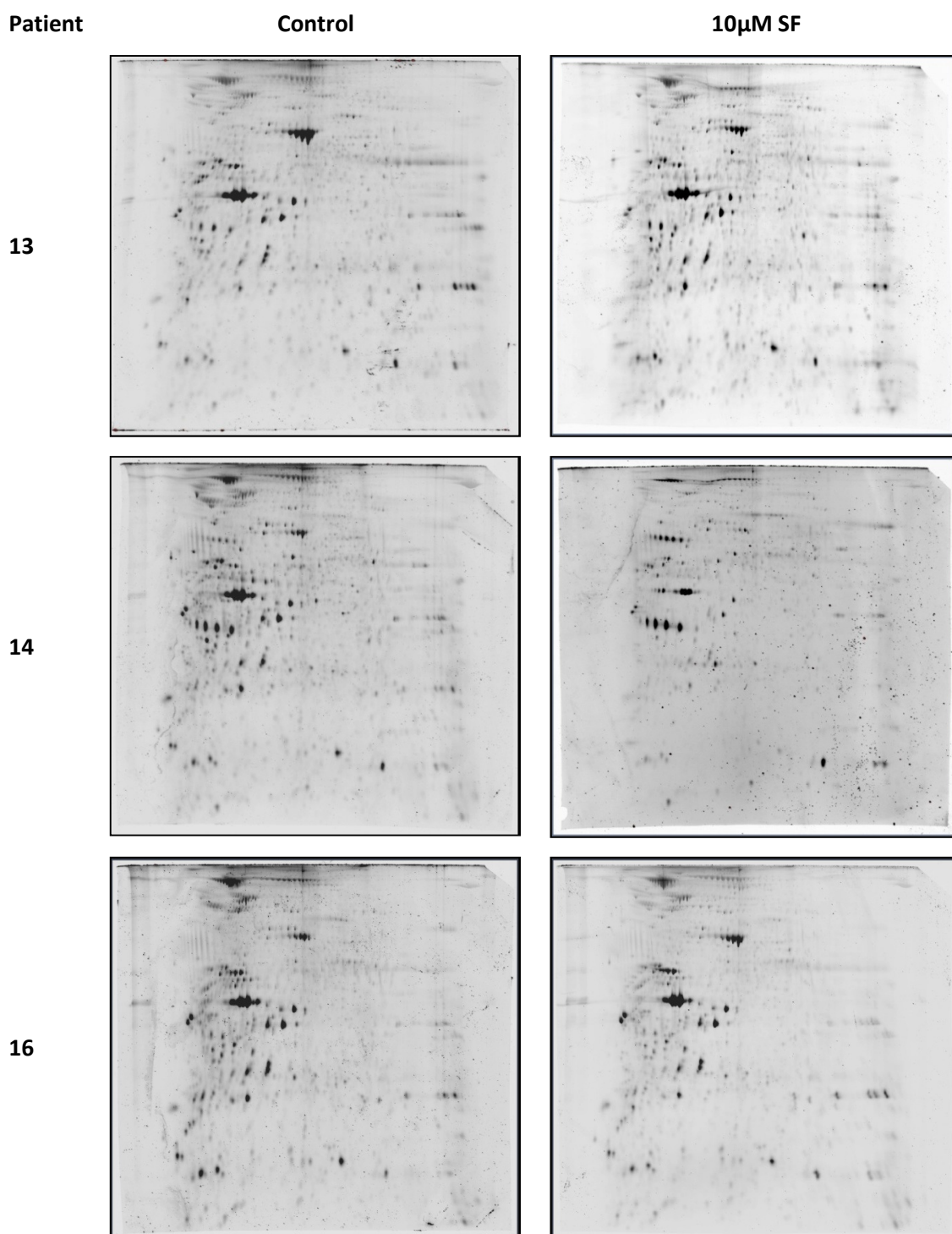


Figure 4.6. 2D Gels of protein extracted from BPH tissue cultured with or without 10 μ M SF.

BPH tissue from three patients was cultured with or without 10 μ M SF for 24 hours with 3 biological replicates. Protein was extracted and 100 μ g run using 2D gel electrophoresis. A representative 2D gel for each patient with or without 10 μ M SF is shown here.

Table 4.2. Statistical analysis of the sources of variation within the 2D gels.

Variable	Patient	Replicate	p-value	
Replicate	All	All	<0.001	
	All	Replicate 2 removed	0.0462*	
	All control	All	0.068	
	13 control	All	0.649	
	14 control	All	0.614	
	16 control	All	0.0072	
			1 vs 3	0.734
			2 vs 3	0.0073
			1 vs 2	0.061
	All 10 μ M SF	All	0.672	
	13 10 μ M SF	All	0.645	
	14 10 μ M SF	All	0.812	
	16 10 μ M SF	All	0.503	
	Patient	All control	Replicate 2 removed	0.001*
		13 vs 14 control	All	0.343
		13 vs 16 control	Replicate 2 removed	0.037*
14 vs 16 control		Replicate 2 removed	<0.001*	
Treatment (10μM SF)	All	Replicate 2 removed	<0.001*	
	13	All	0.0037	
	14	All	<0.001	
	16	Replicate 2 removed	0.9265*	

BPH tissue from three patients (patients 13, 14 and 16) was cultured with or without 10 μ M SF for 24 hours with three biological replicates. Protein was separated by 2D gel electrophoresis and the resulting gels compared using SameSpots software. Statistical analysis was performed to determine the sources of variation within the experiment: patient, replicate and treatment. ANOVA (1-way and repeated measures), and Tukey HSD tests were used to calculate significance as appropriate. The data shows replication error from replicate 2 of the patient 16 control group. Patient 16 was significantly different to patients 13 & 14 at baseline whereas patient 13 & 14 were not significantly different. Patients 13 & 14 were significantly affected by treatment whereas patient 16 was not. *Replicate 2 of patient 16 control was found to be statistically significantly different to other replicates, so replicate 2 of all patients, with or without 10 μ M SF, are excluded from analysis when the analysis includes patient 16 control group.

4.3.2 Selection of protein spots for identification

After analysis of the sources of variation within the 2D gels, individual spots were then analysed to identify individual spots that were significantly altered either due to natural variation between the patients at baseline (patient variation), or due to the effect of the 10 μ M SF, either on all the patients as a population, or on each patient individually (treatment variation).

All protein spots were assigned an ID by the SameSpots software, and a value calculated from the spot volume and intensity. These values were then compared between gels using 1-way ANOVA for each spot ID to identify any changes (Table 4.3). Results were not corrected for multiple testing. Instead all spots that were reported to be significantly changed were manually visually assessed to verify the statistical result. Any 'false positives' obtained due to artefacts, such as excess SYPRO staining, were eliminated resulting in a list of spots to be picked for identification (Table 4.3). Spots chosen for identification are shown in Figure 4.7 which demonstrates the position of the spots on the gel for each variable in which the spots selected were altered.

Ten spots were identified as significantly variable between patients without SF treatment (Figure 4.7a), and 4 spots were significantly altered in all 3 patients after SF treatment (Figure 4.7b). For patients 13, 14 and 16, 20, 38 and 5 spots, respectively, were identified as altered by SF (Figure 4.7a, b, c). From the spots identified as significantly altered, it is clear to see that the greatest number of changes was observed in patient 14, and that patient 13 had almost half that number. In comparison, very few changes were observed in patient 16 as a result of SF treatment. These results correlate with the statistical analysis (Table 4.2), which showed that a greater statistical variation was observed in patient 14 (p-value <0.001) as a result of SF treatment compared to patient 13 and 16 (p-values = 0.0037 and 0.9265 respectively).

Comparison of the spots chosen for identification from the three patients (Figure 4.8) shows there is little overlap between the spots altered and the patients, in fact there is only one spot overlap between patients 13 and 14, another between patient 13 and 16 but none between patient 14 and 16, and none that overlap between all three.

This once again highlights how different patients respond in very different manners to SF treatment. The spread of the spots on the gels also demonstrates that there is no correlation between mass or pI, and the proteins that SF modulated (Figure 4.7).

Table 4.3. Number of spots found to be statistically significantly altered (p-value <0.05) and chosen for identification.

Variable	Statistically Significantly Altered Spots	Spots Picked For Identification
Patient	188	10
Treatment All patients	59	4
Patient 13	78	20
Patient 14	199	38
Patient 16	65	5
TOTAL*	482	70

BPH tissue from three patients (patients 13, 14 and 16) was cultured with or without 10 μ M SF for 24 hours in triplicate. Protein was run on by 2D gel electrophoresis and the resulting gels compared using SameSpots software. The spots found to be statistically significantly altered were identified by statistical analysis of the data generated by the SameSpots software. Each spot was then manually assessed and any ‘false positives’ obtained due to artefacts were eliminated resulting in the spots picked for identification. The effect of patient was measured in the control group. Statistics were not adjusted for multiple testing. *Due to overlap between spot IDs in the different variable groups the totals are less than the sum of spots in each column.

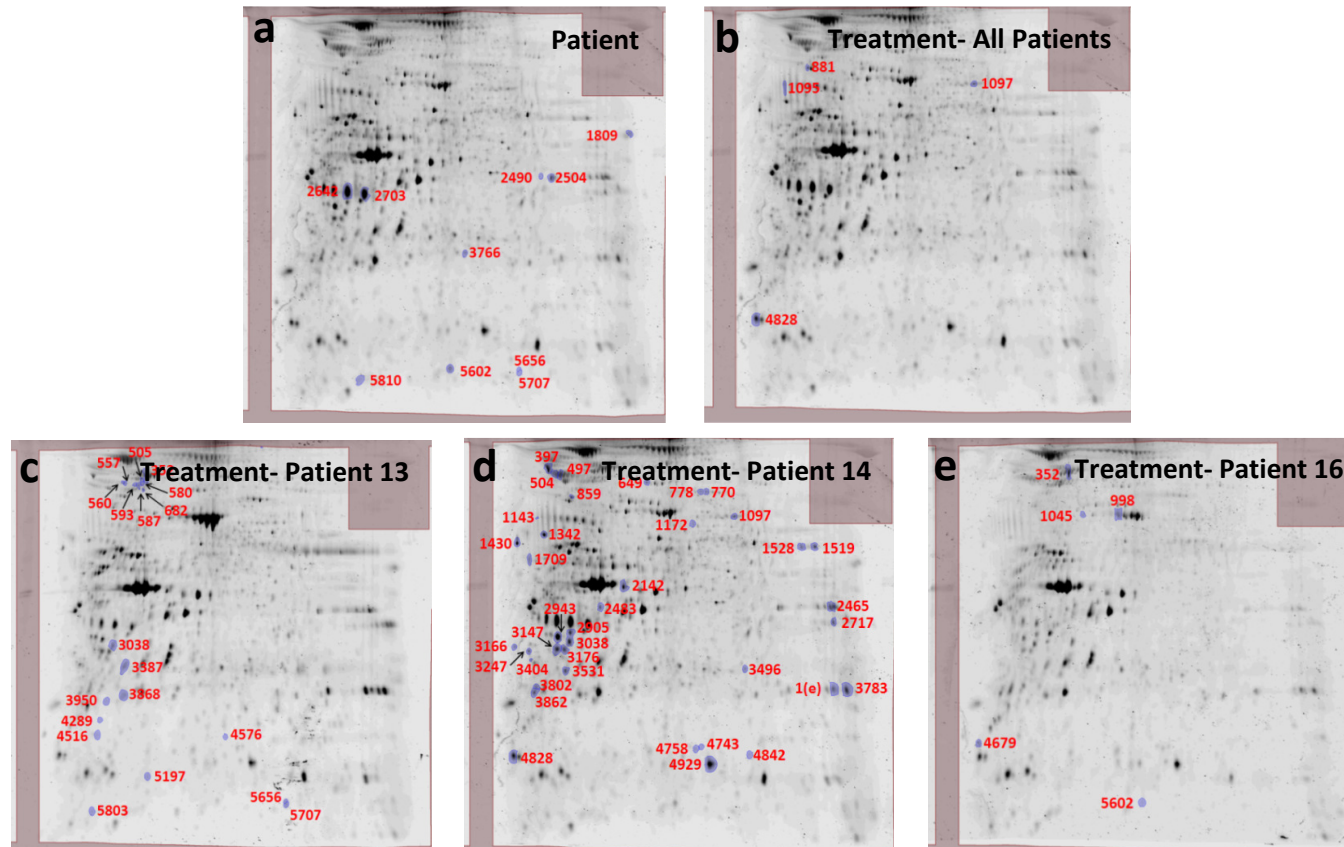


Figure 4.7. Spots picked for identification.

BPH tissue from three patients (patients 13, 14 and 16) was cultured with or without 10 μ M SF for 24 hours in triplicate. Protein was run by 2D gel electrophoresis and the resulting gels compared using SameSpots software. Spots found to be significantly altered and chosen for identification due to different sources of variation are shown on example gels: (a) patient variation, and treatment effect on (b) all patients, (c) patient 13, (d) patient 14 and (e) patient 16.

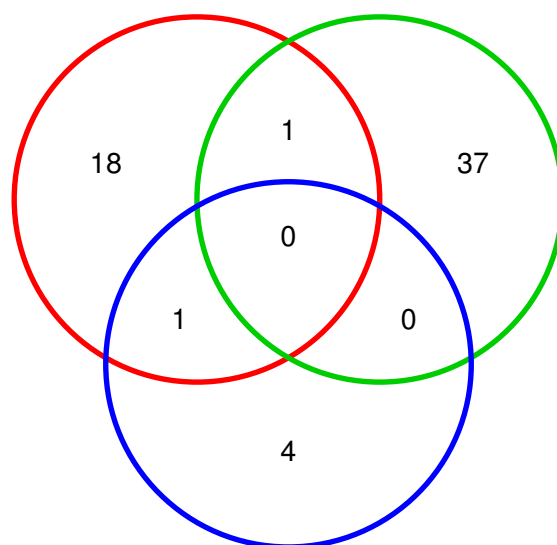


Figure 4.8. Overlap between spots picked for identification due to the effect of SF on each patient.

This Venn diagram shows the overlap between the spot IDs identified as altered due to the effect of 10 μ M SF on BPH tissue in culture, and selected for protein identification in the tissue samples from the three patients. Red = patient 13, green = patient 14, blue = patient 16.

4.3.3 Identification of proteins

Spots chosen for identification were picked and underwent in-gel Trypsin digestion. The resulting peptides were analysed on an LTQ-Orbitrap Mass Spectrometer and the proteins identified by Mascot. From the 70 spots analysed (Table 4.3), 55 positive identifications were made, the remaining 15 were not identified, either as protein levels were below the detectable limit, or the score returned in Mascot did not reach the arbitrary threshold of significance. The positions of the spots that were successfully identified are shown in Figure 4.9, and their corresponding protein identifications listed in Table 4.4.

Proteins were identified from Mascot results using the method described in Chapter 4.2.8. In most cases where proteins were identified, several were found in each spot. To reduce the complexity, those identifications that returned a score of <100 were immediately eliminated as these were assumed to be minor components within the spot. The mass and pI of the remaining IDs were compared to the position of the spot on the gel, and any that did not correspond were also discounted.

Finally, sequence coverage was assessed to determine the likelihood of a true identification. In some cases, if there was good coverage in a specific section of the sequence, fragmentation of the protein was considered, and the mass and pI of the proposed fragment calculated. The calculated mass and pI was compared to the position of the spot on the gel to decide whether this was a possible ID.

Of the 55 spots that were positively identified, 12 were identified as possible fragments. The pI and mass for both the whole protein, and the possible fragment, is listed in Table 4.4.

For some spots more than one possible identification was made as, using the above steps, a single identification could not be arrived at, so both possible IDs have been listed. From the 55 spots that returned a positive ID, 11 of these have more than one possible protein ID.

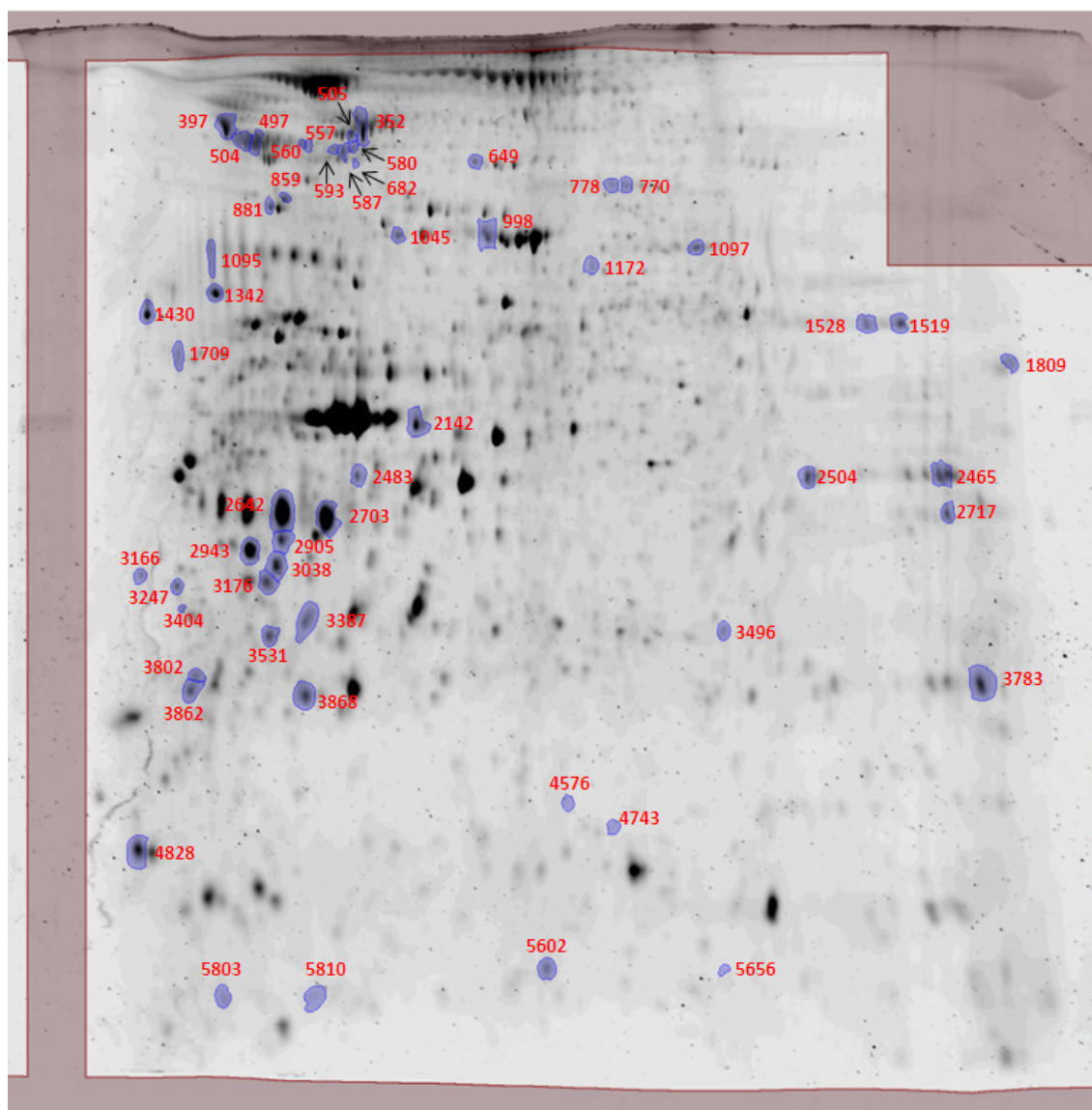


Figure 4.9. Spots identified from 2D Gels.

BPH tissue from three patients (patients 13, 14 and 16) was cultured with or without 10 μ M SF for 24 hours in triplicate. Protein was run by 2D gel electrophoresis, the resulting gels compared using SameSpots software and spots selected for identification. Protein spots of interest were excised from the gel using the ProPick (Genomic Solutions), and in-gel Trypsin digested. The resulting peptides were analysed on an LTQ-Orbitrap Mass Spectrometer (Thermo), and the proteins identified by Mascot (Matrix Sciences). An example gel is shown, with spots labelled corresponding to Spot ID in table 4.4, spots that were picked but had no positive ID returned by mass spectrometry are not shown.

Table 4.4. Identification of protein spots by mass spectrometry.

Spot ID	Protein	Score	Coverage (%)	Accession No.	Mass (kDa)	pI
352	Myosin-11	5523	18	Q3MIV8	225(86)	5.44(5.17)
397	Endoplasmic	2212	38	P14625	92696	4.76
497	Fibulin-1	1698	22	P23142	81	5.07
504	Fibulin-1	923	13	P23142	81	5.07
505	Myosin-11	2506	20	Q3MIV8	224(85)	5.44(5.16)
	Collagen Alpha-3(VI) Chain	409	5	P12111	345(131)	6.26(5.54)
557	Myosin-11	647	8	P35749	228(85)	5.42(5.13)
	Collagen Alpha-3(VI) Chain	266	3	P12111	345(145)	6.26(5.6)
560	Protein Disulfide- Isomerase A4	327	10	P13667	73	4.96
580	Myosin-11	119	3	P35749	228(59)	5.42(5.1)
587	Myosin-11	3259	19	Q3MIV8	224(106)	5.44(5.22)
593	Myosin-11	464	6	Q3MIV8	224(79)	5.44(5.15)
649	Collagen Alpha-3(VI) Chain	759	5	P12111	345(157)	6.26(5.48)
	Filamin-A	487	3	P21333	283(141)	5.7(5.15)
	Alpha-Actinin-1	328	10	P12814	103	5.25
682	Myosin-11	962	11	P35749	228 (85)	5.42 (5.13)
	Collagen Alpha-3(VI) Chain	732	5	P12111	345(119)	6.26 (5.59)
770	Serotransferrin	864	24	P02787	79	6.81
778	Serotransferrin	812	23	P02787	79	6.81
859	Protein Disulfide- Isomerase A4	366	10	P13667	73	4.96
881	Lumican	282	15	P51884	38	6.16
998	Serum Albumin	692	29	P02768	71	5.92

[CONTINUED]

[TABLE 4.4 CONTINUED]

1045	Collagen Alpha-3(VI) Chain	338	3	P12111	345(116)	6.26 (5.53)
	Heat Shock 70 kDa Protein 1A/1B	211	17	P08107	70	5.48
1095	78 kDa Glucose- Regulated Protein	1897	37	P11021	72	5.07
1097	ATP Synthase Subunit Alpha, Mitochondrial	1463	34	P25705	59	9.16
1172	Keratin, Type II Cytoskeletal 1	392	8	P04264	66 (31)	8.15 (4.83)
1342	Protein Disulfide- Isomerase	334	19	P07237	57	4.76
1430	Calreticulin	226	15	P27797	48	4.29
1519	ATP Synthase Subunit Alpha, Mitochondrial	1950	42	P25705	59	9.16
1528	ATP Synthase Subunit Alpha, Mitochondrial	1218	36	P25705	59	9.16
1709	Fibulin-5	424	17	Q9UBX5	52	4.58
1809	Trifunctional Enzyme Subunit Beta, Mitochondrial	418	19	P55084	51	9.45
	Elongation Factor 1- Alpha	250	12	P68104	50	9.10
2142	Creatine Kinase B-Type	777	27	P12277	42	5.34
2465	Glyceraldehyde-3- Phosphate Dehydrogenase	216	44	P04406	36	8.57
2483	Actin, Cytoplasmic 2	399	16	P63261	42	5.3
2504	Annexin A2	1148	58	P07355	38	7.57
2642	Tubulin Beta-2C Chain Actin, Alpha Skeletal Muscle	208	14	P68371	50	4.79
		204	14	P68133	42	5.23

[CONTINUED]

[TABLE 4.4 CONTINUED]

2703	Actin, Alpha Skeletal Muscle Microfibril- Associated Glycoprotein 4	175	12	P68133	42	5.23
		150	23	P55083	28	5.38
2717	L-Lactate Dehydrogenase A Chain	318	17	P00338	36	8.44
2905	Actin, Gamma-Enteric Smooth Muscle Keratin, Type 1 Cytoskeletal 10- Fragment	664	28	P63267	42	5.31
		374	16	P13645	34	4.62
2943	Annexin A5	2239	42	P08758	35	4.94
3038	Actin, Aortic Smooth Muscle	793	44	P62736	42	5.23
3166	Keratin, Type I Cytoskeletal 16- Fragment	152	22	P08779	51(41)	4.99(4.82)
3176	Keratin, Type II Cytoskeletal 1- Fragment	710	13	P04264	66	8.15
3247	14-3-3 Epsilon	2634	55	P62258	29	4.63
3387	Actin, Cytoplasmic 2	434	18	P63261	42	5.31
3404	14-3-3 Theta	671	32	P27348	28	4.68
3496	Triosephosphate Isomerase	703	61	P60174	26	6.45
3531	Actin, Alpha Skeletal Muscle	377	20	P68133	42	5.23
3783	Transgelin	889	47	Q01995	22	8.87

[CONTINUED]

[TABLE 4.4 CONTINUED]

3802	Keratin, Type II					
	Cytoskeletal 1	908	15	P04264	66(32)	8.15(4.9)
	Desmin- Fragment	607	21	P17661	53	5.21
3862	Desmin	469	14	P17661	53	5.21
3868	Actin, Aortic Smooth					
	Muscle	733	23	P62736	42	5.23
4576	Heat Shock Protein Beta					
	6	426	30	O14558	17	5.95
4743	Transgelin- Fragment	321	47	Q01995	22	8.87
4828	Myosin Light Chain 6B	1249	22	P14649	22	5.56
5602	Keratin, Type II					
	Cytoskeletal 1- Fragment	636	9	P04264	66	8.15
5656	Keratin, Type II					
	Cytoskeletal 1- Fragment	230	6	P04264	66	8.15
5803	Keratin, Type II					
	Cytoskeletal 1- Fragment	197	6	P04264	66	8.15
	Actin, Aortic Smooth Muscle- Fragment	171	7	P62736	42	5.23
5810	Keratin, Type I					
	Cytoskeletal 10- Fragment	315	9	P13645	59	5.13

BPH tissue from three patients (patients 13, 14 and 16) was cultured with or without 10 μ M SF for 24 hours in triplicate. Protein was run on by 2D gel electrophoresis, the resulting gels compared using SameSpots software and spots selected for identification. Protein spots of interest were excised from the gel using the ProPick (Genomic Solutions) and in-gel Trypsin digested; the resulting peptides were analysed on an LTQ-Orbitrap Mass Spectrometer (Thermo) and the proteins identified by Mascot (Matrix Sciences). Masses and pIs given in brackets are estimated for a predicted fragment according to the sequence coverage.

4.4 Discussion

4.4.1 Sources of Variation

Within the experiment there were four main sources of variation: replication, patient, treatment and technology. The aim of this experiment was to measure the variation of the SF treatment, but to ensure high quality significant results, the effect of replication, patient and technical variation first had to be assessed.

4.4.1.1 Replication

Analysis of replication variability revealed little difference between replicates, the only variation that was observed was that replicate 2 of patient 16 in the control group was significantly different to the other replicates (Table 4.2). As the variability between all other replicates was insignificant, it was decided to exclude replicate 2 of all patients and treatments when performing analysis that would otherwise include replicate 2 of the patient 16 control group. This decision was made to ensure balanced statistical analysis, although as a result some statistical power was lost.

The source of this variation could be either of two things, either this replicate was biologically different to the other replicates, or technical error may have occurred resulting in the significant variation. Without running this replicate again by 2D gel electrophoresis, to confirm or eliminate technical error, it is difficult to identify the cause of the variation. Due to the good replication seen in all other samples, treating this replicate as an anomaly, and excluding it from analysis, seemed the fairest decision to prevent any skewing of results.

4.4.1.2 Patient

To understand any effect of SF treatment, it was first necessary to look at variability in the untreated patient samples, due to the natural variation that is known to exist in humans.

Altered gene expression is commonly used to describe and explain many diseases, including cancer, but it is possible that many of these changes may not actually be specific to disease, but related to other factors such as polymorphisms among individuals and populations. Natural variation within humans arises not only from inherited genes but also from

environmental factors such as lifestyle, diet, and aging. Natural variation has been widely reported, but little research has investigated how significant this effect can be.

To investigate this precise question, Whitehead and Crawford examined the expression of 192 metabolic genes in a fish model. They reported that the expression of 48% of the genes altered between individuals in the same population, despite being raised in controlled conditions [184]. As a result, they suggested the same variation in gene expression would be expected in humans, and highlighted the need for biological replicates in order to ascribe differences in gene expression to treatment, rather than inter-individual variation.

The variation between individuals found by Whitehead and Crawford [184] was very high compared to other studies, in which natural variation of 24 and 25% has been reported in yeast and *Drosophila* respectively. The high variation in the study by Whitehead and Crawford may be explained by the targeted measurement of metabolic genes only. A separate study, by Oleksiak and colleagues [185], using the same fish model reported 18% of genes varied. However, they measured 907 genes, compared to the 192 assayed by Whitehead and Crawford. The 18% variation observed by Oleksiak and colleagues more closely matched the variation reported in other models.

Variation has also been investigated in human samples, with a study of gene expression patterns in human blood reporting variation in 370 genes between samples. These changes were attributed to factors such as relative proportions of specific cell subsets, gender, age, and time of day that the samples were collected at [186]. Human variation was also considered an important factor in a study by Bouwman and colleagues, who noted the importance of replicate number as a result of this variation, and also due to the subtlety of the effects that are normally induced by dietary agents [178].

In the study performed here, out of the tissue from three patients analysed, it was interesting to note that global protein expression at baseline in patients 13 and 14 was similar, but that in patient 16 was significantly different (Table 4.2). Out of the 1817 spots assigned an ID, 188 (10%) were noted as statistically significantly varied between patients at baseline, but after manual assessment only 10 were selected for identification (Table 4.3). Whether the natural variation observed between patients resulted from the expression of different proteins (eg. patient 13 expressed protein A whilst patient 14 expressed protein B), or significant

differences in the levels of protein expression (eg. patients 13 and 14 both expressed protein A but it is expressed at a significantly higher level in patient 14) is unknown. However, this highlights the natural variation which exists between patients, and therefore needs to be considered when analysing the effect of SF treatment on the different patients.

4.4.1.3 Technical

A further source of error arose in the automatic selection and value calculation of the spots by SameSpots software, leading to the need for the manual assessment of the spots. During the initial stages of spot selection and gel alignment, such error occurred due to the size or shape of the spot, as sometimes the automatic selection would create multiple spots from a spot that, upon manual inspection, would be analysed as a whole (Figure 4.10a). Once the gels were correctly aligned and the spot selection verified, the gels were analysed, producing a list of spot IDs that were statistically significantly altered. All such spots were then manually assessed for any artefacts that may affect the analysis and produce false positives. The two main factors that were looked for were excess Sypro spots and watermark spots.

Excess Sypro spots occur where the surface of the gel is not perfectly smooth forming small pockets where the Sypro stain gets trapped, causing small intense spots. Although these pockets are very small and the program does not identify them as spots, if they are within the selection boundary of a spot they are included in the calculation of the spot value. As they are often intensely stained, their inclusion can skew the spot value, so that upon statistical analysis a false positive or negative may be obtained (Figure 4.10b).

Further to this, the SameSpots programme is highly sensitive, and can therefore detect very small changes in the gel image. Due to this, it can detect and select altered spots that would be missed by the naked eye. However, this sensitivity can lead to the detection of spots that appear to be no more than a watermark, so these kinds of spots were eliminated as they may not be a true result of the sample. In addition, the level of any protein in such spots is at the limit of detection so would result in huge variability in identification (Figure 4.10c).

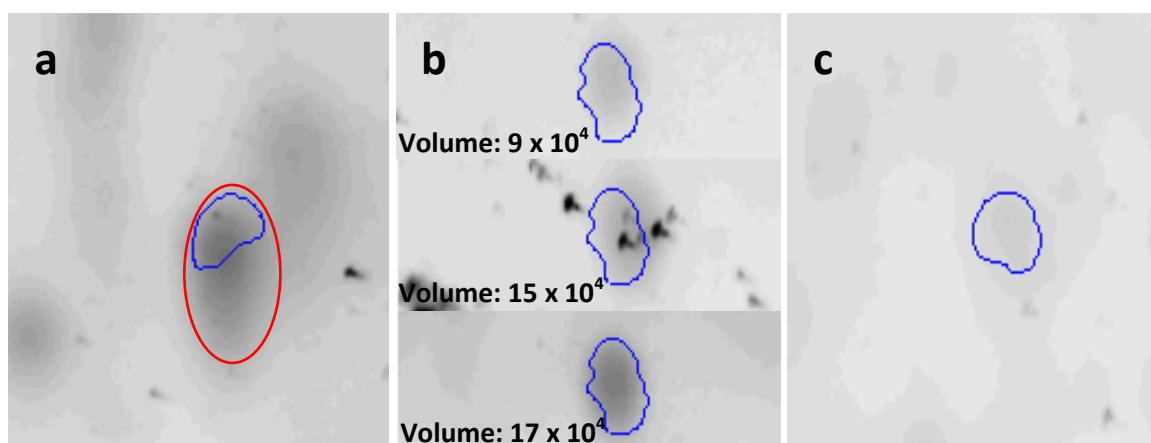


Figure 4.10. Technical Sources of Error in 2D Gel Analysis.

Example images of sources of error that can affect the analysis of 2D gels. All gels are assessed manually to identify and correct these errors. (a) Spot splitting: Automatic spot selection using SameSpots can sometimes result in spots being ‘split’ by the software but can be corrected manually. The blue selection is the spot selected by SameSpots, the red selection shows the approximate area that would be selected as a spot after manual correction. (b) Excess Sypro staining: small indents in the gel surface form pockets trapping Sypro stain, and producing small intense spots that can interfere with spot value calculation, and therefore analysis. In the middle image, within the blue boundary is a Sypro spot, without this spot the staining of the selected area is visibly less intense than that in the lower image and at a similar level to that in the top image. However, due to the Sypro spot the calculated value of the spot in the middle image (15×10^4 units) is closer to that of the lower image (17×10^4 units) than the top image (9×10^4 units). This would therefore affect any statistical analysis performed, so such spots need to be identified manually and this artefact noted, so as not to produce any false results. (c) Watermark spot: SameSpots is highly sensitive and can detect changes in the gel image that the naked eye would otherwise miss leading to the selection of spots that look like watermarks. Such spots are not selected for identification as these spots may not be a true result of the sample, and the level of protein in such spots is at the limit of detection so would result in huge variability in identification.

4.4.2 The effect of SF on global protein expression

Treatment with 10 μ M SF had a highly significant effect on the global protein expression (p-value <0.001) in the patients when analysed as a whole population. A total of 59 spots were identified as altered, although only 4 were chosen for identification (Table 4.3).

When analysed individually, both patient 13 and 14 responded significantly (p-values = 0.0037 and <0.001 respectively), patient 14 especially so, but no effect was observed on patient 16 (p-value = 0.9265) (Table 4.2). These results correspond with the number of spots that were found to be statistically significantly altered; 78 in patient 13, 199 in patient 14, and 65 in patient 16. However, only 20, 38 and 5 spots were selected for identification respectively (Table 4.3). Interestingly, there was very little overlap between the proteins altered in the three patients (Figure 4.8).

These results show that in a population you would expect sulforaphane, or the consumption of broccoli, to have an effect on protein expression in the prostate. This corresponds with previous research that has shown the consumption of cruciferous vegetables can modify disease risk [52, 70, 72-75]. However, the individual nature of the response of each patient highlights the natural variation present in human tissue. This demonstrates the different ways by which tissue can respond to the same treatment, and therefore the necessity for larger patient numbers when dealing with human samples in order to obtain data of wider significance.

4.4.3 Spots chosen for identification

Out of all the spots chosen for identification it is interesting to note that the positions of the spots are widely spread over the gel, indicating that none of the sources of variation affect proteins with a particular mass or pI (Figures 4.7). There are some areas of the gel that comparatively have a higher percentage of the gel IDs within them, but these correspond to areas that have a greater protein density, in particular towards the lower end of the pH scale and in the top half of the mass scale. Some of these spots appear to be in 'sets' or run together, so it may be these proteins are highly homologous, or belong to the same family of proteins. Therefore, they may have similar properties, so in samples where one member of a family has greater expression, another member of the same family may be reduced, the expression pattern of which may then be reversed in a different sample.

4.4.4 Identification of proteins

Out of the 70 proteins that were picked for identification, only 55 returned a positive ID (Table 4.4). This may be because the amount of protein in the spot was too low, and therefore below the detection limit of the mass spectrometry. In other cases protein was detected, but the score returned was <100, which was set as an arbitrary threshold of significance. Scores below this were rejected and therefore no positive ID made.

It is difficult to assess the success of the identification rate, here it was 71%, as papers do not generally state whether the number of spots identified was the same as the number picked. However, from the data that is available I would suggest that the identification rate compares favourably. Polley and colleagues [187] did not specify how many spots were picked for identification but they identified 26 spots out of a possible 291 as they stated that the others were too weakly expressed to be identified. Lee and colleagues [180] successfully identified all spots selected, but as they only selected the 9 spots from a possible 300 which were noted as altered, they increased their chances of success by only selecting spots with high expression. In comparison, in the study performed here, all spots identified as altered were selected. As a result, it is not surprising that not all spots picked were identified in this study as they were not selected based on expression strength, so it is in line with previous data that weaker spots were not identified.

After Trypsin-digestion, the resulting peptides were analysed by mass spectrometry in batches on a number of different runs. On the first run, an error occurred with the machine and only partial identifications obtained. These spots were re-picked and identified. For the majority of the samples that had returned a result on the original run, the new run produced the same outcome further verifying these identifications. As the same results could be obtained from the same spot from different gels, this indicates good reproducibility of results, and therefore greater confidence that the results obtained are correct. It is good practice to replicate analysis of proteins by mass spectrometry to demonstrate reproducibility of results but this is often not done due to cost limitations.

Some of the spots identified had more than one possible protein ID returned that could not be eliminated, and as a result, all probable IDs for that spot are listed (Table 4.4). For example, spot 649 returned three possible IDs, two of which may be fragments, whilst spot 2642 could be one of two proteins, or a combination of both. Such results suggest sequence homology

between proteins, or may be due to more than one protein being present in the spot, so the multiple identifications may actually be representative of the spot picked. In the majority of cases, a single identification could be reached by comparison of mass, pI and sequence coverage, but in some cases all values were highly comparable and therefore no single ID could be arrived at.

4.4.5 Conclusions

2D gel electrophoresis produced good replication, and was a reliable method for the unbiased detection of protein changes, although there were limits, such as the identification of low volume spots. The results demonstrate that global protein expression naturally varies in BPH samples between individuals.

It is also clear to see that biologically relevant levels of SF can significantly alter global protein expression in BPH tissue after 24 hours of culture, but that individual patients respond in varying manners. These results demonstrated that natural variation was highly apparent in the patients, both at baseline and in their response to SF. This highlights the need to use large sample numbers to obtain results that can be considered representative of the general population. The biological role of the proteins identified and any previously reported relationships with SF are discussed in the next chapter.

Chapter Five

Analysis of Proteins Altered in BPH Tissue

Chapter 5. Analysis of proteins altered in BPH tissue

5.0.1 Summary

In the previous chapter, protein extracted from BPH tissue from three patients, cultured with or without 10 μ M SF in triplicate, was separated by 2D gel electrophoresis. The resulting protein spots that were altered, either between patients at baseline, or as a result of SF treatment, were identified by mass spectrometry. Of the 70 spots chosen for identification, 55 returned a positive ID, of which there were only 37 unique proteins. The proteins identified are discussed in this chapter.

Analysis of the proteins using the Gene Ontology website, indicated five main biological processes that the proteins were involved in, and the majority of the proteins could be sorted into three molecular function groups. The greatest overlap between the two sets of groups was between the molecular chaperone functional group, and the apoptosis biological process group. Apoptosis is a critical biological process, so the proteins that overlapped between the groups were chosen for further analysis. These proteins were HSP90 β 1, calreticulin, 14-3-3 ϵ , GRP78 and HSP70.

These results demonstrate that SF is capable of altering proteins involved in biological processes critical to normal cell function. Dysregulation of molecular chaperones has been implicated in disease, including cancer, so it is interesting that SF can alter these proteins. Little research has been done with regard to the effect of SF on molecular chaperones, so this may be a promising area of research.

5.1 Introduction

Previously, protein extracted from BPH tissue, cultured with and without 10 μ M SF for 24 hours, was analysed using 2D gel electrophoresis. From this untargeted approach, a number of spots that altered either between patients due to natural variation, or as a result of SF, either in one patient, or in the patients as a whole population, were selected. Using mass spectrometry, the protein identity of these spots was discovered. In this chapter, the proteins identified as altered are discussed, and any patterns in the molecular functions and biological processes these proteins are involved in are analysed. This analysis was performed to identify a possible novel target of SF activity for further investigation.

The proteins are classified using the Gene Ontology (GO) website [188]. The GO website is a database designed to provide consistent descriptions of gene products in terms of their associated biological processes, molecular functions, and cellular components. In this chapter, the biological processes and molecular functions are discussed. According to the GO website a biological process is defined as being a 'collection of molecular events with a defined beginning and end', whilst molecular function refers to the job or abilities of a particular protein [189]. Therefore, a molecular function can describe the job that a protein does within a biological process. Depending on the particular abilities of a protein, a single protein can be capable of performing multiple molecular functions in multiple biological processes. Use of the GO classifications will allow the proteins identified to be grouped and compared more easily in order to identify any patterns in the functions and processes altered.

5.2 Methods

5.2.1 Classification of proteins by molecular function and biological process

The 55 spots (Table 4.4) successfully identified in the Chapter 4 were searched on the GO website (www.geneontology.org) [188], and grouped according to molecular functions and biological processes. Many proteins were involved in multiple molecular functions and biological processes, therefore, proteins were classified so as to minimise the number of groups in order to discover the most common biological processes and molecular functions the proteins were involved in.

5.3 Results

5.3.1 Analysis of proteins significantly altered between 2D gels

Spots that were found to be significantly altered were identified by mass spectrometry (see Chapter 4), and separated into groups depending on the variable, baseline variation or effect of SF, due to which they altered.

In total, fifty five spots were positively identified (Figure 5.1). Seven varied between the patients at baseline (Table 5.1), three were altered as a result of 10 μ M SF in the patients analysed as a population (Table 5.2), and fifty were altered in the individual patients treated with SF: fourteen altered in patient 13 (Table 5.3), thirty two in patient 14 (Table 5.4) and four in patient 16 (Table 5.5). There was a total overlap of five spots between all the groups (baseline and SF treated).

Two of the spots which naturally varied between the patients at baseline were also found to be altered by 10 μ M SF, one in patient 13 (spot 5656) and the other in patient 16 (spot 5602). Of the three spots identified as altered by SF in the patients analysed as a population one of these was also altered in patient 14 (spot 4828) when analysed individually. Of the spots found to be altered in the individual patients in response to SF, one spot was found to be altered in patient 13 and 14 (spot 3038), and another was altered in patients 13 and 16 (spot 352), but there was no overlap between patients 14 and 16.

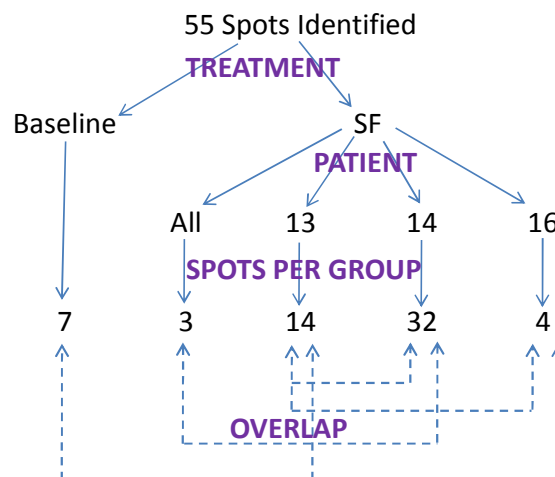


Figure 5.1. Spots significantly altered between BPH samples ran by 2D gel electrophoresis.

Diagram showing the grouping of the spots identified from the 2D gels as they were found to be altered due to either baseline variation or in response to 10 μ M SF. Overlap between groups also displayed.

Of the seven spots that were altered between the patients without SF treatment, three were found to have multiple possible IDs, whilst the other four all had a single ID, three of which were keratins (Table 5.1).

Table 5.1. Fold-change of proteins identified as statistically significantly ($p \leq 0.05$) different between individuals at baseline.

Spot ID	Protein	Fold-Change		
		13vs14	13vs16	14vs16
1809	Trifunctional Enzyme Subunit Beta, Mitochondrial Elongation Factor 1-Alpha 1	0.87	0.43	0.49
2504	Annexin A2	0.84	0.54	0.65
2642	Tubulin Beta-2C Chain Actin, Alpha Skeletal Muscle	1.50	0.49	0.32
2703	Actin, Alpha Skeletal Muscle Microfibril-Associated Glycoprotein 4	1.74	0.49	0.28
5602	Keratin, Type II Cytoskeletal 1- Fragment	1.48	0.69	0.47
5656	Keratin, Type II Cytoskeletal 1- Fragment	0.44	0.22	0.50
5810	Keratin, Type I Cytoskeletal 10- Fragment	1.22	2.63	2.16

BPH tissue from three patients (patients 13, 14 and 16) was cultured for 24 hours in triplicate. Protein was run by 2D gel electrophoresis, the resulting gels compared using SameSpots software, and spots selected for identification.

In the patients analysed as a population, three spots were altered, all of which were identified as single and differing IDs (Table 5.2).

Table 5.2. Fold-change of proteins identified as statistically significantly ($p > 0.05$) altered in the population as a whole as a result of sulforaphane treatment.

Spot ID	Protein	Fold-Change
881	Lumican	1.21
1095	78 kDa Glucose-Regulated Protein	0.62
4828	Myosin Light Chain 6B	0.76

BPH tissue from three patients (patients 13, 14 and 16) was cultured with or without 10 μ M SF for 24 hours in triplicate. Protein was run by 2D gel electrophoresis, the resulting gels compared using SameSpots software, and spots selected for identification.

Of the fourteen spots altered by SF in patient 13, four spots returned multiple possible IDs, but three of these spots were identified as myosin-11 (MYH11) and collagen alpha-3 (VI) chain (COL6A3). The remaining ten spots each had single IDs, four of which were identified as MYH11, three as actins, and the remaining three all had different IDs (Table 5.3).

Table 5.3. Fold-change of proteins identified as statistically significantly ($p \leq 0.05$) altered in patient 13 as a result of 10 μ M SF treatment.

Spot ID	Protein	Fold-Change
352	Myosin-11	1.29
505	Myosin-11	1.21
	Collagen Alpha-3(VI) Chain	
557	Myosin-11	0.42
	Collagen Alpha-3(VI) Chain	
560	Protein Disulfide-Isomerase A4	0.59
580	Myosin-11	1.45
587	Myosin-11	2.01
593	Myosin-11	1.83
682	Myosin-11	0.26
	Collagen Alpha-3(VI) Chain	
3038	Actin, Aortic Smooth Muscle	1.71
3387	Actin, Cytoplasmic 2	1.44
3868	Actin, Aortic Smooth Muscle	2.03
4567	Heat Shock Protein Beta-6	1.78
5656	Keratin, Type II Cytoskeletal 1- Fragment	0.48
5803	Keratin, Type II Cytoskeletal 1- Fragment	1.25
	Actin, Aortic Smooth Muscle- Fragment	

BPH tissue from patient 13 was cultured with or without 10 μ M SF for 24 hours in triplicate. Protein was run by 2D gel electrophoresis, the resulting gels compared using SameSpots software, and spots selected for identification.

Thirty two spots were found to be altered by SF in patient 14, with only three having multiple possible IDs. Of the spots with single IDs, only three spots were found to be increased by SF, two of which were both identified as serotransferrin (TF). The other twenty six spots were all reduced by SF, and included three spots each identified as fibulin (FBLN), ATP synthase subunit alpha (ATP5A1), and actin. Whilst protein disulfide isomerase, keratin, transgelin (TAGLN), and 14-3-3 proteins, were found in two spots each. The remaining nine spots all had different IDs (Table 5.4).

Table 5.4. Fold-change of proteins identified as statistically significantly ($p \leq 0.05$) altered in patient 14 as a result of 10 μ M SF treatment.

Spot ID	Protein	Fold-Change
397	Endoplasmin	0.41
497	Fibulin-1	0.50
504	Fibulin-1	0.51
649	Collagen Alpha-3(VI) Chain	0.75
	Filamin-A	
	Alpha-Actinin-1	
770	Serotransferrin	2.19
778	Serotransferrin	2.93
859	Protein Disulfide-Isomerase A4	0.25
1097	ATP Synthase Subunit Alpha, Mitochondrial	0.40
1172	Keratin, Type II Cytoskeletal 1	2.32
1342	Protein Disulfide-Isomerase	0.31
1430	Calreticulin	0.15
1519	ATP Synthase Subunit Alpha, Mitochondrial	0.25
1528	ATP Synthase Subunit Alpha, Mitochondrial	0.42
1709	Fibulin-5	0.35
2142	Creatine Kinase B-Type	0.52
2465	Glyceraldehyde-3-Phosphate Dehydrogenase	0.43
2483	Actin, Cytoplasmic 2	0.51
2717	L-Lactate Dehydrogenase A Chain	0.33

[CONTINUED]

[TABLE 5.4 CONTINUED]

2905	Actin, Gamma-Enteric Smooth Muscle Keratin, Type 1 Cytoskeletal 10- Fragment	0.59
2943	Annexin A5	0.46
3038	Actin, Aortic Smooth Muscle	0.54
3166	Keratin, Type I Cytoskeletal 16- Fragment	0.32
3176	Keratin, Type II Cytoskeletal 1- Fragment	0.53
3247	14-3-3 Epsilon	0.26
3404	14-3-3 Theta	0.37
3496	Triosephosphate Isomerase	0.46
3531	Actin, Alpha Skeletal Muscle	0.57
3783	Transgelin	0.34
3802	Keratin, Type II Cytoskeletal 1 Desmin- Fragment	0.42
3862	Desmin	0.41
4743	Transgelin- Fragment	0.53
4828	Myosin Light Chain 6B	0.43

BPH tissue from patient 14 was cultured with or without 10 μ M SF for 24 hours with in triplicate. Protein was run by 2D gel electrophoresis, the resulting gels compared using SameSpots software, and spots selected for identification.

In patient 16, four spots were identified as altered, one of which returned multiple IDs. The other three spots had single IDs (Table 5.5).

Table 5.5. Fold-change of proteins identified as statistically significantly ($p \leq 0.05$) altered in patient 16 as a result of 10 μ M SF treatment.

Spot ID	Protein	Fold-Change
352	Myosin-11	0.82
998	Serum Albumin	2.05
1045	Collagen Alpha-3(VI) Chain Heat Shock 70 kDa Protein 1A/1B	1.91
5602	Keratin, Type II Cytoskeletal 1- Fragment	1.29

BPH tissue from patient 16 was cultured with or without 10 μ M SF for 24 hours in triplicate. Protein was run by 2D gel electrophoresis, the resulting gels compared using SameSpots software, and spots selected for identification.

5.3.2 Biological process and molecular function analysis

A number of the spots analysed were identified as being the same protein, so the list of proteins from the forty eight spots altered by sulforaphane resulted in thirty three different protein IDs. Using the Gene Ontology website, these proteins were then classified into the smallest number of biological process and molecular functional groups possible, to identify if there were any patterns or similarities in the proteins altered in the tissue.

To try and understand the biological relevance of the proteins altered by SF (Table 5.2 – 5.5), they were grouped according to the biological processes in which they were involved. The proteins were classified into five biological process groups, although four additional proteins were unable to be grouped with any others, and were therefore listed in a sixth group called 'Other'. The biological processes identified were (in order of descending number of proteins in the group): apoptosis; metabolism; muscle development and contraction; cell proliferation, adhesion and angiogenesis; cytoskeleton organization; and other (Table 5.6).

According to molecular function the proteins could be sorted in three broad groups, plus a final 'Other' group for those that did not correspond with any other protein molecular functions. The most common molecular function was structure and adhesion, followed by molecular chaperones, and then enzymatic activity (Table 5.7).

Comparison of the Molecular Function and Biological Process groups revealed the greatest overlap between the Enzymatic Activity molecular function group and the Metabolism biological process group with all seven proteins found in both groups. Five proteins overlapped between the Molecular Chaperone molecular functional group and the Apoptosis biological process group. All the members of the Cell Proliferation, Adhesion and Angiogenesis biological process group and all but one of the seven members, HSPB6, of the Muscle Development and Contraction biological process group, were in the Structure and Adhesion molecular function group.

Table 5.6. Proteins identified from 2D gels classified by biological process.

Apoptosis				Metabolism			
14-3-3 Epsilon				ATP synthase subunit alpha, mitochondrial			
Alpha-Actinin-1				Glyceraldehyde-3-phosphate			
Annexin A5				dehydrogenase			
Calreticulin				L-lactate dehydrogenase A chain			
78 kDa Glucose-Regulated Protein				Creatine kinase B-type			
Endoplasmin				Protein Disulfide-Isomerase			
Heat Shock 70 kDa Protein 1A/1B				Protein disulfide-isomerase A4			
Serum Albumin				Triosephosphate Isomerase			
Cell Proliferation, Adhesion and Angiogenesis				Muscle Development and Contraction			
Collagen alpha-3(VI) chain				Actin, alpha skeletal muscle			
Fibulin-1				Actin, gamma-enteric smooth muscle			
Fibulin-5				Desmin			
Keratin, Type I Cytoskeletal 16				Heat shock protein beta-6			
Keratin, Type II Cytoskeletal 1				Myosin-11			
Lumican				Myosin light-chain 6B			
Cytoskeletal Organization				Other			
Actin, cytoplasmic 2				Keratin, Type I Cytoskeletal 10			
Filamin-A				14-3-3 Theta			
				Serotransferrin			

Three BPH tissue samples (patients 13, 14 and 16) were cultured with or without SF for 24 hours in triplicate. Protein was run by 2D gel electrophoresis, the resulting gels compared using SameSpots software, and spots selected for identification. Identified proteins grouped into smallest number of biological processes possible as classified by www.geneontology.org as the majority of proteins are involved in multiple GO biological processes.

Table 5.7. Proteins identified from 2D gels organised into molecular functional groups.

Enzymatic Activity	Structure and Adhesion (ECM, Cytoskeleton, and Muscle)
L-Lactate Dehydrogenase A Chain	Actin, Cytoplasmic 2
Glyceraldehyde-3-Phosphate Dehydrogenase	Actin, Gamma-Enteric Smooth Muscle
Protein Disulfide-Isomerase	Actin, Alpha Skeletal Muscle
Protein Disulfide-Isomerase A4	Alpha-Actinin-1
Creatine Kinase B-Type	Desmin
ATP Synthase Subunit Alpha, Mitochondrial	Filamin-A
Triosephosphate Isomerase	Keratin, Type II Cytoskeletal 1
	Keratin, Type I Cytoskeletal 10
	Keratin, Type I Cytoskeletal 16
	Transgelin
	Collagen Alpha-3(VI) Chain
	Lumican
	Fibulin-1
	Myosin Light-Chain 6B
	Myosin-11
	Fibulin-5
Molecular Chaperones	
14-3-3 Epsilon	
14-3-3 Theta	
Calreticulin	
Endoplasmin	
78 kDa Glucose-Regulated Protein	
Heat Shock 70 kDa Protein 1A/1B	
Others	
Serum Albumin	
Serotransferrin	
Annexin A5	
Heat Shock Protein Beta 6	

BPH tissue from three patients (patients 13, 14 and 16) was cultured with or without 10 μ M SF for 24 hours in triplicate. Protein was run by 2D gel electrophoresis, the resulting gels compared using SameSpots software, and spots selected for identification. Identified proteins grouped into smallest number of molecular functions possible as classified by www.geneontology.org as the majority of proteins have multiple GO Molecular functions.

5.3.3 The link between protein binding proteins and apoptosis

Comparison of the most common molecular functions and biological processes the proteins altered by 10 μ M SF were found to be involved in, revealed overlap between proteins that acted as molecular chaperones and were involved in the apoptotic biological process. These proteins were then selected as possible novel targets for SF activity as, although the effect of SF on apoptosis has been investigated, little research has been conducted regarding SF and molecular chaperones, and their role in the biological process. The five proteins are endoplasmic reticulum chaperone protein (HSP90 β 1), calreticulin (CALR), 14-3-3 ϵ , 78 kDa glucose-regulated protein (GRP78) and heat shock 70 kDa protein 1A/1B (HSP70).

As discussed in the previous chapter, variation was observed in replicate two of patient 16 in the control group, so this data was excluded from any analysis performed. Therefore, the data shown below for the altered spots, includes replicate two in the analysis of patients 13 and 14, but replicate two of patient 16 with and without SF is excluded. When analysed as a population, replicate two of all patients and conditions is excluded, as this corresponds with handling of data in Chapter 4 to ensure balanced statistical analysis.

SF was seen to significantly reduce HSP90 β 1 (Figure 5.2) in patient 14 by 60% (p-value = 0.023), but had very little effect on its expression in the other patients, although a slight increase was observed in patient 16 (p-value = 0.098). Overall, the reduction of HSP90 β 1 in the patients analysed as a whole was not significant (p-value = 0.327).

Calreticulin (Figure 5.3) was also seen to be significantly reduced (p-value = 0.018) by SF in patient 14, although it appeared to be non-significantly increased in patients 13 and 16 (p-values = 0.307 and 0.374 respectively). Overall, in the population, SF did not have a significant effect on calreticulin (p-value = 0.389).

A similar pattern was seen for the effect of SF on 14-3-3 ϵ (Figure 5.4), with its expression being reduced in patient 14 (p-value = 0.02), whilst no significant effect was observed on the other patients (p-values = 0.406 and 0.938 respectively). When analysed as a population no effect was seen (p-value = 0.244).

GRP78 (Figure 5.5) was observed to be significantly decreased in both patients 14 and 16 (p-values = 0.015 and 0.013 respectively), but no effect seen on patient 13 (p-value = 0.645). Due

to the significant effect seen on two patients, the reduction of GRP78 in the group was highly significant (p-value <0.001).

The effect of SF on HSP70 (Figure 5.6) was more complex, with patient 13 showing no effect (p-value = 0.839), patient 14 was observed to be slightly decreased (p-value = 0.057), whilst in patient 16 it was increased (p-value = 0.041). However, overall no effect was noted (p-value = 0.649).

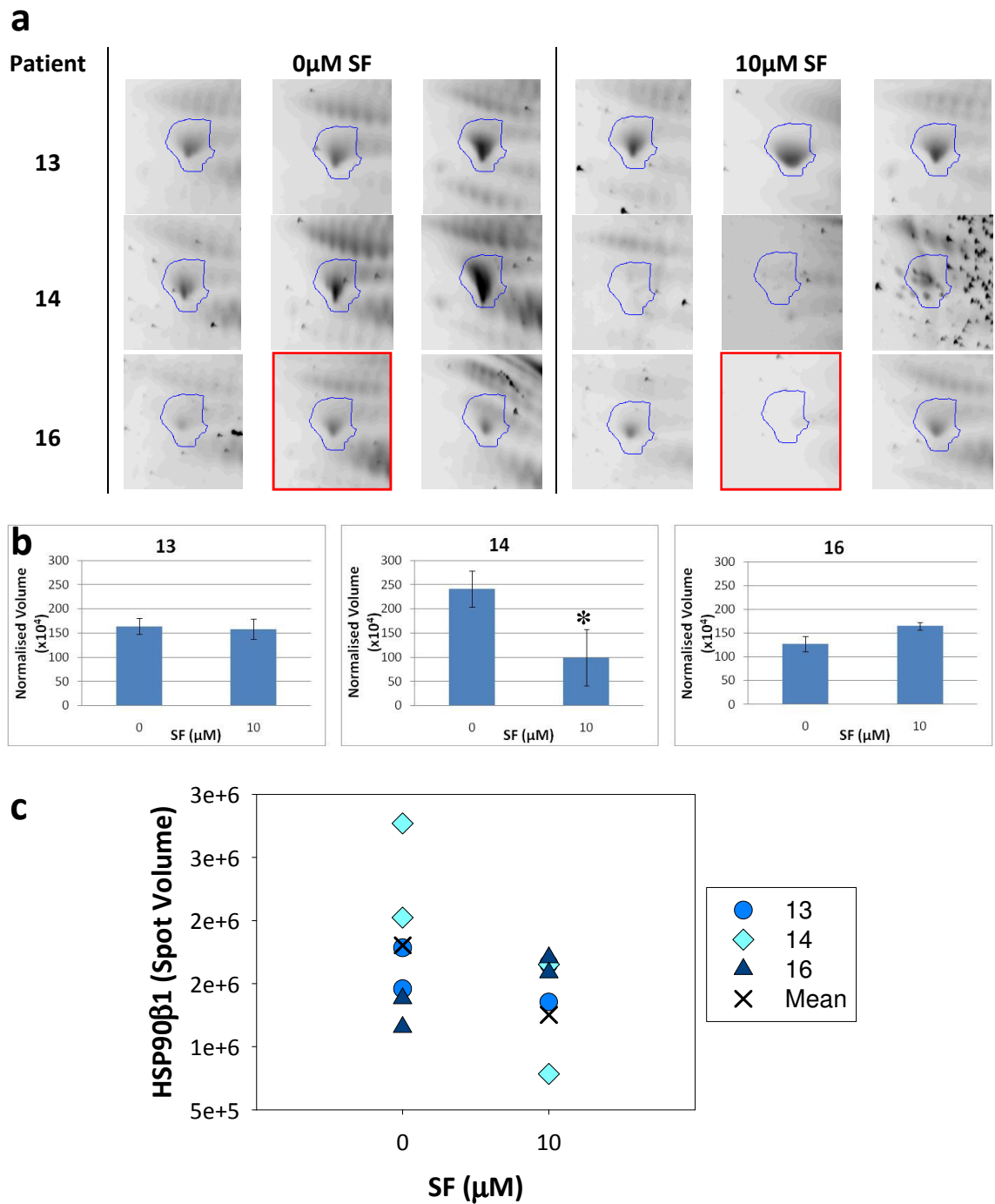


Figure 5.2. The effect of SF on HSP90β1.

BPH tissue from three patients (patients 13, 14 and 16) was treated with or without 10μM SF for 24 hours in triplicate. Protein was extracted, run on 2D gels, and analysed using SameSpots software to identify altered spots which were then identified using mass spectrometry. (a) Images of spot 397, identified as HSP90β1, taken from the 2D gels for each patient with or without 10μM SF in triplicate are shown, and (b) quantified to statistically determine the effect of 10μM SF (Means ± standard deviation are plotted; p-values = 0.735, 0.023, 0.098 respectively). Replicate 2 of patient 16 was excluded from the analysis due to previously noted replication variation (outlined in red in (a)). (c) The effect of SF on the patients as a whole population with replicate 2 removed from all patients (p-value = 0.327). * p-value <0.05.

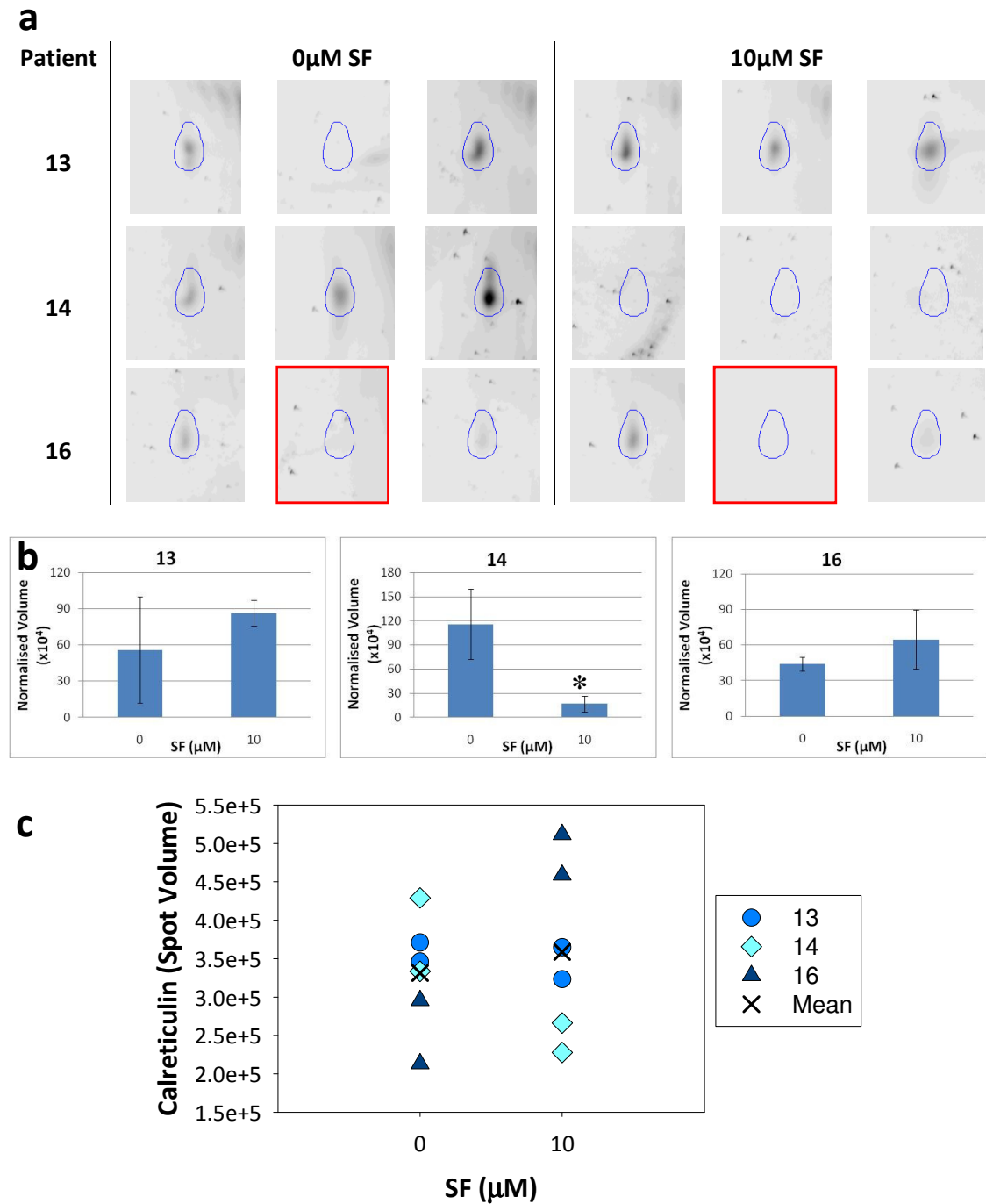


Figure 5.3. The effect of SF on calreticulin.

BPH tissue from three patients (patients 13, 14 and 16) was treated with or without 10μM SF for 24 hours in triplicate. Protein was extracted, run on 2D gels, and analysed using SameSpots software to identify altered spots which were then identified using mass spectrometry. (a) Images of spot 1430, identified as Calreticulin taken, from the 2D gels for each patient with or without 10μM SF in triplicate are shown, and (b) quantified to statistically determine the effect of 10μM SF (Means ± standard deviation are plotted; p values: 0.307, 0.018, 0.374 respectively). Replicate 2 of patient 16 was excluded from the analysis due to previously noted replication variation (outlined in red in (a)). (c) The effect of SF on the patients as a whole population with replicate 2 removed from all patients (p-value = 0.389). * p-value <0.05.

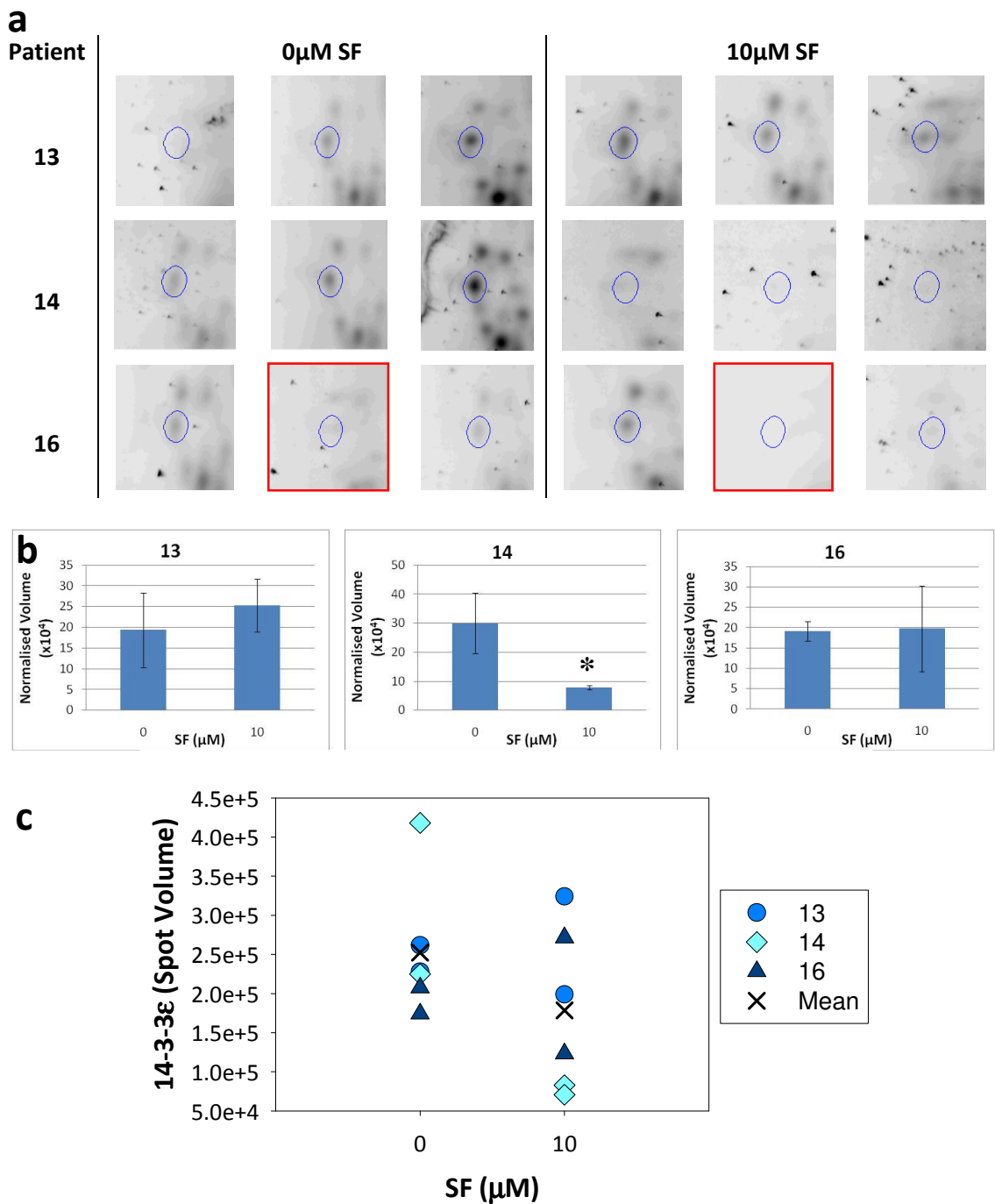


Figure 5.4. The effect of SF on 14-3-3ε.

BPH tissue from three patients (patients 13, 14 and 16) was treated with or without 10 μM SF for 24 hours in triplicate. Protein was extracted, run on 2D gels, and analysed using SameSpots software to identify altered spots which were then identified using mass spectrometry. (a) Images of spot 3247, identified as 14-3-3ε, taken from the 2D gels for each patient with or without 10 μM SF in triplicate are shown, and (b) quantified to statistically determine the effect of 10 μM SF (Means ± standard deviation are plotted; p values: 0.406, 0.02, 0.938 respectively). Replicate 2 of patient 16 was excluded from the analysis due to previously noted replication variation (outlined in red in (a)). (c) The effect of SF on the patients as a whole population with replicate 2 removed from all patients (p-value = 0.244). * p-value < 0.05.

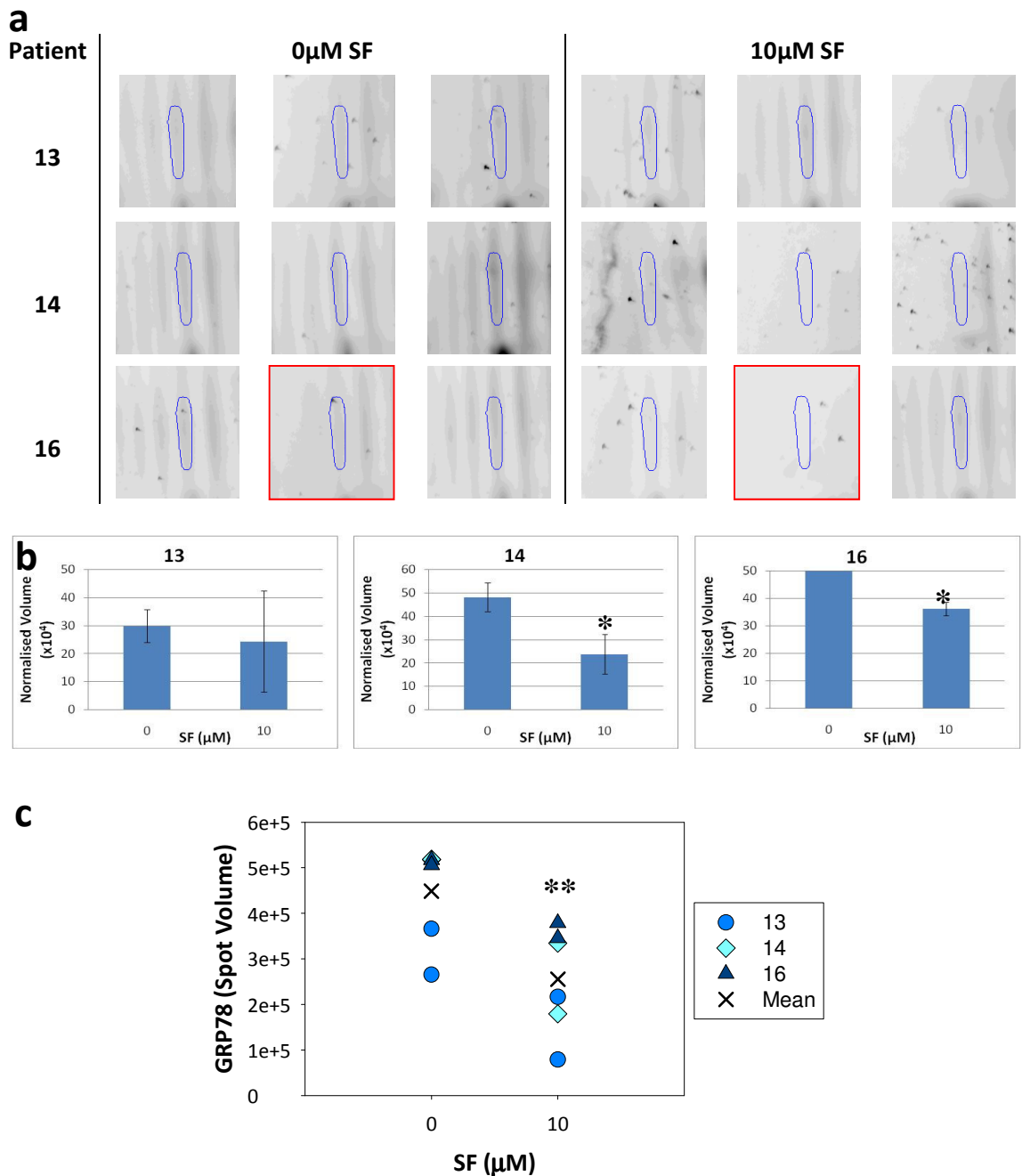


Figure 5.5. The effect of SF on GRP78.

BPH tissue from three patients (patients 13, 14 and 16) was treated with or without 10 μ M SF for 24 hours in triplicate. Protein was extracted, run on 2D gels, and analysed using SameSpots software to identify altered spots which were then identified using mass spectrometry. (a) Images of spot 1095, identified as GRP78, taken from the 2D gels for each patient with or without 10 μ M SF in triplicate are shown, and (b) quantified to statistically determine the effect of 10 μ M SF (Means \pm standard deviation are plotted; p values: 0.645, 0.015, 0.013 respectively). Replicate 2 of patient 16 was excluded from the analysis due to previously noted replication variation (outlined in red in (a)). (c) The effect of SF on the patients as a whole population with replicate 2 removed from all patients (p-value <0.001). * p-value <0.05., ** p-value <0.005.

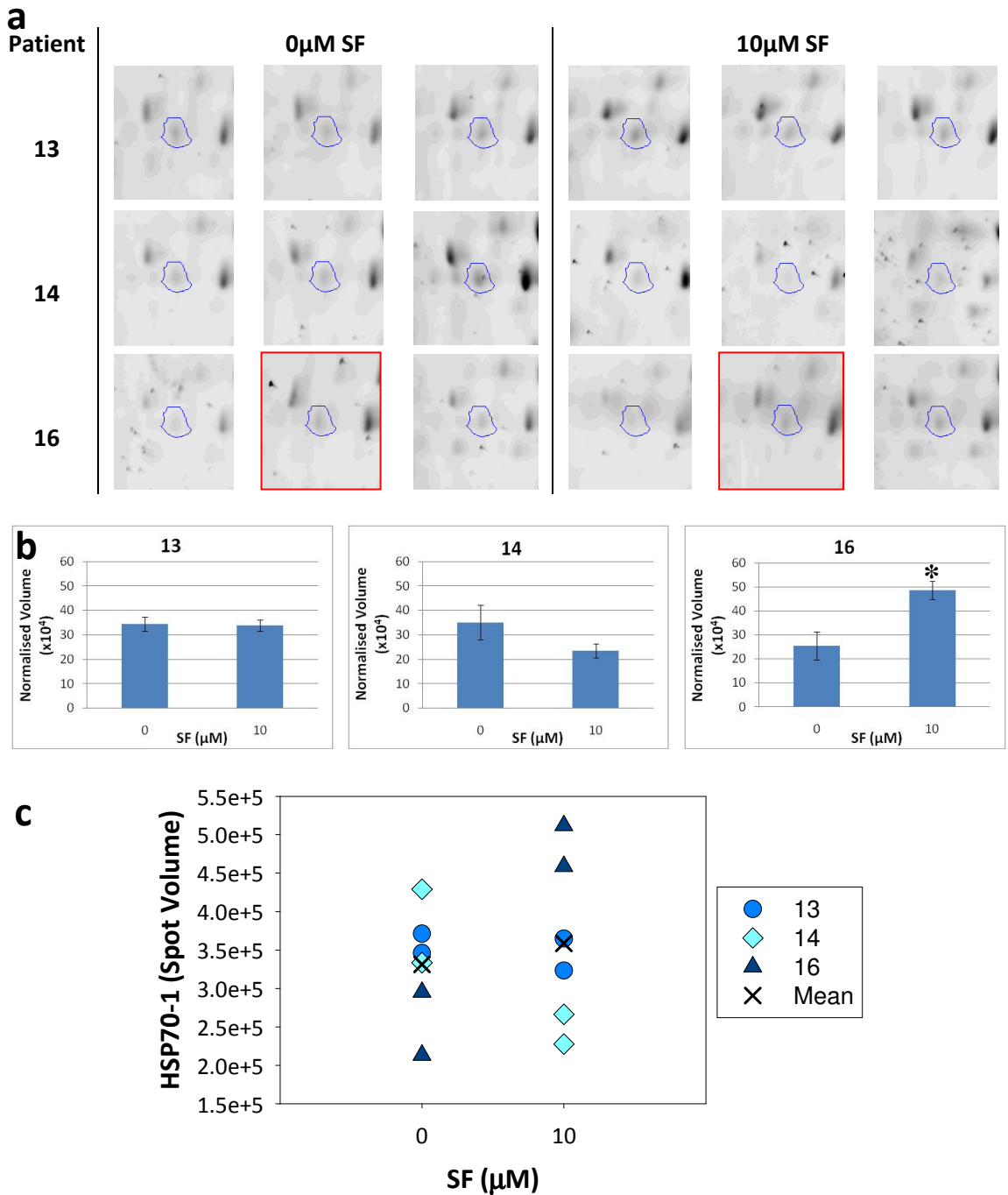


Figure 5.6. The effect of SF on HSP70.

BPH tissue from three patients (patients 13, 14 and 16) was treated with or without 10μM SF for 24 hours in triplicate. Protein was extracted, run on 2D gels, and analysed using SameSpots software to identify altered spots which were then identified using mass spectrometry. (a) Images of spot 1045, identified as HSP70, taken from the 2D gels for each patient with or without 10μM SF in triplicate are shown, and (b) quantified to statistically determine the effect of 10μM SF (Means ± standard deviation are plotted; p values: 0.839, 0.056, 0.041 respectively). Replicate 2 of patient 16 was excluded from the analysis due to previously noted replication variation (outlined in red in (a)). (c) The effect of SF on the patients as a whole population with replicate 2 removed from all patients (p-value = 0.649). * p-value <0.05.

5.4 Discussion

In the previous chapter, protein extracted from BPH tissue from three patients cultured with or without 10 μ M SF in triplicate for 24 hours, was separated by 2D gel electrophoresis, and the resulting images compared. Protein spots were selected that were altered due to either natural variation between patients, or due to SF treatment, and then identified using mass spectrometry.

Little data has previously been collected regarding the expression of the proteins identified in BPH. However, from the known function of these proteins, and the data that is available regarding their expression in the prostate, suggestions as to why they may vary, and what effect this variation may have in the tissue, are discussed.

5.4.1 Natural variation of protein expression in BPH tissue

From the 2D gels seven spots were identified that naturally varied between the patients without treatment (Table 5.1). Of the seven, two spots were found to have multiple IDs, and the final list of proteins identified from the seven spots was: keratins (KRT1 and 10); tubulin beta-2C chain (TUBB2C); actin (ACTA1); microfibril-associated glycoprotein 4 (MFAP4); elongation factor 1-alpha 1 (EEF1A1); annexin A2 (ANXA2); and trimolecular functional enzyme subunit beta (TFP- β).

5.4.1.1 Keratin

Multiple spots were identified as keratin, although often sequence coverage was low, suggesting fragmentation of the protein. It is well known that keratin is a common contaminant of human samples, meaning the keratin identified in these spots may have come from a source other than the BPH tissue, so may not reflect a true variation in protein expression between the patients. Keratin is present in all human tissues, so it is easy to contaminate samples with keratin from hair or skin during handling. However, the presence of keratins in BPH has previously been investigated, so it may be that the results observed here is not a consequence of contamination.

Hudson and colleagues [190] suggested that the keratin expression pattern in cells of the BPH epithelium alters as they differentiate. They reported that basal stem cells express only

keratins 5 and 14, which give rise to a proliferating population, which also express keratins 15, 17 or 19. These cells then differentiate into luminal cells that express keratins 8, 18 and 19, prior to full differentiation, at which point they express only keratins 8 and 18 [190]. However, the keratins identified in the present study were KRT1 and 10, which have both previously been recorded as expressed in the prostate [191]. Although the exact role of KRT10 and KRT4 in the prostate is unknown, KRT10 has been associated with differentiation in the epidermis [192], so it could play a similar role in the prostate.

In summary, the variation in keratin expression observed here may be due to contamination, or it may suggest that the patients had different percentages of differentiated cells, which could explain the varied expression (eg. those with higher levels of KRT10 may have a higher percentage of differentiated cells). The expression pattern of the keratins within each patient could therefore determine the proliferative abilities and differentiation state of the samples, which may affect their behaviour *ex vivo*.

5.4.1.2 Tubulin

Tubulin beta-2C chain (TUBB2C), a cytoskeletal protein, dimerizes with tubulin α , subsequently polymerizing to form microtubules, which are structural components within the cell that are involved in mitosis and vesicular transport. The formation and disassembly of microtubules is a dynamic process, and essential for formation of the spindle during mitosis. Drugs have been developed that interfere with this process, preferentially killing dividing cells, and have been used to treat some cancers [193].

Tubulin β exists as many isoforms, the expression of which has been examined in BPH and PCa samples. Tubulin β_{IV} has the highest expression in both BPH and PCa, but β_{II} expression increases greatly in PCa compared to both BPH and normal tissue [194]. The β_{III} isoform has also been correlated with PCa progression and aggressiveness [195]. The isoform of the tubulin β identified here is not known, so no comparison to the data above can be drawn, but the variation observed may suggest a difference in isoform expression and therefore cell proliferation between the samples.

5.4.1.3 Actin

Like TUBB2C, actin is a cytoskeletal protein, but it is also found in thin filaments in muscle. Actin can participate in a wide range of processes including muscle contraction, cell division, vesicle and organelle movement, cell signalling, and cell junctions [193].

As actin is expressed in muscle, the difference in expression of actin between the patients, may be due to the percentage of muscle within each sample. In addition, an increase in α -actin expression has been correlated with elevated IL-8 expression, and can its expression can be induced by IL-8 [196]. Therefore, it may be that the samples secreted varying concentrations of IL-8, resulting in the altered actin expression as observed.

Actin has been reported as decreased in both PCa and BPH compared to normal prostate tissue samples, and a change in distribution also observed, suggesting it may be related to alterations in adhesion, shape and proliferation [197]. The altered expression of actin may therefore be due to differences in the pre-dominant cell type of the sample, such as muscle cells, or may reflect a change in expression, which could result in alterations in cell interactions, division and signalling.

5.4.1.4 Microfibril-associated glycoprotein 4

Microfibril-associated glycoprotein 4 (MFAP4) is the member of a family of glycoproteins that forms microfibrils and covers elastin, forming elastic fibres in the extracellular matrix (ECM) [193]. Literature regarding its role and expression in the prostate is sparse, but it has been investigated in the context of bladder and ovarian cancer. Microfibril-associated glycoprotein 4 expression was found to be down-regulated in bladder cancer [198], and has been proposed as a biomarker of poor prognosis in ovarian cancer [199]. Therefore, MFAP4 expression may be the result of, or may be related to, the viability of the samples.

5.4.1.5 Elongation factor 1-alpha 1

Elongation factor 1-alpha 1 (EEF1A1) is a subunit of the elongation factor-1 complex (EEF1), which is responsible for the delivery of amino-acyl tRNAs to the ribosome during protein synthesis, and has also been shown to have a role in the nuclear export of proteins [193]. Expression of EEF1 has been correlated with androgen-independent proliferation in PCa [200],

and suppression of EEF1 in cancer cell lines can inhibit proliferation [201]. The EEF1 expression status of the BPH samples may therefore alter its proliferative ability, and it would be interesting to investigate whether EEF1 is overexpressed in BPH compared to healthy prostates.

5.4.1.6 Annexin A2

Annexin (ANX) A2, a member of the annexin calcium-dependent phospholipid-binding protein family, is pleiotropic in nature and can be involved in a wide range of cellular processes. Such processes include: epithelial cell motility, cell-ECM interactions, and linkage of membrane-associated proteins to the actin cytoskeleton.

In BPH, ANXA2 is only expressed in the basal cells, whilst in comparison it also expressed in luminal cells in the healthy prostate. The expression pattern observed in BPH was also seen in PIN, but ANXA2 expression is further reduced in PCa [202]. However, ANXA2 has been observed in some cases of PCa, and has been found to increase IL-6 expression, giving rise to a subset of PCa with an aggressive phenotype [203]. Further work has demonstrated that ANXA2 can regulate adhesion, growth and migration, in PCa [204-205].

The variation in the level detected in the patients in the current study, may therefore be explained by the disease state of the tissue, with BPH in the patients with the lower ANXA2 expression likely to be more advanced.

5.4.1.7 Trifunctional enzyme subunit beta

Trifunctional enzyme subunit beta (TFP- β) is a subunit of the mitochondrial trifunctional protein, an enzyme involved in beta oxidation, converting fats into energy. Mutations in either subunit can result in deficiency of the enzyme, which can be lethal or result in disease. Previously, it has been suggested that beta-oxidation is altered in PCa [206], so it may be the case that this also occurs in BPH. Therefore, the altered expression could be in line with this suggestion, and reflects variation in beta-oxidation between the samples.

5.4.1.8 Summary

For all the above discussed proteins, it is important to note the small sample number used, and the lack of understanding of the relevance of these proteins in BPH. As such, little can be drawn from the above discussion, and no conclusions reached, other than to say protein expression varies between individuals. Further research needs to be conducted to elucidate whether the varied expression observed has any significant relevance. In addition, it would be interesting to see whether variation in the expression of these proteins is still observed in a larger sample number.

5.4.2 The biological processes and molecular functions altered by SF

Of the spots identified from the 2D gels, the majority were chosen due to the observation that they were altered by SF treatment. Of the fifty five spots selected and identified, fifty were altered by SF, only three of which were seen to be altered by SF in the population as a whole: lumican, GRP78 and myosin-11 (Table 5.2).

As discussed previously, patient 14 exhibited the greatest effect of SF treatment, which was reflected in the number of proteins identified, thirty two (Table 5.4), compared to fourteen and four for patient 13 and 16 respectively (Table 5.3 and 5.5). Global protein expression in patient 16 was not statistically significantly altered as a result of SF treatment (Table 4.2).

Of the fifty proteins altered by SF, fifteen were increased, thirty three were decreased, and two were both increased and decreased in different patients, in response to SF.

The proteins were grouped by biological process and molecular function to identify the processes and functions most commonly altered by SF in this model. The proteins were grouped according to GO classification into the smallest number of groups, as the proteins were typically associated with multiple functions and processes (Table 5.6). In order of the number of proteins per group, the processes altered were: apoptosis (eight proteins) metabolism, muscle contraction and development (both seven proteins), cell proliferation, adhesion and angiogenesis (six proteins), and cytoskeletal organization (two proteins). Three proteins did not fit into any of these groups. Of the processes of which the proteins altered were involved, many have been implicated in dysregulation and disease, in particular apoptosis, and cell proliferation, adhesion and angiogenesis.

5.4.2.1 Apoptosis

Apoptosis, also known as programmed cell death, is the process by which cells commit 'suicide'. It can be triggered by a number of factors and results in the fragmentation of DNA and shrinkage of the cytoplasm, ultimately leading to cell death without lysis or damage to surrounding cells. The process of apoptosis is tightly regulated, with a wide number of pro- and anti-apoptotic factors controlling the balance between cell survival and death. Dysregulation due to mutation or alteration in the expression of proteins involved in the process can result in excess or reduced cell death, leading to diseases such as cancer. Correct control of apoptosis is therefore vital for maintaining homeostasis [193].

Apoptosis was found to be the biological process in which the greatest number of proteins altered by SF, were involved. Previous research has shown that SF has pro-apoptotic properties, so it would follow that it may therefore effect the expression of proteins involved in this process (Table 5.8).

Annexin A5 is often measured as a marker of apoptosis, including SF-induced apoptosis [207-208]. It is interesting that here it was observed to be decreased by SF, suggesting a decrease in apoptosis in response to SF, which is contradictory to what would be expected.

HSP70, a known anti-apoptotic protein, was, in contrast, the only protein in the apoptosis group that was increased by SF. This suggests that SF was exerting an anti-apoptotic, not pro-apoptotic, effect as would be expected. SF has previously been reported to increase the expression of HSP70 and other heat shock proteins by an Nrf2-dependent pathway in the liver of mice [116], so the increase in HSP70 observed here is not unprecedented. Confusingly though, HSP70 has also been observed to be increased in cells in which SF-induced apoptosis has been blocked [209]. Thus suggesting that SF-induced apoptosis would lead to reduced levels of HSP70, in contradiction to the reduction we observed.

Serum albumin, here seen to be increased by SF, has previously been shown to form adducts with SF in the plasma, with levels of these adducts higher after chronic exposure than a single dose [210]. The formation of SF protein adducts in the cell correlates with induction of apoptosis, and has been postulated as a critical early event in the induction of apoptosis by SF [181]. However, the specific interaction of SF and albumin has not been implicated in apoptosis.

No relationship or interaction has been reported regarding SF and the remaining proteins in the apoptosis group. Instead a brief description of evidence suggesting a correlation for these proteins with apoptosis is reported.

14-3-3 ϵ is known to be an anti-apoptotic protein whose increased expression is correlated with inhibition of apoptosis [211], whilst disruption of α -actinin-1 (ACTN1) interactions have been shown to increase susceptibility of cells to apoptotic stimuli [212]. Furthermore, ACTN1 has been found to undergo alternative splicing in cancer [213]. Another protein in this group, calreticulin, is a calcium (Ca²⁺)-binding protein that can protect against apoptosis by protecting against Ca²⁺ overload-induced apoptosis, by maintaining calcium homeostasis [214].

As with the majority of glucose-regulated or heat shock proteins (GRP/HSP), GRP78 is believed to be anti-apoptotic, and has been shown to protect against drug-induced apoptosis by blocking casase-7 activation preventing cytochrome c release. In contrast, other research has suggested it may have pro-apoptotic properties, but this activity may be dependent on its expression on the cell surface. GRP78 is primarily found in the endoplasmic reticulum, however increased cell death due to membrane bound GRP78 has been observed, but only in carcinogenic cell lines, not normal cells [215].

Endoplasmin (HSP90 β 1), another GRP/HSP is also suggested to have anti-apoptotic properties which have primarily been attributed to its Ca₂⁺ binding properties [216].

Overall, these data suggest that SF altered the expression of a number of apoptotic proteins in such a manner that would suggest SF induced apoptosis in the BPH tissue. Although SF increased the expression of one anti-apoptotic protein, HSP70, which should inhibit apoptosis, it decreased the expression of multiple anti-apoptotic proteins, suggesting the balance between the two opposing actions would most likely result in increased apoptosis. Therefore, it is likely that in these samples SF induced apoptosis. Thus indicating a beneficial activity of SF in BPH, which is characterized by excess proliferation.

Table 5.8. Apoptotic proteins altered by SF: Their role in apoptosis and relationship with SF.

Protein	Role in apoptosis and previous evidence of relationship with SF
<i>Decreased by SF</i>	
Annexin A5	Marker of apoptosis, including SF-induced [207-208]
Serum Albumin	Forms adducts with SF [210] Formation of SF protein adducts in the cell correlates with induction of apoptosis [181]
14-3-3ε	Increased expression is correlated with inhibition of apoptosis [211]
α-actinin-1	Disruption of α-actinin-1 interactions sensitize cells to apoptotic stimuli [212]
Calreticulin	Protects against Ca ²⁺ overload-induced apoptosis by maintaining calcium homeostasis [214]
GRP78	Protects against drug-induced apoptosis by blocking casase-7 activation preventing cytochrome c release [217-218] Cell surface expression can induce cell death in carcinogenic cell lines [215]
Endoplasmin	Protects against Ca ²⁺ overload-induced apoptosis by maintaining calcium homeostasis [216]
<i>Increased by SF</i>	
HSP70	Increased in cells in which SF-induced apoptosis has been blocked [209] Increased by an Nrf2-dependent pathway by SF [116]

Table summarising previous literature discussing the apoptotic properties of the proteins identified from the 2D gels as involved in apoptosis, and any previous data suggesting a link with SF activity.

5.4.2.2 Muscle Development and Contraction

BPH occurs when the balance between proliferation and apoptosis is lost, and involves over-proliferation of cells, both in the epithelium and the stroma. Common in the stroma of the prostate are smooth muscle cells (SMCs), which along with other cell types over-proliferate in BPH.

In response to SF, the majority of the proteins found to be involved in muscle development and contraction, were reduced. In combination with the suggestion above, that SF induced apoptosis in the BPH samples, it may be that the reduction of the muscle related proteins was due to a reduction in muscle cell number as a result of increased apoptosis of SMCs. It is likely that the proteins involved in muscle development and contraction are primarily expressed in the SMCs in the BPH stroma, so an increase in SMC apoptosis would likely result in a reduction in their expression.

Increased expression of gamma-enteric smooth muscle actin (ACTG2) and transgelin (TAGLN), has been correlated with transdifferentiation of fibroblasts into myofibroblasts, which exhibit increased expression of SMC-associated proteins in response to TGF β 1 treatment [219]. Transdifferentiation is a process associated with BPH progression, and SF is known to interact with TGF β 1, which is critical in prostate regulation. As such, the reduction of ACTG2 and TAGLN observed may have occurred due to SF inhibiting TGF β 1-induced transdifferentiation.

Desmin is often used for the identification of SMCs in prostate stroma [220-221], so as proposed above, a reduction in desmin could likely suggest a reduction in the SMC population.

Also reduced by SF, were alpha skeletal muscle actin (ACTA1) and myosin light-chain 6B, (MYL6B) although little is know about their specific function in the prostate. Due to the lack of information regarding their role in the prostate, all that can be suggested is that they were reduced in the samples due to SF-induced apoptosis of SMCs in which they are expressed.

The only protein in this group whose expression was increased by SF was heat shock protein beta-6 (HSPB6). Heat shock protein beta-6 is a small heat shock protein involved in contraction in smooth muscle. Little is known about its role in BPH, but its function in intimal hyperplasia, hyperplastic thickening of the inner layer of a blood vessel, has been investigated. Heat shock protein beta-6 has been seen to inhibit intimal hyperplasia, in particular by reducing cell

migration, and in some cases proliferation [222]. As BPH is also a hyperplastic condition it may be that HSP6B acts in a similar manner and can inhibit migration, and possibly proliferation, in BPH. However, HSPB6 was increased by SF in the BPH samples, which suggests a mechanism by which SF could promote migration and proliferation in BPH, but without specific information regarding HSPB6 expression and function in the prostate, no conclusions can be made.

The final protein in the group was myosin-11 (MYH11). From the 2D gels, eight spots that were altered by SF were identified as MYH11, although interestingly seven of these spots were found in patient 13, whilst the other was found in patient 16, and no spots identified as MYH11 in patient 14, which was the patient which exhibited the greatest effect. Of the spots identified as MYH11, five were increased, and three were decreased by SF. As a result, little can be deduced regarding the effect of SF, or how SF may be altering MYH11. A possible explanation is that as multiple spots were identified as MYH11, MYH11 may have fragmented or undergone post-translational modification. Such events would alter the mass and pI of the protein, altering the position at which it ran on the 2D gel, resulting in multiple spots of MYH11. This could therefore suggest that SF can alter post-translational modification of MYH11, thereby increasing and decreasing the expression of differently modified forms.

5.4.2.3 Metabolism

The expression of all the proteins identified as involved in metabolism were reduced by SF.

Three spots were identified as ATP-synthase subunit alpha (ATP5A1), a subunit of mitochondrial ATP-synthase an enzyme involved in ATP synthesis. Increased expression of ATP-synthase has been reported in a metastatic, highly tumorigenic PCa cells compared to a slow growing, poorly tumorigenic PCa cell line [223]. The reduction of ATP5A1 by SF observed here, could suggest a decrease in growth in the sample in response to SF treatment, indicating SF reduced cell proliferation in the BPH tissue *ex vivo*.

Three of the proteins, glyceraldehyde-3-phosphate dehydrogenase (GAPDH), L-lactate dehydrogenase A chain (LDHA), and triosephosphate isomerise (TPI1), are involved in glycolysis, a process often upregulated in cancer. Glyceraldehyde-3-phosphate dehydrogenase is routinely used as a housekeeping gene [224-225], so it is interesting to note that here it was

altered by SF. However, its expression has previously been reported as increased in PCa compared to BPH [226-227], suggesting its expression may relate to prostate dysregulation, and thereby the reduction of GAPDH by SF may have a beneficial effect on prostate health.

In both the studies that noted GAPDH expression was increased in PCa, they also reported the same observation for lactate dehydrogenase (LDH) expression [226-227]. Lactate dehydrogenase has five isoforms which are differentially expressed throughout the body. The ratio of two of these isoforms, LDH-1 and -5, was investigated in prostatic secretions, with the mean ration of LDH-5/LDH-1 significantly higher in PCa compared to BPH [228]. This suggests that LDH isoform expression alters in correlation with prostate disease, but here it was LDH-A, a subunit of LDH, which was altered, which is predominantly expressed in muscle cells. It may be that SF can alter the isoform expression, but the isoform of the protein identified is not known, so this can not be fully discussed. LDH is released from cells when membrane integrity is lost, such as in apoptosis. As such, the reduction of LDH protein within the tissue sample as a result of SF treatment, may be due to release of LDH into the media in response to SF-induced apoptosis, resulting in less LDH in the tissue, thereby suggesting lower expression. Therefore, the reduced expression observed may not be a reduction in expression at all, but a loss of LDH from the tissue into the media.

The final identified protein involved in glycolysis, triosephosphate isomerase, has been linked to PCa [227], with its expression increased compared to BPH [229].

A further protein in the metabolism group, creatine kinase B-type (CKB), is involved in the conversion of creatine to phosphocreatine in muscle to create an energy reservoir for muscle contraction. Separate studies have reported conflicting results regarding CKB expression in prostate disease [230-231], so as with many of these proteins, the reduction of CKB by SF may just be a reflection of increased apoptosis.

The final members of the metabolism biological process group were protein disulfide isomerase (PDI) and protein disulfide isomerase A4 (PDIA4). Both PDI and PDIA4, the latter is also known as ERP70 or ERP72, catalyze the formation and breakage of disulphide bonds during protein folding. The expression of PDI has been shown to be increased in PCa compared to BPH [232-233], whilst PDIA4 has been correlated with metastatic potential in hepatocellular carcinoma [234].

5.4.2.4 Cell Proliferation, Adhesion and Angiogenesis

The six proteins involved in cell proliferation, adhesion, and angiogenesis were collagen alpha-3(VI) (COL6A3), fibulin-1 and -5 (FBLN1/5), keratin type II cytoskeletal 1 (KRT1), keratin type I cytoskeletal 16 (KRT16) and lumican (LUM).

Both COL6A3 and KRT1 were identified in multiple spots which were both up- and down-regulated, so it is unlikely that SF actually increases or decreases their expression. However, it may instead be altering the splice variants expressed, as previously COL6A3 splice variant expression has been correlated with cancer, although not specifically in the prostate [213]. Previously, SF has been shown to modulate keratin expression, although this was observed in skin epithelia [235], so SF may be able to have a similar effect in the prostate.

The other three proteins in this group, FBLN1, FBLN5 and KRT16 were all reduced by SF. Fibulins are involved in cell adhesion, and FBLN5 has previously been suggested to have anticancerous function. It has been recorded as reduced in PCa [236], so it would appear on first glance that downregulation of FBLN5 by SF would most likely enhance BPH progression. However, the down-regulation of FBLN5 would most likely reduce cell adhesion which, although beneficial for migration and metastasis in PCa, can actually trigger apoptosis in healthy cells, so it could be that this down-regulation may contribute to apoptosis of BPH cells.

Keratin type I cytoskeletal 16 is primarily expressed in the epithelium suggesting it would most likely effect the proliferation of basal and luminal cells in the prostate. Previously KRT16 expression has been reported as upregulated in psoriatic lesions which are characterized by hyperproliferation [237]. KRT16 may be involved in the hyperplasia seen in BPH, so by reducing the expression of KRT16, SF may exert an anti-proliferative on BPH tissue.

Lumican (LUM) is an ECM protein involved in collagen-fibril organization, and can regulate cell growth and migration. It has been shown to be upregulated in BPH [238], although it is down-regulated in PCa [239-240]. That in this study it was increased by SF is interesting considering previous data that it is upregulated in BPH compared to normal prostate anyway. However, as it is down-regulated in cancer, the increase in LUM by SF may help prevent development of PCa.

5.4.2.5 Cytoskeletal Organization

The final defined biological process group was cytoskeletal proteins. These proteins are often involved in adhesion, and thereby cell migration, but using the GO classification were not listed as involved in these processes, so are grouped separately.

Actin cytoplasmic 2 (ACTG1) is a component of the cytoskeleton expressed in the cytoplasm of non-muscle cells. In the 2D gels, two spots were identified as ACTG1 one of which was increased by SF, whilst the other was decreased. Transdifferentiation of fibroblasts is a key event in BPH pathogenesis and one which is associated with increased ACTG1 expression [219], so a reduction of ACTG1 would most likely inhibit the progression of BPH. However, as here both a reduction and increase in ACTG1 expression in response to SF was seen, it is unlikely that SF has any meaningful effect on this protein and any processes it is involved in in BPH.

The other cytoskeletal protein identified was filamin-A (FLNA), which is involved in the anchoring of the actin cytoskeleton. Its expression has been reported to be decreased in PCa compared to BPH [241], suggesting that its reduction may be involved in prostate dysregulation. However, FLNA has been shown to form a complex with AR which leads to cell migration [242], so by reducing FLNA SF may inhibit androgen-driven cell migration.

5.4.2.6 Other

The remaining proteins could not be included in any of the other groups discussed above.

Serotransferrin (TF) is an iron-binding protein that controls the level of free iron in the blood and tissues. Interestingly, its levels are decreased in inflammation [243], so the increase in TF in response to SF may be due to the anti-inflammatory effect of SF.

14-3-3 theta (YWHAQ) is involved in protein targeting and has been implicated as involved in Akt-induced cell cycle progression by assisting the cytoplasmic localization of WEE1 [244]. Therefore, the reduction of YWHAQ by SF may inhibit cell cycle proliferation.

The remaining protein, Keratin type I cytoskeletal 10 (KRT10) was decreased by SF, but was also recognised as naturally varying between the patients. The deletion of KRT10 in mice led to a reduction in tumour formation in the epidermis due to increased keratinocyte turnover [245]. Whilst in the prostate, KRT10 is expressed in the terminally differentiated squamous epithelial cells [191]. The reduction of SF observed here may therefore help prevent tumour formation in the prostate, or may inhibit the process of squamous metaplasia, which was seen in the samples that underwent histological assessment (see Chapter 2).

5.4.2.7 Function Comparison

By classifying the above discussed proteins in terms of molecular function, the proteins altered were seen to fall into three main groups; enzymes, molecular chaperones, and structural and adhesion proteins, with seven, six and sixteen proteins in each group respectively (Table 5.7). Four proteins did not belong in any of these groups.

Comparison of the processes and functions groups revealed that all the proteins involved in metabolism, functioned as enzymes, catalyzing reactions. It was of interest to note, that of the eight proteins involved in apoptosis, five acted as molecular chaperones. All but one of the proteins, HSPB6, involved in cell proliferation, adhesion and angiogenesis, muscle development and contraction, and the cytoskeleton, functioned in structure and adhesion in some way.

All the proteins found to be altered by SF were all investigated for previous research demonstrating a link between their expression and SF activity. However, very few of these proteins had previously been reported with regard to SF, but data from those which have is included in the discussion above (Chapter 5.4.2.1).

5.4.3 Apoptosis and chaperone proteins

Comparison of the biological processes and molecular functions that the proteins are involved in, revealed an overlap between the apoptosis process and molecular chaperone function groups. Of these groups, there were five proteins that were in both; HSP90 β 1, calreticulin, 14-3-3 ϵ , GRP78 and HSP70. The expression, role and control of these proteins in the prostate has previously been investigated, in particular in PCa, but little research has reported a

relationship with BPH, or in response to SF. SF has long been linked with increased apoptosis but little work has reported, or focussed, on the role of molecular chaperones in SF-induced apoptosis.

The control of apoptosis is crucial to maintain homeostasis as its dysregulation is common in disease. It is of great importance to understand the apoptotic process in order to be able to prevent, treat, and hopefully cure diseases in which apoptosis plays a role. The current evidence indicating the function of these proteins in apoptosis, and in particular their importance in the prostate, is reviewed below, and the relevance of the effect of SF observed discussed (see Table 5.9 for a summary).

Table 5.9. The role of molecular chaperones in apoptosis.

Protein	Pro-Apoptotic	Anti-Apoptotic
<i>Decreased by SF</i>		
HSP90β1		Down-regulation sensitizes cells to drug-induced apoptosis [216, 246] Protects against apoptosis by maintaining Ca ²⁺ homeostasis [247] Androgen-responsive [248-249] Correlated with metastatic potential [250]
GRP78	Expression on the cell surface induces cell death in carcinogenic cell lines [215]	Induced by (extended exposure to) etoposide [246, 250] Blocks caspase-7 activation [250] Stabilizes Raf-2 preventing cytochrome c release [217] Androgen-responsive [218, 251-252] Essential for PTEN-induced PCa development [253]
Calreticulin	Down-regulated in PCa, over-expression associated with inhibition of tumour growth and metastasis [254]	Androgen-responsive [255] Protects against Ca ²⁺ -induced apoptosis in androgen-sensitive cells [214] Over-expressed in metastatic cell lines [182, 248]
14-3-3ε	Essential role in NADE-induced apoptosis [256]	Binds phosphorylated Bad, inhibiting apoptosis [211] Promotes cell cycle progression [257-258] Increases TGFβ1 signalling [259]
<i>Increased by SF</i>		
HSP70		Essential for survival of carcinogenic cells [260] Correlated with prostate carcinogenesis and protects against apoptosis by stabilizing mutant p53 [261-262] Interacts with CD10 which is increased in BPH but decreased in PCa [262] Androgen-responsive [263]

A summary of the evidence for the pro- and anti-apoptotic properties of the molecular chaperones involved in apoptosis. The proteins were identified by proteomic analysis of 2D gels as altered by SF in BPH tissue.

5.4.3.1 HSP90β1

Heat shock protein 90 beta -1 (HSP90β1) is a member of the heat shock family of proteins, and is also known as glucose regulated protein 94 (GRP94), gp96, and endoplasmic reticulum chaperone protein.

A reduction in HSP90β1 expression is proposed to reduce cell viability, and has been demonstrated in human acute T cell leukaemia cells, where a reduction of HSP90β1 sensitised the cells to etoposide⁴-induced apoptosis. In the same cell line, it was demonstrated that in response to etoposide treatment, HSP90β1 is cleaved by calpain, a cysteine protease, in a Ca²⁺-dependent manner, concurrent with the activation of caspase CPP32 and initiation of DNA fragmentation [216]. In neuroblastoma cells, suppression of HSP90β1 was once again associated with a decrease in cell viability in response to an apoptosis inducer, this time A23187, a calcium ionophore. Interestingly treatment with A23187 increased HSP90β1 expression, but it also activated calpain [246].

HSP90β1 has been suggested to protect against apoptosis by maintaining endoplasmic reticulum (ER) calcium (Ca²⁺) homeostasis. Ca²⁺ overload can cause ER stress and trigger apoptosis by activating calpain, which in turn triggers the caspase cascade resulting in cell death. As a result of etoposide-induced apoptosis in HUVEC cells, HSP90β1 was reduced to undetectable levels [247].

With particular reference to its importance in the prostate, HSP90β1 is believed to be regulated by N-myc downstream regulated gene 1 (NDRG1) protein, as inhibition of NDRG1 reduces HSP90β1 expression. NDRG1 plays an important role in androgen-induced cell differentiation and inhibition of PCa metastasis, and can itself be induced by androgen, PTEN, and p53 [249]. This suggests that HSP90β1 can be indirectly regulated by androgen, which is essential in the development of prostate disease, and PTEN, which plays a key role in many cases of PCa.

The regulation of HSP90β1 by androgen has been demonstrated in the androgen-responsive PCa cell line, LNCaP, which showed an increase in HSP90β1 gene expression in response to androgen treatment. Further evidence for androgen regulation was provided by the observation that DU145 and PC3 PCa cell lines, which lack a functional androgen receptor, express HSP90β1 at significantly lower levels [248]. Comparison of the poorly metastatic

⁴ A drug used to as a chemotherapy drug against some cancers including PCa. It causes errors in DNA synthesis and promotes apoptosis of the cancer cell.

LNCaP, and highly metastatic LNCaP-LN3, PCa cell lines revealed that the expression of HSP90 β 1, GRP78 and calreticulin, were all increased in the metastatic cells [250]. This result was corroborated by a separate study who noted HSP90 β 1 and calreticulin expression was higher in the highly metastatic 1E8-H cell line compared to the lowly metastatic 2B4-L cells, although these cell lines are androgen-independent [182].

5.4.3.2 GRP78

Glucose regulated protein, GRP78, is an ER chaperone and member of the HSP70 protein family. As with many ER proteins, it participates in Ca²⁺ homeostasis, influencing apoptosis, as well as facilitating protein folding and assembly. It is essential for embryonic cell survival, and its overexpression has been reported in drug-resistant primary lung and ovarian cancer cell lines. As with HSP90 β 1, GRP78 has been suggested to protect against apoptosis by maintaining endoplasmic reticulum (ER) calcium (Ca²⁺) homeostasis.

As a result of etoposide-induced apoptosis in HUVEC cells, GRP78 was unexpectedly increased 2.23-fold [247]. The increase in GRP78 is counter-intuitive and suggests a mechanism by which the cell was attempting to prevent apoptosis, although in this case it was not enough. In other studies it has been reported that cells that survive long exposure to etoposide treatment over-express GRP78, so it may be that 24 hours is a long enough period to induce this response [217]. It has been suggested that this overexpression of GRP78 can protect against etoposide-induced apoptosis by associating with procaspase-7, an activity dependent on its ATP binding domain, blocking caspase-7 activation [217]. Furthermore GRP78 can stabilize Raf-1, preventing cytochrome c release, and in turn inhibiting ER stress-induced apoptosis [218].

GRP78 has also been associated with AR status and the development of androgen-insensitive PCa [251-252]. Androgen treatment resulted in an increase in GRP78 expression at 24 hours reducing cell death, but this was only transient with the levels of GRP78 subsequently decreasing, coinciding with an increase in cell death [253]. Using a mouse model, Fu and colleagues showed that knockout of GRP78 from the prostate epithelium cells suppressed AKT activation, and prevented the development of PCa in response to PTEN deletion [260].

However, in contrast, overexpression of GRP78 has also been linked to increased apoptosis in carcinogenic prostate cell lines. Burikhanov and colleagues noted that both normal and cancer

cells in culture secreted prostate apoptosis response-4 (Par-4), a pro-apoptotic protein. Although GRP78 is primarily an ER protein, further investigation revealed that most cancer cells, and some normal cells, expressed GRP78 on the cell membrane. Secreted Par-4 was shown to bind to GRP78 at the cell surface, triggering ER stress. This resulted in overexpression of GRP78, and its translocation to the cell surface, leading to activation of caspases 8 and 3 via Fas-Associated protein with Death Domain (FADD), ultimately promoting apoptosis. Interestingly though, ER stress and apoptosis in response to extracellular Par-4 was only observed in cancer cells, not normal cells [215].

5.4.3.3 HSP70

Of the five proteins selected for investigation HSP70, also known as HSP70-1, was the only one increased by SF treatment. It belongs to the same family as GRP78, and much like GRP78, has been shown to have anti-apoptotic properties and is correlated with cancer progression.

Deletion of HSP70 results in cell death of tumorigenic cell lines, including PCa cells, but not of normal prostate epithelial cells, indicating it is essential for the survival of tumorigenic cells [262]. Increased HSP70 expression has been correlated with prostate carcinogenesis, and it has been shown to stabilize mutant p53, but not the native protein, protecting the cell from apoptosis. The loss of HSP70 has been observed to increase apoptosis and reduce viability in PC3 cancer cells [261, 263].

Also of interest, is the finding that HSP70 interacts with CD10. CD10 is a transmembrane metallo-endopeptidase which is strongly expressed by normal prostate epithelium. The expression of CD10 is increased in BPH tissue, but reduced in PCa. In PCa, its expression is observed in only 30% of primary prostate tumours, although conflictingly, CD10 is strongly expressed by the majority of lymph node metastases. The exact function of CD10 in PCa is unknown, but it has been hypothesised that the loss of CD10 may facilitate androgen independent growth of PCa [261]. It has also been shown that HSP70 is under androgen regulation, as DHT enhances its expression in androgen-sensitive, but not androgen-insensitive PCa cell lines [255].

Considering the evidence above it is interesting then that SF increased the expression of HSP70, as by doing this it would protect the cell against apoptosis, when previously SF has been shown to induce apoptosis.

However, all the data above has been collected from PCa cells, not BPH, and it may be that the role of HSP70 depends upon disease state. Little data exists regarding the role and expression of HSP70 in BPH, but using 2D gel electrophoresis, Lin and colleagues reported that HSP70 is expressed at higher levels in BPH than PCa. However, multiple spots were identified as HSP70 leading to the suggestion that there were different post-translationally modified isoforms in BPH and PCa needle biopsies [241].

5.4.3.4 Calreticulin

Calreticulin is a Ca²⁺ binding protein that localizes to the ER and is involved in Ca²⁺ homeostasis, cell adhesion and apoptosis. The expression of calreticulin is induced by androgens which are essential in prostate development and disease, suggesting that calreticulin may be of importance in prostate dysregulation [254]. Downregulation of calreticulin has been observed in PCa, and its overexpression has been associated with reduced tumour growth and inhibition of metastasis [264].

In comparison however, two separate studies have noted an increase in calreticulin expression in highly metastatic cell lines compared to poorly metastatic cell lines, although one of these studies used androgen-independent cell lines [182, 250]. Increased calreticulin has also been shown to protect against apoptosis induced by Ca²⁺ overload, with androgen treatment inhibiting Ca²⁺ overload-induced apoptosis in the androgen-sensitive LNCaP, but not in the androgen-insensitive PC3 PCa cell lines [214].

5.4.3.5 14-3-3ε

14-3-3ε is part of the highly-conserved 14-3-3 family of proteins which are ubiquitously expressed in many cell types, and of which approximately 50 genes have been identified in plants, animals and yeast. They have been implicated in the regulation of a number of kinases involved in signalling pathways, including Rap, Ras, Bcr and protein kinase C, although they can perform diverse roles in different systems [265].

In neural cells, it has been suggested that 14-3-3 ϵ can modulate apoptosis by binding to p75NTR-associated cell death executor (NADE), a protein that interacts with p75 neurotrophin receptor (p75NTR), which mediates apoptosis in neural cells. It was seen that a mutant form of 14-3-3 ϵ inhibited apoptosis, although it still bound to NADE, suggesting 14-3-3 ϵ plays an essential role in the p75NTR/NADE apoptotic pathway [256]. 14-3-3 ϵ upregulation has also been shown to increase binding to phosphorylated Bad, a pro-apoptotic protein, preventing apoptosis [211].

Further research has linked 14-3-3 ϵ to cell cycle progression, as it has been shown that 14-3-3 ϵ interacts with cdc25 phosphatases, which activate cyclin-dependent kinases, promoting the continuation of the cell cycle [257]. Furthermore, it also been shown to compete with importin α 5, which is involved in its transport to the nucleus, sequestering it in the cytoplasm, preventing inhibition of the cell cycle [258].

All these data combine to suggest mechanisms by which 14-3-3 ϵ can promote cell cycle progression, acting in an anti-apoptotic manner. Furthermore, 14-3-3 ϵ overexpression can lead to increased TGF β 1 signalling via the human type 1 TGF β receptor (T β R1), a pathway which has been implicated in PCa progression, although the relationship between TGF β 1 and the prostate is complex [259]. TGF β 1 is also involved in inflammation suggesting a role for 14-3-3 ϵ in BPH. In addition, 14-3-3 ϵ has been reported as increased in PCa samples compared to BPH tissue [232].

5.4.3.6 Summary

It is interesting that of the five proteins, three of these, HSP90 β 1, GRP78 and HSP70, are heat-shock or glucose-regulated proteins. It is also interesting that the majority of these proteins are localized to the ER, and are involved in Ca²⁺ homeostasis, a critical factor in the balance between cell survival and apoptosis.

Little work has been conducted investigating the effect of SF on these proteins but the effect of other dietary agents has been investigated. In DU145 PCa cells, resveratrol, a polyphenol found in red wine and grapes, was seen to reduce cell proliferation and viability, coinciding with an increase in HSP70 [266]. Selenium induced ER stress, increasing the expression of anti-

apoptotic proteins including GRP78 and GRP94, as well as the expression of pro-apoptotic proteins in PC3 PCa cells, although they hypothesised that low doses of selenium promotes cell survival, whilst high doses may initiate the apoptotic process [267].

Due to the importance of the apoptotic process in disease, including BPH and PCa, and data demonstrating induction by SF, further investigation of the proteins above may increase our understanding of this process. Of the proteins above, a number of papers have suggested a role for HSP90 β 1 in PCa, but none have reported a relationship with SF. However, the cytoplasmic homolog of HSP90 β 1, HSP90, is well researched and a relationship with SF reported. HSP90 β 1 will be investigated further as a possible novel target of SF to gain greater understanding of the relationship between the two, and also to try and discover what biological relevance this may have in the prostate.

5.4.4 Conclusions

From the results obtained, it is interesting to note that the majority of the proteins that naturally varied between the patients were cytoskeletal or ECM proteins, suggesting differences in the proliferation, adhesion and migration characteristics of the samples. That SF altered the expression of proteins involved in essential cell processes that are often dysregulated in disease, such as apoptosis, metabolism, proliferation and adhesion, suggests that SF may be able to modulate signalling in BPH.

Furthermore, SF primarily altered the protein expression in such way that should, from our understanding of the proteins, have a beneficial effect in BPH. It is likely that SF can beneficially alter protein expression, thereby influencing processes in BPH, promoting prostate health. It was observed that in particular SF altered the expression of a number of molecular chaperones involved in apoptosis. A review of the literature regarding these proteins led to the decision to investigate HSP90 β 1 as a novel target of SF, and to try and elucidate its biological relevance in the prostate, the results of which are reported in the next chapter.

Chapter Six

Biological Relevance of HSP90 β 1

Chapter 6. Biological Relevance of HSP90β1

6.0.1 Summary

The previous chapter discussed the proteins whose expression was altered by SF in the *ex vivo* model. Among them SF altered a number of molecular chaperones that have been implicated in the control of apoptosis. From these results a single protein, HSP90β1, was selected for further investigation regarding the effect of SF on its expression and biological relevance, the results of which form this chapter. HSP90β1 was selected due to its proposed anti-apoptotic function, and its reported correlation with PCa. Furthermore, its cytoplasmic homologue, HSP90, which has been more highly researched, has been suggested as a target of SF activity.

In the 2D gels, HSP90β1 was found to be significantly altered in one of the three patients. Analysis of a further nine samples revealed that HSP90β1 was significantly reduced by SF in three of the individuals, and a further two showed a reduction, but not significantly so. In addition, both protein and mRNA levels were analysed in healthy and cancerous prostate cell lines. An increase in HSP90β1 mRNA was observed in the cancerous cell line in response to SF, but this did not translate to an alteration in protein expression. No significant effect was observed on either HSP90β1 mRNA or protein after SF treatment in the healthy cell line. To investigate the biological relevance of HSP90β1 reduction, siRNA was used to knockdown the expression of HSP90β1, with a maximum reduction of 60 and 30% obtained for mRNA and protein levels respectively. As analysis from the previous chapter had suggested a link between HSP90β1 and apoptosis, the effect of this knockdown on cell viability and proliferation was assayed, but no effect was observed.

Combined with data garnered from literature, this may indicate that a total knockout of HSP90β1, and additional apoptotic stimuli, are necessary to obtain a significant effect. Furthermore, it is hypothesised that epithelium-stroma interactions, tissue type, and disease state may play a role.

6.1 Introduction

In the previous chapter, it was identified that 10 μ M SF altered the expression of a number of proteins in BPH tissue *ex vivo*, including a number of molecular chaperones involved in apoptosis. The control of apoptosis is a key process in tissue homeostasis and is often disrupted in disease [193]. To be able to understand, and manipulate, proteins involved in its control can provide novel targets for therapy to help prevent and treat diseases. In BPH and PCa where there is excess proliferation of cells, to be able to manipulate such proteins to increase apoptosis could help inhibit the development of these diseases [268].

I had hoped to investigate a number of the molecular chaperones involved in apoptosis, however many were undetectable by western blotting so were not pursued in further samples. One of the proteins identified, endoplasmic reticulum chaperone, was detectable by western blotting and was selected for investigation as a possible novel target of SF, and in particular SF-induced apoptosis. No relationship between endoplasmic reticulum chaperone and SF has previously been reported, but a role in the prostate, and more specifically PCa, has been suggested. Furthermore, its cytoplasmic homologue, HSP90, has been suggested as an indirect target for SF activity, indicating that the HSP90 family of proteins may provide a novel mechanism by which SF can exert a beneficial effect. As such, in this chapter, further work attempts to elucidate the biological relevance of the effect observed in the previous chapter, with particular reference to its significance in apoptosis.

Endoplasmic reticulum chaperone or heat shock protein 90 beta -1 (HSP90 β 1), is a member of both the heat shock and glucose-regulated families of proteins, and is also known as glucose regulated protein 94 (GRP94) or gp96. Glucose regulated proteins (GRPs) are ubiquitously expressed molecular chaperones that are localized in the endoplasmic reticulum (ER) of the cell. Their expression is induced in conditions where there is glucose deprivation, chronic anoxia, and acidic pH, such as in poorly vascularised solid tumours, and they are therefore suggested to protect cells against adverse physiological conditions. Increased expression of GRPs is implicated in carcinogenesis [269], and associated with tumour size. Furthermore, they have been shown to protect carcinoma cells against cytotoxic T-lymphocyte-mediated cytotoxicity, and from treatment with drugs, such as some chemotherapeutic agents [270].

Increased expression of HSP90 β 1 has been demonstrated in transformed cells, where it is able to form a stable complex with p185^{erbB2}, a protein commonly expressed in many prostate,

breast and ovarian carcinomas, and associated with poor prognosis. Disruption of this complex results in degradation of existing p185^{erbB2}, and an altered distribution of newly synthesized p185^{erbB2} protein. The expression of HSP90β1 is increased in a number of breast cancer cell lines compared to normal breast epithelial cells, and is also further induced in glucose deprived conditions [270]. In a number of human haematopoietic cell lines stably transfected with a wild type or mutated form of p53, a correlation between resistance to 2-deoxyglucose (a known inducer of GRPs)-induced apoptosis, and the cells' ability to induce HSP90β1 was observed, suggesting that HSP90β1 has anti-apoptotic properties.

During etoposide (an apoptotic drug) -induced apoptosis, a subpopulation of HSP90β1 associated with the ER membrane co-localizes with calpain, an apoptosis associated Ca₂⁺ activated neutral protease, in the perinuclear region. This subpopulation is then specifically cleaved by calpain in a Ca₂⁺ dependent manner, resulting in a 80kDa carboxyl peptide, concurrent with the progression of apoptosis induced by DNA damage mediated by etoposide [216].

The expression of HSP90β1 has also been noted as increased in malignant prostate epithelium compared to benign. In addition, it has been correlated with increased metastatic potential in prostate cell lines, both androgen-sensitive and androgen-independent [182, 250].

The expression of HSP90β1 is increased by androgen-stimulation, and it is expressed at much lower levels in PCa cell lines lacking a functional AR, suggesting it to be an androgen-response gene [248]. Androgen, acting via the AR, down-regulates the expression of trichorhinophalangeal syndrome I (TRPS1), a transcription factor that inhibits the secretion of PSA. As a result, the expression of TRPS1 is higher in comparison in androgen-independent cells. Using the androgen-independent cell line DU145, which does not express TRPS1, artificial expression of TRPS1 reduced HSP90β1 expression, and was hypothesized to induce apoptosis. Therefore, increased TRPS1 may inhibit the secretion of PSA, a key marker of PCa progression, reduce HSP90β1, and induce apoptosis in PCa cells [271]. Androgen may inhibit TRPS1 expression, thereby preventing TRPS1-mediated reduction of HSP90β1. Further to this, androgen induces the expression of the N-myc downstream regulated gene 1 (NDRG1) gene, which is implicated in differentiation, and can thereby inhibit tumour growth and metastasis. NDRG1, in turn, increases HSP90β1, suggesting a mechanism by which androgen can up-regulate HSP90β1 expression [249].

In contradiction of the results indicating HSP90β1 is increased in PCa, Howard and colleagues reported HSP90β1 expression to be decreased in malignant tissue compared to BPH, and was further reduced in circulating tumour cells (CTCs) [183]. It may be hypothesised that this apparent discrepancy may be due to androgen-response status, as this may differ between the two sets of patients tested. Although HSP90β1 expression is altered by androgen, increased HSP90β1 has been correlated to metastatic potential in both androgen-sensitive and independent cells, so this is unlikely to explain the difference. However, as HSP90β1 has been implicated in tumour immunogenicity, it may be that reduced expression may be beneficial for CTCs, allowing them to escape detection and establishing new metastatic sites.

Both HSP90β1 and HSP90, its cytoplasmic homologue, are involved in ensuring the correct folding conformation of a number of signal transduction proteins. Disruption of this process results in the destabilisation of these proteins, many of which are critical for cell survival or proliferation, and their disruption can result in cell death or cell cycle arrest. With particular reference to inhibition of HSP90β1, the resulting accumulation of misfolded proteins in the ER causes ER stress, initiating the upregulation of GRP78, another ER chaperone, and in some circumstances can result in apoptosis [272].

Geldanamycin (GA) and herbimycin A (HMA), inhibitors of HSP90β1 and its cytoplasmic homolog HSP90, have attracted interest as potential anticancer agents. GA and HMA can induce apoptosis and augment sensitivity to cytotoxic drugs in chronic lymphocytic leukaemia, specifically targeting malignant cells, and in some cases even conferring modest cytoprotective effects to normal cells. In CLL cells, GA increased HSP70 and GRP78, but decreased Akt, a key mediator of cell survival in CLL cells, and a target of HSP90. However, the increase of HSP70 and GRP78 could result in a decrease in cell death, as HSP70 blocks the recruitment of procaspase 9 to the Apaf-1 apoptosome, and GRP78 may inhibit caspase activation directly [273]. In a small cell lung cancer cell line, inhibition of HSP90 by 0.1μM GA decreases cell viability by 40%, an effect which reached a plateau up to 3μM, and it took 4μM to decrease cell viability to zero. During the first phase of the response, the number of live cells was similar to the total number of cells, but during the second phase, the number of dead cells greatly increased. This indicated that the initial response was due to inhibition of cell proliferation, followed by increased cell death during the second phase of the response. Up to concentrations of 50nM GA, the effect on cell proliferation was reversible, but at higher

concentrations there remained a population of viable cells that did not recover. The experiment was repeated with a human glioblastoma cell line in which cell proliferation arrest was observed, but the effect was not sustained after removal of the drug [274].

Further to its proposed anti-apoptotic effects, HSP90β1 has been shown to induce anti-tumour immune responses to pre-existing cancers. HSP90β1 has an amino-terminal signal sequence and a carboxyterminal ER retention/retrieval signal, targeting it to the ER, but a small fraction has been seen to localise to the cell surface in transformed cells [275]. At the cell surface HSP90β1 interacts with antigen presenting cells (APCs) in two separate events, first by interacting with toll-like receptors (TLRs) 2 and 4, activating the APC and leading to secretion of pro-inflammatory cytokines, and secondly by interaction with CD91 and scavenger receptor-A leading to internalization of the HSP90β1-peptide complex, and cross-presentation of the HSP90β1-associated peptide, eliciting a peptide-specific T_C immune response [276]. The specificity of the response was demonstrated by Srivastava and colleagues, who were the first to identify HSP90β1 as a possible tumour rejection antigen (TRA). They noted that injection of HSP90β1 isolated from a chemically induced tumour into mice provided protective immunity to transplantation of cells from the parent tumour. Tumour rejection antigens (TRAs) induce resistance to tumour transplants in specifically immunized syngeneic recipients. Each sarcoma appears to have its own unique antigen, or set of antigens, because immunisation against any one tumour provides no protection against any other syngeneic sarcoma. [277].

More recently, it has been suggested that the post-translation glycosylation of HSP90β1 is crucial in its function. In particular, the sialic acid content of HSP90β1 affects its interactions with APCs, and differences in glycosylation patterns have been observed in normal and cancerous tissues. Thus suggesting that the glycosylation status of the protein determines its anti-carcinogenic activity [276, 278].

With regards to previous research investigating the effect of external agents on HSP90β1, particularly in the prostate, its expression has been shown to be upregulated by copper. Copper is an essential trace element that can also cause oxidative damage, and that is often accumulated in cancerous tissue, corresponding with an increase in the inflammatory response pathway in prostate cells [279]. Dietary agents have also been shown to modulate HSP90β1 expression. Diindolylmethane, a derivative of the dietary phytochemical indole-3-carbinol, is, like SF, derived from cruciferous vegetables. Diindolylmethane has been suggested to have

protective effects against cervical cancer, and can induce apoptosis in tumour cells. Confusingly, it increased HSP90β1 expression in both cervical and prostate cancer cell lines [280]. Furthermore, HSP90β1 expression was induced in PCa cells, by methylseleninic acid, a selenium metabolite, which triggers ER stress and can lead to apoptosis [267].

Up until now SF has not been reported to alter HSP90β1 expression, although data has suggested a link between SF and HSP90. It has been shown that SF increases HSP90 acetylation by inhibiting the enzymatic function of HDAC6, a cytoplasmic non-histone protein deacetylase. The increased acetylation causes dissociation of HSP90 from the androgen receptor (AR), resulting in a reduction of AR protein levels and reduced expression of AR targets [117].

The data above provides evidence of a role for HSP90β1 in disease, especially cancer, and more specifically in the prostate. It has also been seen that HSP90β1 can be altered by dietary agents, and that its cytoplasmic homolog has been shown to be altered by SF. The above evidence also highlights the dual function for HSP90β1 in disease, by firstly modulating apoptosis, and secondly by its immunogenic properties. This indicates the importance of the reduction of HSP90β1 observed in BPH tissue *ex vivo*, and highlights the relevance of investigating the effect of SF on HSP90β1 expression in the prostate in this chapter.

6.2 Materials & Methods

6.2.1 Tissue culture and sample collection

BPH tissue samples were collected, processed and cultured with four biological replicates with or without 10 μM SF as previously described in Chapter 3.2.1-3. Three biological replicates were washed in PBS and immediately frozen on dry ice and stored at -80°C for subsequent protein extraction and western blotting. The final biological replicate samples were placed in Accustain® Formalin Solution 10% Neutral Buffered (Sigma-Aldrich) for 24 hours and then transferred to 70% ethanol, both at 4°C prior to transfer to the Cotman Centre (Norwich, UK) for paraffin wax-embedding and sectioning using standard methods for subsequent immunohistochemical staining. Tissue sections were mounted on Probe-On Plus Slides (Fisher Scientific).

Dependent on the tissue sample size received, some samples were unable to be used for both western blotting and immunohistochemistry (IHC). The samples received, and whether they were used for western blotting and/or IHC, are listed in the Annex.

6.2.1.1 Protein Extraction

Protein was extracted and quantified as described in Chapter 4.2.2-3. Protein was run by western blot for immunodetection of HSP90β1 as described in Chapter 6.2.3.

6.2.1.2 Immunohistochemistry

BPH samples that had been fixed and wax-embedded were sectioned for immunohistochemical staining for the detection of HSP90β1 following the protocol in Figure 6.1. Where a specific temperature is stated, sections were warmed using a slide warmer (Cole-Parmer). Xylene, ethanol and 3% H₂O₂ were obtained from Sigma Aldrich. Citric acid buffer from Dako. Tris-buffered saline (TBS) was made as followed: 50 mM Tris, pH 7.4; 200 mM NaCl, all Sigma Aldrich. Supplemented with 0.1% Tween 20 (Sigma-Aldrich) to produce TBST. Incubation buffer: 1% bovine serum albumin (BSA) (Sigma-Aldrich) and 10% horse serum (Vector) in TBST. Primary antibody solution: HSP90β1 antibody (ab53075, Abcam) 1:100 in 1% BSA TBST. Secondary antibody solution: Elite ABC Anti-Rabbit Kit (3 drops serum and 1 drop Ab in 10ml TBST; Vector Laboratories). Vectastain Elite ABC Reagent prepared as follows: 2 drops Reagent A and 2 drops Reagent B in 5ml TBST pre-equilibrated at room temperature for 30 minute, and DAB Peroxidase Substrate Solution: 2 drops buffer, 4 drops DAB, 2 drops H₂O₂ in

5ml distilled H₂O (both Vector Laboratories). Haematoxiniln from SurgiPath Europe Ltd, Vectamount from Vector Laboratories and coverslips from VWR International.



Figure 6.1. Immunohistochemistry Protocol.

Method for the immunohistochemical detection of HSP90B1 expression in wax-embedded tissue sections.

6.2.2 Cell Line Culture

6.2.2.1 Cell Lines

Human healthy prostate PNT1a cells were obtained from European Collection of Cell Cultures (ECACC), and human prostate cancer DU145 were obtained from American Type Culture Collection (ATCC). PNT1a cells were maintained in RPMI and DU145 in EMEM media, both supplemented with 2mM L-glutamine (Sigma-Aldrich), 5mg/ml penicillin/streptomycin antibiotics, 1X non-essential amino acids (Invitrogen) and 10% (v/v) foetal bovine serum (Sigma).

6.2.2.2 Cell Culture

All cells were maintained in an incubator at 37°C with 5% CO₂. Cells were sub-cultured when reaching 70% confluency in 10cm dishes and experiments were performed in 6- and 96-well plates as appropriate. Cell treatments occurred in complete media with less than 0.1% dimethyl sulphoxide (DMSO, Sigma-Aldrich). Unless specified, cells were treated when at 70% confluency. Sulforaphane (LKT Laboratories) diluted in DMSO to 100mM and then diluted to 1mM in PBS. SF was added to media at final concentration of 10 or 25µM as applicable.

6.2.2.3 siRNA

Non-targeting (NT), glyceraldehyde 3-phosphate dehydrogenase (GAPDH) and HSP90β1 siRNA, DharmaFECT transfection reagent 2, 5x siRNA Buffer and RNase-Free Water were all obtained from ThermoScientific. siRNA was reconstituted to approximately 100µM as per instructions: 5nmol siRNA was reconstituted in 40µl RNase-Free Water and RNA concentration determined using the NanoDrop, 5x siRNA buffer was added to give a final concentration of 1x buffer, and the concentration calculated and noted. NT and GAPDH siRNA were used as negative and positive controls respectively. The NT siRNA used consisted of a pool of four NT siRNAs which were all confirmed to have at least 4 mismatches with all known human genes by BLAST analysis, and to have minimum off-target effects. Untreated cells and cells treated with transfection reagent but no siRNA were also used as controls. All experiments with siRNA were performed in antibiotic-free RPMI media, complete media is antibiotic-free RPMI supplemented with 10% FCS. Experiments were performed in 6-well plates (Greiner Bio-One), for protein and RNA extraction, and black-sided clear-bottomed 96-well plates (Perkin-Elmer),

for the cell viability and proliferation assays, as appropriate, and cultured for up to 7 days post-transfection. siRNA transfection was carried out as per Figure 6.2.

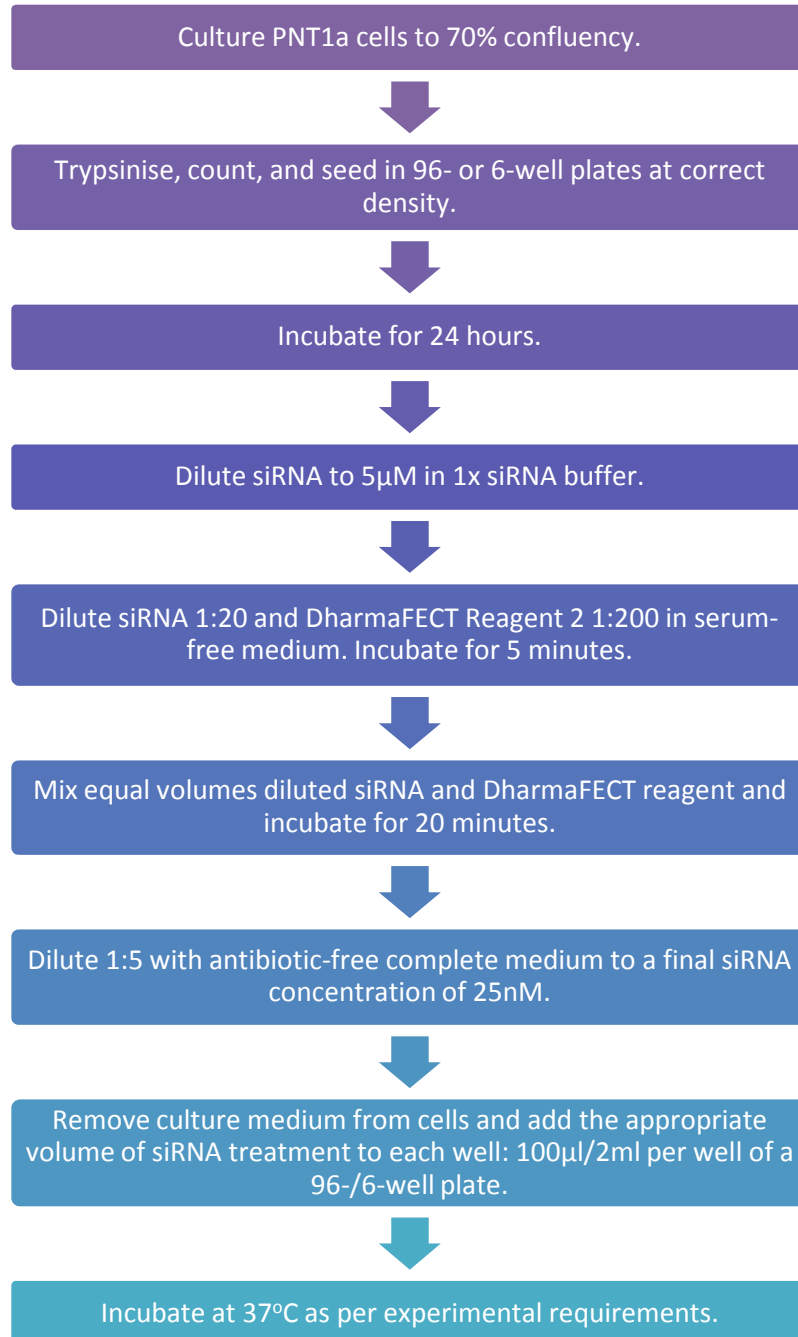


Figure 6.2. siRNA Transfection Protocol.

Method for the transfection of PNT1a using siRNA. Adapted from protocol provided by Thermo Scientific.

6.2.2.4 Protein Extraction

Cells were sub-cultured in 6 well plates and treated as per experimental design. Media was removed and the cells washed with ice-cold 10% phosphate buffered saline (PBS, Sigma-Aldrich). 100µl RIPA buffer (50µl of 50mM Tris-Hcl, pH7.4; 150mM NaCl; 1% Triton X-100; 0.5% sodium deoxycholate; 0.2% SDS; 200mM sodium orthovanadate; plus one Roche complete protease inhibitor cocktail tablet and 37.5 units/ml Benzonase (Novagen)) added to each well and the plate placed on ice for 2 minutes. Cells were removed from the plate using a cell scraper (SPL Lifesciences, Korea), collected and vortexed. Lysates were placed on ice for 5 minutes and vortexed, repeated 3 times for a total of 15 minutes, and then spun at 13,000 g for 10 minutes at 4°C to remove cell debris. Supernatants were stored at -20°C.

6.2.2.5 Protein Quantification

Protein collected from cells was quantified using the bicinchoninic acid (BCA) assay (Sigma-Aldrich). A standard curve was prepared using BSA (range: 100 – 1200µg/ml) diluted in NaPi buffer (50mM sodium phosphate pH 6 plus 5mM EDTA) and samples diluted 1:3 in NaPi buffer prior to quantification. 25µl of each standard and sample were pipetted in duplicates into a 96-well plate and 200µl BCA working reagent (Reagent B diluted 1:50 in Reagent A) added to each well. The plate was then incubated at 37°C for 30 minutes and the absorbance read at 550nm using the MRXII plate reader with Revelation 3.2 software (both Dynex Technologies). The BSA standards were used to prepare a standard curve which was then used to calculate the concentration of the samples.

6.2.2.6 RNA Extraction

Cells were sub-cultured in 6 well plates and treated as per experimental design. Media was removed and the cells washed with warm 10% PBS (Sigma-Aldrich). 350µl buffer RLT (Qiagen) supplemented with 1% β-Mercaptoethanol (Sigma) was added to each well. Cells were removed by scraping and collected in a QIAshredder tube (Qiagen), centrifuged at 13,000 rpm for 2 minutes and the filter disposed of. RNA was extracted from lysate using RNeasy kit (Qiagen) following the manufacturers' protocol for 'Purification of Total RNA from Animal Cells Using Spin Technology'. Store at -20°C

6.2.2.7 RNA Quantification

RNA samples kept on ice were quantified using a NanoDrop ND-1000 Spectrophotometer (Thermo Scientific) using ND-1000 v3.7.1 software. 1µl RNA sample was placed on the pedestal and absorbance was measured at 260nm to calculate concentration. Duplicate readings were performed per sample and average was calculated. Samples with a 260/280nm ratio of approximately 2.0 were considered acceptable for further use in experiments.

6.2.2.8 Cell Viability Assay

PNT1a cells were seeded in 96-well plates and transfected with siRNA. They were then incubated for up to 7 days post-transfection. At the time-point at which cell viability was to be measured 10µl alamarBlue (Invitrogen) was added to each well and cells were incubated for 3 hours. Fluorescence was measured every hour using a fluorescence excitation wavelength of 540nm and fluorescence emission was read at 590nm using the FLUOstar OPTIMA plate reader (BMG Labtech). Viability of all treatments was calculated as a percentage of the viability of the untreated cells.

6.2.2.9 Cell Proliferation Assay

Cell proliferation assay was performed over a period of 7 days on PNT1a cells cultured in 96-well plates with siRNA (see section 6.2.2.3). At the selected time-point cell proliferation was measured using the BrdU Assay (Roche) as per the kit protocol: 10µl/well BrdU labelling solution was added and incubated overnight at 37°C. Media was removed, 200µl/well FixDenat added, and incubated for 30 minutes at room temperature. FixDenat was removed and 100µl/well Anti-BrdU-POD working solution was added, and incubated for a further 90 minutes at room temperature. Solution was removed and washed three times with 300µl/well Washing Solution leaving the wash solution on for up to 5 minutes each time. Washing solution was removed and the bottom of the plate sealed using a black adhesive foil. 100µl/well Substrate Solution was added and luminescence measured immediately using the Luminoskan Ascent plate reader (Thermo Labsystems).

6.2.3 Western Blotting

6.2.3.1 SDS-Page Gel

20µg protein samples, extracted from either cell or tissue samples, were prepared by the addition of NuPAGE LDS Sample Buffer (Invitrogen) and dithiothreitol (DTT; Sigma) and denatured at 70°C for 10 minutes. Samples were loaded onto a 10% NuPage Bis-Tris gel in MOPS running buffer supplemented with NuPAGE Antioxidant (all Invitrogen) to maintain reducing conditions. 2µl of the protein ladder MagicMark XP (Invitrogen) was also loaded. Gels were run for 50 minutes at 200V using the XCell SureLock system (Invitrogen).

6.2.3.2 Western Transfer

Proteins run on gel were transferred to nitrocellulose membrane (BioRad) by western blotting. Three sponges were placed in the XCell II Blot Module (Invitrogen) followed by one piece blotting paper (Whatman), the protein gel, nitrocellulose membrane (Biorad), a further layer of blotting paper and three more sponges. The blot module was placed in the XCell SureLock system and the running chamber filled with NuPAGE Transfer Buffer (Invitrogen), with 10% methanol (Sigma) and 0.1% antioxidant. The outer chamber of the running system was filled with water. The transfer was run at 30V for 60 minutes.

6.2.3.3 Western Blot

The nitrocellulose membrane was checked for successful protein transfer using reversible Ponceau S staining (Sigma-Aldrich). Membranes were blocked in 10ml 5% milk in Tris-Buffered Saline Tween-20 (TBST) (50mM Tris, pH 7.4; 200mM NaCl and 0.1% Tween 20; all Sigma) for 1 hour at room temperature with rocking, and washed 3 x for 5 minutes in TBST. All primary antibodies were diluted in 10ml 5% milk TBST and incubated with the membrane overnight with rocking at 4°C, apart from β-Actin which was incubated for 1 hour at room temperature with rocking. The blot was washed as before and then incubated for 1 hour at room temperature with rocking with the secondary antibody in 5% milk TBST. The membrane was washed once more as previously described. Primary antibodies were both obtained from Abcam and diluted as follows; HSP90B1 1:500 (ab53075), and β-actin 1:10,000 (ab8227). The secondary antibody anti-rabbit IgG (Sigma-Aldrich) diluted 1:10,000 was used for both primary antibodies.

6.2.3.4 Immunodetection

The membrane was incubated with 4ml working reagent from SuperSignal West Pico Chemiluminescent Substrate (2ml Reagent A, 2 ml Reagent B; Thermo Scientific) for 5 minutes in the dark. The fluorescence intensity was measured using the BioRad Fluor-S Multilimager. For re-probing of the membranes, the previous antibodies were stripped for 40 min at room temperature using Restore™ Western blot stripping buffer (Pierce).

6.2.4 Taqman

RNA samples extracted from cells were prepared for Taqman analysis using the CAS-1200 robot and Robotics 4 software (both Corbett Life Science). Briefly MicroAmp Optical 96-well Reaction Plates (Applied Biosystems) were prepared including a standard curve with 20µl/well containing TaqMan RNA-to-C_T 1-Step Kit (Applied Biosystems), 4ng RNA and either 1x Pre-Developed TaqMan Assay Reagents (PDAR) mix (HSP90β1, assay ID: Hs00427665_g1; and GAPDH, assay ID: Hs03929097_g1, both Applied Biosystems) or 400 nM forward and reverse primers and 200 nM probe dye labelled with 5'-FAM™ (6-carboxyfluorescein) and 3'-TAMRA (6-carboxytetramethylrhodamine) for 18S detection (Table 6.1; Sigma Genosys, UK). Plates were analysed using the 7500 Real Time PCR System (Applied Biosystems) and reaction conditions consisted of 48°C for 30 minutes, 95°C for 10 minutes, followed by 40 PCR cycles of 95°C for 15 seconds and 60°C for 1 minute. Transcript levels were calculated from the standard curve.

Table 6.1. 18S Primers and probe sequences.

	Sequence
Forward primer	5' GGC TCA TTA AAT CAG TTA TGG TTC CT 3'
Reverse primer	5' GTA TTA GCT CTA GAA TTA CCA CAG TTA TCC A 3'
Probe	5' TGG TCG CTC GCT CCT CTC CCA C 3'

Where possible biological triplicates were performed, and technical triplicates run, for Taqman analysis. However, for the optimization of the siRNA delivery (Figure 6.6), due to the number of conditions to be tested, only a single biological replicate, and two technical replicates were performed. This was due to the preference to perform all treatments simultaneously, and so that Taqman analysis could be ran on a single plate, to reduce technical variation for better comparison of results.

6.2.5 Statistics

Statistical analysis performed in Minitab 15 (LEAD Technologies, Ltd), GraphPad Prism (GraphPad Software) and R as necessary. Analysis in R was performed by Dr Jack Dainty. Data for the effect of SF on HSP90 β 1 expression (Figure 6.3) was log-transformed to ensure normal distribution of residuals. Data was analysed in R using repeated measures ANOVA, with subsequent 1-way ANOVA of each patient. Minitab was used to perform Student's paired t-tests to compare treatment to control for both protein and mRNA in the two cell lines (Figure 6.5). Student's paired t-tests were also performed to compare each time point to time 0 for mRNA and protein (Figure 6.8). Data for the effect of HSP90 β 1 siRNA on cell viability and proliferation (Figure 6.9 and 6.10) was analysed in GraphPad Prism. 1-way ANOVA was performed for each day with subsequent Tukey *post hoc* tests to control each treatment to control.

6.3 Results

6.3.1 The effect of SF on HSP90β1 in BPH tissue

In the previous chapter, 24 hour treatment of 10μM SF significantly reduced HSP90β1 protein expression in one of the three patients. To investigate whether this effect was prevalent throughout the population, BPH tissue from nine independent patients was cultured with or without 10μM SF for 24 hours with in triplicate. The protein was extracted and run on western blots to detect HSP90β1 protein levels. The results were normalised by the housekeeping gene β-actin, and the results log-transformed so that the residuals were normally distributed (Figure 6.3). Repeated measures ANOVA revealed that both patient (p-value ≤0.001) and treatment (p-value = 0.025) had a statistically significant effect. Comparison of the means showed an average reduction of 22% in HSP90β1 expression as a result of 10μM SF treatment. Individual analysis of each patient using 1-way ANOVA revealed HSP90β1 expression was significantly reduced in patients 31, 32 and 38 by an average of 62% (p-values = 0.003, 0.019 and 0.021 respectively). Although there was a reduction in a further two patients, 29 and 34, these were not statistically significant.

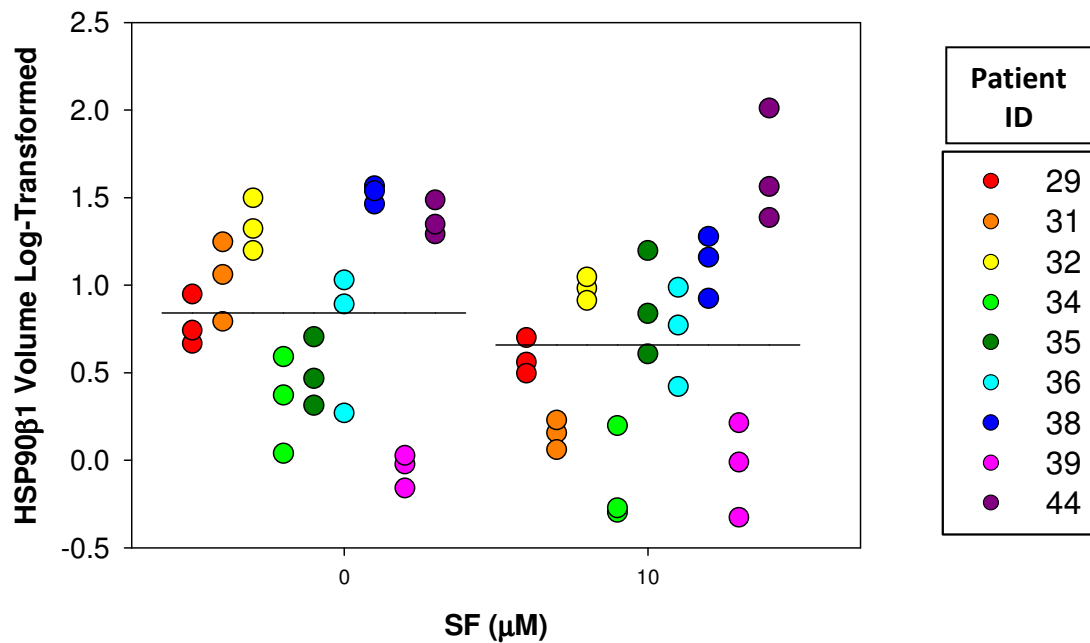


Figure 6.3. The effect of SF on HSP90 β 1.

BPH tissue from nine independent patients was cultured with or without 10 μ M SF for 24 hours in triplicate. Protein was extracted, run by western blot and quantified. Results were normalised by the house-keeping gene β -actin. Data was log-transformed and analysed by repeated measures ANOVA, revealing that both patient and treatment had a statistically significant effect (p -values ≤ 0.001 and 0.025 respectively). Biological triplicates for each patient plotted, mean value for all patients also plotted (black line through each group).

The expression of HSP90β1 in the BPH tissue cultured with or without 10μM SF was also investigated using immunohistochemical staining. Tissue samples from six patients were examined in this manner and representative images shown (Figure 6.4). HSP90β1 was seen to be expressed throughout the tissue, but most strongly in the epithelium. It is difficult to quantify any effect of SF due to heterogeneity between the samples, but in some samples, particularly 38, 42 and 43, staining of the epithelium appears to be less pronounced in the samples treated with 10μM SF.

Of the patients examined using IHC, HSP90β1 expression was also examined by western in patients 38, 39 and 44 (See Figure 6.3). HSP90β1 expression was noted to be significantly reduced in patient 38 analysed by western blot, which corresponds with the IHC results in that staining for HSP90β1 appeared less pronounced in the epithelium of the 10μM SF treated sample compared to the control. No significant effect was seen on HSP90β1 expression by western blot in samples 39 and 44, correlating with the IHC results in which no clear change in staining was observed as a result of SF treatment.

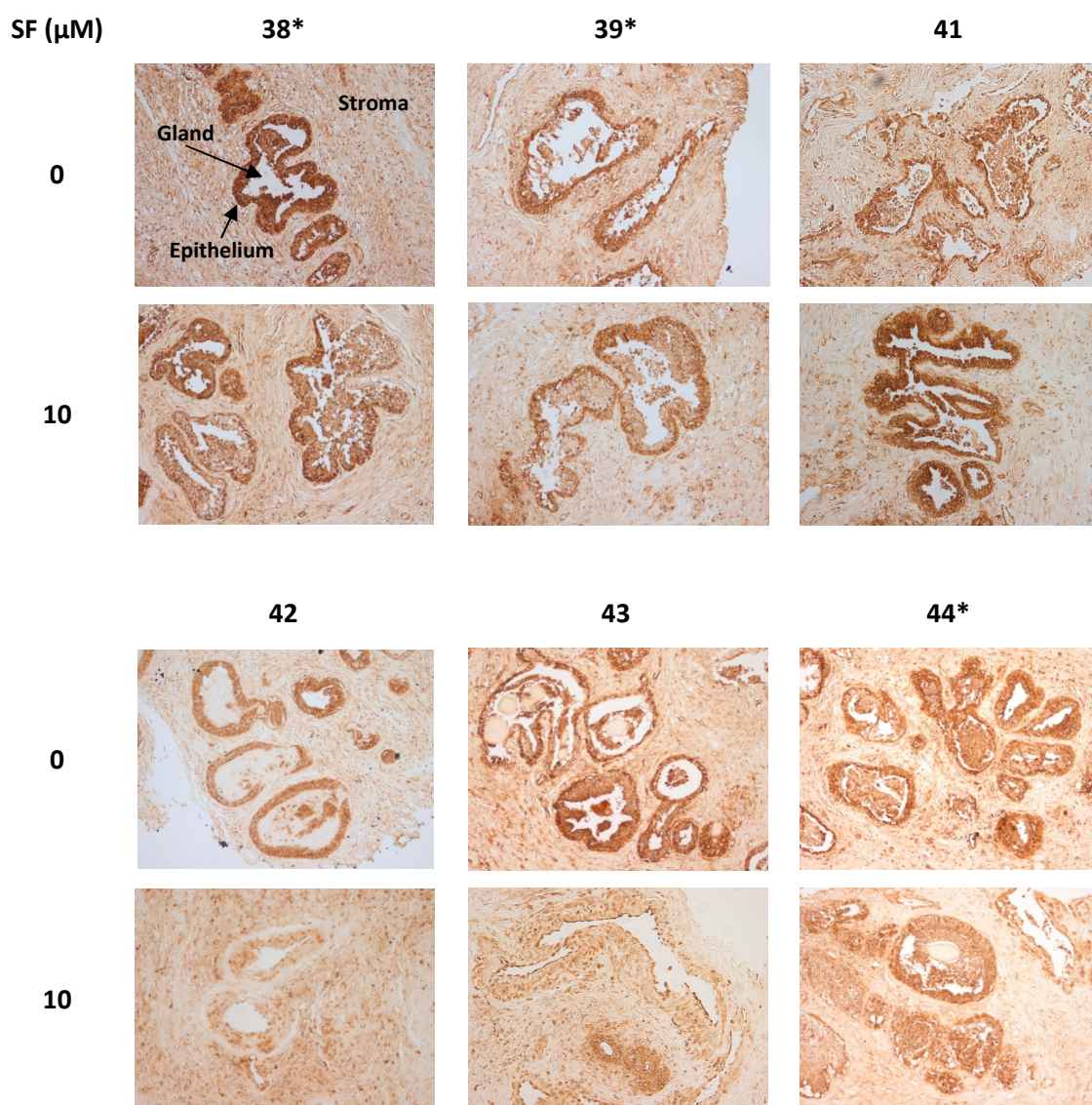


Figure 6.4. HSP90β1 expression in BPH tissue.

BPH tissue from six patients was incubated with or without 10μM SF for 24 hours, fixed in formalin, wax-embedded and sectioned. Tissue was probed for HSP90β1 expression by immunohistochemistry. Representative images shown, all images x10 magnification. *HSP90β1 expression was also examined by western in patients 38, 39 and 44 (See Figure 6.3).

6.3.2 Modulation of HSP90B1 by SF in cell lines

To further investigate the effect of SF on HSP90β1, prostate cell lines were used, and the expression of both HSP90β1 mRNA and protein measured (Figure 6.5). In the PNT1a cells, a healthy prostate cell line, no effect on mRNA expression was observed with either 10 or 25μM SF, but protein expression was reduced with the 10μM SF (p-value = 0.051). In the cancerous cell line, DU145, mRNA expression was seen to be significantly increased by 25μM SF treatment (p-value <0.05), but this did not translate into a significant effect on protein levels.

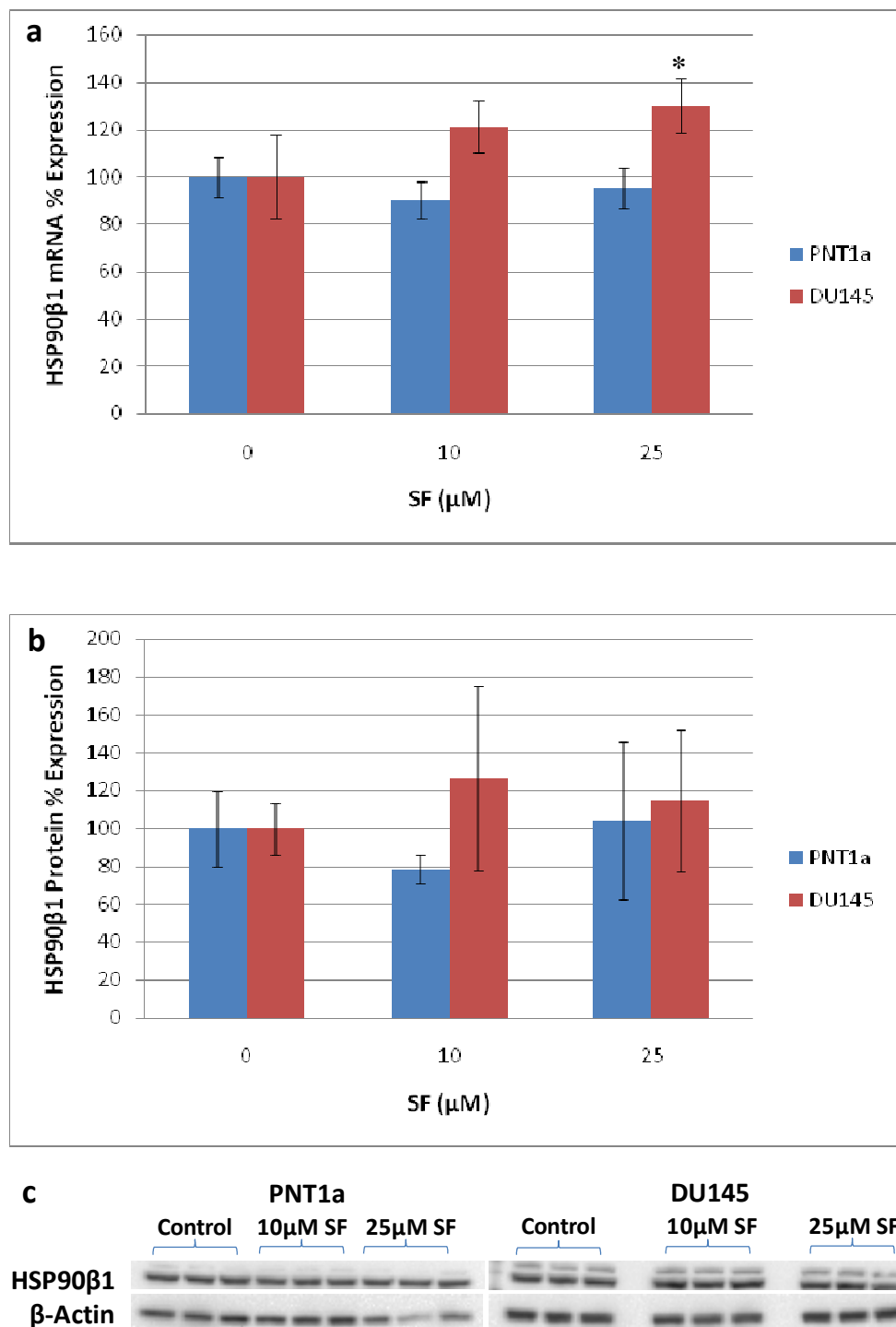


Figure 6.5. The effect of SF on HSP90β1 in cell lines.

Cells were cultured with 0, 10 or 25μM SF for either 24 or 48 hours. At 24 hours, (a) mRNA was extracted and at 48 hours, (b) protein was extracted (triplicates performed for all and the experiment performed twice). HSP90β1 mRNA was measured by Taqman and protein by western blot. (c) Representative western blots shown. Results were normalised for 18S and β-actin respectively. Means ± standard deviation are shown. *p ≤ 0.05

6.3.3 siRNA Method Optimization

HSP90β1 protein expression was reduced by 10μM SF in BPH prostate tissue, but SF had no significant effect on protein expression in both healthy and cancerous prostate cell lines. Little research has been conducted regarding the biological activity of HSP90β1, and in particular its role in the prostate. To understand the biological significance of the reduction in HSP90β1 protein expression seen in BPH tissue *ex vivo* in response to 10μM SF, expression of HSP90β1 was artificially knocked down using siRNA in PNT1a cells.

Initially, the method for siRNA delivery had to be optimized to determine the most effective cell plating density, and which concentration of transfection reagent was the most efficient. Cell viability was measured to ensure the transfection did not reduce cell viability by more than 20%, and GAPDH gene expression was assayed, as GAPDH siRNA was used as a positive control to ensure successful transfection. Non-targeting siRNA was used as a negative control to confirm the specificity of any effect observed.

Increasing the concentration of the transfection reagent decreased the viability of the cells, but as cell plating density increased the effect was less pronounced (Figure 6.6). Due to the necessity that cell viability remained above 80%, the lowest cell seeding density, 1.5×10^4 cells/cm², was found to be unsuitable, as all conditions reduced viability to below this level.

Expression of GAPDH was measured in all samples, and a minimum of 80% knockdown was set as the threshold of efficient transfection. At all conditions, excluding the lowest transfection reagent dilution with the highest cell seeding density, this was achieved (Figure 6.6). The non-targeting siRNA had no effect on GAPDH expression, confirming this was a specific targeted effect of the GAPDH siRNA.

As the transfection reagent did have an effect on cell viability, but was essential for good transfection, it was decided to use the lowest possible dilution at which no more than a 20% reduction in cell viability was seen, but that still displayed good GAPDH knockdown. Comparison between all the conditions resulted in the selection of a dilution of 1:666.66 of the transfection reagent, with the cell seeding density of 3×10^4 cells/cm² for all subsequent experiments.

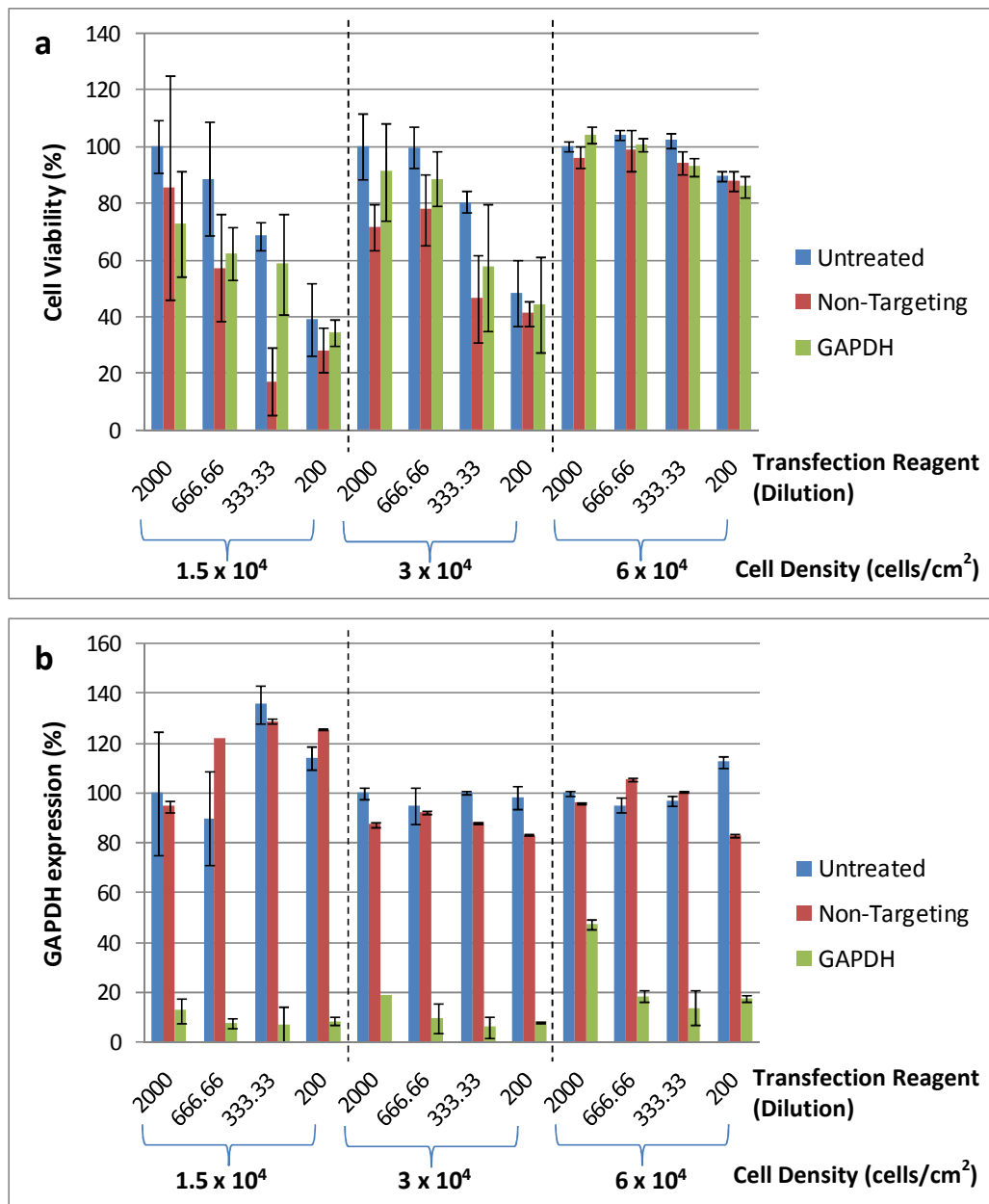


Figure 6.6. Optimisation of siRNA delivery.

To optimize the siRNA delivery conditions in PNT1a cells two conditions were altered: cell seeding density, and transfection reagent concentration. (a) Cell viability was measured by alamarBlue (4 biological replicates), and (b) GAPDH expression assayed by RT-PCR (2 technical replicates). Means \pm standard deviation are shown. Increasing transfection reagent concentration reduced cell viability, although the loss in cell viability became less notable the higher the seeding density. GAPDH siRNA successfully knocked down GAPDH expression, with a higher knock down noted at the higher transfection reagent concentrations. The transfection reagent dilution of 1:666.66 and seeding density of 3×10^4 cells/cm² were selected for all further experiments. (Untreated contained transfection reagent but no siRNA).

6.3.4 Optimising HSP90β1 knockdown

Subsequent to the optimization of the transfection conditions, the concentration of HSP90β1 siRNA for the most effective knockdown needed to be assessed. Knockdown using concentrations of between 5-50nM HSP90β1 siRNA revealed no variation between the effectiveness of the different concentrations, and a 40% knockdown was achieved (Figure 6.7). Both the GAPDH and non-targeting siRNA were used at the concentration of 25nM, so in line with this, 25nM HSP90β1 siRNA was selected for all further HSP90β1 knockdown experiments.

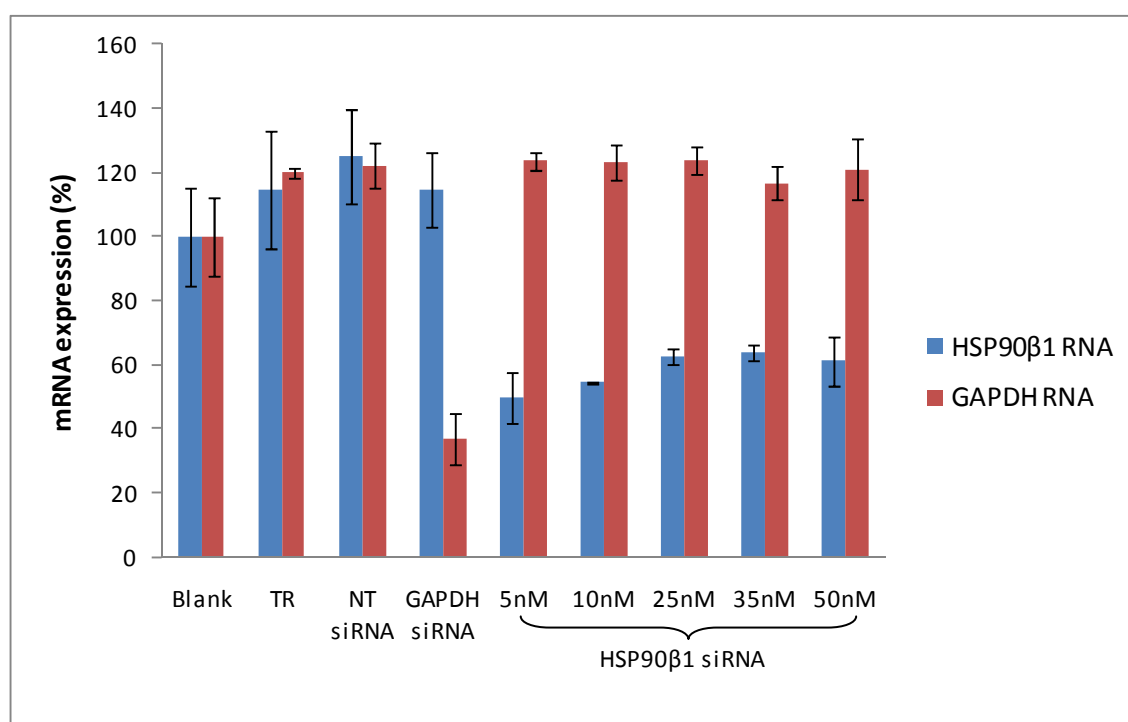


Figure 6.7. HSP90β1 siRNA dose effect.

PNT1a cells were seeded in 6 well plates and treated with siRNA to knockdown either GAPDH or HSP90β1 at different concentrations. After 24 hours mRNA was extracted and HSP90β1 and GAPDH measured using Taqman. Means \pm standard deviation (three biological replicates). (TR = transfection reagent, NT = non-targeting)

mRNA from the siRNA experiments had been routinely collected after 24 hours, so a time course was performed to determine the knockdown over time for both mRNA and protein HSP90β1 expression (Figure 6.8).

HSP90β1 knockdown was apparent from 12 hours after transfection with a 35% decrease, reducing further until at 48 hours, a 60% knockdown was recorded. At 72 hours, the last point measured, HSP90β1 expression was at a highly similar level to that seen after 24 hours, at just below 50% of the expression at time zero.

As expected, the subsequent reduction in HSP90β1 protein levels was delayed, with no noticeable reduction observed until a 20% reduction at 48 hours, further reducing at 72 hours to 70% of the original protein level.

A greater reduction of protein levels than that achieved here may make it easier to observe any effect on the biological phenotype of the cells, as it is expected that the greater the reduction of the protein, the more pronounced any behavioural changes would be. However, the reduction in protein recorded, no more than 30%, is comparable to the 22% reduction that was on average seen in the tissue, so any results may more accurately represent the biological relevance of HSP90β1 reduction by SF in the tissue.

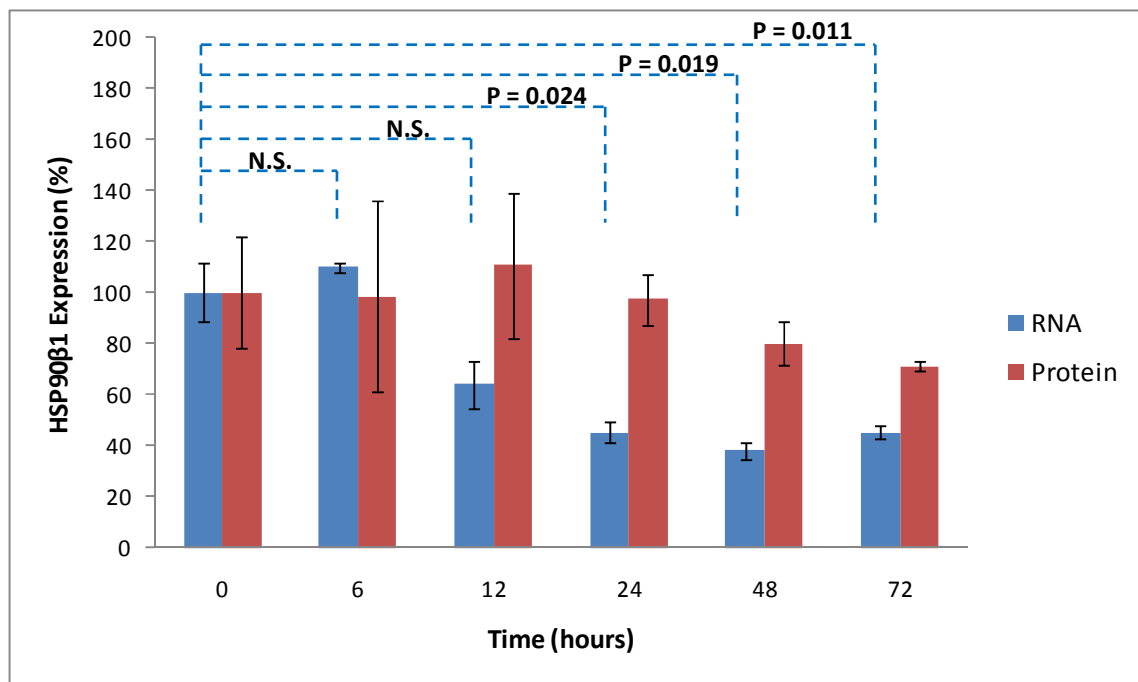
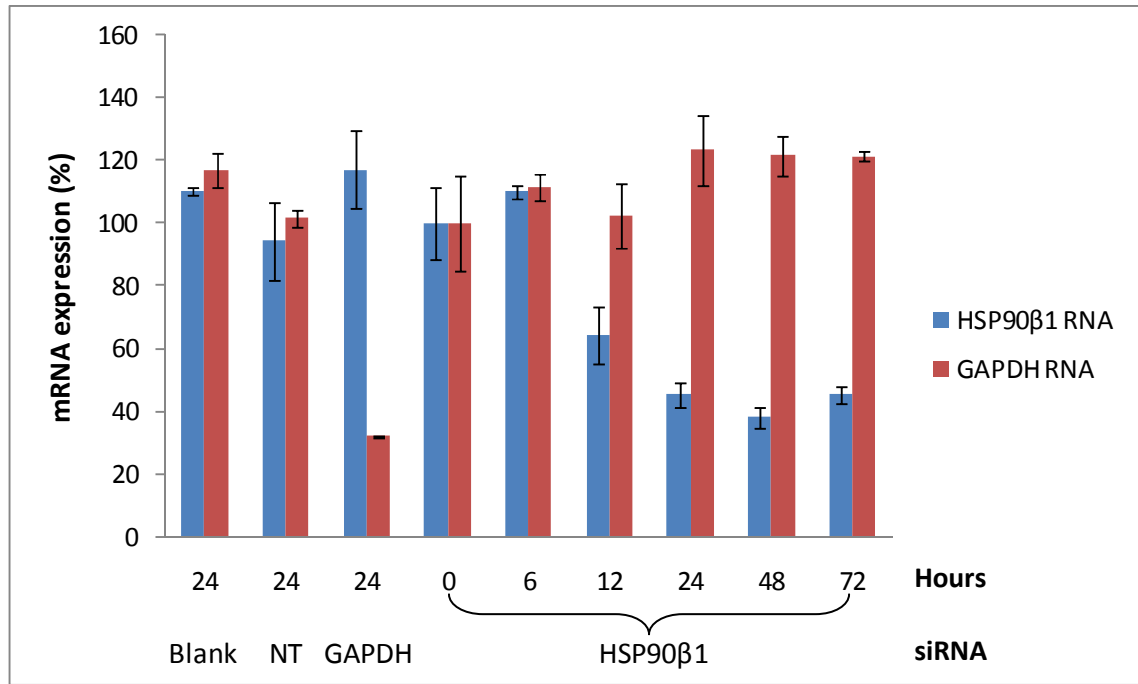


Figure 6.8. Time course for HSP90β1 knockdown.

PNT1a cells were seeded in 6 well plates and treated with HSP90B1 siRNA. RNA and protein were extracted at different time points. mRNA was measured by Taqman and protein by western blotting. Mean ± standard deviation (biological triplicates) shown. N.S. = non-significant. Protein was not significantly reduced at any time point compared to 0 hours (p-values not shown). NT = non-targeting.

6.3.5 The effect of HSP90β1 knockdown on the cell

As HSP90β1 was originally selected for further investigation due to its proposed role in apoptosis, it was decided to measure the effect of HSP90β1 knockdown on cell viability, as any effect on apoptosis would alter cellular viability. Cells were cultured for up to 7 days after transfection, and viability measured using AlamarBLUE (see Chapter 6.2.2.8). Over the time period measured, no effect was observed on viability as a result of HSP90β1 knockdown (Figure 6.9).

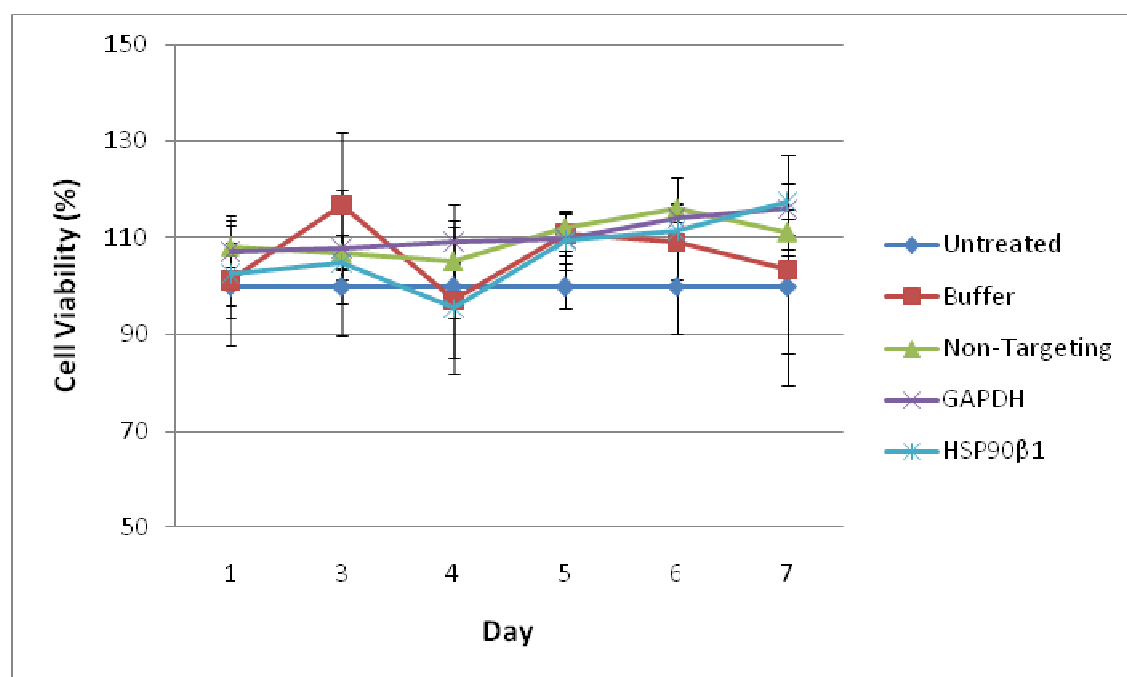


Figure 6.9. Effect of HSP90β1 siRNA on cell viability.

PNT1a cells were seeded on 96-well plates and treated with HSP90β1 siRNA. Cell proliferation was measured by alamarBlue. Values normalised to untreated cells with no siRNA or transfection reagent. Means \pm standard deviation (9 biological replicates).

As no effect was observed on viability, it was then decided to measure whether the knockdown had any influence on cell proliferation. Cells were once again cultured for up to 7 days after transfection and cell proliferation determined using the BrdU Cell Proliferation assay (see Chapter 6.2.2.9). No effect on cell proliferation was observed (Figure 6.10).

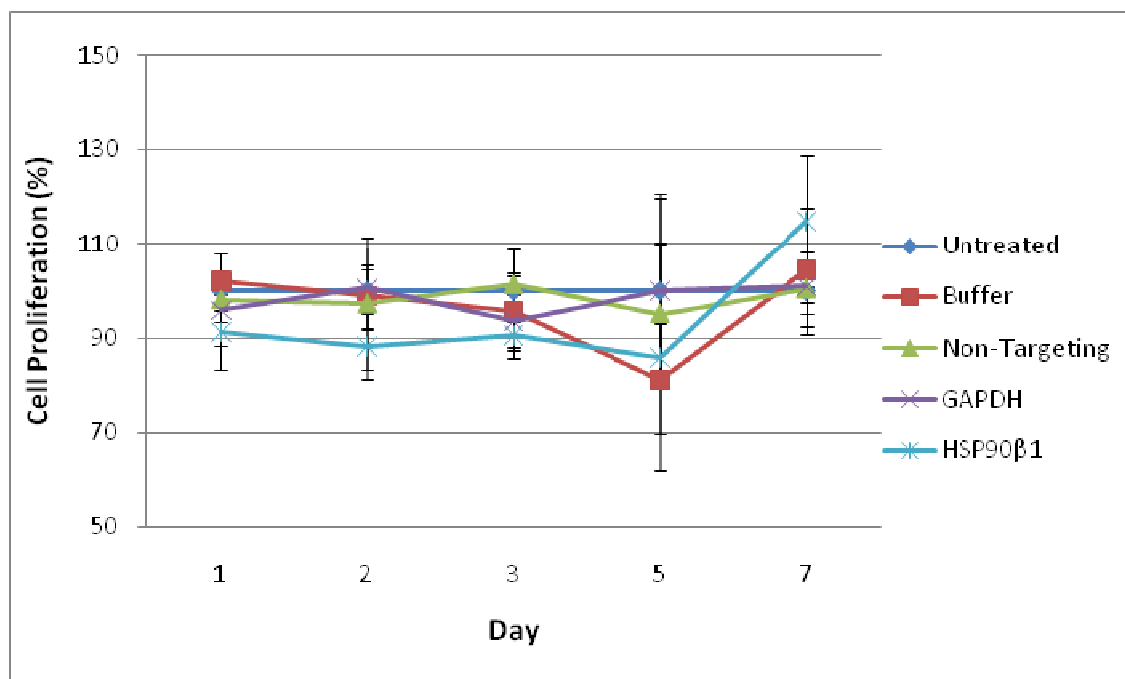


Figure 6.10. Effect of HSP90β1 siRNA on cell proliferation.

PNT1a cells were seeded on 96-well plates and treated with HSP90β1 siRNA. Cell viability was measured by BrdU Assay. Values normalised to untreated cells with no siRNA or transfection reagent. Means \pm standard deviation (9 biological replicates).

6.4 Discussion

6.4.1 Modulation of HSP90β1 by SF

6.4.1.1 Ex Vivo Model

In the previous chapter, it was reported that HSP90β1 was significantly reduced by 10μM SF in one of the BPH samples from three patients analysed by 2D gel electrophoresis. To investigate whether this result could be observed in further patients, further BPH tissue samples were obtained and treated as before, and analysed using western blotting for the immunodetection of HSP90β1.

Analysis of the results from the nine patients, using repeated measures ANOVA, showed that both patient and treatment had a statistically significant effect (p-values <0.001 and 0.025 respectively) (Figure 6.3). On average, a significant reduction of 22% was observed after SF treatment, indicating that the effect observed in the 2D gels was repeatable and applicable to a larger population. Individual assessment of each patient by 1-way ANOVA, indicated HSP90β1 was significantly reduced by SF by an average of 62% in three patients (patients 31, 32 and 38). Visual assessment showed a non significant reduction in a further two patients (patients 29 and 34), whilst two showed a possible increase (patients 35 and 44), and the final two remained unaltered (patients 36 and 39).

The different response of the patients demonstrates once again the variation that exists between individuals, and the necessity for large sample numbers in order to observe trends in a population. Despite the individual nature of the responses, the reduction seen in five of the nine patients and the statistically significant reduction seen in the group as a whole, suggests that the modulation of HSP90β1 by SF, may be of importance to the larger population. As such, this effect is worth investigating further in the hope that it may help us to understand more about SF activity, and how SF can be beneficial to prostate health.

6.4.1.2 Immunohistochemistry

To further investigate the expression of HSP90β1 in BPH, samples were fixed and wax-embedded, and immunohistochemically examined for HSP90β1 staining (Figure 6.4). From the sections, it is clear that HSP90β1 is expressed throughout the epithelium and stroma of the tissue, but with darker staining in the epithelium, suggesting higher expression in this region. Due to the heterogeneous nature of the tissue samples it is difficult to determine the effect of

SF on the expression of HSP90β1, but in a number of the samples the epithelial staining appears less pronounced in the samples cultured with SF, suggesting that SF may reduce the expression of HSP90β1 in the epithelium. This effect was observed in a select number of patients, and would correlate with results from the western, where some patients showed no effect of SF on HSP90β1 expression, whilst others did.

This result is also interesting as it suggests that SF only alters HSP90β1 in epithelial, but not stromal cells. This observation may help explain the limited reduction in HSP90β1 seen, as stroma typically constitutes a greater percentage of the samples compared to epithelium. If SF only reduces HSP90β1 in epithelial cells, and not stromal cells, there is a lower percentage of cells on which SF can act. Therefore, any effect in HSP90β1 expression in epithelial cells may be hidden when looking at reduction in the whole sample. For example, if 80% of the sample is comprised of stroma, and the remaining 20% is epithelium, and they both express HSP90β1 at the same level, then the stroma and epithelium will contribute 80 and 20% of the total HSP90β1 expression respectively. If SF reduces HSP90β1 expression by 50% in the epithelium, but has no effect on the stroma, then the 80% of HSP90β1 expression contributed by the stroma is unchanged, but the 20% from the epithelium is reduced by half to only 10%. In turn, this would therefore lead to an observation of only a 10% reduction in total HSP90β1. As such, if HSP90β1 expression was assessed in the stroma and epithelium independently, it would then be revealed that SF had a significant effect on HSP90β1 expression in epithelial cells, but no effect in the stroma.

However, in the control tissue HSP90β1 expression is greater in the epithelium compared to the stroma. As a result, you may expect an effect on HSP90β1 in the epithelium to be more noticeable when examining total expression than in the example given above. However, it is still likely that this reduction would be partially obscured by the prevalence of stroma in the tissue, which may help explain why a significant reduction was seen in so few samples. It would also be more likely that the samples which had a higher percentage of epithelium compared to stroma would show a greater reduction of HSP90β1 expression in response to SF.

6.4.1.3 Cell Lines

The variation between tissue samples from different patients and the differing degrees to which SF can reduce HSP90β1 in each sample, makes the use of tissue very difficult and

complex in further investigating this relationship. Therefore, it was decided to use prostate cell lines for further experiments, as this less complex system allows greater reproducibility of results. The two cell lines selected were PNT1a, a healthy prostate cell line, and DU145, a cancerous prostatic cell line, to see whether there was any variation in the effect of SF on HSP90β1 in the different diseases states, due to the suggested relationship between HSP90β1 and cancer.

In the cells, the only significant effect observed was on the mRNA in DU145 cells treated with 25μM SF. However, despite this, the effect on protein expression was not significant (Figure 6.5). It has previously been reported that HSP90β1 mRNA and protein levels do not always correlate [270], so this is not unprecedented. That the effect seen *ex vivo* can not be replicated *in vitro*, may be due to a number of factors.

As the immunohistochemistry (IHC) results suggest that SF reduced HSP90β1 in the epithelial cells, and not the stroma, it was expected that a reduction of HSP90β1 in response to SF would be seen *in vitro*, as the cell lines used were both of epithelial origin. That an effect was not seen, suggests that the interactions between the epithelium and stroma play a crucial role in the result seen *ex vivo*.

The importance of epithelial-stromal interactions in the normal prostate is well established, and is known to be mediated by growth factors including FGF, IGF and EGF [3]. Epithelial cells secrete factors that alter the behaviour of stromal cells, which in turn secrete factors to modulate epithelial cell proliferation and differentiation. The expression of these growth factors is often altered in BPH, altering the behaviour of both the stroma and epithelial cells [173]. For example, FGF-2 secretion by basal cells is increased in BPH and can promote stromal cell proliferation. In addition, TGFB1, which has a complex role in prostate regulation, is also secreted by basal cells and can, at low concentrations, increase cell proliferation, but at higher concentration, inhibits stromal cell proliferation [219, 281]. Therefore, the interactions between the two cell types play a crucial role in the development of BPH.

In culture, cell lines lack the signals that *in vivo* are crucial to their function and behaviour, and may therefore respond differently to outside stimuli. As such, it may be suggested that reduction of HSP90β1 by SF is dependent on cross-talk between the stromal and epithelial cells.

Further to this, the reduction of HSP90β1 by SF was only seen in a select number of the tissue samples analysed, indicating variation in how each individual responds. In the same way that not all tissue samples responded in the same way, not all cell lines will, as each cell line is established from a different patient, so variation will exist between cell lines in the same manner it exists between tissue samples. Therefore, if tissue samples were taken from the patients from which the cell lines were initially established, it may be that SF would not reduce HSP90β1 expression in these samples, explaining why HSP90β1 was not reduced in the cell lines.

Cell lines are typically well documented and major mutations characterised, so careful selection of cell lines can help elucidate and understand the mechanisms by which stimuli can elicit a response. The knowledge of specific mutations in cell lines was implemented to great success in a study by Traka and colleagues who sought to investigate the effect of PTEN-deletion on SF activity. PTEN is a major tumour suppressor which is commonly mutated or deleted in PCa. Using the PC3 PCa cell line, in which PTEN is not expressed, and the healthy PNT1a cell line, in which PTEN is expressed, it was observed that the PC3 cells were more sensitive to growth inhibition by SF. These results suggested that the mechanism by which SF reduced growth was via altering the PTEN pathway. As there are other unspecified genetic differences between the two cell lines, a mouse model in which PTEN was specifically deleted was used, and confirmed that PTEN-deficient cells were more sensitive to SF. Thus suggesting that SF can specifically target cells in which PTEN is deleted, helping protect against carcinogenesis [160].

In addition, in the current study the tissue was taken from patients with BPH, whilst the cell lines used were representative of healthy and carcinogenic prostate, so it may be that the result observed is disease state specific. For example, TGFβ1 is able to inhibit the growth and proliferation of non-malignant cells, but conversely promotes survival and proliferation of tumour cells [36]. In BPH, stromal cells proliferate in response to IFN-γ, IL-2 and IL-7 and are not affected by IL-4, but in healthy stromal cell the opposite is true [19]. These examples provide evidence that the response to stimuli can vary in relation to prostate disease.

It must therefore be considered that the reduction of HSP90β1 by SF may be BPH specific. If this is the case, then it would be expected that treatment of an established cell line, isolated

from BPH, with SF, would result in a reduction of HSP90β1. Furthermore, if tissue samples taken from healthy or cancerous prostate were treated and analysed in the same way as the BPH tissue, then a reduction in HSP90β1 would not be expected.

If the reduction of HSP90β1 by SF is disease state specific, and occurs in BPH cell lines but not those representative of other disease states, then understanding the differences between the cell lines may help discover the mechanism by which SF reduces HSP90β1 expression. It would therefore be likely, that this mechanism is dependent on a pathway or protein which is specifically altered in BPH, and identification of this difference would help elucidate the mechanism by which SF alters HSP90β1.

From these results, it is apparent to see that the reduction of HSP90β1 by SF in the prostate is a complex process in which it is likely that stroma-epithelium interactions, inter-individual variation and disease state play a crucial role.

6.4.2 Artificial knockdown of HSP90β1

As SF did not reduce the expression of HSP90β1 *in vitro*, to investigate the biological relevance of the effect seen *ex vivo*, HSP90β1 had to be suppressed artificially. To this end, siRNA targeted to the HSP90β1 gene was used. Although the siRNA was pre-designed (DharmaFECT, ThermoScientific), the delivery method had to be optimised for the cell line used, and the specificity of the siRNA knockdown confirmed (Figure 6.6).

A number of controls were used for the experiment, including: no treatment, as a complete blank for all conditions; transfection reagent only, to determine whether transfection reagent alone altered the cells; non-targeting siRNA, a negative control to demonstrate the specificity of the siRNA effect; and GAPDH siRNA, a positive control to show whether the transfection was successful. Using these controls, the concentration of transfection reagent, and density of cells, was determined for optimum transfection of PNT1a cells. Successful transfection was determined as >80% GAPDH knockdown and <20% reduction in cell viability.

It was apparent from the results that increased transfection reagent concentration decreased cell viability, with a greater effect seen on cells with a lower seeding density. However, a greater concentration of transfection reagent allowed for a greater knockdown of GAPDH due

to increased siRNA uptake by the cells. A balance between these two observations had to be reached, so a transfection reagent dilution of 1:666.66, and seeding density of 3×10^4 cells/cm², was selected for all further experiments.

Increasing concentrations of HSP90β1 siRNA did not induce a greater knockdown of gene expression. Therefore, a concentration of 25nM was selected to correspond with the concentrations used of the control siRNA (Figure 6.7). In comparison to GAPDH, with which >80% knockdown was achieved, the maximum knockdown of HSP90β1 observed was 60%. Commonly the main sources of insufficient knockdown are siRNA degradation, poor delivery and inappropriate detection methods [282]. However, as both the GAPDH and HSP90β1 siRNA were stored, handled and delivered in the same manner, with GAPDH being reduced by >80%, it is unlikely that degradation or delivery are the reason why only a 60% knockdown of HSP90β1 could be achieved. The final common cause is incorrect detection of the knockdown, which here was measured using real-time RT-PCR and western blotting to quantify mRNA and protein respectively. Methods with poor sensitivity may produce false results, which may be a factor in western blotting, but Taqman is highly sensitive [283], and it is therefore unlikely that this was the source of the insufficient reduction.

A time course revealed that mRNA levels decreased from 12 hours post-transfection decreasing steadily until 48 hours although at 24, 48 and 72 hours the level of HSP90β1 was highly comparable. As expected there was a time delay for this to translate to protein expression, with a reduction first seen at 48 hours reducing further at 72 hours (Figure 6.8).

Both mRNA and protein were measured, as although siRNA exerts its effect at the mRNA level, it is the protein level which dictates the biological phenotype of the cell. As such, it is essential to determine that the mRNA knockdown translates into a reduction in protein. As protein and mRNA levels were only measured up to 72 hours post transfection, at which point protein levels were still decreasing, it would be interesting to see if studied over a longer time period whether protein levels carried on reducing, and what the ultimate reduction would be. Alongside this, it would then be interesting to note the mRNA levels to discover the longevity of this knockdown, and at what time point the levels started to recover, if at all. Typically siRNA-mediated silencing lasts between 5-7 days [282], and taking into account the delay between mRNA and protein reduction, a behavioural change may therefore be expected to be observed from days 2-9. Here, the mRNA and protein expression were measured up to three

days post-transfection, but it would be expected that the reduction of mRNA would last twice as long. Therefore, the reduction in protein may become more pronounced if measured over a longer time period.

6.4.3 The effect of HSP90β1 reduction on cell function

In the previous chapter, HSP90β1 was chosen for investigation due to its reduction by SF in BPH, and its postulated role in apoptosis, a process essential to normal tissue homeostasis, and which SF has previously been reported to induce.

To investigate its biological relevance, it was hypothesised that a reduction of HSP90β1 would lead to a decrease in cell viability as a result of increased apoptosis. However, here, the reduction of HSP90β1 by siRNA had no effect on cell viability (Figure 6.9). As no effect was seen on cell viability it was decided to investigate whether a reduction of HSP90β1 would reduce cell proliferation, a process of critical importance in BPH. A previous paper had also reported that inhibition of HSP90β1 by geldanamycin (GA) resulted in reduced cell proliferation at low concentrations, whilst inducing apoptosis at higher doses, leading to the hypothesis that this may have been what was happening in this study [274]. However, no significant effect was observed on cell proliferation (Figure 6.10).

It is intriguing that no effect on either viability or proliferation was observed when previous data reports a link. However, in previous research they have often measured HSP90β1 expression after apoptosis has been induced, so it may be that a reduction in HSP90β1 alone does not trigger apoptosis, but sensitizes the cell to apoptotic stimuli. It would of great interest to repeat the experiment with some external apoptotic stimulus, such as the apoptotic drug etoposide, to see whether the reduction of HSP90β1 leads to greater induction of apoptosis than etoposide alone. Although no effect was observed on HSP90β1 expression *in vitro* by SF, it would also be interesting to see whether artificial HSP90β1 knockdown would sensitize the cells to SF-induced apoptosis.

Pan and colleagues [284] performed a similar experiment to the one here, and found that HSP90β1 knockdown promoted apoptosis. However, there were three major differences between the two experiments. Firstly, they were working with a pancreatic cancer cell line, secondly they were able to achieve a greater knockdown (70% at 48 hours increasing to 90% at

72 and 96 hours and reaching 98% at 120 hours), and lastly they treated the cells with actinomycin D to stimulate apoptosis. All these differences may be the reason that they reported an increase in apoptosis, whilst here none was seen.

It may be that the induction of apoptosis is cell type specific, so may not occur in prostate cells, or may be dependent on disease state, as the cells used here were healthy, whilst Pan and colleagues were working with a cancerous cell line. With regards to tissue type specificity, very few studies have looked directly at HSP90β1 silencing and apoptosis as Pan and colleagues have done, but the reduced expression of HSP90β1 has been correlated with apoptosis in a number of cell lines, including prostate. This suggests that the effect Pan and colleagues observed is unlikely to be unique to pancreatic cells, and that it is probable the same effect would occur in prostate cells.

A second possible explanation could be the disease state of the cells, as the prostate cells used were healthy, whilst the pancreatic cells were cancerous. This suggestion is not without precedence as GA and HMA, inhibitors of HSP90β1 and HSP90, have been seen to induce apoptosis and sensitivity to cytotoxic drugs in CLL cells whilst conferring cytoprotective effects to normal cells [273]. Thus, suggesting that whilst the silencing of HSP90β1 may lead to increased apoptosis in cancerous cells, it may actually protect healthy cells. This may explain why no effect in the prostate cells was seen. To test this, it would be necessary to perform the experiment in both healthy and cancerous prostate cell lines to discover whether there is any difference in the level of apoptosis as a result of HSP90β1 siRNA.

It may also be that the knockdown achieved here was not sufficient to observe an effect, as the maximum knockdown observed was 60% at 48 hours, compared to 70% at the same time point in the experiment by Pan and colleagues. At 72 hours, the knockdown had not increased further, whilst theirs had reached to 90%. However, we did not measure mRNA at any later time points, whilst they measured it again at 96 and 120 hours, so it would be interesting to see whether the reduction of HSP90β1 mRNA further increases over a longer period.

Using a mouse model, null mutation of HSP90β1 results in embryonic lethality, but in embryonic stem cells (ESCs), HSP90β1 $-/-$ prevents cells from differentiating into muscle cells due to lack of insulin-like growth factor II. Complete knockout of HSP90β1 also resulted in upregulation of other ER chaperones, including GRP78 and calreticulin (see Chapter 5.3.3 and

5.4.3), but not protein disulfide isomerase, suggesting some form of compensatory mechanism, but this effect was only observed in the HSP90β1 heterozygotes [272]. As this effect was only seen in the HSP90β1 null ESCs, this suggests that total knockdown of HSP90β1 may be necessary to see any effect, which may be why the 60% knockdown we achieved did not elicit a response. However, the compensatory mechanism seen may result in other chaperones being upregulated, taking on the functions of HSP90β1, and may therefore allow the cell to function as normal. It would be interesting to investigate whether any ER chaperones were upregulated as a result of the knockdown in the PNT1a cells.

Finally, the last difference noted was that they used actinomycin D to induce apoptosis, so it may be, that as discussed above, the knockdown on HSP90β1 alone is not sufficient to increase apoptosis, but sensitizes the cell to apoptotic stimuli. Therefore, repeating the experiment but with the addition of a pro-apoptotic drug, such as actinomycin D or etoposide, could determine whether the knockdown of HSP90β1 sensitizes the cell to apoptotic stimuli.

Due to time constraints further investigations were not possible. As well as the suggestions made above regarding apoptotic stimuli, disease state, and knockdown status, there are other possible experiments that could be performed. Cell viability was measured as an indicator of apoptosis as HSP90β1 is suggested to have anti-apoptotic properties. However, the cell viability assay was not specific for apoptotic cell death, and could also measure different types of cell death, such as necrosis. Instead, there are other more specific markers of apoptosis that could be investigated. These include annexin V, DNA fragmentation, and caspase 3 activity.

Annexin V binds to phosphatidylserine (PS) on the cell surface, the amount of which increases in apoptotic cells. As such, annexin V binds to cells with PS exposed on their surface, acting as a marker of apoptosis. Annexin V can be coupled with a fluorescent dye and added to the cells under investigation before being analysed by flow cytometry. The number of cells to which the annexin V has bound is then detected, indicating the level of apoptosis within a sample [207-208]. Furthermore, DNA fragmentation is a hallmark of apoptosis, and assays can detect either low molecular weight DNA which increases in apoptosis, or high molecular weight DNA that decreases in apoptosis. DNA fragmentation can be measured in the nuclei of lysed cells by ELISA, or using extracted DNA can be analysed by gel electrophoresis [285]. A further marker of the apoptosis is caspase 3 activity, which plays a key role in initiating cellular events during

the early stages of the process. As with DNA fragmentation, caspase 3 activity can be assayed by ELISA but it is also detectable by western blotting [125].

6.4.4 Conclusions

In conclusion, the results reported in the previous chapter that SF can reduce HSP90β1 protein expression *ex vivo* has been confirmed in tissue from further patients, although the variation in responses obtained, once again highlights natural variation between individuals, and therefore the need for a large sample number. However, SF was not seen to significantly alter HSP90β1 expression *in vitro*, suggesting the effect was dependent on interactions between cell types or was specific to BPH. Despite research suggesting a role for HSP90β1 in apoptosis, artificial reduction of HSP90β1 using siRNA did not reduce cell viability or inhibit cell proliferation. Further research is needed to investigate the role of HSP90β1 in apoptosis, its biological relevance in BPH and prostate health in general, and to clarify its relationship with SF.

Chapter Seven

Final Discussion

Chapter 7. Final Discussion

7.1 Contributions to thesis aims

The rationale behind this thesis was strongly influenced by previous work, which has primarily focussed on investigating the bioactivity of SF with the use of *in vitro* cell models. However, such models have limitations, as discussed in Chapter 1, notably poor replication of conditions *in vivo*. To address this issue, this current study developed an *ex vivo* BPH tissue culture method to more closely replicate *in vivo* conditions. The majority of BPH samples exhibit inflammatory infiltrates, so this system was used as a model of inflammation, which is also suggested to have a role in the aetiology of PCa. To investigate the effect of SF on this system, two approaches were used. Initially, a targeted approach was used to measure the effect of SF on inflammatory cytokine secretion. Following on from this, an untargeted approach was then employed to investigate the effect of SF on global protein expression. Further work was then conducted to investigate the biological relevance of HSP90 β 1, a protein found to be reduced by SF *ex vivo*.

In this chapter I will discuss the results of the five results chapters, their contributions to my original thesis aims, and also their context within the wider field of research. The original aims of my thesis as stated out the end of Chapter 1 were:

1. Develop a method for the culture of BPH tissue to replicate *in vivo* conditions using an *ex vivo* model.
2. Establish whether SF is able to reduce inflammation in the *ex vivo* model as has been previously demonstrated using *in vitro* models.
3. Determine what effect SF has on global protein expression in BPH tissue *ex vivo*.
4. Confirm the effect of SF on a selected protein, as identified from aim 3, using a greater sample number, and investigate further to determine whether this effect may have any biological significance for prostate health.

7.1.1 *Ex vivo* model of prostate inflammation

The first aim of my thesis was to establish an *ex vivo* tissue culture method in order to replicate *in vivo* conditions in the prostate. Previously, the use of tissue culture as a model has been limited, with researchers instead favouring the use of established cell lines. These cell lines provide a good starting point for investigating biological mechanisms, but do not provide as close a model to *in vivo* conditions as *ex vivo* tissue culture can offer.

Established immortalised cell lines are easy to grow and manipulate, but due to the single cell type, are a lot less complex than, and therefore a poor model, for conditions *in vivo*. Using a tissue culture method still allows for targeted treatment, as with cell culture models, but due to the complexity of the system, there is interaction between different cell types, resulting in a response which is more representative of what happens *in vivo*. However, as this system is more complex and the cells have not been immortalized, establishing a viable culture method is difficult.

Although culture of prostate tissue has been performed previously [136, 139, 141-144], a standard method has not yet been established. A review of previous protocols (see Chapter 2), was used as a starting point for my own method, influencing the types of media tested, and whether the addition of DHT was necessary, as well as the assays used to determine the success of the procedure. Of all the conditions tested, and the markers of viability and function measured, there was seen to be no significant difference between them. It was, however, obvious in all conditions that sections of the tissue, in particular the epithelium, rapidly died (see Chapter 2). Other studies noted that the tissue adjusted to the conditions after time in culture [138-139], but due to this rapid loss of the epithelium, which was felt to be of importance for the biological relevance of this model, the tissue was not cultured for longer than 24 hours.

One issue that may have affected the success of the culture may be the size of the culture pieces, which were $\sim 2\text{mm}^3$. It is known that the size of a tumour without new vascularisation is limited to about 200nm due to the oxygen diffusion limit [193]. If this work were repeated, it may be of interest to investigate the effect the size of tissue piece has on viability, and therefore the success of the culture.

The use of an *ex vivo* tissue culture model may be a promising technique that can, and should, be expanded due to its closer representation of *in vivo* conditions compared to *in vitro* established cell lines. However, work still needs to be done to establish a standard culture procedure, and to improve viability. In addition, factors such as the availability of tissue, natural variation, and ethical issues, will most likely always limit the use of *ex vivo* models.

7.1.2 Reduction of inflammation by sulforaphane

It has been previously suggested that SF can reduce inflammation [103, 111, 113-114], but this work has been primarily performed using *in vitro* models. The current study is novel, as it investigates whether this still holds true in an *ex vivo* model.

In *in vitro* models it is often necessary to induce an inflammatory response before measuring any effect of treatment, but, in correspondence with literature, the BPH samples used here all secreted inflammatory cytokines, so no induction of inflammation was necessary.

Inflammatory cytokines were measured as a marker of inflammation and were selected due to their reported importance in BPH. Six cytokines were selected for investigation, but only three were detectable in the media by ELISA. Of the three cytokines detected, it was observed that IL-6 and IL-8 were secreted at similar concentrations, but FGF-2 levels were 4-fold lower (Figure 3.3).

Tissue was initially treated with 25 μ M SF, in line with previous studies [117, 132-133, 135, 162]. At this concentration, SF was seen to significantly reduce the secretion of IL-6 and IL-8, but had no effect on FGF-2 (Figure 3.4). In terms of physiologically relevant levels, 25 μ M SF is greater than has been recorded *in vivo*, but possible through the use of supplements. A dose-dependent experiment was then performed using lower, more physiologically relevant concentrations, and IL-6 secretion measured. Using SF concentrations ranging from 2-25 μ M, the lowest concentration at which a significant effect on IL-6 secretion was seen was 10 μ M (Figure 3.5). In comparison to 25 μ M SF, 10 μ M is physiologically achievable through diet. This was demonstrated by Gasper and colleagues who recorded SF at 7.4 μ M \pm 3.08 after high-glucosinolate broccoli consumption [100].

In the experiment performed with 25 μ M SF, a greater reduction was seen on IL-8 secretion than IL-6. IL-6 was chosen for the dose-dependent experiment as evidence commonly correlates IL-6 levels with inflammation and disease risk [163, 170-171]. However, it may have been interesting to see whether the secretion of IL-8 was also more sensitive at lower SF concentrations than IL-6.

When evaluating the results obtained, the biological relevance must be considered. Although previous work has suggested 10 μ M SF to be physiologically achievable, this level was measured in the plasma, not the tissue. In this experiment, 10 μ M SF was directly added to the tissue, but it may be that even if plasma levels are this high, the concentration which reaches the tissue *in vivo* is much lower. Studies in which subjects have consumed either broccoli or SF have observed changes in the prostate, providing evidence that SF does reach the prostate at biologically active levels *in vivo* [95, 160]. In the plasma, the concentration of SF after broccoli consumption is transient, peaking at two hours, after which it rapidly reduces [100]. In addition, repeated consumption of broccoli, every day for 10 days, does not result in an accumulation of SF in plasma [286]. As such, it would be interesting to investigate the concentration of SF in the prostate, and also whether there is accumulation of SF in tissue if broccoli is regularly consumed. This would provide further evidence for the biological relevance of the SF concentrations used in this study, and the results obtained from this.

One of the aims of this work was to investigate whether the previous results observed in *in vitro* studies could be replicated *ex vivo*. In agreement with previous work [103, 158-159], SF was seen to reduce IL-6 concentrations. Also, previous work in prostate cancer cell lines, has demonstrated that SF can inhibit IL-6-induced activation of oncogenic signalling pathways involved in PCa progression, highlighting the relevance of the result observed here [177]. It is also of note that a significant effect was observed with 10 μ M SF, which is at the upper limit of levels achieved in plasma, demonstrating that these results are therefore biologically relevant [100].

Although not investigated in this study, the mechanism by which SF can reduce the secretion of IL-6 has been previously described. Therefore, it may be possible that such mechanisms (Figure 7.1) can explain how SF reduced IL-6 secretion in the *ex vivo* model.

One mechanism by which SF is proposed to reduce IL-6 secretion is by inhibiting the TLR4 pathway. TLR4, a membrane-spanning receptor protein, is activated by LPS, increasing the production of cytokines, including IL-6, and inducing inflammation. Youn and colleagues demonstrated that SF binds to cysteine residues in the extracellular domain of TLR4, inhibiting its oligomerization, an essential step in its activation [112]. Furthermore, SF was found to inhibit NF κ B activation induced by the overexpression of myeloid differentiation primary response gene 88 (MyD88) or I κ B kinase (IKK β), both downstream signalling components of TLR4 activation. Coupled with previous evidence, Youn and colleagues suggested that SF directly inhibited the activity of IKK β and NF κ B. Using a mouse model, injection of LPS was observed to significantly increase levels of circulating cytokines, including IL-6, an effect which was strongly inhibited by oral administration of SF [112].

Xu and colleagues further demonstrated inhibition of NF κ B transcriptional activity by SF, subsequently reducing the expression of NF κ B-regulated genes. Their results suggested that SF primarily acted by inhibiting IKK phosphorylation, and preventing p65 nuclear translocation. Thus, this prevented IKK from catalysing the phosphorylation, ubiquitination and degradation of IK β , which sequesters NF κ B in the cytoplasm. As a result, NF κ B, which is formed from a heterodimer of p50 and p65, is not phosphorylated, and does not translocate to the nucleus [287].

In a number of previous studies, other isothiocyanates have been shown to have similar biological activity to SF, including the study by Xu and colleagues who showed PEITC to be biologically active at lower concentrations than SF [287]. Furthermore, it has been shown that a range of other phytochemicals, such as resveratrol, epigallocatechin-3-gallate and curcumin, which are derived from red grapes, green tea, and tumeric, respectively, can act through similar mechanisms [288], demonstrating how a range of dietary components can reduce inflammation. However, this work was conducted in cell line models, and as such, it remains to be seen whether the same effect would occur in humans.

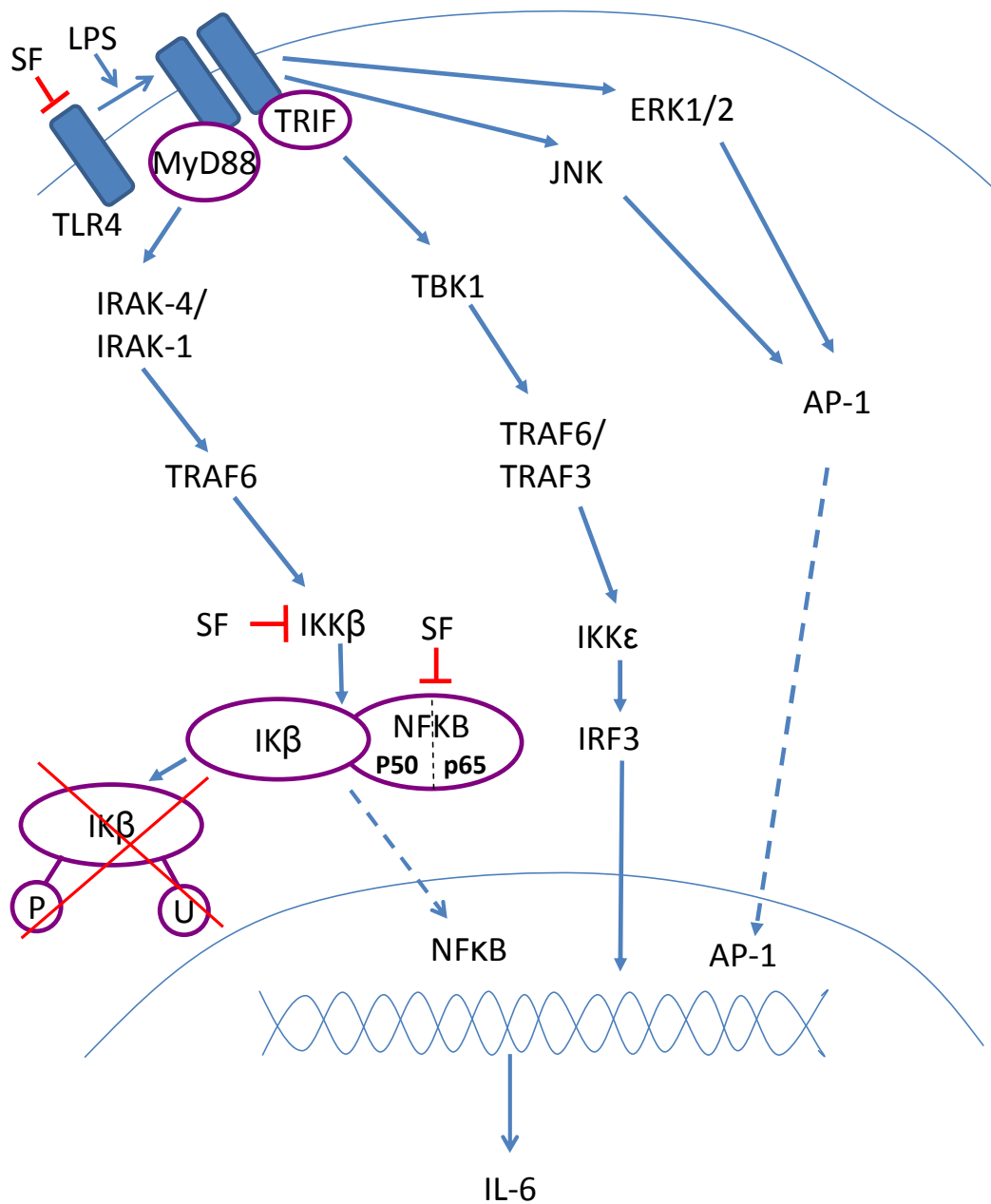


Figure 7.1. Inhibition of IL-6 production by sulforaphane.

Diagram demonstrating the induction of IL-6 via TLR4. Blue arrows represent the normal pathway of activation following TLR4 oligomerization. Red arrows indicate components of the pathway which SF can exert an inhibitory effect, thereby inhibiting IL-6 production. The red cross indicates degradation of IK β . The dotted lines indicate translocation to the nucleus.

7.1.3 Sulforaphane and protein expression in BPH tissue *ex vivo*

Once it was established that SF was able to alter the secretion of inflammatory markers from BPH tissue using a targeted method, it was decided to investigate the effect of SF on BPH tissue using an untargeted approach to look at changes in global protein expression.

The method decided upon was 2D gel electrophoresis which allows the separation of proteins extracted from the BPH tissue using both iso-electric focussing point and mass. Subsequent overlay and comparison of gels allowed the selection of spots that altered between gels for protein identification. Biological triplicates were performed for tissue from three patients, with and without SF treatment, and showed little replicate variation demonstrating the homogeneity of the sample replicates (Table 4.2). Technical replicates were not performed due to the quantity of protein required per gel, and the limitation of the amount of protein that could be extracted from each sample. Collecting a larger sample from each patient would have allowed a greater amount of protein to be recovered, allowing technical replicates, which would have acted as a further control for the reliability of the results obtained. However, the size of the sample obtained was itself limited.

From comparison of the gels, it was evident that variation exists between individuals, as there were significant differences in protein expression between the patients at baseline (Table 4.2). Further variation was observed when treated with 10 μ M SF, as only two of the three patients exhibited a significant effect on global protein expression in response to SF (Table 4.2 and Table 4.3). Of the two that did alter, there was very little overlap between the spots that had changed in each patient (Figure 4.6). This highlighted the natural variation that exists, not only in the baseline protein expression in human tissue, but in the varying ways in which our bodies can respond to the same stimulus. In order to elucidate the relevance of any data to the general population, it would be beneficial to use as large a number of patients as possible.

From the data, 70 spots were selected as significantly altered and chosen for identification, although only 55 spots were positively identified, of which there were only 37 unique proteins. Analysis of the proteins using the Gene Ontology website, indicated five main processes that the proteins were involved in: apoptosis; metabolism; muscle development and contraction; cell proliferation, adhesion and angiogenesis; and cytoskeleton organization (Table 5.4). In addition, the majority of proteins could be sorted into three functional groups; enzymes, molecular chaperones, and structural and adhesion proteins (Table 5.6). The two lists of

groups, function and process, were compared, and the greatest overlap observed was the involvement of molecular chaperones in the apoptotic process. The spots of these proteins, HSP90 β 1, calreticulin, 14-3-3 ϵ , GRP78 and HSP70-1, from the 2D gels were then more closely examined (Figure 5.1-5), and HSP90 β 1 selected for further investigation.

In summary, it is apparent that SF can alter a wide range of proteins in BPH tissue *ex vivo*, including proteins involved in cell processes critical for normal tissue homeostasis, such as apoptosis, cell adhesion, and transcription and translation. Dysregulation of both molecular chaperones and apoptosis has been implicated in disease, including cancer, so it is interesting that SF can alter these proteins. These results highlight the variation that exists between individuals, as well as the diverse activity of SF, and the many pathways by which it may exert a beneficial effect on prostate health.

7.1.4 Novel target for sulforaphane activity

The final aim of the thesis was to identify and investigate a possible novel target for SF activity. From the 2D gel work, it was discovered that SF modulated a number of molecular chaperones involved in apoptosis, so it was decided to investigate one of these further, the protein selected was HSP90 β 1.

In the tissue samples analysed by 2D gel electrophoresis, HSP90 β 1 was found to be reduced by SF in one of the three patients. A further nine independent tissue samples were then analysed to investigate whether this result could be repeated in other patients. In these samples it was apparent that the effect of SF on HSP90 β 1 varied between patients, but overall a reduction in HSP90 β 1 expression was seen.

HSP90 β 1 was selected due to its proposed anti-apoptotic function, along with its correlation with cancer progression. Furthermore, no work has previously been published with regard to SF activity, although, it has been suggested that SF is capable of modulating HSP90, the cytoplasmic homologue of HSP90 β 1 [117, 289].

The biological function of HSP90 β 1 was discussed in detail in Chapter 6, but briefly, its anti-apoptotic properties are suggested to be due to its calcium-binding properties [216] (Figure 7.2).

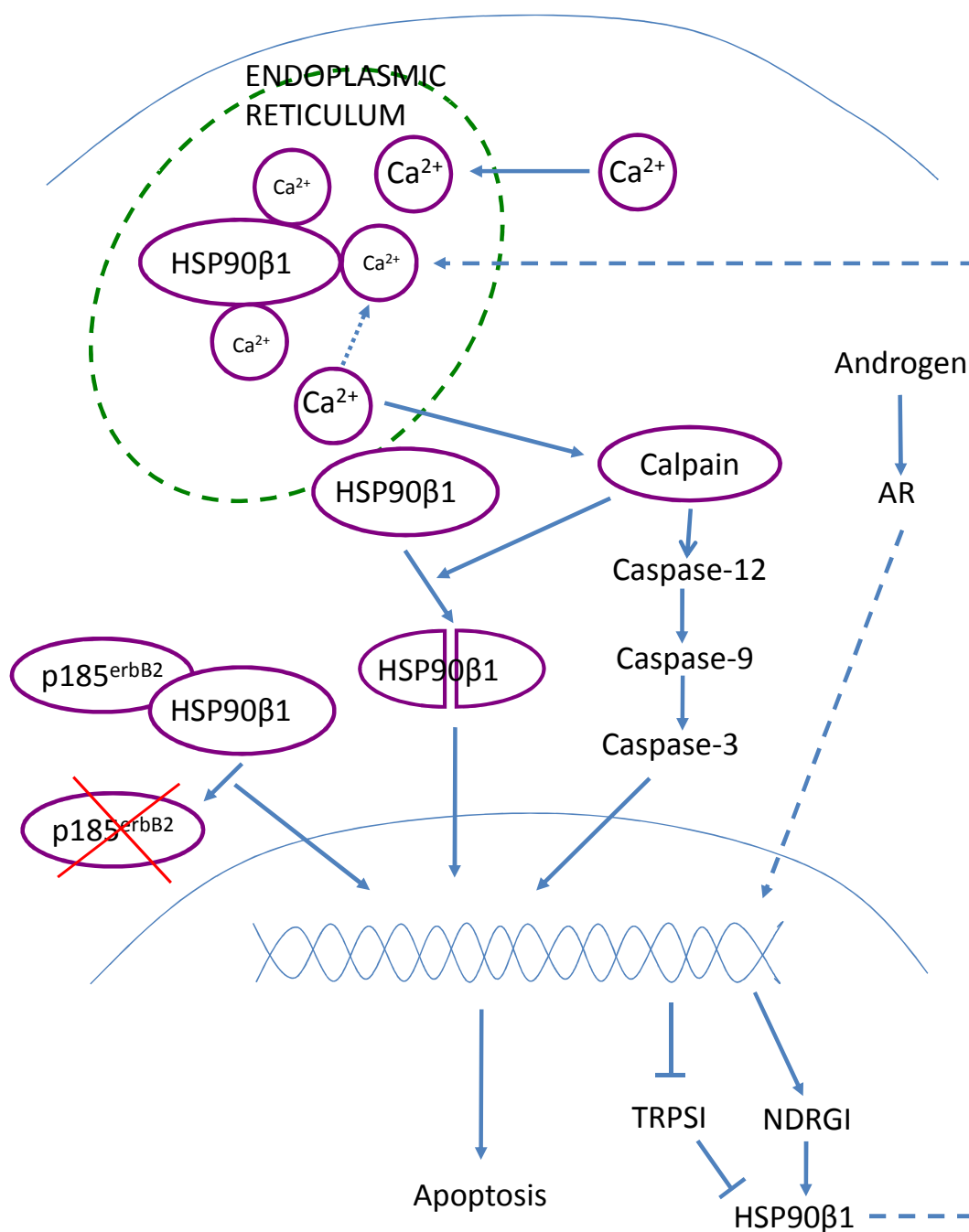


Figure 7.2. HSP90β1 and apoptosis.

Diagram outlining the proposed anti-apoptotic functions of HSP90β1. Briefly, HSP90β1 binds to calcium (Ca²⁺) in the endoplasmic reticulum preventing apoptosis. If the cell is overloaded with Ca²⁺, beyond the binding capacity of HSP90β1 (and other Ca²⁺-binding proteins), the free Ca²⁺ can activate calpain, subsequently triggering the caspase cascade. In addition, calpain can cleave HSP90β1, preventing it from binding Ca²⁺, thereby promoting apoptosis. In contrast, androgen can promote the expression of HSP90β1 inhibiting the apoptotic process. The dotted lines represent translocation, and the red cross indicates degradation.

By binding calcium, HSP90 β 1 can modulate calcium homeostasis, preventing calcium overload-induced apoptosis. In the absence of HSP90 β 1, calcium levels within the cell can promote apoptosis by activating calpain, triggering the caspase cascade [127]. Calpain, in turn, can cleave HSP90 β 1, which has been seen to coincide with DNA damage, thus further promoting apoptosis [216]. In addition, its expression can be induced by androgen [271], suggesting a mechanism by which HSP90 β 1 expression can be specifically modulated in the prostate. Furthermore, HSP90 β 1 can form a stable complex with p185^{erbB2}, a protein often upregulated in PCa, and associated with poor prognosis. Disruption of this complex leads to degradation of p185^{erbB2} [270], demonstrating how reduction of HSP90 β 1 expression could be beneficial to prostate health. As such, the reduction of HSP90 β 1 by SF, may contribute to the pro-apoptotic activity of SF.

As no previous work has investigated a relationship between HSP90 β 1 and SF, the mechanism of action is unknown. However, using previous knowledge of SF activity, a possible pathway can be hypothesised. Previously, SF has been shown to increase intracellular free Ca²⁺, activating calpain [127], which in turn cleaves HSP90 β 1. The cleaved HSP90 β 1 may then be degraded, or if not degraded, when run on a 2D gel, the two fragments would run at a different position, explaining the reduction observed *ex vivo*. This reduction of HSP90 β 1 within the cell would therefore reduce the calcium binding capacity of the cell, further increasing intracellular free Ca²⁺, driving apoptosis. As such, this indicates a possible mechanism by which SF may be able to reduce HSP90 β 1 expression.

Up until this point all experiments had been performed using the *ex vivo* tissue culture model, due to its closer replication of *in vivo* conditions, but to further investigate the relationship between SF and HSP90 β 1, it was decided to use *in vitro* established prostate cell lines. This approach was used as the simpler model allows for better manipulation, and greater reproducibility of results. It also allowed the investigation of the effect of SF in different states of prostate dysregulation by using both healthy, PNT1a, and carcinogenic, DU145, cell lines.

In contrast to the results from the tissue, very little effect was seen in the cells, with no effect seen on mRNA or protein levels in the healthy PNT1a cells with either 10 or 25 μ M SF. 25 μ M SF significantly increased mRNA levels in the DU145 cells, but this did not translate into any effect on protein levels. It is interesting that no effect was seen on protein expression in the cell lines, but this could be due to a number of factors.

The cell lines were all epithelial in origin, but it may be that in the tissue, SF has more effect on the stromal cells than the epithelium, or that the effect is due to some interaction between the cell types that does not occur in the less complex *in vitro* model. It may also be related to the disease state of the prostate as the tissue was from those diagnosed with BPH, whilst the cell lines were established from healthy and cancerous prostate respectively, so it may be that SF only reduces HSP90 β 1 in BPH.

Although no effect was observed on the cell lines treated with SF, the relevance of the effect seen *ex vivo* still needed to be investigated. As the reduction of HSP90 β 1 in tissue cannot be guaranteed in each patient, and due to culture viability issues, the use of the *ex vivo* model was not appropriate to investigate this question. Established cell lines remove issues associated with variability and viability, but as HSP90 β 1 was not reduced by SF *in vitro*, it was decided to artificially reduce HSP90 β 1 using siRNA.

Using the healthy PNT1a cells, a maximal reduction of 60% in HSP90 β 1 protein expression was observed. As HSP90 β 1 had been selected due to its role in the apoptotic process, the effect on cell viability was initially investigated, but no effect was seen. Further investigation measuring the effect on cell proliferation also revealed no effect. Therefore, the biological relevance of the reduction of HSP90 β 1 by SF as seen *ex vivo* is undetermined.

Given further time, it would be interesting to try and determine what role HSP90 β 1 plays in the cell (see Chapter 7.4), and whether its reduction by SF, is relevant to the mechanism by which SF can promote a beneficial effect on health. The reduction of HSP90 β 1 expression by SF in BPH tissue, which was originally observed in one of the three patients analysed by 2D gel electrophoresis, was further confirmed in three out of nine independent BPH tissue samples. However, further investigation into its biological relevance and possible impact on prostate health was inconclusive, as no effect on cell behaviour was observed.

7.2 Further Contributions

7.2.1 *Ex Vivo* models versus *In Vitro* Models

In this thesis the use of an *ex vivo* prostate model has been described as a viable alternative to *in vitro* models. However, in the final results chapter of the thesis, *in vitro* models were also employed. Such a shift was necessary due to limitations and disadvantages intrinsic to both models, an understanding of which is essential in selecting the correct model to best answer the question being asked (Table 7.1).

Initially, the *ex vivo* model was used, as this provides greater replication of conditions *in vivo*, due to the complexity of the system. Of particular relevance are the epithelial-stromal interactions, which, as discussed previously, are of great importance in the prostate. In comparison, cell lines are established from a single cell type, and are therefore a far simpler model, and much less representative of conditions *in vivo*.

However, due to the complexity, and the variation present between patients, reproducibility of results is low, so to obtain statistically significant results, larger numbers of patients must be analysed. In contrast, established cell lines are genetically identical, providing greater reproducibility of results, and reducing the need for larger numbers of replicates.

Cell lines are often well described, with any mutations or deletions documented, allowing greater understanding of the cell response to external conditions. Due to the genetic variation that exists between patients, samples are genetically uncharacterised, and any differences unidentified, leading to unexplained variations in sample responses.

As *ex vivo* models are infrequently used, there are no standard methods for the culture of tissue, so method optimisation must be performed prior to starting experimental investigations. However, protocols for the culture and experimental use of cell lines are well established. Furthermore, due to the simplicity of the system, cell lines are easier to manipulate, and collection of the necessary measurements simpler. For example, techniques such as the delivery of siRNA have been optimized in cells, and whilst delivery to tissue is possible, it is much more complex [290]. To further complicate matters, whilst the extraction of protein and RNA from cells is straightforward, the extraction of these from tissue is less routine. Procedures have been established for the collection of mRNA from fresh tissue, however, mRNA could not be successfully extracted from the cultured tissue (data not shown),

limiting the investigative techniques that could be used on this model. The reason as to why mRNA was not successfully extracted was undetermined despite multiple attempts, suggesting that the mRNA in the culture samples had degraded.

A further advantage of cell lines is the ease of availability, and the number of cell lines available that are representative of the different disease states of the prostate. These range from healthy cells to cancerous cells, including those which are androgen-dependent or independent, or poorly or highly metastatic, thus allowing investigation and comparison of the different stages of prostate dysregulation.

In contrast to this, prostate tissue is less readily available with tight regulation in place to ensure its ethical use. Tissue is often removed as part of routine clinical care in prostate diseases, including BPH and PCa, so can be obtained without the need for patients to undergo non-essential surgery. However, obtaining healthy tissue is more complex as this would most likely require volunteers to undergo elective surgery for this to be collected, which obviously has associated health, cost, and ethical issues. Thus, it is common for studies analysing tissue samples to use BPH samples as a healthy comparison to PCa tissue, although normal prostate samples can be obtained from cadavers [291]. However, studies in which normal, BPH and PCa samples have been used, have often demonstrated the variation between normal and BPH tissue, providing evidence that BPH tissue should not be used as a 'normal' control. Although the use of BPH as a healthy control for PCa is not ideal, due to the issues associated with the collection of healthy tissue, its use is understandable and almost unavoidable. It is therefore apparent that the use of cell lines can be of great value when comparing disease states.

The use of the two models in this study provides evidence for the complementary nature of the results obtained from each, and the benefits of using the two models in combination. Unfortunately, within the time constraints of this study, the biological relevance of results obtained *ex vivo* were unable to be determined *in vitro*. However, using a similar combination of techniques, a global approach followed by a targeted *in vitro* approach, Sreekumar and colleagues were able to identify the metabolite sarcosine as elevated in PCa, and using cell lines demonstrated its role in the development of an invasive phenotype [292]. A similar metabolomic approach in the *ex vivo* BPH model may therefore be successful in identifying novel targets of SF activity.

In summary, the use of both *ex vivo* and *in vitro* models can complement each other by taking advantage of the strengths, and considering the weaknesses, of each technique. Together the two models can be used to further our knowledge of cellular processes, and the behaviour of tissue as a complex whole, providing greater understanding of biological systems than either model alone.

Table 7.1. Advantages and limitations of *ex vivo* and *in vitro* models

<i>Ex Vivo</i> Models	<i>In Vitro</i> Models
High genetic variability	Genetically identical
Complex system (interactions between cell types)	Simple system
Closer replication of conditions <i>in vivo</i>	Poor replication of <i>in vivo</i> conditions
Novel	Well documented
Ethical issues	No ethical approval needed
Not freely available	Readily available
Difficult to obtain healthy tissue	Numerous cell lines representative of different disease states

Summary of the major advantages and limitations in the use of *ex vivo* tissue culture compared to *in vitro* established cell lines.

7.2.2 Targeted versus Untargeted Approaches

Along with the use of both *ex vivo* and *in vitro* models to investigate the thesis aims, two major approaches were used: targeted and untargeted. The targeted methods included ELISA, western blotting and RT-PCR (Chapter 3 and 6), whilst the untargeted approach chosen was 2D gel electrophoresis (Chapter 4).

BPH tissue was selected as a model of inflammation, as although the aetiology of BPH is yet to be determined, inflammation is proposed to play a crucial role [10]. More recently inflammation has been implicated in the development of some cancers, including PCa [29], highlighting the impact inflammation can have on health. Furthermore, inflammation is a critical component in the aetiology of a wide range of other diseases, such as cardiovascular disease and arthritis, the treatment of which places a huge burden on healthcare budgets. Moreover, the occurrence of these diseases increase with age which, in an aging population, means that in the future, the burden from these diseases is only likely to increase. Therefore, finding ways in which changes in our diet could help prevent the onset or slow development of these diseases is a major challenge.

Previous research has suggested that the consumption of cruciferous vegetables can have a beneficial effect on health [72, 75], and in particular broccoli has been shown to positively impact the prostate [52, 73-74]. Furthermore, SF, which is believed to be the main bio-active compound derived from broccoli, has been proposed to have anti-inflammatory properties.

To build on this previous research, BPH tissue was used as a model of prostate inflammation. A number of inflammatory cytokines were selected for targeted analysis based on previous data regarding the expression of inflammatory cytokines in BPH, some of which SF has previously been reported to alter. Using a targeted analysis allows the investigation of specific molecules, in this case inflammatory cytokines, but this means you must know what you are looking for.

Initially, this answered the question as to whether SF can alter the secretion of inflammatory cytokines *ex vivo*. However, targeted methods have limitations in that they require previous knowledge of the system being investigated, whereas untargeted methods allow multiple measurements to be made without specificity. The most commonly used example of this method are microarrays, in which changes in gene expression throughout the genome can be detected. Further techniques include the fields of metabolomics and proteomics.

As it is proteins which determine the biological response of a cell, the global protein expression in the tissue was investigated using 2D gel electrophoresis. This allowed protein extracted from BPH tissue to be separated by both isoelectric focussing point and mass on 2-dimensional gels, which can then be overlaid to identify differences in the protein spots. Selected spots are then analysed using mass spectrometry to identify the protein. This allows all proteins that are altered in a system to be detected without any bias or previous decisions as to what to look for.

However, 2D gel electrophoresis is not without its limitations. Although 2D gels are considered to be of high resolution and can separate many proteins, the resolution is still not great enough to separate all proteins, due to the huge diversity that exists. The use of reduced-range pH gradient gels partially combats this issue, allowing better separation of proteins within this range, but obviously leads to poorer resolution outside this range. Furthermore, it is not uncommon for proteins to migrate together, leading to multiple proteins within a spot, as seen in some spots in Chapters 4 and 5, reducing the clarity of the results.

2D gels, however, do allow for the recognition of different isoforms and post-translational modifications of proteins. Identification is based on sequence recognition, and the peptides derived from modified and unmodified proteins rarely differ, therefore allowing correct identification by mass spec. Whereas the use of a targeted approach such as antibodies may produce false results, as the antibody may not recognise that particular isoform, or post-translational modification, depending on the specificity of the antibody, and where on the protein it binds. Antibodies that are specific for particular post-translation modifications, such as phosphorylation, are available, but to test for all possible modifications would require numerous antibodies which are not necessary in 2D gel electrophoresis.

A further limitation of 2D gels, results from the differing abundance of proteins in the sample, so low abundance proteins are not detected, as 2D gels have a 10^4 dynamic range. Therefore, if some proteins are expressed at 10^8 molecules per cell, and some at 10^2 molecules per cell, the proteins expressed below 10^4 molecules per cell will not be detected. Proteins with certain properties are also poorly separated by 2D gel electrophoresis, especially poorly soluble hydrophobic proteins, such as many membrane and nuclear proteins [293]. Due to the limitations in the proteins that can be detected by 2D gel electrophoresis inflammatory

cytokines, such as interleukins, are not measurable by this method, so for investigating inflammatory markers another method may be more appropriate.

The analysis of 2D gel data can be complicated due to the volume of data generated, and the multiple sources of error. These sources were discussed in detail in Chapter 4 but briefly resulted from technical, replication, patient and treatment variation. Although software used to analyse the 2D gels is highly sensitive and can detect low volume spots, it is also necessary to manually assess the spots identified by the software, which is time-consuming. Statistical analysis of the data needs to be dealt with carefully, as correction for multiple-testing due to the volume of data produced is often impractical because it removes all statistical significance.

When dealing with human data, large sample numbers are required due to the vast amount of natural variation that exists. 2D gel electrophoresis is not high throughput so is not suited to dealing with the necessary sample numbers. As such, once proteins of interest are identified, the use of targeted methods is often more practical for further investigations.

Despite the limitations associated with 2D gel electrophoresis it is currently the best technique available for unbiased analysis of complex protein mixtures, and can be successfully used to identify novel changes in protein expression. Results from 2D gel electrophoresis can then be built on using targeted methods, so, in the same way that *in vitro* and *ex vivo* models can be used to provide complementary information, so may targeted and untargeted approaches.

7.3 Summary

In line with the first aim of the thesis, a method for the culture of BPH tissue *ex vivo* was successfully established, and it is shown that the use of an *ex vivo* model is a novel but viable method for the investigation of the response of human tissues.

This model has been used to show that SF is able to reduce the secretion of known pro-inflammatory cytokines by BPH tissue, which confirms data obtained from *in vitro* models, fulfilling the second aim of this work.

Furthermore, as set out for investigation in the third aim, this model also demonstrated that global protein expression naturally varies between individuals, and that SF at a biologically relevant concentration can alter global protein expression, although the nature of the response differs between individuals.

The proteins altered were seen to fall into three main functional groups: enzymes, molecular chaperones, and structural and adhesion proteins. These were involved in apoptosis, muscle development and contraction, cell adhesion, cellular component moving, glycolysis, transcription and translation, metabolism, cell redox homeostasis, proliferation and angiogenesis. The greatest overlap between function and process resulted from the molecular chaperones involved in apoptosis, which were HSP90 β 1, calreticulin, 14-3-3 ϵ , GRP78 and HSP70-1.

In accordance with the fourth aim, a single protein, HSP90 β 1, was selected for further investigation as a novel target of SF activity, due to its correlation in the literature with disease progression. However, its biological relevance, and therefore possible influence on prostate health, was not ascertained.

The reduction of HSP90 β 1 protein expression by SF observed in the one of the three initial patients was confirmed in further patients, although once again the effect varied between individuals. Interestingly, SF did not alter HSP90 β 1 protein expression in established healthy and carcinogenic prostate cell lines, suggesting the effect may be due to disease state, cell type, or may rely on interactions between cell types within the tissue sample. Transfection of a healthy prostate cell line with HSP90 β 1 siRNA resulted in a maximum reduction of 60%, but did not affect cell viability or proliferation.

This study demonstrated that the use of an *ex vivo* model is a viable approach for the investigation of the effects of dietary agents on prostate health. Further to this, it showed that the use of an untargeted approach, such as the 2D gel electrophoresis, is a suitable method for the identification of novel targets of SF. Further investigation is required to better understand the biological role of HSP90 β 1, and thereby what effect the reduction by SF may have on the prostate, and any relevance there may be to the beneficial effects of SF on prostate health.

7.4 Future Work

There are a number of areas on which future work could build and investigate further, including the tissue culture method, the biological effect of HSP90 β 1 reduction, and its biological relevance in the prostate.

7.4.1 Further *Ex Vivo* Tissue Culture Optimization

The initial experimental work focussed on the development of an *ex vivo* tissue culture method which extra work could further optimise. Possible factors for investigation include sample piece size and the viable culture period length. In this study, the sample piece size was not investigated and the size selected based on previous studies. However, other studies have investigated different sectioning methods, and considering the diffusion limit of oxygen, it may be that the centre of the pieces were starved of oxygen and other nutrients which may have impacted the results. Therefore, culturing smaller pieces or using precision cut slices may positively impact the success of the culture.

Furthermore, the viability of the tissue rapidly decreased, with little epithelium remaining after 24 hours. If it were possible to extend the viable culture period this would allow investigation of the model over longer time periods, providing greater understanding of the system. Alteration of the sample piece size may possibly impact this, but other factors such as culture medium, including the possible addition of DHT, may further improve viability.

7.4.2 HSP90 β 1

Using the *ex vivo* model, it was discovered that SF could reduce the expression of HSP90 β 1, a previously unidentified target for SF activity. However, this result was not replicated in established cell lines, as no significant effect was seen on HSP90 β 1 protein expression in response to SF treatment. In order to investigate the biological effect *in vitro*, HSP90 β 1 expression was artificially reduced using siRNA. Using this approach, a maximum reduction of 60 and 30% was seen in RNA and protein expression respectively. As HSP90 β 1 is suggested to play a role in apoptosis, the effect of HSP90 β 1 siRNA on cell viability and proliferation was investigated, but no effect found. To further this work, there are two major areas that can be addressed: the knockdown of HSP90 β 1, and the biological relevance of this reduction.

7.4.2.1 Knockdown of HSP90β1

In this study, siRNA was used to knockdown the expression of HSP90β1 from which a maximum reduction of 60 and 30% was seen in RNA and protein expression respectively. Previous work suggests that a total knockout of HSP90β1 may be necessary to observe a response [272, 294], which may explain no effect was seen here. Therefore, if HSP90β1 can not be knocked down to a greater degree using siRNA, an alternative approach may be more appropriate. Two possible methods may be the creation of a cell line or mouse model in which HSP90β1 is permanently deleted.

To investigate the effect of HSP90β1 knockout *in vitro*, a transgenic cell line could be created in which HSP90β1 is permanently deleted. This would facilitate the investigation of the biological relevance of HSP90β1, and whether HSP90β1 deletion reduces cell viability or proliferation.

Using a conventional mouse model, null mutation of HSP90β1 results in embryonic lethality [272]. To create a mouse model in which HSP90β1 knockout can be investigated, the Cre/loxP system could be used to create a conditional model in which HSP90β1 expression is specifically knocked-out in the prostate. This would then allow the investigation of the effect of the specific knockout of HSP90β1 in the prostate in a whole organism.

7.4.2.2 Biological Relevance of HSP90β1

As SF was observed to reduce HSP90β1 expression *ex vivo*, using siRNA HSP90β1 was reduced *in vitro*. The biological relevance of this reduction was investigated by measuring the effect on cell viability and proliferation, due to the suggested anti-apoptotic properties of HSP90β1 but no difference was observed. To understand the biological function of HSP90β1 in the prostate, and the importance of the reduction by SF observed *ex vivo*, further work is necessary.

Previous work has correlated increased HSP90β1 expression with cancer progression, whilst another paper reported it as reduced in circulating tumour cells suggesting a negative correlation. To try and clarify the relationship between HSP90β1 and prostate disease, two approaches could be used. Firstly, public databases, such as The Human Protein Atlas and the Gene Expression Atlas, could be used to gather information regarding the expression of HSP90β1 protein and RNA in different prostate disease states. However, often these databases only sort data as being from either normal or cancerous tissue so it may be necessary to gather fresh data. Tissue samples representative for normal, BPH, PIN and PCa prostate could be

analysed for HSP90 β 1 protein expression, providing greater understanding of the correlation of HSP90 β 1 with prostate dysregulation.

To begin to understand the mechanism by which SF reduces HSP90 β 1, it would be beneficial to know whether it acts at a transcriptional or translational level. To accomplish this it would be necessary to extract RNA from the tissue in which a reduction in protein level is observed, but unfortunately it was not possible to achieve this. However, it has been reported that HSP90 β 1 mRNA and protein levels do not always correlate, so even if RNA could be successfully extracted from the cultured tissue the results may be inconclusive.

The reduction of HSP90 β 1 was initially investigated for its effect on cell viability due to its proposed anti-apoptotic function, but no significant effect was observed. However, it may be that a reduction in HSP90 β 1 does not induce apoptosis, but instead sensitizes the cell to apoptotic stimuli. Further work may be to induce apoptosis using a chemical such as etoposide, which has previously been shown to sensitize cells to SF induced apoptosis. Cells treated with both etoposide and HSP90 β 1 siRNA in combination may therefore have reduced viability compared to cells treated with either etoposide or HSP90 β 1 siRNA alone.

The use of siRNA to knockdown HSP90 β 1 was necessary as SF had no effect on HSP90 β 1 expression *in vitro*, despite the effect seen *ex vivo*. There were four main hypothesis that were suggested to explain this result; cell type, stroma-epithelial interactions, inter-individual variation and disease state.

The first explanation as to why the effect seen *ex vivo* was not replicated *in vitro* was due to the cell type. The cell lines were of epithelial origin, but it may be that SF reduces HSP90 β 1 expression in stromal cells in the tissue. However, IHC suggested that it was the epithelial cells in which HSP90 β 1 was reduced. As a result, it was suggested that the reason for the discrepancy between the cell lines and tissue was due to stromal-epithelial interactions which are essential in normal prostate development in function. In which case, SF may be more likely to reduce SF expression in a co-culture of stromal and epithelial cells, or epithelial cells grown in Matrigel which acts as an extracellular matrix. This may then more closely replicate the *ex vivo* model and if the stroma-epithelial interactions are key to the reduction of HSP90 β 1 by SF, then an effect may be observed.

The reduction of HSP90 β 1 by SF was only seen in a select number of the tissue samples analysed, indicating variation in how each individual responds. The cell lines used were each established from a single patient, so it may be that in the same way HSP90 β 1 expression was not altered in the tissue samples from all patients that the cell lines used were established from patients who do not respond in this way. It would be interesting to isolate primary epithelial and stromal cells from a number of BPH samples and to culture these alongside tissue from the same patients and to compare if whether HSP90 β 1 expression is reduced in the primary epithelial cells obtained from tissue samples in which a reduction is observed. If no effect is seen in the cells isolated from tissue samples in which a reduction is observed, this would be further evidence for the importance of stromal-epithelial interactions.

Finally, the last reason suggested for SF not reducing HSP90 β 1 expression *in vitro* may be related to disease state. The *ex vivo* model used was BPH tissue whilst the established cell lines investigated were PNT1a, a healthy cell line, and DU145, a PCa cell line. It may be that the reduction of HSP90 β 1 by SF only occurs in BPH through BPH-specific mechanisms and does not occur in other disease states. To investigate this hypothesis, healthy and PCa tissue samples may be cultured to see whether the reduction of HSP90 β 1 expression by SF can be observed in samples other than BPH tissue. This would provide further evidence for whether baseline HSP90 β 1 expression alters in correlation with prostate dysregulation as current evidence is inconclusive.

7.4.3 In Vivo Models

The aim of studies concerning the role of diet in health is to understand the impact consumption of particular dietary components can have on a whole organism. To investigate this there are two options, animal models and human studies.

The use of an animal model has already been suggested in investigating the importance of HSP90 β 1 knockdown. Here an animal model can be used to answer the question as to whether SF can reduce HSP90 β 1 expression *in vivo*. There are a wide range of mouse models available, including a number of PCa models [295], such as TRAMP mice [296], but to investigate whether SF reduces HSP90 β 1 expression a healthy mouse model, such as C57BL/6, may be more appropriate. The diet of the mice could be supplemented with SF, and the prostates collected for analysis of HSP90 β 1 expression in comparison to mice on a control diet.

The ultimate aim to investigate the relationship between SF and HSP90 β 1 expression in the prostate is a human study. To follow-on from the work performed in this thesis, volunteers with BPH could be recruited to a study, in which they would consume broccoli, as a vehicle for SF delivery, for 6 months. Prostate samples could be collected at the beginning and end of the study period, and analysed for HSP90 β 1 expression.

As the BPH tissue was originally cultured *ex vivo* as a model of prostate inflammation, it may also be of interest to look at the effect of broccoli consumption on inflammatory markers. This could be achieved either by measuring the levels of cytokines in the blood to assess the effect on systemic inflammation, or by quantifying cytokines in seminal plasma [167] to investigate prostate inflammation.

Annex

Annex

BPH Tissue Patients

No.	Tissue Bank Code	Culture Conditions	Thesis
1	-	KGM/RPMI	Figure 2.3
2	-	+/- DHT	Figure 2.4
3	-	+/- DHT	Figure 2.4
4	-	+/- DHT	Figure 2.4
8	09TB00041	+/- 25 μ M SF	Figure 3.3-4
9	09TB00043	+/- 25 μ M SF	Figure 3.3-4
10	09TB00044	+/- 25 μ M SF	Figure 3.3-4
12	09TB00050	2/5/10/25 μ M SF	Figure 3.5
13	09TB00051	2/5/10/25 μ M SF	Figure 3.5 + Chapters 4-5
14	09TB00061	2/5/10/25 μ M SF	Figure 3.5 + Chapters 4-5
15	09TB00062	2/5/10/25 μ M SF	Figure 3.5
16	09TB00063	2/5/10/25 μ M SF	Figure 3.5 + Chapters 4-5
29	09TB00233	+/- 10 μ M SF	Figure 6.3
31	10TB0002	+/- 10 μ M SF	Figure 6.3
32	10TB0007	+/- 10 μ M SF	Figure 6.3
34	10TB0013	+/- 10 μ M SF	Figure 6.3
35	10TB0015	+/- 10 μ M SF	Figure 6.3
36	10TB0016	+/- 10 μ M SF	Figure 6.3
37*	10TB0033	+/- 10 μ M SF (and 24 hr TC.)	-
38	10TB0034	+/- 10 μ M SF (and 24 hr TC.)	Figure 2.8 + 6.3-4
39	10TB0051	+/- 10 μ M SF	Figure 6.3-4
41	10TB0058	+/- 10 μ M SF	Figure 6.4
42	10TB0088	+/- 10 μ M SF	Figure 6.4
43	10TB0089	+/- 10 μ M SF (and 5 day TC.)	Figure 2.6 + 6.4
44	10TB0090	+/- 10 μ M SF (and 5 day TC.)	Figure 2.6 + 6.3-4

TC = Time Course

*Patient 37 was later identified as high grade cancer so excluded from analysis and data not shown.

References

References

1. Aumuller, G., *Postnatal development of the prostate*. Bull Assoc Anat (Nancy), 1991. **75**(229): p. 39-42.
2. McNeal, J.E., *The zonal anatomy of the prostate*. Prostate, 1981. **2**(1): p. 35-49.
3. Kumar, V.L. and P.K. Majumder, *Prostate gland: structure, functions and regulation*. Int Urol Nephrol, 1995. **27**(3): p. 231-43.
4. Huggins, C., W.W. Scott, and J. Henry Heinen, *Chemical composition of human semen and of the secretions of the prostate and seminal vesicles*. Am J Physiol 1942(136): p. 467-473.
5. Fair, W.R. and R.F. Parrish, *Antibacterial substances in prostatic fluid*. Prog Clin Biol Res, 1981. **75A**: p. 247-64.
6. Farnsworth, W.E. and J.R. Brown, *Metabolism of testosterone by the human prostate*. JAMA, 1963. **183**: p. 436-9.
7. Imperato-McGinley, J. and Y.S. Zhu, *Androgens and male physiology the syndrome of 5alpha-reductase-2 deficiency*. Mol Cell Endocrinol, 2002. **198**(1-2): p. 51-9.
8. Ellem, S.J. and G.P. Risbridger, *The dual, opposing roles of estrogen in the prostate*. Ann N Y Acad Sci, 2009. **1155**: p. 174-86.
9. Farnsworth, W.E., *Prostate stroma: physiology*. Prostate, 1999. **38**(1): p. 60-72.
10. Kramer, G., D. Mitteregger, and M. Marberger, *Is benign prostatic hyperplasia (BPH) an immune inflammatory disease?* Eur Urol, 2007. **51**(5): p. 1202-16.
11. Widmaier, E.P., Raff, H. and Strang K.T., *Vander, Sherman, Luciano's Human Physiology: The Mechanims of Body Function*. 9th ed. 2004: McGraw-Hill.
12. McVary, K.T., *BPH: epidemiology and comorbidities*. Am J Manag Care, 2006. **12**(5 Suppl): p. S122-8.
13. Berry, S.J., et al., *The development of human benign prostatic hyperplasia with age*. J Urol, 1984. **132**(3): p. 474-9.
14. Trueman, P., et al., *Prevalence of lower urinary tract symptoms and self-reported diagnosed 'benign prostatic hyperplasia', and their effect on quality of life in a community-based survey of men in the UK*. BJU Int, 1999. **83**(4): p. 410-5.
15. McNeal, J.E., *Origin and evolution of benign prostatic enlargement*. Invest Urol, 1978. **15**(4): p. 340-5.
16. Oesterling, J.E., *The origin and development of benign prostatic hyperplasia. An age-dependent process*. J Androl, 1991. **12**(6): p. 348-55.

17. McConnell, J.D., *The pathophysiology of benign prostatic hyperplasia*. J Androl, 1991. **12**(6): p. 356-63.
18. Steiner, G.E., et al., *Cytokine expression pattern in benign prostatic hyperplasia infiltrating T cells and impact of lymphocytic infiltration on cytokine mRNA profile in prostatic tissue*. Lab Invest, 2003. **83**(8): p. 1131-46.
19. Deshpande, N., et al., *Divergent effects of interferons on the growth of human benign prostatic hyperplasia cells in primary culture*. J Urol, 1989. **141**(1): p. 157-60.
20. Kramer, G., et al., *Increased expression of lymphocyte-derived cytokines in benign hyperplastic prostate tissue, identification of the producing cell types, and effect of differentially expressed cytokines on stromal cell proliferation*. Prostate, 2002. **52**(1): p. 43-58.
21. Handisurya, A., et al., *Differential expression of interleukin-15, a pro-inflammatory cytokine and T-cell growth factor, and its receptor in human prostate*. Prostate, 2001. **49**(4): p. 251-62.
22. Steiner, G.E., et al., *Expression and function of pro-inflammatory interleukin IL-17 and IL-17 receptor in normal, benign hyperplastic, and malignant prostate*. Prostate, 2003. **56**(3): p. 171-82.
23. CancerStats. 2011 [cited 2011 April 4th].
24. Cancer Research UK: CancerStats. 2011 April 4th 2011].
25. Bello-DeOcampo, D. and D.J. Tindall, *TGF-beta1/Smad signaling in prostate cancer*. Curr Drug Targets, 2003. **4**(3): p. 197-207.
26. Pecorino, L., *Molecular Biology of Cancer*. 2005: Oxford University Press.
27. Humphrey, P.A., *Gleason grading and prognostic factors in carcinoma of the prostate*. Mod Pathol, 2004. **17**(3): p. 292-306.
28. Koochekpour, S., *Androgen receptor signaling and mutations in prostate cancer*. Asian J Androl, 2010. **12**(5): p. 639-57.
29. Dennis, L.K., C.F. Lynch, and J.C. Torner, *Epidemiologic association between prostatitis and prostate cancer*. Urology, 2002. **60**(1): p. 78-83.
30. Vasto, S., et al., *Inflammation and prostate cancer*. Future Oncol, 2008. **4**(5): p. 637-45.
31. MacLennan, G.T., et al., *The influence of chronic inflammation in prostatic carcinogenesis: a 5-year followup study*. J Urol, 2006. **176**(3): p. 1012-6.
32. Bardia, A., et al., *Anti-inflammatory drugs, antioxidants, and prostate cancer prevention*. Curr Opin Pharmacol, 2009. **9**(4): p. 419-26.

33. Alcaraz, A., et al., *Is there evidence of a relationship between benign prostatic hyperplasia and prostate cancer? Findings of a literature review.* Eur Urol, 2009. **55**(4): p. 864-73.
34. De Marzo, A.M., et al., *Human prostate cancer precursors and pathobiology.* Urology, 2003. **62**(5 Suppl 1): p. 55-62.
35. Karan, D., J. Holzbeierlein, and J.B. Thrasher, *Macrophage inhibitory cytokine-1: possible bridge molecule of inflammation and prostate cancer.* Cancer Res, 2009. **69**(1): p. 2-5.
36. Haverkamp, J., B. Charbonneau, and T.L. Ratliff, *Prostate inflammation and its potential impact on prostate cancer: a current review.* J Cell Biochem, 2008. **103**(5): p. 1344-53.
37. Fujita, K., et al., *Cytokine profiling of prostatic fluid from cancerous prostate glands identifies cytokines associated with extent of tumor and inflammation.* Prostate, 2008. **68**(8): p. 872-82.
38. Armenian, H.K., et al., *Relation between benign prostatic hyperplasia and cancer of the prostate. A prospective and retrospective study.* Lancet, 1974. **2**(7873): p. 115-7.
39. Greenwald, P., et al., *Cancer of the prostate among men with benign prostatic hyperplasia.* J Natl Cancer Inst, 1974. **53**(2): p. 335-40.
40. Simons, B.D., et al., *The relation of surgery for prostatic hypertrophy to carcinoma of the prostate.* Am J Epidemiol, 1993. **138**(5): p. 294-300.
41. McNeal, J.E., et al., *Zonal distribution of prostatic adenocarcinoma. Correlation with histologic pattern and direction of spread.* Am J Surg Pathol, 1988. **12**(12): p. 897-906.
42. Konig, J.E., et al., *Analysis of the inflammatory network in benign prostate hyperplasia and prostate cancer.* Prostate, 2004. **58**(2): p. 121-9.
43. Mollet, B. and I. Rowland, *Functional foods: at the frontier between food and pharma.* Curr Opin Biotechnol, 2002. **13**(5): p. 483-5.
44. Divisi, D., et al., *Diet and cancer.* Acta bio-medica, 2006. **77**(2): p. 118-123.
45. Denis, L., M.S. Morton, and K. Griffiths, *Diet and its preventive role in prostatic disease.* Eur Urol, 1999. **35**(5-6): p. 377-87.
46. Gu, F., *Changes in the prevalence of benign prostatic hyperplasia in China.* Chin Med J (Engl), 1997. **110**(3): p. 163-6.
47. Bravi, F., et al., *Macronutrients, fatty acids, cholesterol, and risk of benign prostatic hyperplasia.* Urology, 2006. **67**(6): p. 1205-11.

48. Kristal, A.R., et al., *Dietary patterns, supplement use, and the risk of symptomatic benign prostatic hyperplasia: results from the prostate cancer prevention trial*. *Am J Epidemiol*, 2008. **167**(8): p. 925-34.
49. Suzuki, S., et al., *Intakes of energy and macronutrients and the risk of benign prostatic hyperplasia*. *Am J Clin Nutr*, 2002. **75**(4): p. 689-97.
50. Lagiou, P., et al., *Diet and benign prostatic hyperplasia: a study in Greece*. *Urology*, 1999. **54**(2): p. 284-90.
51. Bravi, F., et al., *Food groups and risk of benign prostatic hyperplasia*. *Urology*, 2006. **67**(1): p. 73-9.
52. Rohrmann, S., et al., *Fruit and vegetable consumption, intake of micronutrients, and benign prostatic hyperplasia in US men*. *Am J Clin Nutr*, 2007. **85**(2): p. 523-9.
53. Galeone, C., et al., *Onion and garlic intake and the odds of benign prostatic hyperplasia*. *Urology*, 2007. **70**(4): p. 672-6.
54. Shimizu, H., et al., *Cancers of the prostate and breast among Japanese and white immigrants in Los Angeles County*. *Br J Cancer*, 1991. **63**(6): p. 963-6.
55. Cook, L.S., et al., *Incidence of adenocarcinoma of the prostate in Asian immigrants to the United States and their descendants*. *J Urol*, 1999. **161**(1): p. 152-5.
56. Schuurman, A.G., et al., *Association of energy and fat intake with prostate carcinoma risk: results from The Netherlands Cohort Study*. *Cancer*, 1999. **86**(6): p. 1019-27.
57. Kristal, A.R., et al., *Associations of energy, fat, calcium, and vitamin D with prostate cancer risk*. *Cancer Epidemiol Biomarkers Prev*, 2002. **11**(8): p. 719-25.
58. Deneo-Pellegrini, H., et al., *Foods, nutrients and prostate cancer: a case-control study in Uruguay*. *Br. J. Cancer*, 1999. **80**: p. 591-597.
59. Ohno, Y., et al., *Dietary beta-carotene and cancer of the prostate: a case-control study in Kyoto, Japan*. *Cancer Res*, 1988. **48**(5): p. 1331-6.
60. Key, T.J., et al., *A case-control study of diet and prostate cancer*. *Br. J. Cancer*, 1997. **76**: p. 678-687.
61. Slattery, M.L., et al., *Food-consumption trends between adolescent and adult years and subsequent risk of prostate cancer*. *Am J Clin Nutr*, 1990. **52**(4): p. 752-7.
62. Hayes, R.B., et al., *Dietary factors and risks for prostate cancer among blacks and whites in the United States*. *Cancer Epidemiol Biomarkers Prev*, 1999. **8**(1): p. 25-34.
63. Willett, W.C., *Specific fatty acids and risks of breast and prostate cancer: dietary intake*. *Am J Clin Nutr*, 1997. **66**(6 Suppl): p. 1557S-1563S.

64. Augustsson, K., et al., *A prospective study of intake of fish and marine fatty acids and prostate cancer*. *Cancer Epidemiol Biomarkers Prev*, 2003. **12**(1): p. 64-7.
65. Schuurman, A.G., et al., *Animal products, calcium and protein and prostate cancer risk in The Netherlands Cohort Study*. *Br J Cancer*, 1999. **80**(7): p. 1107-13.
66. Hsing, A.W. and A.P. Chokkalingam, *Prostate cancer epidemiology*. *Front Biosci*, 2006. **11**: p. 1388-413.
67. Rodriguez, C., et al., *Calcium, dairy products, and risk of prostate cancer in a prospective cohort of United States men*. *Cancer Epidemiol Biomarkers Prev*, 2003. **12**(7): p. 597-603.
68. Chan, J.M., *Dairy products, calcium, and prostate cancer risk in the Physicians' Health Study*. *Am. J. Clin. Nutr.*, 2001. **74**: p. 549-554.
69. Giovannucci, E., *Calcium and fructose intake in relation to risk of prostate cancer*. *Cancer Res.*, 1998. **58**: p. 442-447.
70. Kolonel, L.N., et al., *Vegetables, fruits, legumes and prostate cancer: a multiethnic case-control study*. *Cancer Epidemiol Biomarkers Prev*, 2000. **9**(8): p. 795-804.
71. Deneo-Pellegrini, H., et al., *Foods, nutrients and prostate cancer: a case-control study in Uruguay*. *Br J Cancer*, 1999. **80**(3-4): p. 591-7.
72. Verhoeven, D.T.H., et al., *Epidemiological studies on brassica vegetables and cancer risk*. *Cancer Epidemiology Biomarkers & Prevention*, 1996. **5**(9): p. 733-748.
73. Cohen, J.H., A.R. Kristal, and J.L. Stanford, *Fruit and vegetable intakes and prostate cancer risk*. *J Natl Cancer Inst*, 2000. **92**(1): p. 61-8.
74. Giovannucci, E., et al., *A prospective study of cruciferous vegetables and prostate cancer*. *Cancer Epidemiol Biomarkers Prev*, 2003. **12**(12): p. 1403-9.
75. Joseph, M.A., et al., *Cruciferous vegetables, genetic polymorphisms in glutathione S-transferases M1 and T1, and prostate cancer risk*. *Nutrition and Cancer-an International Journal*, 2004. **50**(2): p. 206-213.
76. Richman, E.L., P.R. Carroll, and J.M. Chan, *Vegetable and fruit intake after diagnosis and risk of prostate cancer progression*. *Int J Cancer*, 2011.
77. Kirsh, V.A., et al., *Prospective study of fruit and vegetable intake and risk of prostate cancer*. *J Natl Cancer Inst*, 2007. **99**(15): p. 1200-9.
78. Steinbrecher, A., et al., *Dietary glucosinolate intake and risk of prostate cancer in the EPIC-Heidelberg cohort study*. *Int J Cancer*, 2009. **125**(9): p. 2179-86.
79. Clinton, S.K., et al., *cis-trans lycopene isomers, carotenoids, and retinol in the human prostate*. *Cancer Epidemiol Biomarkers Prev*, 1996. **5**(10): p. 823-33.

80. Norrish, A.E., et al., *Prostate cancer and dietary carotenoids*. Am J Epidemiol, 2000. **151**(2): p. 119-23.
81. Giovannucci, E., et al., *A prospective study of tomato products, lycopene, and prostate cancer risk*. J. Natl Cancer Inst., 2002. **94**: p. 391-398.
82. Helzlsouer, K.J., et al., *Association between alpha-tocopherol, gamma-tocopherol, selenium, and subsequent prostate cancer*. J Natl Cancer Inst, 2000. **92**(24): p. 2018-23.
83. Reichman, M.E., et al., *Serum vitamin A and subsequent development of prostate cancer in the first National Health and Nutrition Examination Survey Epidemiologic Follow-up Study*. Cancer Res, 1990. **50**(8): p. 2311-5.
84. Sichieri, R., J.E. Everhart, and G.A. Mendonca, *Diet and mortality from common cancers in Brazil: an ecological study*. Cad Saude Publica, 1996. **12**(1): p. 53-59.
85. Lee, M.M., et al., *Soy and isoflavone consumption in relation to prostate cancer risk in China*. Cancer Epidemiol Biomarkers Prev, 2003. **12**(7): p. 665-8.
86. Verkerk, R., et al., *Glucosinolates in Brassica vegetables: the influence of the food supply chain on intake, bioavailability and human health*. Mol Nutr Food Res, 2009. **53 Suppl 2**: p. S219.
87. Kristal, A.R. and J.W. Lampe, *Brassica vegetables and prostate cancer risk: a review of the epidemiological evidence*. Nutr Cancer, 2002. **42**(1): p. 1-9.
88. Moreno, D.A., et al., *Chemical and biological characterisation of nutraceutical compounds of broccoli*. Journal of Pharmaceutical and Biomedical Analysis, 2006. **41**(5): p. 1508-1522.
89. Fimognari, C. and P. Hrelia, *Sulforaphane as a promising molecule for fighting cancer*. Mutation Research-Reviews in Mutation Research, 2007. **635**(2-3): p. 90-104.
90. Higdon, J.V., et al., *Cruciferous vegetables and human cancer risk: epidemiologic evidence and mechanistic basis*. Pharmacological Research, 2007. **55**(3): p. 224-236.
91. Conaway, C.C., et al., *Disposition of glucosinolates and sulforaphane in humans after ingestion of steamed and fresh broccoli*. Nutr Cancer, 2000. **38**(2): p. 168-78.
92. Juge, N., R.F. Mithen, and M. Traka, *Molecular basis for chemoprevention by sulforaphane: a comprehensive review*. Cellular and Molecular Life Sciences, 2007. **64**(9): p. 1105-1127.
93. Hayes, J.D., J.U. Flanagan, and I.R. Jowsey, *Glutathione transferases*. Annu Rev Pharmacol Toxicol, 2005. **45**: p. 51-88.

94. Zhang, Y., et al., *Reversible conjugation of isothiocyanates with glutathione catalyzed by human glutathione transferases*. *Biochem Biophys Res Commun*, 1995. **206**(2): p. 748-55.
95. Traka, M., et al., *Broccoli consumption interacts with GSTM1 to perturb oncogenic signalling pathways in the prostate*. *PLoS ONE*, 2008. **3**(7): p. e2568.
96. Spitz, M.R., et al., *Dietary intake of isothiocyanates: evidence of a joint effect with glutathione S-transferase polymorphisms in lung cancer risk*. *Cancer Epidemiol Biomarkers Prev*, 2000. **9**(10): p. 1017-20.
97. Wang, L.I., et al., *Dietary intake of Cruciferous vegetables, Glutathione S-transfrase (GST) polymorphisms and lung cancer risk in a Caucasian population*. *Cancer Causes & Control*, 2004. **15**(10): p. 977-985.
98. Fowke, J.H., et al., *Urinary isothiocyanate levels, brassica, and human breast cancer*. *Cancer Res*, 2003. **63**(14): p. 3980-6.
99. Zhao, B., et al., *Dietary isothiocyanates, glutathione S-transferase -M1, -T1 polymorphisms and lung cancer risk among Chinese women in Singapore*. *Cancer Epidemiol Biomarkers Prev*, 2001. **10**(10): p. 1063-7.
100. Gasper, A.V., et al., *Glutathione S-transferase M1 polymorphism and metabolism of sulforaphane from standard and high-glucosinolate broccoli*. *Am J Clin Nutr*, 2005. **82**(6): p. 1283-91.
101. Steinbrecher, A., et al., *Dietary glucosinolate intake, polymorphisms in selected biotransformation enzymes, and risk of prostate cancer*. *Cancer Epidemiol Biomarkers Prev*, 2010. **19**(1): p. 135-43.
102. Kuroiwa, Y., et al., *Protective effects of benzyl isothiocyanate and sulforaphane but not resveratrol against initiation of pancreatic carcinogenesis in hamsters*. *Cancer Lett*, 2006. **241**(2): p. 275-80.
103. Brandenburg, L.O., et al., *Sulforaphane suppresses LPS-induced inflammation in primary rat microglia*. *Inflamm Res*, 2009.
104. Bergstrom, P., et al., *Repeated transient sulforaphane stimulation in astrocytes leads to prolonged Nrf2-mediated gene expression and protection from superoxide-induced damage*. *Neuropharmacology*, 2010.
105. Maheo, K., et al., *Inhibition of cytochromes P-450 and induction of glutathione S-transferases by sulforaphane in primary human and rat hepatocytes*. *Cancer Res*, 1997. **57**(17): p. 3649-52.

106. Barcelo, S., et al., *CYP2E1-mediated mechanism of anti-genotoxicity of the broccoli constituent sulforaphane*. *Carcinogenesis*, 1996. **17**(2): p. 277-82.
107. Jiang, Z.Q., et al., *Differential responses from seven mammalian cell lines to the treatments of detoxifying enzyme inducers*. *Life Sci*, 2003. **72**(20): p. 2243-53.
108. Bonnesen, C., I.M. Eggleston, and J.D. Hayes, *Dietary indoles and isothiocyanates that are generated from cruciferous vegetables can both stimulate apoptosis and confer protection against DNA damage in human colon cell lines*. *Cancer Res*, 2001. **61**(16): p. 6120-30.
109. Hu, R., et al., *In vivo pharmacokinetics and regulation of gene expression profiles by isothiocyanate sulforaphane in the rat*. *J Pharmacol Exp Ther*, 2004. **310**(1): p. 263-71.
110. Yu, R., et al., *Role of a mitogen-activated protein kinase pathway in the induction of phase II detoxifying enzymes by chemicals*. *J Biol Chem*, 1999. **274**(39): p. 27545-52.
111. Ritz, S.A., J. Wan, and D. Diaz-Sanchez, *Sulforaphane-stimulated phase II enzyme induction inhibits cytokine production by airway epithelial cells stimulated with diesel extract*. *Am J Physiol Lung Cell Mol Physiol*, 2007. **292**(1): p. L33-9.
112. Youn, H.S., et al., *Sulforaphane Suppresses Oligomerization of TLR4 in a Thiol-Dependent Manner*. *J Immunol*, 2009.
113. Zakkar, M., et al., *Activation of Nrf2 in endothelial cells protects arteries from exhibiting a proinflammatory state*. *Arterioscler Thromb Vasc Biol*, 2009. **29**(11): p. 1851-7.
114. Lin, W., et al., *Sulforaphane suppressed LPS-induced inflammation in mouse peritoneal macrophages through Nrf2 dependent pathway*. *Biochem Pharmacol*, 2008. **76**(8): p. 967-73.
115. Gan, N., et al., *Sulforaphane activates heat shock response and enhances proteasome activity through up-regulation of Hsp27*. *J Biol Chem*, 2010. **285**(46): p. 35528-36.
116. Hu, R., et al., *Gene expression profiles induced by cancer chemopreventive isothiocyanate sulforaphane in the liver of C57BL/6J mice and C57BL/6J/Nrf2 (-/-) mice*. *Cancer Lett*, 2006. **243**(2): p. 170-92.
117. Gibbs, A., et al., *Sulforaphane destabilizes the androgen receptor in prostate cancer cells by inactivating histone deacetylase 6*. *Proc Natl Acad Sci U S A*, 2009. **106**(39): p. 16663-8.
118. Myzak, M.C., et al., *A novel mechanism of chemoprotection by sulforaphane: inhibition of histone deacetylase*. *Cancer Res*, 2004. **64**(16): p. 5767-74.

119. Myzak, M.C., et al., *Sulforaphane inhibits histone deacetylase activity in BPH-1, LnCaP and PC-3 prostate epithelial cells*. *Carcinogenesis*, 2006. **27**(4): p. 811-9.
120. Myzak, M.C., et al., *Sulforaphane inhibits histone deacetylase in vivo and suppresses tumorigenesis in Apc-minus mice*. *FASEB J*, 2006. **20**(3): p. 506-8.
121. Parnaud, G., et al., *Mechanism of sulforaphane-induced cell cycle arrest and apoptosis in human colon cancer cells*. *Nutr Cancer*, 2004. **48**(2): p. 198-206.
122. Gamet-Payrastre, L., et al., *Sulforaphane, a naturally occurring isothiocyanate, induces cell cycle arrest and apoptosis in HT29 human colon cancer cells*. *Cancer Res*, 2000. **60**(5): p. 1426-33.
123. Roy, S.K., R.K. Srivastava, and S. Shankar, *Inhibition of PI3K/AKT and MAPK/ERK pathways causes activation of FOXO transcription factor, leading to cell cycle arrest and apoptosis in pancreatic cancer*. *J Mol Signal*, 2010. **5**: p. 10.
124. Traka, M.H., et al., *Involvement of KLF4 in sulforaphane- and iberin-mediated induction of p21(waf1/cip1)*. *Nutr Cancer*, 2009. **61**(1): p. 137-45.
125. Shankar, S., S. Ganapathy, and R.K. Srivastava, *Sulforaphane enhances the therapeutic potential of TRAIL in prostate cancer orthotopic model through regulation of apoptosis, metastasis, and angiogenesis*. *Clin Cancer Res*, 2008. **14**(21): p. 6855-66.
126. Xu, C., et al., *ERK and JNK signaling pathways are involved in the regulation of activator protein 1 and cell death elicited by three isothiocyanates in human prostate cancer PC-3 cells*. *Carcinogenesis*, 2006. **27**(3): p. 437-45.
127. Karmakar, S., et al., *Activation of multiple molecular mechanisms for apoptosis in human malignant glioblastoma T98G and U87MG cells treated with sulforaphane*. *Neuroscience*, 2006. **141**(3): p. 1265-80.
128. Asakage, M., et al., *Sulforaphane induces inhibition of human umbilical vein endothelial cells proliferation by apoptosis*. *Angiogenesis*, 2006. **9**(2): p. 83-91.
129. Bertl, E., H. Bartsch, and C. Gerhauser, *Inhibition of angiogenesis and endothelial cell functions are novel sulforaphane-mediated mechanisms in chemoprevention*. *Mol Cancer Ther*, 2006. **5**(3): p. 575-85.
130. Thejass, P. and G. Kuttan, *Antimetastatic activity of Sulforaphane*. *Life Sci*, 2006. **78**(26): p. 3043-50.
131. Annabi, B., et al., *The diet-derived sulforaphane inhibits matrix metalloproteinase-9-activated human brain microvascular endothelial cell migration and tubulogenesis*. *Mol Nutr Food Res*, 2008. **52**(6): p. 692-700.

132. Bhamre, S., et al., *Temporal changes in gene expression induced by sulforaphane in human prostate cancer cells*. Prostate, 2009. **69**(2): p. 181-90.
133. Kim, S.H. and S.V. Singh, *D,L-Sulforaphane causes transcriptional repression of androgen receptor in human prostate cancer cells*. Mol Cancer Ther, 2009. **8**(7): p. 1946-54.
134. Myzak, M.C., et al., *Sulforaphane retards the growth of human PC-3 xenografts and inhibits HDAC activity in human subjects*. Exp Biol Med (Maywood), 2007. **232**(2): p. 227-34.
135. Yao, H., et al., *Sulforaphane inhibited expression of hypoxia-inducible factor-1alpha in human tongue squamous cancer cells and prostate cancer cells*. Int J Cancer, 2008. **123**(6): p. 1255-61.
136. Bronte, V., et al., *Boosting antitumor responses of T lymphocytes infiltrating human prostate cancers*. J Exp Med, 2005. **201**(8): p. 1257-68.
137. Singh, S.V., et al., *Sulforaphane inhibits prostate carcinogenesis and pulmonary metastasis in TRAMP mice in association with increased cytotoxicity of natural killer cells*. Cancer Res, 2009. **69**(5): p. 2117-25.
138. Nevalainen, M.T., et al., *Hormone regulation of human prostate in organ culture*. Cancer Res, 1993. **53**(21): p. 5199-207.
139. Papini, S., et al., *Selective growth of epithelial basal cells from human prostate in a three-dimensional organ culture*. Prostate, 2004. **59**(4): p. 383-92.
140. Varani, J., et al., *Matrix metalloproteinases (MMPs) in fresh human prostate tumour tissue and organ-cultured prostate tissue: levels of collagenolytic and gelatinolytic MMPs are low, variable and different in fresh tissue versus organ-cultured tissue*. Br J Cancer, 2001. **84**(8): p. 1076-83.
141. Varani, J., et al., *Characteristics of nonmalignant and malignant human prostate in organ culture*. Lab Invest, 1999. **79**(6): p. 723-31.
142. Parrish, A.R., et al., *Culturing precision-cut human prostate slices as an in vitro model of prostate pathobiology*. Cell Biol Toxicol, 2002. **18**(3): p. 205-19.
143. Hernandez, J. and I.M. Thompson, *Prostate-specific antigen: a review of the validation of the most commonly used cancer biomarker*. Cancer, 2004. **101**(5): p. 894-904.
144. Legrand, C., et al., *Lactate dehydrogenase (LDH) activity of the cultured eukaryotic cells as marker of the number of dead cells in the medium [corrected]*. J Biotechnol, 1992. **25**(3): p. 231-43.

145. Decker, T. and M.L. Lohmann-Matthes, *A quick and simple method for the quantitation of lactate dehydrogenase release in measurements of cellular cytotoxicity and tumor necrosis factor (TNF) activity*. J Immunol Methods, 1988. **115**(1): p. 61-9.
146. Abdollahi, A. and M. Ayati, *Frequency and outcome of metaplasia in needle biopsies of prostate and its relation with clinical findings*. Urol J, 2009. **6**(2): p. 109-13.
147. Martz, L., *The root of prostate cancer*. Science-Business eXchange, 2010. **3**(33).
148. Goldstein, A.S., et al., *Identification of a cell of origin for human prostate cancer*. Science, 2010. **329**(5991): p. 568-71.
149. Kurita, T., et al., *Role of p63 and basal cells in the prostate*. Development, 2004. **131**(20): p. 4955-64.
150. . 1997.
151. Lawson, D.A., et al., *Isolation and functional characterization of murine prostate stem cells*. Proc Natl Acad Sci U S A, 2007. **104**(1): p. 181-6.
152. Kopf, M., M.F. Bachmann, and B.J. Marsland, *Averting inflammation by targeting the cytokine environment*. Nat Rev Drug Discov, 2010. **9**(9): p. 703-18.
153. Santer, F.R., et al., *Interleukin-6 trans-signalling differentially regulates proliferation, migration, adhesion and maspin expression in human prostate cancer cells*. Endocr Relat Cancer, 2010. **17**(1): p. 241-53.
154. Ara, T. and Y.A. Declerck, *Interleukin-6 in bone metastasis and cancer progression*. Eur J Cancer, 2010. **46**(7): p. 1223-31.
155. Corcoran, N.M. and A.J. Costello, *Interleukin-6: minor player or starring role in the development of hormone-refractory prostate cancer?* BJU Int, 2003. **91**(6): p. 545-53.
156. Nakashima, J., et al., *Serum interleukin 6 as a prognostic factor in patients with prostate cancer*. Clin Cancer Res, 2000. **6**(7): p. 2702-6.
157. Rojas, A., et al., *IL-6 promotes prostate tumorigenesis and progression through autocrine cross-activation of IGF-IR*. Oncogene, 2011.
158. Hunakova, L., et al., *Modulation of markers associated with aggressive phenotype in MDA-MB-231 breast carcinoma cells by sulforaphane*. Neoplasma, 2009. **56**(6): p. 548-56.
159. Chan, C., H.J. Lin, and J. Lin, *Stress-associated hormone, norepinephrine, increases proliferation and IL-6 levels of human pancreatic duct epithelial cells and can be inhibited by the dietary agent, sulforaphane*. Int J Oncol, 2008. **33**(2): p. 415-9.

160. Traka, M.H., et al., *The dietary isothiocyanate sulforaphane modulates gene expression and alternative gene splicing in a PTEN null preclinical murine model of prostate cancer*. Mol Cancer, 2010. **9**: p. 189.
161. Cornblatt, B.S., et al., *Preclinical and clinical evaluation of sulforaphane for chemoprevention in the breast*. Carcinogenesis, 2007. **28**(7): p. 1485-90.
162. Traka, M., et al., *Transcriptome analysis of human colon Caco-2 cells exposed to sulforaphane*. J Nutr, 2005. **135**(8): p. 1865-72.
163. Bouraoui, Y., et al., *Pro-inflammatory cytokines and prostate-specific antigen in hyperplasia and human prostate cancer*. Cancer Detect Prev, 2008. **32**(1): p. 23-32.
164. Hochreiter, W.W., et al., *Evaluation of the cytokines interleukin 8 and epithelial neutrophil activating peptide 78 as indicators of inflammation in prostatic secretions*. Urology, 2000. **56**(6): p. 1025-9.
165. Castro, P., et al., *Interleukin-8 expression is increased in senescent prostatic epithelial cells and promotes the development of benign prostatic hyperplasia*. Prostate, 2004. **60**(2): p. 153-9.
166. Lee, S.O., et al., *Interleukin-4 stimulates androgen-independent growth in LNCaP human prostate cancer cells*. Prostate, 2008. **68**(1): p. 85-91.
167. Penna, G., et al., *Seminal plasma cytokines and chemokines in prostate inflammation: interleukin 8 as a predictive biomarker in chronic prostatitis/chronic pelvic pain syndrome and benign prostatic hyperplasia*. Eur Urol, 2007. **51**(2): p. 524-33; discussion 533.
168. Hobisch, A., et al., *Immunohistochemical localization of interleukin-6 and its receptor in benign, premalignant and malignant prostate tissue*. J Pathol, 2000. **191**(3): p. 239-44.
169. Giri, D. and M. Ittmann, *Interleukin-8 is a paracrine inducer of fibroblast growth factor 2, a stromal and epithelial growth factor in benign prostatic hyperplasia*. Am J Pathol, 2001. **159**(1): p. 139-47.
170. Fujita, K., et al., *Monocyte chemotactic protein-1 (MCP-1/CCL2) is associated with prostatic growth dysregulation and benign prostatic hyperplasia*. Prostate, 2010. **70**(5): p. 473-81.
171. Drachenberg, D.E., et al., *Circulating levels of interleukin-6 in patients with hormone refractory prostate cancer*. Prostate, 1999. **41**(2): p. 127-33.
172. Veltri, R.W., et al., *Interleukin-8 serum levels in patients with benign prostatic hyperplasia and prostate cancer*. Urology, 1999. **53**(1): p. 139-47.

173. Soultziz, N., et al., *Expression analysis of peptide growth factors VEGF, FGF2, TGFB1, EGF and IGF1 in prostate cancer and benign prostatic hyperplasia*. *Int J Oncol*, 2006. **29**(2): p. 305-14.
174. Boget, S., A. Leriche, and A. Revol, *Basic fibroblast growth factor and keratinocyte growth factor over-expression in benign prostatic hyperplasia*. *Farmaco*, 2001. **56**(5-7): p. 467-9.
175. Ropiquet, F., et al., *FGF7 and FGF2 are increased in benign prostatic hyperplasia and are associated with increased proliferation*. *J Urol*, 1999. **162**(2): p. 595-9.
176. Kong, J.S., et al., *Inhibition of synovial hyperplasia, rheumatoid T cell activation, and experimental arthritis in mice by sulforaphane, a naturally occurring isothiocyanate*. *Arthritis Rheum*, 2010. **62**(1): p. 159-70.
177. Hahm, E.R. and S.V. Singh, *Sulforaphane inhibits constitutive and interleukin-6-induced activation of signal transducer and activator of transcription 3 in prostate cancer cells*. *Cancer Prev Res (Phila)*, 2010. **3**(4): p. 484-94.
178. Bouwman, F.G., et al., *2D-electrophoresis and multiplex immunoassay proteomic analysis of different body fluids and cellular components reveal known and novel markers for extended fasting*. *BMC Med Genomics*, 2011. **4**: p. 24.
179. Mastrangelo, L., et al., *Serotonin receptors, novel targets of sulforaphane identified by proteomic analysis in Caco-2 cells*. *Cancer Res*, 2008. **68**(13): p. 5487-91.
180. Lee, C.H., et al., *Down-regulation of phosphoglucomutase 3 mediates sulforaphane-induced cell death in LNCaP prostate cancer cells*. *Proteome Sci*, 2010. **8**: p. 67.
181. Mi, L., et al., *The role of protein binding in induction of apoptosis by phenethyl isothiocyanate and sulforaphane in human non-small lung cancer cells*. *Cancer Res*, 2007. **67**(13): p. 6409-16.
182. Wu, M., et al., *Proteome analysis of human androgen-independent prostate cancer cell lines: variable metastatic potentials correlated with vimentin expression*. *Proteomics*, 2007. **7**(12): p. 1973-83.
183. Howard, E.W., et al., *Decreased adhesiveness, resistance to anoikis and suppression of GRP94 are integral to the survival of circulating tumor cells in prostate cancer*. *Clin Exp Metastasis*, 2008. **25**(5): p. 497-508.
184. Whitehead, A. and D.L. Crawford, *Variation in tissue-specific gene expression among natural populations*. *Genome Biol*, 2005. **6**(2): p. R13.
185. Oleksiak, M.F., G.A. Churchill, and D.L. Crawford, *Variation in gene expression within and among natural populations*. *Nat Genet*, 2002. **32**(2): p. 261-6.

186. Whitney, A.R., et al., *Individuality and variation in gene expression patterns in human blood*. Proc Natl Acad Sci U S A, 2003. **100**(4): p. 1896-901.
187. Polley, A.C., et al., *Proteomic analysis reveals field-wide changes in protein expression in the morphologically normal mucosa of patients with colorectal neoplasia*. Cancer Res, 2006. **66**(13): p. 6553-62.
188. Consortium, G.O. *The Gene Ontology*. 1999-2011 [cited 2011 26th April].
189. Ashburner, M., et al., *Gene ontology: tool for the unification of biology*. *The Gene Ontology Consortium*. Nat Genet, 2000. **25**(1): p. 25-9.
190. Hudson, D.L., et al., *Epithelial cell differentiation pathways in the human prostate: identification of intermediate phenotypes by keratin expression*. J Histochem Cytochem, 2001. **49**(2): p. 271-8.
191. Moll, R., et al., *The catalog of human cytokeratins: patterns of expression in normal epithelia, tumors and cultured cells*. Cell, 1982. **31**(1): p. 11-24.
192. Zhu, S., et al., *C/EBPbeta modulates the early events of keratinocyte differentiation involving growth arrest and keratin 1 and keratin 10 expression*. Mol Cell Biol, 1999. **19**(10): p. 7181-90.
193. Alberts, B., Johnson, A., Lewis, J., Raff, M., Roberts, K., Walter, P., *Molecular Biology of the Cell*. 4th ed. 2002: Garland Science.
194. Ranganathan, S., et al., *Immunohistochemical analysis of beta-tubulin isotypes in human prostate carcinoma and benign prostatic hypertrophy*. Prostate, 1997. **30**(4): p. 263-8.
195. Ploussard, G., et al., *Class III beta-tubulin expression predicts prostate tumor aggressiveness and patient response to docetaxel-based chemotherapy*. Cancer Res, 2010. **70**(22): p. 9253-64.
196. Schauer, I.G., et al., *Elevated epithelial expression of interleukin-8 correlates with myofibroblast reactive stroma in benign prostatic hyperplasia*. Urology, 2008. **72**(1): p. 205-13.
197. Arenas, M.I., et al., *E-, N- and P-cadherin, and alpha-, beta- and gamma-catenin protein expression in normal, hyperplastic and carcinomatous human prostate*. Histochem J, 2000. **32**(11): p. 659-67.
198. Zaravinos, A., et al., *Identification of common differentially expressed genes in urinary bladder cancer*. PLoS One, 2011. **6**(4): p. e18135.

199. Spivey, K.A. and J. Banyard, *A prognostic gene signature in advanced ovarian cancer reveals a microfibril-associated protein (MAGP2) as a promoter of tumor cell survival and angiogenesis*. *Cell Adh Migr*, 2010. **4**(2): p. 169-71.
200. Mohler, J.L., et al., *Identification of differentially expressed genes associated with androgen-independent growth of prostate cancer*. *Prostate*, 2002. **51**(4): p. 247-55.
201. Zhu, G., et al., *Inhibition of proliferation, invasion, and migration of prostate cancer cells by downregulating elongation factor-1alpha expression*. *Mol Med*, 2009. **15**(11-12): p. 363-70.
202. Lehnigk, U., et al., *Localization of annexins I, II, IV and VII in whole prostate sections from radical prostatectomy patients*. *Histol Histopathol*, 2005. **20**(3): p. 673-80.
203. Inokuchi, J., et al., *Annexin A2 positively contributes to the malignant phenotype and secretion of IL-6 in DU145 prostate cancer cells*. *Int J Cancer*, 2009. **124**(1): p. 68-74.
204. Shiozawa, Y., et al., *Annexin II/annexin II receptor axis regulates adhesion, migration, homing, and growth of prostate cancer*. *J Cell Biochem*, 2008. **105**(2): p. 370-80.
205. Liu, J.W., et al., *Annexin II expression is reduced or lost in prostate cancer cells and its re-expression inhibits prostate cancer cell migration*. *Oncogene*, 2003. **22**(10): p. 1475-85.
206. Liu, Y., *Fatty acid oxidation is a dominant bioenergetic pathway in prostate cancer*. *Prostate Cancer Prostatic Dis*, 2006. **9**(3): p. 230-4.
207. Fimognari, C., et al., *Growth inhibition, cell-cycle arrest and apoptosis in human T-cell leukemia by the isothiocyanate sulforaphane*. *Carcinogenesis*, 2002. **23**(4): p. 581-6.
208. Jakubikova, J., Y. Bao, and J. Sedlak, *Isothiocyanates induce cell cycle arrest, apoptosis and mitochondrial potential depolarization in HL-60 and multidrug-resistant cell lines*. *Anticancer Res*, 2005. **25**(5): p. 3375-86.
209. Sharma, R., et al., *Role of lipid peroxidation in cellular responses to D,L-sulforaphane, a promising cancer chemopreventive agent*. *Biochemistry*, 2010. **49**(14): p. 3191-202.
210. Kumar, A. and G. Sabbioni, *New biomarkers for monitoring the levels of isothiocyanates in humans*. *Chem Res Toxicol*, 2010. **23**(4): p. 756-65.
211. Wu, J.S., et al., *Ligand-activated peroxisome proliferator-activated receptor-gamma protects against ischemic cerebral infarction and neuronal apoptosis by 14-3-3 epsilon upregulation*. *Circulation*, 2009. **119**(8): p. 1124-34.
212. Triplett, J.W. and F.M. Pavalko, *Disruption of alpha-actinin-integrin interactions at focal adhesions renders osteoblasts susceptible to apoptosis*. *Am J Physiol Cell Physiol*, 2006. **291**(5): p. C909-21.

213. Thorsen, K., et al., *Alternative splicing in colon, bladder, and prostate cancer identified by exon array analysis*. Mol Cell Proteomics, 2008. **7**(7): p. 1214-24.
214. Zhu, N. and Z. Wang, *Calreticulin expression is associated with androgen regulation of the sensitivity to calcium ionophore-induced apoptosis in LNCaP prostate cancer cells*. Cancer Res, 1999. **59**(8): p. 1896-902.
215. Burikhanov, R., et al., *The tumor suppressor Par-4 activates an extrinsic pathway for apoptosis*. Cell, 2009. **138**(2): p. 377-88.
216. Reddy, R.K., J. Lu, and A.S. Lee, *The endoplasmic reticulum chaperone glycoprotein GRP94 with Ca(2+)-binding and antiapoptotic properties is a novel proteolytic target of calpain during etoposide-induced apoptosis*. J Biol Chem, 1999. **274**(40): p. 28476-83.
217. Reddy, R.K., et al., *Endoplasmic reticulum chaperone protein GRP78 protects cells from apoptosis induced by topoisomerase inhibitors: role of ATP binding site in suppression of caspase-7 activation*. J Biol Chem, 2003. **278**(23): p. 20915-24.
218. Shu, C.W., et al., *GRP78 and Raf-1 cooperatively confer resistance to endoplasmic reticulum stress-induced apoptosis*. J Cell Physiol, 2008. **215**(3): p. 627-35.
219. Untergasser, G., et al., *Profiling molecular targets of TGF-beta1 in prostate fibroblast-to-myofibroblast transdifferentiation*. Mech Ageing Dev, 2005. **126**(1): p. 59-69.
220. Zhang, J., et al., *Human prostatic smooth muscle cells in culture: estradiol enhances expression of smooth muscle cell-specific markers*. Prostate, 1997. **30**(2): p. 117-29.
221. Kyprianou, N., et al., *Induction of prostate apoptosis by doxazosin in benign prostatic hyperplasia*. J Urol, 1998. **159**(6): p. 1810-5.
222. Dreiza, C.M., et al., *The small heat shock protein, HSPB6, in muscle function and disease*. Cell Stress Chaperones, 2010. **15**(1): p. 1-11.
223. Liu, X., et al., *Proteomic analysis of the tumorigenic human prostate cell line M12 after microcell-mediated transfer of chromosome 19 demonstrates reduction of vimentin*. Electrophoresis, 2003. **24**(19-20): p. 3445-53.
224. Mavridis, K., et al., *Expression analysis and study of the KLK15 mRNA splice variants in prostate cancer and benign prostatic hyperplasia*. Cancer Sci, 2010. **101**(3): p. 693-9.
225. Calo, L.A., et al., *Effect of doxazosin on oxidative stress-related proteins in benign prostatic hyperplasia*. Urol Int, 2006. **76**(1): p. 36-41.
226. Sharief, F.S., et al., *Expression of human prostatic acid phosphatase and prostate specific antigen genes in neoplastic and benign tissues*. Biochem Mol Biol Int, 1994. **33**(3): p. 567-74.

227. van den Bemd, G.J., et al., *Mass spectrometric identification of human prostate cancer-derived proteins in serum of xenograft-bearing mice*. Mol Cell Proteomics, 2006. **5**(10): p. 1830-9.
228. Grayhack, J.T., et al., *Biochemical profiles of prostatic fluid from normal and diseased prostate glands*. Prostate, 1980. **1**(2): p. 227-37.
229. Alaiya, A., et al., *Polypeptide expression in prostate hyperplasia and prostate adenocarcinoma*. Anal Cell Pathol, 2000. **21**(1): p. 1-9.
230. Truong, T., et al., *Creatine phosphokinase isoenzymes in human prostatic tissues: a comparison between benign hyperplasia and adenocarcinoma*. Prostate, 1985. **7**(2): p. 143-9.
231. Feld, R.D., et al., *The presence of creatine kinase BB isoenzyme in patients with prostatic cancer*. Clin Chim Acta, 1980. **100**(3): p. 267-73.
232. Alaiya, A.A., et al., *Proteomics-based signature for human benign prostate hyperplasia and prostate adenocarcinoma*. Int J Oncol, 2011. **38**(4): p. 1047-57.
233. Lexander, H., et al., *Proteomic analysis of protein expression in prostate cancer*. Anal Quant Cytol Histol, 2005. **27**(5): p. 263-72.
234. Chen, N., et al., *Quantitative proteome analysis of HCC cell lines with different metastatic potentials by SILAC*. Proteomics, 2008. **8**(23-24): p. 5108-18.
235. Kerns, M., et al., *Differential modulation of keratin expression by sulforaphane occurs via Nrf2-dependent and -independent pathways in skin epithelia*. Mol Biol Cell, 2010. **21**(23): p. 4068-75.
236. Wlazlinski, A., et al., *Downregulation of several fibulin genes in prostate cancer*. Prostate, 2007. **67**(16): p. 1770-80.
237. van Lingen, R.G., et al., *Distribution of dipeptidyl-peptidase IV on keratinocytes in the margin zone of a psoriatic lesion: a comparison with hyperproliferation and aberrant differentiation markers*. Arch Dermatol Res, 2008. **300**(10): p. 561-7.
238. Luo, J., et al., *Gene expression signature of benign prostatic hyperplasia revealed by cDNA microarray analysis*. Prostate, 2002. **51**(3): p. 189-200.
239. Coulson-Thomas, V.J., et al., *Fibroblast and prostate tumor cell cross-talk: fibroblast differentiation, TGF-beta, and extracellular matrix down-regulation*. Exp Cell Res, 2010. **316**(19): p. 3207-26.
240. Holland, J.W., et al., *Purification of the keratan sulfate proteoglycan expressed in prostatic secretory cells and its identification as lumican*. Prostate, 2004. **59**(3): p. 252-9.

241. Lin, J.F., et al., *Identification of candidate prostate cancer biomarkers in prostate needle biopsy specimens using proteomic analysis*. Int J Cancer, 2007. **121**(12): p. 2596-605.
242. Castoria, G., et al., *Androgen-induced cell migration: role of androgen receptor/filamin A association*. PLoS One, 2011. **6**(2): p. e17218.
243. Ritchie, R.F., et al., *Reference distributions for the negative acute-phase serum proteins, albumin, transferrin and transthyretin: a practical, simple and clinically relevant approach in a large cohort*. J Clin Lab Anal, 1999. **13**(6): p. 273-9.
244. Katayama, K., N. Fujita, and T. Tsuruo, *Akt/protein kinase B-dependent phosphorylation and inactivation of WEE1Hu promote cell cycle progression at G2/M transition*. Mol Cell Biol, 2005. **25**(13): p. 5725-37.
245. Reichelt, J., G. Furstenberger, and T.M. Magin, *Loss of keratin 10 leads to mitogen-activated protein kinase (MAPK) activation, increased keratinocyte turnover, and decreased tumor formation in mice*. J Invest Dermatol, 2004. **123**(5): p. 973-81.
246. Bando, Y., et al., *GRP94 reduces cell death in SH-SY5Y cells perturbed calcium homeostasis*. Apoptosis, 2004. **9**(4): p. 501-8.
247. Bruneel, A., et al., *Proteomics of human umbilical vein endothelial cells applied to etoposide-induced apoptosis*. Proteomics, 2005. **5**(15): p. 3876-84.
248. Romanuik, T.L., et al., *Identification of novel androgen-responsive genes by sequencing of LongSAGE libraries*. BMC Genomics, 2009. **10**: p. 476.
249. Tu, L.C., et al., *Proteomics analysis of the interactome of N-myc downstream regulated gene 1 and its interactions with the androgen response program in prostate cancer cells*. Mol Cell Proteomics, 2007. **6**(4): p. 575-88.
250. Glen, A., et al., *iTRAQ-facilitated proteomic analysis of human prostate cancer cells identifies proteins associated with progression*. J Proteome Res, 2008. **7**(3): p. 897-907.
251. Pootrakul, L., et al., *Expression of stress response protein Grp78 is associated with the development of castration-resistant prostate cancer*. Clin Cancer Res, 2006. **12**(20 Pt 1): p. 5987-93.
252. Tan, S.S., et al., *GRP78 up-regulation is associated with androgen receptor status, Hsp70-Hsp90 client proteins and castrate-resistant prostate cancer*. J Pathol, 2010.
253. Bennett, H.L., et al., *Androgens modulate autophagy and cell death via regulation of the endoplasmic reticulum chaperone glucose-regulated protein 78/BiP in prostate cancer cells*. Cell Death Dis, 2010. **1**(9): p. e72.

254. Zhu, N., et al., *Calreticulin: an intracellular Ca⁺⁺-binding protein abundantly expressed and regulated by androgen in prostatic epithelial cells*. *Endocrinology*, 1998. **139**(10): p. 4337-44.
255. Lu, S., et al., *Regulation of heat shock protein 70-1 expression by androgen receptor and its signaling in human prostate cancer cells*. *Int J Oncol*, 2010. **36**(2): p. 459-67.
256. Kimura, M.T., et al., *14-3-3 is involved in p75 neurotrophin receptor-mediated signal transduction*. *J Biol Chem*, 2001. **276**(20): p. 17291-300.
257. Conklin, D.S., K. Galaktionov, and D. Beach, *14-3-3 proteins associate with cdc25 phosphatases*. *Proc Natl Acad Sci U S A*, 1995. **92**(17): p. 7892-6.
258. Sekimoto, T., M. Fukumoto, and Y. Yoneda, *14-3-3 suppresses the nuclear localization of threonine 157-phosphorylated p27(Kip1)*. *EMBO J*, 2004. **23**(9): p. 1934-42.
259. McGonigle, S., M.J. Beall, and E.J. Pearce, *Eukaryotic initiation factor 2 alpha subunit associates with TGF beta receptors and 14-3-3 epsilon and acts as a modulator of the TGF beta response*. *Biochemistry*, 2002. **41**(2): p. 579-87.
260. Fu, Y., et al., *Pten null prostate tumorigenesis and AKT activation are blocked by targeted knockout of ER chaperone GRP78/BiP in prostate epithelium*. *Proc Natl Acad Sci U S A*, 2008. **105**(49): p. 19444-9.
261. Dall'Era, M.A., et al., *HSP27 and HSP70 interact with CD10 in C4-2 prostate cancer cells*. *Prostate*, 2007. **67**(7): p. 714-21.
262. Nylandsted, J., K. Brand, and M. Jaattela, *Heat shock protein 70 is required for the survival of cancer cells*. *Ann N Y Acad Sci*, 2000. **926**: p. 122-5.
263. Zhao, Z.G., Q.Z. Ma, and C.X. Xu, *Abrogation of heat-shock protein (HSP)70 expression induced cell growth inhibition and apoptosis in human androgen-independent prostate cancer cell line PC-3m*. *Asian J Androl*, 2004. **6**(4): p. 319-24.
264. Alur, M., et al., *Suppressive roles of calreticulin in prostate cancer growth and metastasis*. *Am J Pathol*, 2009. **175**(2): p. 882-90.
265. Pan, S., et al., *Specific interactions with TBP and TFIIB in vitro suggest that 14-3-3 proteins may participate in the regulation of transcription when part of a DNA binding complex*. *Plant Cell*, 1999. **11**(8): p. 1591-602.
266. Cardile, V., et al., *Involvement of HSP70 in resveratrol-induced apoptosis of human prostate cancer*. *Anticancer Res*, 2003. **23**(6C): p. 4921-6.
267. Wu, Y., et al., *Endoplasmic reticulum stress signal mediators are targets of selenium action*. *Cancer Res*, 2005. **65**(19): p. 9073-9.

268. Novara, G., et al., *Inflammation, apoptosis, and BPH: What is the evidence?* European Urology Supplements, 2006. **5**(4): p. 401-409.
269. Takahashi, H., et al., *Overexpression of GRP78 and GRP94 is involved in colorectal carcinogenesis.* Histol Histopathol, 2011. **26**(6): p. 663-71.
270. Gazit, G., J. Lu, and A.S. Lee, *De-regulation of GRP stress protein expression in human breast cancer cell lines.* Breast Cancer Res Treat, 1999. **54**(2): p. 135-46.
271. Chang, G.T., et al., *Proteomic analysis of proteins regulated by TRPS1 transcription factor in DU145 prostate cancer cells.* Biochim Biophys Acta, 2007. **1774**(5): p. 575-82.
272. Mao, C., et al., *Targeted mutation of the mouse Grp94 gene disrupts development and perturbs endoplasmic reticulum stress signaling.* PLoS One, 2010. **5**(5): p. e10852.
273. Jones, D.T., et al., *Geldanamycin and herbimycin A induce apoptotic killing of B chronic lymphocytic leukemia cells and augment the cells' sensitivity to cytotoxic drugs.* Blood, 2004. **103**(5): p. 1855-61.
274. Restall, I.J. and I.A. Lorimer, *Induction of premature senescence by hsp90 inhibition in small cell lung cancer.* PLoS One, 2010. **5**(6): p. e11076.
275. Nicchitta, C.V., *Biochemical, cell biological and immunological issues surrounding the endoplasmic reticulum chaperone GRP94/gp96.* Curr Opin Immunol, 1998. **10**(1): p. 103-9.
276. Suriano, R., et al., *Sialic acid content of tissue-specific gp96 and its potential role in modulating gp96-macrophage interactions.* Glycobiology, 2009. **19**(12): p. 1427-35.
277. Srivastava, P.K., A.B. DeLeo, and L.J. Old, *Tumor rejection antigens of chemically induced sarcomas of inbred mice.* Proc Natl Acad Sci U S A, 1986. **83**(10): p. 3407-11.
278. Suriano, R., et al., *Differences in glycosylation patterns of heat shock protein, gp96: implications for prostate cancer prevention.* Cancer Res, 2005. **65**(14): p. 6466-75.
279. Bigagli, E., et al., *Extremely low copper concentrations affect gene expression profiles of human prostate epithelial cell lines.* Chem Biol Interact, 2010. **188**(1): p. 214-9.
280. Sun, S., et al., *Endoplasmic reticulum stress as a correlate of cytotoxicity in human tumor cells exposed to diindolylmethane in vitro.* Cell Stress Chaperones, 2004. **9**(1): p. 76-87.
281. Untergasser, G., S. Madersbacher, and P. Berger, *Benign prostatic hyperplasia: age-related tissue-remodeling.* Exp Gerontol, 2005. **40**(3): p. 121-8.
282. *Dharmacon RNAi Technologies.* [cited 2011 27th April].
283. Huggett, J., et al., *Real-time RT-PCR normalisation; strategies and considerations.* Genes Immun, 2005. **6**(4): p. 279-84.

-
284. Pan, Z., et al., *Silencing of GRP94 expression promotes apoptosis in pancreatic cancer cells*. *Int J Oncol*, 2009. **35**(4): p. 823-8.
285. Herman-Antosiewicz, A., D.E. Johnson, and S.V. Singh, *Sulforaphane causes autophagy to inhibit release of cytochrome C and apoptosis in human prostate cancer cells*. *Cancer Res*, 2006. **66**(11): p. 5828-35.
286. Hanlon, N., et al., *Repeated intake of broccoli does not lead to higher plasma levels of sulforaphane in human volunteers*. *Cancer Lett*, 2009. **284**(1): p. 15-20.
287. Xu, C., et al., *Suppression of NF-kappaB and NF-kappaB-regulated gene expression by sulforaphane and PEITC through IkappaBalpha, IKK pathway in human prostate cancer PC-3 cells*. *Oncogene*, 2005. **24**(28): p. 4486-95.
288. Zhao, L., J.Y. Lee, and D.H. Hwang, *Inhibition of pattern recognition receptor-mediated inflammation by bioactive phytochemicals*. *Nutr Rev*, 2011. **69**(6): p. 310-20.
289. Qazi, A., et al., *Anticancer activity of a broccoli derivative, sulforaphane, in barrett adenocarcinoma: potential use in chemoprevention and as adjuvant in chemotherapy*. *Transl Oncol*, 2010. **3**(6): p. 389-99.
290. Baskin, L., S. Urschel, and B. Eiberger, *A novel ex-vivo application of RNAi for neuroscience*. *Biotechniques*, 2008. **45**(3): p. 338-9.
291. Zachara, B.A., et al., *Selenium level in benign and cancerous prostate*. *Biol Trace Elem Res*, 2005. **103**(3): p. 199-206.
292. Sreekumar, A., et al., *Metabolomic profiles delineate potential role for sarcosine in prostate cancer progression*. *Nature*, 2009. **457**(7231): p. 910-4.
293. Rabilloud, T., *Two-dimensional gel electrophoresis in proteomics: old, old fashioned, but it still climbs up the mountains*. *Proteomics*, 2002. **2**(1): p. 3-10.
294. *Cancer Research UK: CancerStats*. [April 4th 2011].
295. Valkenburg, K.C.a.W., B. O., *Mouse Models of Prostate Cancer*. *Prostate Cancer*, 2011. **2011**.
296. Hurwitz, A.A., et al., *The TRAMP mouse as a model for prostate cancer*. *Curr Protoc Immunol*, 2001. **Chapter 20**: p. Unit 20 5.